2017

# A Novel Synthesis and Subsequent Decyclization of Iminothiozolidinones: Expansion of Thiourea Chemistry for Biological Applications

Constance D. Franklin
*Virginia Commonwealth University*

# A NOVEL SYNTHESIS AND SUBSEQUENT DECYCLIZATION OF IMINOTHIOZOLIDINONES: EXPANSION OF THIOUREA CHEMISTRY FOR BIOLOGICAL APPLICATIONS

A dissertation submitted in partial fulfillment of the requirements of the degree of Doctor of Philosophy in Chemistry at Virginia Commonwealth University.

by

CONSTANCE D. FRANKLIN
Bachelor of Science, University of Virginia, 2011

Director: DR. VLADIMIR A. SIDOROV
ASSOCIATE PROFESSOR, DEPARTMENT OF CHEMISTRY

Virginia Commonwealth University
Richmond, VA
May, 2017

Acknowledgements

I would first like to thank my advisor, Dr. Vladimir Sidorov, for accepting me into his group. I came to the Chemistry Department at VCU with the intention to pursue Chemical Biology. Instead I began a project in organic synthesis and never looked back. I am lucky to have had the opportunity to work with someone who has such a strong dedication to scientific inquiry and discovery. Thank you for your support and encouragement and for teaching me to be a better scientist.

I want to thank the VCU Chemistry Department. I have enjoyed my time here as a graduate student, and I attribute that to the positive, collaborative atmosphere that this department fosters. I would specifically like to thank Dr. Ashton Cropp, Dr. Matthew Hartman, Dr. Indika Arachchige, and Dr. Hamid Akbarali who have been a wonderfully supportive committee. Likewise, Dr. Nicholas Farrell, Dr. Julio Alvarez, and Dr. Galya Abdrakhmanova have been very helpful to me during these past few years. I would like to think Galya in particular for her patience with me when we did the patchclamp experiments together, even when I kept breaking things. I would also like to thank Ms. Lucy Moses for her encouragement and support. I have enjoyed working for her as a teaching assistant and I appreciate all she has taught me about better lab management.

I was lucky enough to meet some excellent people over the past six years. To Mike Wood, AJ Pagan, Nick Abrigo, Vivek Kaushik, and Andrew Vogel I wish to express how grateful I am to have had the opportunity to work with you. I found working with you highly

motivating and I will remember this time fondly. I believe science is a collaborative venture of creative minds and nowhere was that more true than in our lab. Although not an official member of the Sidorov lab, Christine Ring has also been a significant source of scientific discussion and moral support and I will miss our lunch breaks. I was also fortunate to get to know Madhura Damle and Anita Gharse through the program. Thank you all for your friendship and support.

The work I have presented here is vastly different from the work I set out to do. I want to thank Dave Lebron, Ashley Groth, and Courtney Diamond for all of their help in this quest. You guys turned a weird and frustrating problem into a remarkable body of work and being in the lab with you has been a joy. I wish you all the best.

During my time at UVA, Dr. Derewenda was kind enough to allow me to work in his lab for a year, Dr. David Cooper was my mentor in the lab, and I would like to thank him for his support and guidance. He was an excellent teacher and my time in that lab shaped my decision to apply to the graduate program.

I would like to acknowledge my friends outside the lab as well for keeping me grounded and reminding me why I chose this path in the first place. I met Saša Jusofovic at UVA where we began our journey into science together. It was a long four years, but I will always treasure them. Bethany Kliewer has been my friend since kindergarten and it is impossible to quantify how important her support has been during this process.

Finally, I want to thank all of my parents—Donna and Bryan and Sharon and Carl—and my brother Neil for their support and encouragement. They always believed in me and because of this I have never questioned my ability to do whatever I set out to do. It is because of them that I have reached this goal.

Table of Contents

Page

List of Figures

Page

# List of Schemes

Page

# List of Tables

Page

# List of Abbreviations

| | |
|---|---|
| APTS | 8-Aminopyrene-1,3,6-trisulfonic acid trisodium salt |
| BOC | Di-tert-butyl dicarbonate |
| BrAcBr | Bromoacetyl bromide |
| $CD_3CN$ | Deuterated acetonitrile |
| CF | Carboxyfluorescein |
| Cyclen | 1,4,7,10-Tetraazacyclododecane |
| DCM | Dichloromethane |
| DMF | Dimethyl formamide |
| DMSO | Dimethyl sulfoxide |
| DMSO-$d_6$ | Deuterated dimethyl sulfoxide |
| DNA | Deoxyribose nucleic acid |
| DOPE | Dioleoyl-L-α-phosphatidylethanolamine |
| ELISA | Enzyme-linked immunosorbent assay |
| ESI | Electrospray ionization |
| EtOAC | Ethyl acetate |
| $Et_3N$ | Triethylamine |
| EtOH | Ethanole |
| EYPC | Egg yolk phosphatidylcholine |
| FISH | Fluorescent in situ hybridization |
| GABA | Gamma-aminobutyric acid |
| GFP | Green fluorescent protein |

| | |
|---|---|
| GlyR | Glycine receptor |
| HEK 293 | Human embryonic kidney cells 293 |
| HEPES | 4-(2-hydroxyethyl)-1-piperazineethanesulfonic acid |
| HIV-1 RTI | Human Immunodeficiency Virus Reverse Transcriptase Inhibitor |
| HMBC | Heteronuclear multiple bond correlation spectroscopy |
| HPTS | 8-Hydroxypyrene-1,3,6-trisulfonic acid trisodium salt |
| Hse | Homoserine |
| HSQC | Heteronuclear single quantum correlation |
| ITC | Isothermal titration calorimetry |
| LGIC | Ligand gated ion channel |
| MeCN | Acetonitrile |
| MeOH | Methanol |
| MS | Mass spectrometry |
| NBD | 4-Chloro-7-nitrobenzofurazan |
| NMDA | N-Methyl-D-aspartic acid |
| NMR | Nuclear magnetic resonance |
| OMe | Methoxy |
| PBS | Phosphate buffer saline solution |
| PETT | Phenethylthiazolylthiourea |
| PKD1 | Polycystic kidney disease |
| PTA | 1,3,6,8-Pyrenetetrasulfonic acid tetrasodium salt |
| Pyranine | 8-Hydroxypyrene-1,3,6-trisulfonic acid trisodium salt |
| SDS | Sodium dodecyl sulfate |
| TBAF | Tetrabutylammonium fluoride |
| TFA | Trifluoroacetic acid |

| | |
|---|---|
| THF | Tetrahydrofuran |
| TMSCl | Trimethylsilyl chloride |
| TsCl | Tosyl chloride |
| VEGF | Vascular epithelial growth factor |

# Abstract

A NOVEL SYNTHESIS AND SUBSEQUENT DECYCLIZATION OF IMINOTHIOZOLIDINONES: EXPANSION OF THIOUREA CHEMISTRY FOR BIOLOGICAL APPLICATIONS

By Constance D. Franklin, Ph.D.

A dissertation submitted in partial fulfillment of the requirements for the degree of Doctor of Philosophy in Chemistry at Virginia Commonwealth University

Virginia Commonwealth University, 2017

Major Director: Dr. Vladimir A. Sidorov
ASSOCIATE PROFESSOR, DEPARTMENT OF CHEMISTRY

Small molecule synthesis has become a valuable tool in the study of biological systems. Biologically active compounds can be designed based on well-characterized endogenous systems or they can be found through the screening of large libraries of small molecules. This work involves the development of a small library of cyclic thiourea-based small molecules by use of an unreported synthetic pathway. Briefly, parent thioureas were cyclized by reaction with bromoacetyl bromide, and one or two isomeric heterocycles were found to form. Further studies indicated that the reaction could be easily manipulated by temperature or solvent to effectively control the product distribution. These iminothiozolidinones were characterized by single crystal

x-ray analysis. The new reaction was explored in an effort to uncover the factors influencing the control of the isomer formation. Furthermore, these iminothiozolidinones underwent a novel decyclization reaction that resulted in the loss of the parent thiourea connectivity and incorporation of an external nucleophile to yield an aminooxoethylcarbamothionate. The reaction proceeds through a termolecular mechanism. These reactions can be combined to a one-pot reaction series. These compounds share similarities with a class of compounds reported to be known HIV-1 reverse transcriptase inhibitors[94]. In addition to these new synthetic reactions, work was conducted with a previously developed cyclen thiourea receptor for the anionic dye HPTS and its derivatives[50-52]. This system was used to develop a cell labeling assay that led to the amplification of fluorescent labeling of target cells through the use of liposomes. Briefly, a dye-ligand conjugate for the glycine receptor was synthesized. Liposomes functionalized with the cyclen receptor were prepared encapsulating Rhodamine B. Confocal microscopy studies demonstrated the binding of the HPTS-ligand to the cell membranes. Addition of the liposomes resulted in quenching of the green fluorescence, indicating binding of the cyclen to HPTS. Subsequent excitation of Rhodamine B showed red fluorescence associated with the cells. The intensity of the red signal was demonstrably higher than for the signal resulting from the binding of the ligand-dye to the receptor. Together, these projects increase the synthetic usefulness of thiourea based small molecules and demonstrate the potential biological applications of related compounds.

# Chapter 1.

# Introduction

## 1.1 Fluorescent Imaging of Cells

Fluorescent imaging of cells has been a technique used for many years and is useful for studying many diverse targets.[1] A common approach is to fluorescently tag a ligand through covalent bonding to a fluorophore and apply the dye-conjugate to a cell culture.[2] The ligand would bind to the cells expressing the target, and these cells can then be excited and imaged using confocal microscopy. Many different components of a cell can be labeled, including DNA sequences. For example, the FISH assay can be used to fluorescently label cells that express target RNA strands through tagged DNA and therefore diagnose the presence of disease markers.[3,4] This assay is done in collected cells and requires an hour or more hybridization time. Alternatively, ELISA assays are very effective in searching for markers from cell lysate samples[5].

Vascular endothelial growth factor (VEGF) is responsible for providing an adequate oxygen supply to tissues when there is minimal blood circulation.[6] Tumors overexpress VEGF so that they can grow and metastasize. This makes VEGF a useful biomarker for the detection of cancer in blood serum.[7] The traditional method of detection for VEGF is an ELISA protocol, however this requires a large sample volume and the use of antibodies.[8,9] A new development in the detection of VEGF is the use of aptamers to recognize VEGF. Because aptamers bind one to

one, there needs to be a method for increasing the signal for enhanced sensitivity. After recognition of the target, DNA can be replicated, providing the amplification. The DNA-dye probe is then added, and fluorescence indicates presence of the cancer biomarker.[7]

Regardless of which part of a cell is targeted, most techniques rely on the introduction of a fluorophore. Methods of labeling to be done in vivo require a shorter time scale. This can be achieved by tagging the ligand, which binds immediately, rather than having to wait for the hybridization to occur. The field of real-time imaging has seen a number of advances recently, allowing long-standing questions to be answered.[10,11] The discovery of protein-based fluorophores has been instrumental to this growth. Fluorescent proteins, such as GFP, can be introduced to a protein target through genetic engineering.[12] The advantage to this method is that movement of a fusion protein product can be monitored via the fluorescent protein. Although GFP has become a powerful tool for the study of proteins, the fluorescent protein approach limits the fluorophore that can be used, as it must be genetically encoded, and depending on the size, it might cause deviations from wild type behavior.[13,14] Modern approaches have combined genetic engineering and the use of synthetic fluorophores. As an example, the SNAP-tag technology has become a widely used method to couple a protein of interest with a synthetic probe, such as a fluorophore, through the covalent bond formation between the tag and benzylguanine derivatives.[15-17]

### 1.2 Single Molecule Probes for Real-Time Imaging

Fluorescence microscopy is used in innumerable ways by modern biochemists for the study of biological systems. Activities that can be studied include the detection of a specific DNA sequence responsible for gene expression, visualization of organelles, and cell tracking.[13] It

is a necessary tool in modern research and has recently seen significant advancements. Indeed, the 2014 Nobel prize in Chemistry was awarded to Betzig, Hell, and Moerner for the development of super-resolved fluorescence microscopy, or nanoscopy.[18-22] The wide-spread availability of these microscopes has led to the emergence of fluorescence detection of tumors during surgery as a means to getting better margins in removal of cancerous tissue. Since many cancers require the excision of tumors as the best path to a cure, and since it is necessary to minimize the removal of healthy tissue (especially if the tumor is in a sensitive area such as the brain) it is imperative that fluorescent imaging techniques for this purpose are fast, specific, and have a high signal compared to non-targeted tissue.[23,24]

There are two main modes for fluorescent imaging of tissue to guide surgery. The first is the use of endogenous fluorophores. This method relies on the fact that cancer cells autofluoresce more than healthy tissue.[25] The main benefit with this approach is that it does not require the addition of any other agent, which would have to be approved after time-consuming and costly clinical trials. This also makes it a potential tool for diagnosis.[26] The major drawback to this method is the low signal of tumor to background tissue ratio.

The other technique requires the use of exogenous fluorophores, or fluorophores that are applied to the system. This is advantageous because there are many biocompatible dyes that fluoresce at a high intensity, and the emission range can be selected. There are a number of probes already approved for fluorescence guided surgery. The biggest challenge in this method is the need to target these fluorophores to the specific group of cells to be removed without any other labelling of healthy tissue.[23,24]

Antibodies can be used to provide specificity to a target. Direct immunolabeling comes from linking a primary antibody to a fluorophore. This is advantageous because small molecule

organic dyes will likely not perturb the system to the extent that a larger fluorescent protein might and compounds are available that cover a range of wavelengths. This would make them useful in multiplexed imaging. The biotin-streptavidin system is another powerful tool to provide specificity between a probe and a target.[14]

### 1.3 Use of Nanotechnology in Theranostics

An important characteristic of any fluorophore is excitation and emission at ranges that are different from the biological environment (in the body or a cell growth medium). It should also have a high molar absorption coefficient and quantum yield as well as be biocompatible. It should be easily conjugated to a probe of some kind such as DNA, peptides, streptavidin or other protein ligand for use in targeted imaging,.[27] Organic dyes are the classical choice of fluorophore, as they are cheap, readily available, and already approved for in vivo studies. However quantum dots such as CdSe and CdTe are becoming more common in biosensing.[28,29] The optical properties of quantum dots are in part controlled by their size, so a range of different potential fluorophores can be synthesized with relative ease.[30] Because nanoparticle synthesis often already requires organic capping agents, the surface of quantum dots can be modified to bind to a targeting probe.[31-33] This is also how their dispersion in water can be controlled.[34] Quantum dots generally exhibit more favorable optical properties while organic dyes are more easily incorporated into the cell and do not face issues with aggregation. For the labeling of cell surfaces, however, quantum dots have been successfully used by functionalization with antibodies specific for cell membrane receptors.[35-37] Another potential advantage in the use of nanoparticles is that they often exhibit some biological activity and may be used as both an imaging agent and a therapeutic.[38-40] As with any method, the specific needs of the particular

system in question will define the limitations of an experiment and subsequently dictate the choice in fluorophore.

Liposomes have long been used as a means to deliver drugs or imaging agents to a targeted system.[41-43] Liposomes, a self-assembled lipid bilayer vesicle with an aqueous core, are biocompatible and easy to synthesize encapsulating any desired compound. The lipid bilayer may also be embedded with a compound of interest, letting both hydrophilic and hydrophobic agents be used.[44] Liposome-nanoparticle hybrid development is another growing field. One such system involves the formation of liposomes encapsulating a drug with quantum dots that partition into the lipid bilayer. This system is used for both imaging from the quantum dots as well as drug delivery, which has been the traditional role of liposomes.[45-47]

### 1.4 Thiourea Chemistry: Synthesis and Applications

Thiourea and thiourea derivatives have a long history of both industrial and medicinal applications. Each year, around 8,000 tons of thiourea is produced for use in textile modification, photography, production of flame-retardant polymers, and in removing mercury from water.[48-50] Thiourea is a versatile precursor that allows for the inclusion of sulfur into different scaffolds. The presence of this sulfur contributes to the thermal stability and metal-binding properties of these different materials. Thiourea is a synthetically versatile precursor; it tautomerizes into isothiourea, shown in **Scheme 1.1.**, and it participates in a number of different reactions.

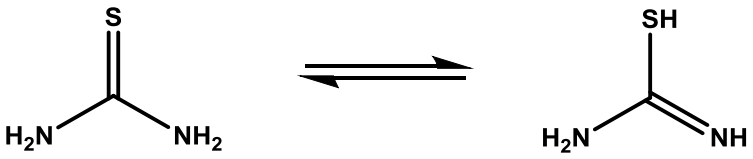


**Scheme 1.1:** Tautomerism of thiourea into isothiourea.

Substituted thioureas can be synthesized through a number of simple, high-yielding reactions using a range of different starting materials. A few selected examples are shown in **Scheme 1.2**.[48,51] The ease of formation from a variety of precursors makes this class of compounds readily accessible which has led to a wide variety of compounds that have found applications in a number of diverse areas **(Figure 1.1)**. Some of those applications include use as antifungal agents,[52-55] herbicides,[56] and as a rodenticide.[57] Functionalized thioureas may act alone or bind metals such as Ni(II), Pt(II), or Cu(II) when exhibiting activity. In the past ten years, these compounds have seen a rise in applications for treatment of HIV as reverse transcriptase inhibitors, as with Trovirdine (PETT) and Trovirdine analogs.[58-62]

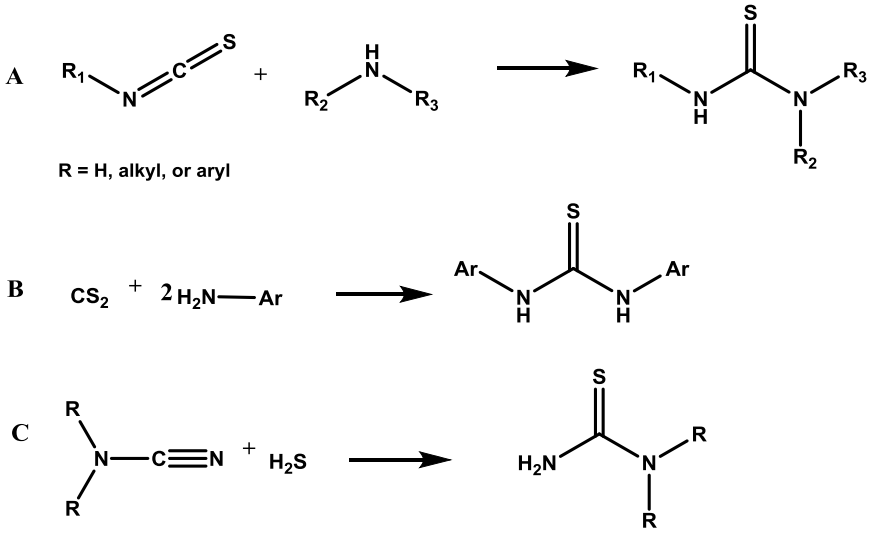


**Scheme 1.2:** Different reactions to form substituted thioureas. **(A)** Shows the formation of di- or tri-substituted thioureas. **(B)** Shows the formation of aryl-substituted thioureas, and **(C)** shows the formation of asymmetric di-substituted thioureas.[48]

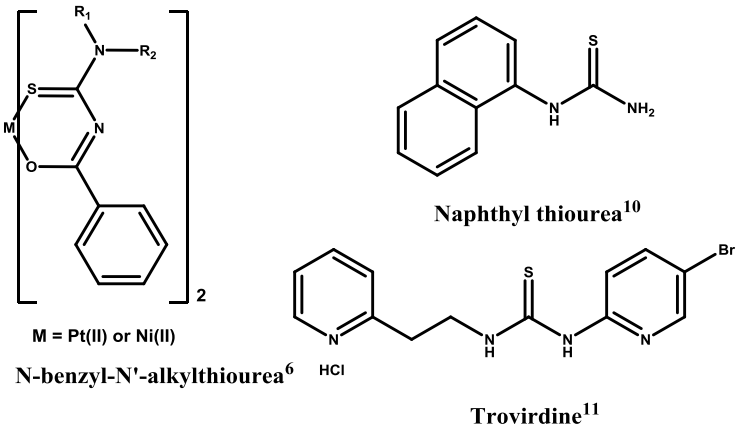


**Figure 1.1:** Examples of selected biologically active thioureas.

Substituted thioureas can act as both hydrogen bond donors and acceptors. Thioureas have also been seen to play a role in metal-free organocatalysis through hydrogen bond interactions.[63] The variety of reactions to form them as well as ones in which they act as a precursor make this class of compounds a synthetically interesting one. They are relatively stable in biological systems as they are neutral and not a target for common enzymes such as esterase. This makes them useful as a linker moiety for potential drugs. This also means that they are easily customized. It is this synthetic versatility that led to the use of functionalized thioureas in our group's work in developing a method of selective cell labelling and amplification.

# Chapter 2.

## Liposome-based Amplification of Cell Labeling Using a Cyclen Thiourea Receptor and Pyranine

### 2.1 Development of the Cyclen Thiourea Receptor

Previous work in the Sidorov group has focused on the development of a macromolecular complex that reversibly binds the class of sulfonated pyrene based dyes.[64-66] This macromolecule consists of a cyclen core that has been modified to include four thiourea-based arms bound to the core through the amine groups **(Figure 2.1)**. These arms consist of ester linkages, a thiourea moiety and terminate in aromatic groups. All of these regions are suspected to be involved in the binding of pyranine. Much work was conducted by the Sidorov group to characterize the selectivity and affinity of the receptor, cyclen **1**, to the sulfonated pyrene dyes.[64,67] Binding of cyclen **1** to HPTS, shown in **Figure 2.2**, results from a combination of hydrogen bonding between the thiourea groups with the sulfonate groups as well as π-π stacking between the planar body of pyrene and the naphthalene groups that terminate the arms. Additional stabilization comes from the interaction of a $Na^+$ ion with the ester bonds. It had been shown previously that the tetraester cyclen compounds will form this upright conformation in the presence of sodium ions.[68,69] HPTS and the related dyes exist as trisodium trisulfonate salts, thus $Na^+$ will always be present in the form of the counter ion.

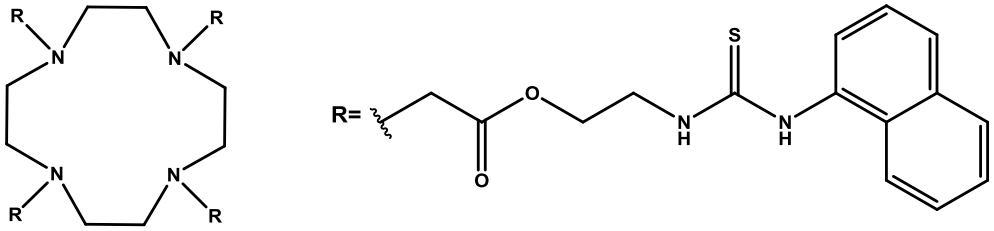


**Figure 2.1:** Structure of the synthetic cyclen thiourea receptor, cyclen **1**.

Experiments were done to show that all elements of the receptor are necessary for binding and quenching the dye.[64] When HPTS was mixed with a solution of either cyclen tetra-NH-boc or the free ester arm monomer (**Figure 2.3**), there was no change in the fluorescent emission. The formation of the complex was further characterized by isothermal titration calorimetry and fluorescence titration studies.[64,67] The titrations were carried out in PBS (10 mM sodium phosphate, 100 mM NaCl, pH 6.4) and were used to determine the $K_a$ of cyclen **1** binding HPTS, APTS, and PTA. The cyclen receptor was able to quench over 90% of the fluorescence of each dye. The structures of the dyes that bind and their $K_a$'s are given in **Figure 2.4**. Studies were also done to show the selectivity of the cyclen receptor for sulfonated pyrene dyes over other dyes such as 5-CF, 6-CF, and calcein which are anionic but non-planar, and safranin O, which is cationic. The isothermal titration calorimetry studies, reproduced in **Figure 2.5**, were carried out in methanol and found that cyclen **1** binds to pyranine in a 1:1 or 1:4 HPTS/receptor binding mode. The envisioned 1:1 mode is shown in **Figure 2.2**. As stated, the binding comes from a combination of interactions

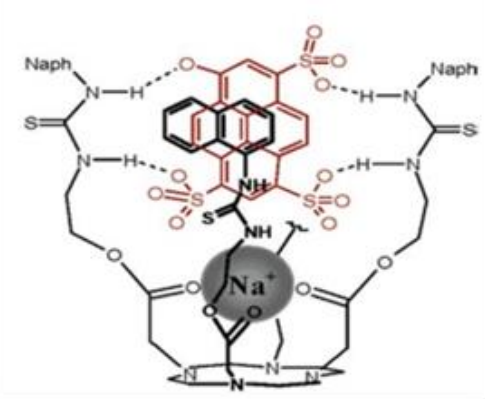


**Figure 2.2:** Envisioned binding mode of cyclen **1** and pyranine dye. The back arms are truncated for clarity.[64] Reprinted with permission from Winschel, C. A.; Kalidinid, A.; Zgani, I.; Magruder, J. L.; Sidorov, V. Receptor for Anionic Pyrene Derivatives Provides the Basis for New Biomembrane Assays. *J. Am. Chem. Soc.* **2005**, *127*, 14704-14713. Copyright 2005 American Chemical Society

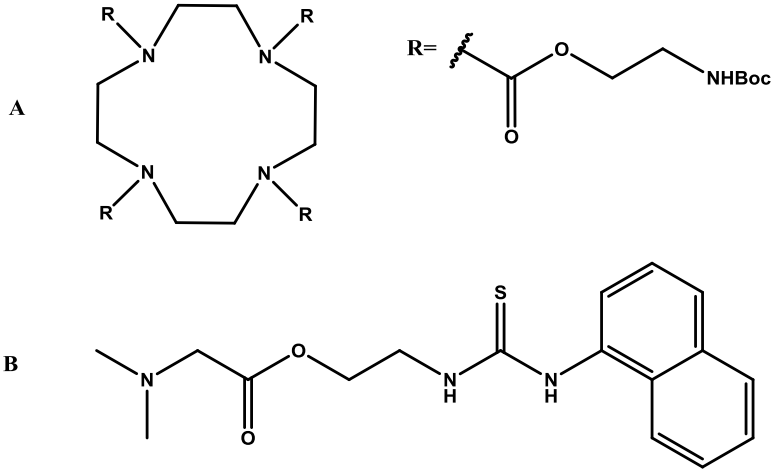


**Figure 2.3:** Structures of receptor control compounds. These were used to test the necessity of different elements in the complex formation between the cyclen receptor and pyranine. **(A)** Cyclen tetra-NH-boc and **(B)** the naphthyl thiourea arm monomer.

between the dye and the receptor, with the $\pi$-$\pi$ interactions being the most important. This complexation appears to be driven by the solvophobic effect. When mixed in methanol or aqueous solutions, the insoluble complex forms and binding is quenched. However, binding is

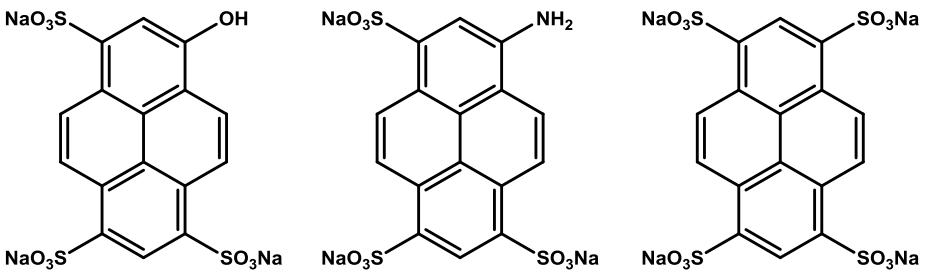


**Figure 2.4:** Structures of dyes that are bound by cyclen **1**: $K_a$ was measured by fluorimetric titrations using 50 nM solutions in PBS (10 mM sodium phosphate, 100 mM NaCl, pH 6.4)

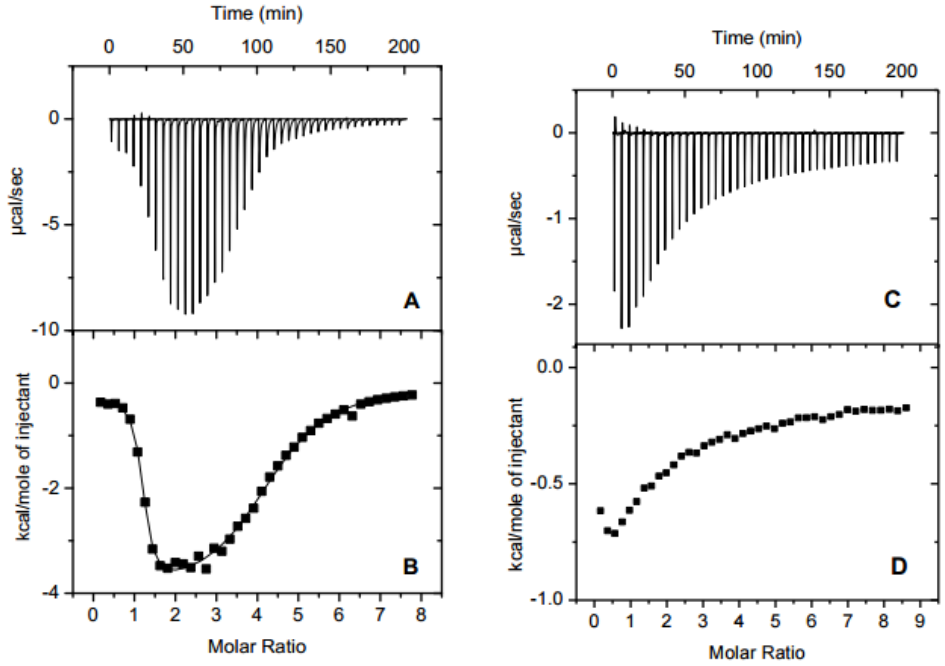


**Figure 2.5:** Microcalorimetric characterization of interactions of cyclen **1** with pyranine and calcein in methanol: (**A**) Raw data for the titration of a 0.25 mM solution of pyranine with a 10 mM solution of cyclen 1. (**B**) Integrated data from (**A**), corrected by the heat of cyclen 1 dilution, normalized to moles of injectant and plotted as a function of cyclen 1/pyranine ratios (solid squares). A continuous line represents the data fit in two sets of sites binding model. (**C**) Raw data for the titration of a 0.25 mM solution of calcein with a 10 mM solution of cyclen 1. Note the difference in vertical scales for plots (**A**) and (**C**). (**D**) Integrated data from (**C**), corrected by the heat of cyclen 1 dilution, normalized to moles of injectant and plotted as a function of cyclen 1/calcein ratios.[64] Reprinted with permission from Winschel, C. A.; Kalidinid, A.; Zgani, I.; Magruder, J. L.; Sidorov, V. Receptor for Anionic Pyrene Derivatives Provides the Basis for New Biomembrane Assays. *J. Am. Chem. Soc.* **2005**, *127*, 14704-14713. Copyright 2005 American Chemical Society.

not observed in DMSO or acetonitrile.. The 1:4 HPTS/receptor binding is weaker by two orders of magnitude and relies primarily on electrostatic interactions and hydrogen bonding.

### 2.1.1 Lipid Flip Assay

The cyclen receptor was used in an assay to monitor lipid flip.[65] Lipid flip can be controlled by enzymes such as flippases, floppases, and scramblases.[70] Proper function of these enzymes is important for maintaining cell membrane composition and lipid flip is part of a number of processes such as apoptosis and blood clotting.[71-77] Although there are several known methods to monitor lipid flip in membranes of cells or model systems, these have certain disadvantages.[78-80] The NBD-dithionite assay involves the use of NBD labeled lipids that are introduced into liposomes or cells. The fluorescence of NBD is then quenched with 10-60 mM sodium dithionite ($Na_2S_2O_4$) through the reduction of the nitro group to the amine. The two major drawbacks to this method are the high concentration of sodium dithionite that is required to quench the fluorescence, as well as the fact that this quenching is irreversible, Additionally, it is possible that the sodium dithionite, which is a small anionic salt, may be taken up into the cell, which would lead to quenching both inside and outside the cell.

The pyranine-cyclen **1** receptor system was modified for use in an assay to monitor lipid flip in both liposomes as well as in vitro studies. DOPE labeled with HPTS (known as cascade blue) was synthesized and incorporated into the membranes. Previous work had shown that cyclen **1** is not cell permeable.[64] and it was later shown that it does not inhibit cell growth. When 10 uM cyclen **1** was added to the solution of liposomes, the fluorescence decreased by 43%, indicating that the fluorescence from outer-facing cascade blue was quenched while the cascade blue facing the inside of the liposome remained. The addition of porcine liver esterase resulted in

the restoration of fluorescence up to 90% of the original intensity. This demonstrated that the pyranine-cyclen **1** system was suitable for monitoring lipid flip, and that the quenching interaction was reversible. Similar results were found when the cascade blue lipid was incubated with HEK 293 cells and a solution of 20 uM cyclen **1** was added.

### 2.1.2 Chemoselective Precipitation Assay

One of the characteristics of the complex that forms between the cyclen **1** receptor and pyranine dyes is the formation of an insoluble complex in aqueous and methanolic solutions. This is true even though both compounds when isolated have a degree of solubility in the two solutions. This led Kaushik et al to develop a chemoselective precipitation assay based on the cyclen **1** receptor and APTS.[66] Using this method, they were able to isolate lactose from a mixture of sucrose and lactose using the following protocol. APTS was added to a solution (1:9 $H_2O$:MeOH) of lactose and sucrose. Because lactose has a reducing end and APTS has the amine function on the ring, the two compounds could undergo reductive amination selectively in the presence of sucrose. A solution of cyclen **1** receptor was added and the resulting precipitate was collected. Back extraction with chloroform released the complex and APTS labeled lactose. 70% of the sucrose was recovered in this manner.

This method, however, required the formation of an irreversible bond between the APTS and lactose. This protocol was further refined to allow the separation of the two sugars with reversible binding to the dye. 1 M acetic acid was used to cause the formation of the imine bond between APTS and lactose. Cyclen **1** was then added to form the precipitate and this was collected as before. The precipitate was hydrolyzed with 2 M acetic acid. The solvent was removed after 2 hrs and the solid residue was treated with 1 N aqueous ammonia and then back

extracted with chloroform to give the cyclen **1** receptor in the organic layer and APTS and lactose in the aqueous layer. The lactose could be further purified by the addition of cyclen **1** to remove the free APTS. This method led to the purification of lactose from the solution with recovery of the cyclen receptor and APTS, but due to the reversible nature of imine formation, the sucrose was not entirely purified of lactose. However, each of these two methods led to purification of one of the sugars, demonstrating the usefulness of this system for chemoselective precipitation as a purification scheme for mixtures of sugars which would otherwise be difficult to separate.[81,82]

### 2.1.3 Modification of the Cyclen Receptor

Following this work, cyclen **2** was developed.[67] This compound is a variant of cyclen **1**, in which the cyclen core contains a p-nitro-benzoyl group. The arms were conjugated to the cyclen group and the nitro group was reduced to an amine **(Scheme 2.1)**. This variant binds to the pyrene based dyes in the same fashion but also contains a site that can be easily modified. Cyclen **2** was developed so that the cyclen receptor could be conjugated for further use. For this work, the cyclen receptor was conjugated to palmitoyl chloride to form the cyclen receptor lipid **(Scheme 2.2)**.

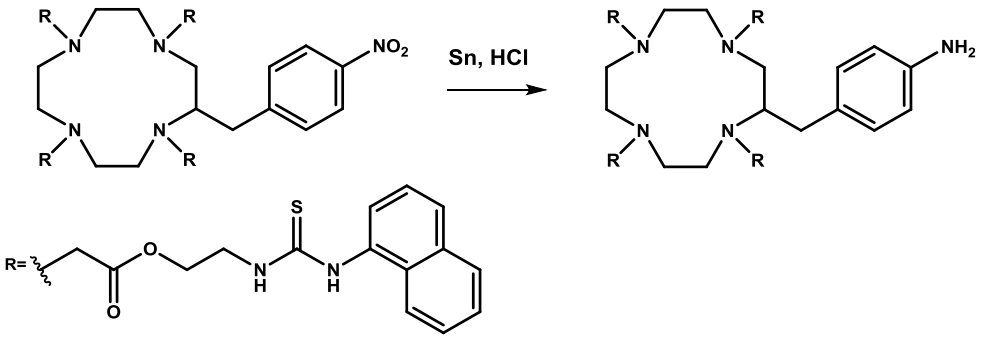


**Scheme 2.1:** Synthesis of cyclen **2** receptor. Reduction of the cyclen receptor using Sn and HCl to form cyclen **2**.

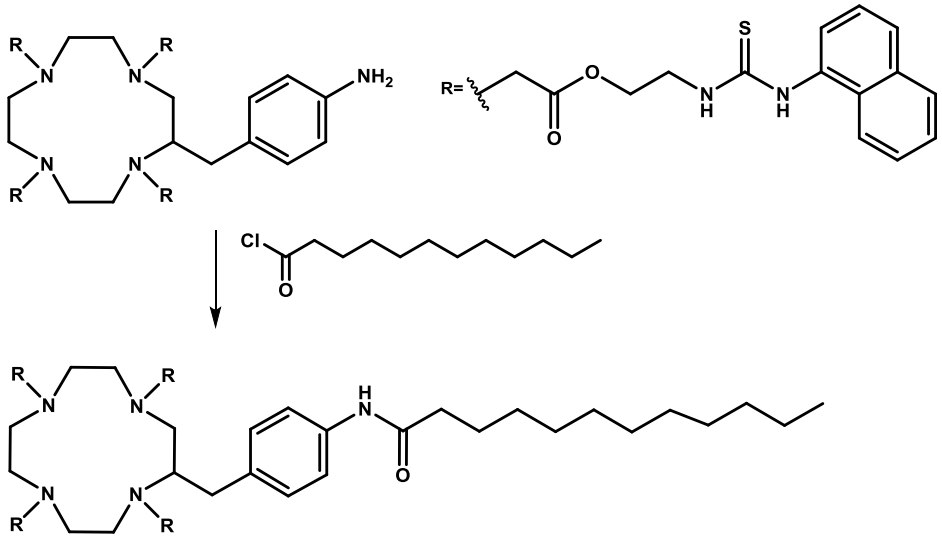

**Scheme 2.2:** Synthesis of the cyclen receptor lipid. This lipid was synthesized using cyclen **2** and palmitoyl chloride.

## 2.2 Experimental Design

The fact that this receptor is both easily modified as well as biocompatible led us to design a cell imaging assay dependent on the selective binding of HPTS to cyclen **1**. We chose a cell-membrane receptor to study based on several criteria. First, the receptor needed to be a ligand-gated ion channel (LGIC). This is a large class of cell-membrane receptors that are responsible for a number of diseases including epilepsy, autism, and alzheimers.[83-86] We chose this class so that potential ligands could be studied via the patch-clamp technique.[87] Patch-clamp is a method that measures the voltage generated when a ligand binds to a LGIC. The voltage comes from the flow of ions which is triggered by the binding of the ligand to the receptor. The proof of concept experiment was developed by conjugating HPTS to a ligand capable of binding to a LGIC, GlyR, and preparing liposomes functionalized with the cyclen receptor and encapsulating a second dye, Rhodamine B **(Figure 2.6)**. The glycine receptor (GlyR) is a ligand-gated ion channel that is activated by endogenous glycine.[88,89] The dye-ligand conjugate would

bind to the receptor when applied to the cells and fluoresce green. The liposomes, when added, would quench the dye via cyclen **1** binding to the HPTS moiety, and the second dye could be excited, leading to fluorescence associated with the cells and a greater intensity, up to a million fold amplification.

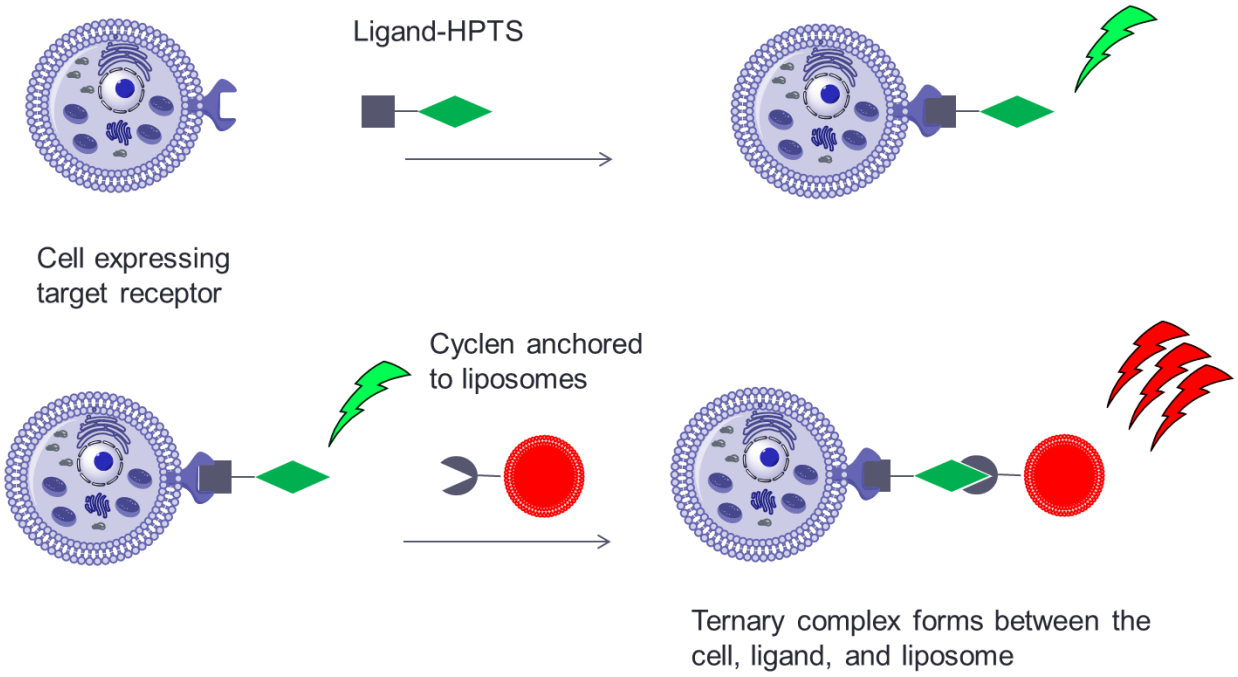


**Figure 2.6:** Liposome-based amplification of cell labeling. The method relies on the formation of a ternary complex between the cell, dye-ligand conjugate, and cyclen receptor conjugated liposomes.

### 2.3 Target Choice: α1GlyR as a Model System

Cells express many diverse proteins on their membranes. Many of these proteins act as channels to allow the flow of molecules and ions into or out of the cell, since most cannot freely pass through the dense, hydrophobic lipid bilayer.[90] Others play roles in complex signaling pathways.[91,92] Membrane proteins may be present in small amounts, or they may be highly expressed. Changes in the expression levels of proteins are often characteristic of disease

phenotypes. For example, VEGF is largely undetectable in healthy neuronal cells, but is over-expressed in cancerous cells, and participates in angiogenesis of gliomas.[6,93,94] Autosomal dominant polycystic kidney disease is another common genetic disease characterized by overexpression of a membrane protein, PKD1.[95]

Ligand gated ion channels comprise a diverse class of membrane proteins. These channels control the flow of ions through the lipid bilayer in response to physiological events. Activation occurs when a specific molecule, the receptor's ligand, binds to the activation site of the receptor, inducing a conformational shift. This change in conformation opens a channel for ions to travel through. Diffusion may be passive or active, depending on the direction of the gradient.[96]

This particular study focuses on the glycine receptor (GlyR), which is a ligand gated ion channel that is found in the central nervous system, specifically the spinal cord, brainstem, and cerebellum, as well as retinal tissues.[88,89] These receptors control the flow of chloride ions into the cell. They are activated by L-glycine, an inhibitory neurotransmitter, but can also be allosterically modulated by many chemicals such as ethanol, Zn(II), and other endogenous amino acids such as taurine. GlyRs are prevalent in nervous tissue, but they can be composed of different combinations of α and β subunits. The composition of subunits determines the characteristics of the receptors. All of them, however, are activated by glycine and are important in maintaining intracellular Cl- balance. Activation of these receptors results in hyperpolarization, when the Cl- ions enter the cell due to the extracellular concentration of Cl- being higher than the intracellular concentration.[97]

Properly functioning GlyRs are necessary for many biological functions such as voluntary motor control, reflex responses, and sensory input. Certain mutations cause the GlyR

to be less sensitive to glycine by up to 100 fold, and this results in what is known as hyperekplexia, or startle disorders. These diseases are characterized by heightened responses to startlement followed by muscle stiffness. It has been characterized in humans, cows, and mice.[98,99] Others have suggested that GlyRs are involved in pain perception, autism, and epilepsy.[83-85] Furthermore, these receptors are known to interact with other receptors such as GABA and NMDA, suggesting the GlyR plays a large role in neuronal homeostasis.[97] Despite all this, there is still much unknown about glycine receptors such as their composition in different tissues and many of their roles may still be unknown. Thus GlyR may become an important therapeutic target, and any further characterization of the receptor is valuable.

In addition to the GlyR being a good target for functional studies, it also makes an ideal candidate for development of enhanced visualization methods. As a ligand gated ion channel, its ligand binding can be well-characterized by patchclamp techniques, and extracellular binding ligands means that a fluorescent labeling technique could be a good way to visualize cells with specificity. This could be used to detect the presence of cells, such as cancer cells, that need to be removed fully during a surgery. However, if there are only a small number of cells present, visualization in an in vivo situation would require increased sensitivity.[93]

The aim of this work was to take advantage of the ligand-receptor interaction to provide specificity to a target, in this case cells expressing α1GlyR, while at the same time utilizing the complex that could be formed between pyranine and cyclen **1** functionalized liposomes. When the interior of the liposome is filled with a fluorescent dye, such as Rhodamine B, then the fluorescence associated with this dye can be used as an indication of the presence of α1GlyRs. The fact that the fluorescence comes from a liposome encapsulating a solution of dye, and not one dye molecule that has been conjugated to the ligand is the key to generating up to a million-

fold amplification of the signal, and thereby increased sensitivity in the visualization of cells expressing the receptor.

### 2.4 Synthesis of HPTS-Ligand for α1GlyR

A survey of the literature indicated that glycine binds to the receptor through the amino acid's backbone. Therefore, we hypothesized that modifying glycine at either the COOH or $NH_2$ sites would compromise binding to the receptor due to the bulky nature of pyranine. We found that several other endogenous amino acids were capable of binding to GlyR with a reasonable affinity.[100,101] These are shown in **Figure 2.7**. We selected homoserine as a potential precursor to form the HPTS-ligand conjugate because of it was similar to serine, which is known to bind, but has a longer side chain. This would allow a suitable distance between the two moieties to prevent any negative impact on the ability of the conjugate to bind to the receptor.

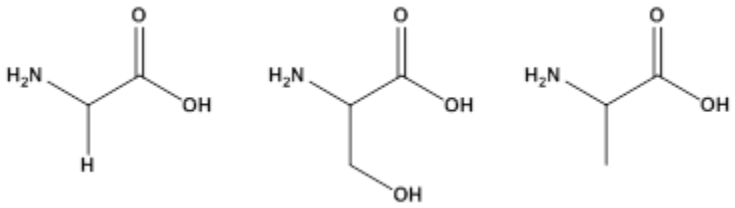


**Figure 2.7:** Structures of known GlyR ligands. (Left) glycine, (middle) serine, and (right) alanine.

Before synthesizing the HPTS-Hse conjugate, the binding of homoserine to GlyR was measured using the patch-clamp technique. HEK 293 cells designed to over-express a homonuclear variant of the receptor, α1GlyR, were obtained from Jensen and Kristiansen.[102] This variant was shown to behave in the same manner as wild-type GlyR. For each patch-clamp experiment, the plate of cultured cells were placed onto the stage and bathed in an extracellular solution (ECS) (140 mM NaCl, 3.5 mM KCl, 1.25 mM $Na_2HPO_4$, 2 mM $MgCl_2$, 2 mM $CaCl_2$, 10 mM glucose, 10 mM HEPES, pH 7.35). Solutions of glycine and homoserine of

concentrations ranging from 1 to 100 uM were made in the same extracellular solution. The intracellular solution (ICS) (140 mM KCl, 1 mM $MgCl_2$, 1 mM $CaCl_2$, 10 mM EGTA, 2 mM MgATP, 10 mM HEPES, pH 7.3) was used inside the pipet with the silver wire electrode. **Figure 2.8** summarizes the findings of the patch-clamp study, which was conducted using the same conditions as reported in the initial characterization of this receptor.[102] Glycine was found to have an $EC_{50}$ of 90 uM, which is similar to values reported in the literature, and homoserine was found to have an $EC_{50}$ of 190 uM. Since the aim of our study was to develop a model system for the amplification of fluorescent imaging, we concluded that homoserine was a suitable ligand.

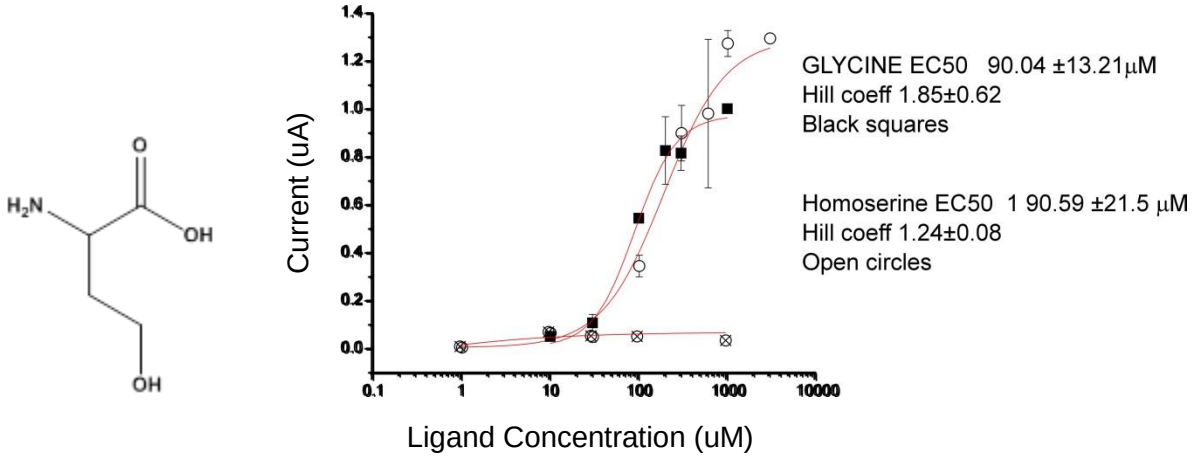


**Figure 2.8:** Patch-clamp measurements of L-homoserine affinity to α1GlyR. (Left) Structure of L-homoserine. (Right) Graph of current (uA) vs concentration of ligand (uM). The open circles with x's represent cells that had no response to glycine. These were not included in the calculation of the $EC_{50}$.

**Scheme 2.3A** shows the complete synthesis of HPTS-Hse. The first two steps in the synthesis of HPTS-Hse was to protect the carboxylic acid and amine groups of the amino acid. Homoserine was suspended in methanol and TMSCl was added to form the Hse methyl ester HCl salt. This was used in the next step without further purification. Next, boc anhydride was used with triethylamine to form N-boc-Hse methyl ester. The alcohol functional group was replaced with Br using carbon tetrabromide and triphenylphosphine. The yield for this reaction

was low (15%) due to the formation of an exceptionally stable five-membered lactone that homoserine forms between the carboxylic acid and the hydroxyl of the side chain, seen in **Scheme 2.3B**. The next step was to conjugate this brominated variant of Hse with HPTS via an ether linkage, using $CsCO_3$ to deprotonate the phenolic group of the dye, and the phase transfer catalyst TBAF. The reaction was heated to 45°C. This step resulted in a yield of 70%. Alkylation of HPTS causes a blue shift in the emission spectrum and we used this to monitor the reaction by fluorimetry. Finally, the protecting group was removed by TFA in DCM to give HPTS-Hse. The overall yield for this synthesis was 10.5%, with the major loss resulting from the formation of the lactone.

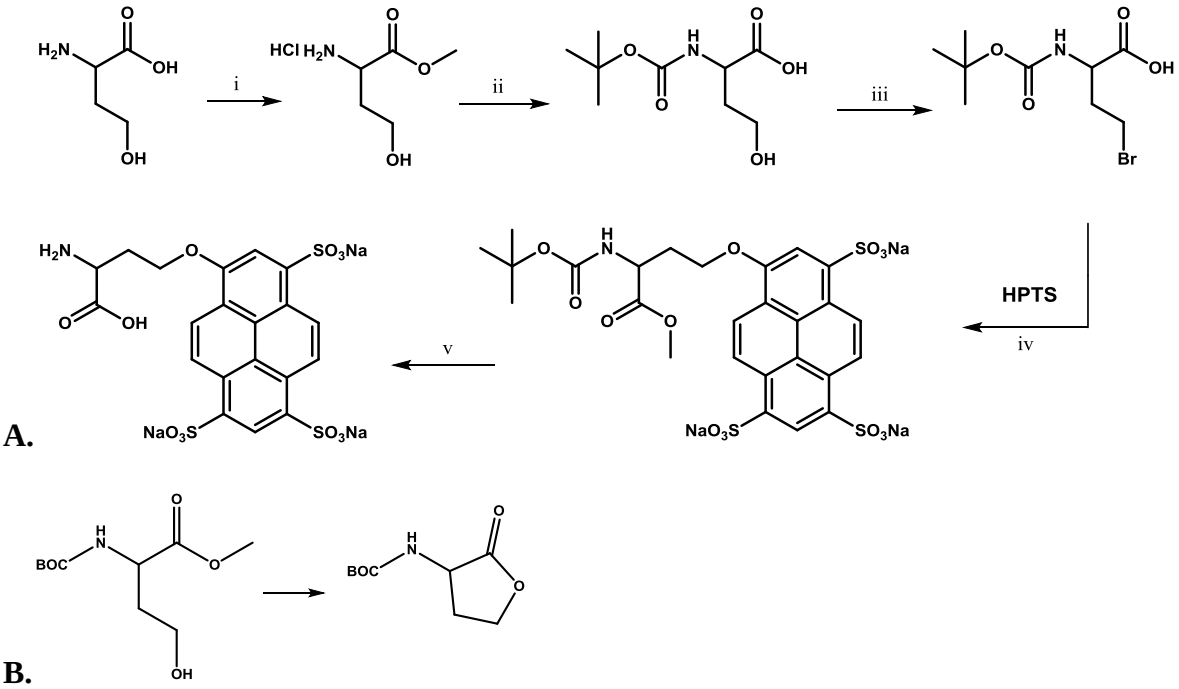


**Scheme 2.3:** Synthesis of HPTS-Homoserine. **(A)** Synthesis of HPTS-Hse. (i) Formation of the methyl ester HCl salt using TMSCl in methanol. (ii) Boc-protection of the amino acid using boc anhydride and triethylamine in MeCN. (iii) Conversion of the alcohol side group to the alkyl bromide using $CBr_4$ and $Ph_4P$. Yield from i-iii was 15%. (iv) Alkylation of HPTS with the Br-Hse intermediate using $CsCO_4$, TBAF in acetone at 45°C. Yield for this step was 70%. (v) Deprotection of the amino acid using TFA in DCM. This reaction gave quantitative yield. The overall yield for i-v was 10%. **(B)** Depiction of the formation of the homoserine lactone. This product accounted for nearly 80% of the homoserine used in the boc-protection step.

This compound was titrated against the cyclen **1** receptor to show that conjugation to homoserine did not diminish binding, (**Figure 2.9)**. HPTS in PBS (pH 7.0) has a $\lambda_{ex}$ = 405 nm and $\lambda_{em}$ = 510 nm and HPTS-Hse in PBS (pH 7.0) has $\lambda_{ex}$ = 402 nm and $\lambda_{ex}$ = 427 nm. The titrations show a $K_a$ of approximately 5 x $10^4$ $M^{-1}$ and a loss of 60% of fluorescence.

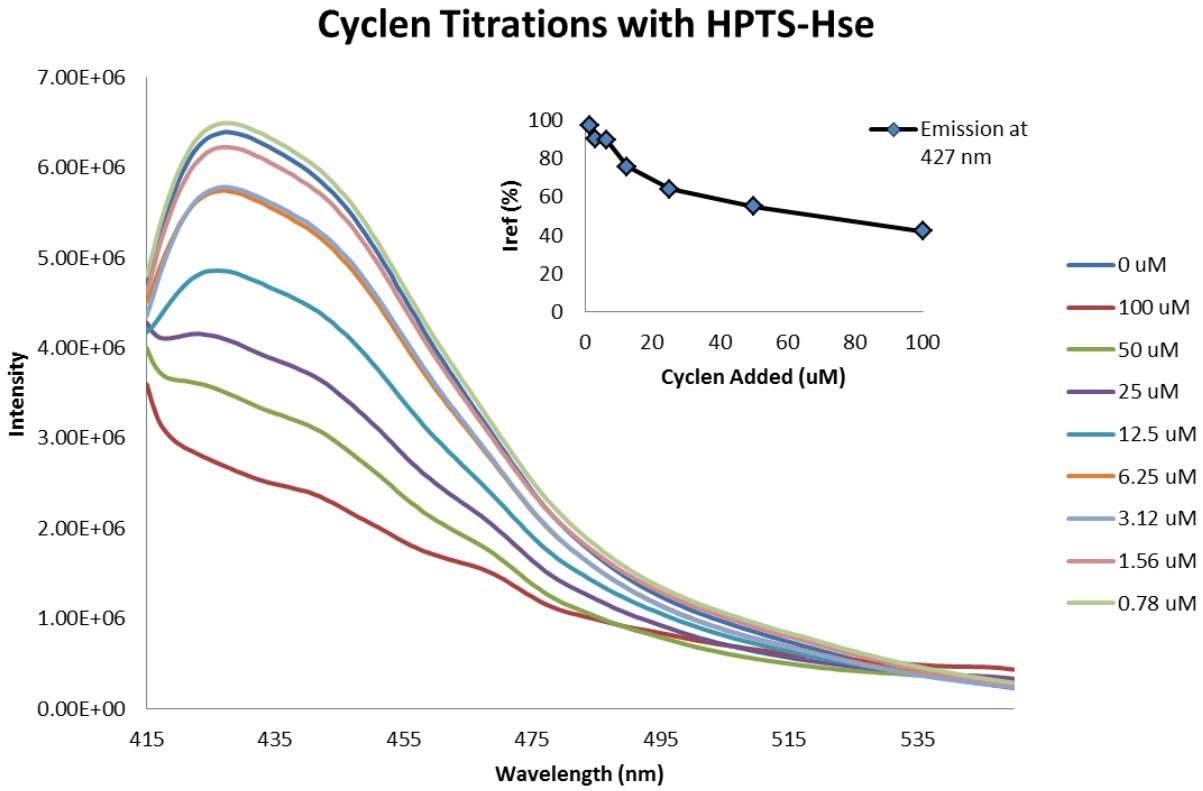


**Figure 2.9:** Fluorimetric titrations of HPTS-Hse with cyclen **1**. $K_a$ was found to be 5 x $10^4$ $M^{-1}$. The inset shows the amount of fluorescence that is quenched from binding with cyclen. The dye was dissolved in phosphate saline buffer (10 mM sodium phosphate, 100 mM NaCl, pH 7.0) with stock solutions (100x) of cyclen in DMSO. Excitation was 402 nm with emission monitored at 427 nm.

## 2.5 Synthesis of a Negative Control

One of the aims of this project was to show that it is the interaction between the cyclen receptor and pyranine that results in associated fluorescence from the liposomes containing the reporter dye. To demonstrate that there is no nonspecific binding between the liposomes and the

cells expressing the GlyR, a control compound was synthesized **(Figure 2.10B)**. We believed that homoserine conjugated to aniline would still bind to the GlyR but would not be bound by the cyclen receptor (**Figure 2.10A**). The brominated homoserine intermediate was reacted with aniline in water with SDS and $NaHCO_3$ to give boc-Hse-OMe aniline. This was deprotected in the same manner that the HPTS-Hse was to give the final product with an overall yield of 30%. Initially, fluorimetric titrations were attempted to demonstrate lack of binding to the cyclen receptor, however the alkylated aniline fluoresced at such a low intensity that the results were inconclusive. Instead, isothermal titration calorimetry was used to measure the interactions between Hse-aniline and the cyclen receptor. **Figure 2.11** shows the results from the ITC experiment, indicating that there is no significant binding of Hse-aniline to the cyclen receptor. Note the difference in the magnitude of the y axis when compared to that shown in **Figure 2.4**.

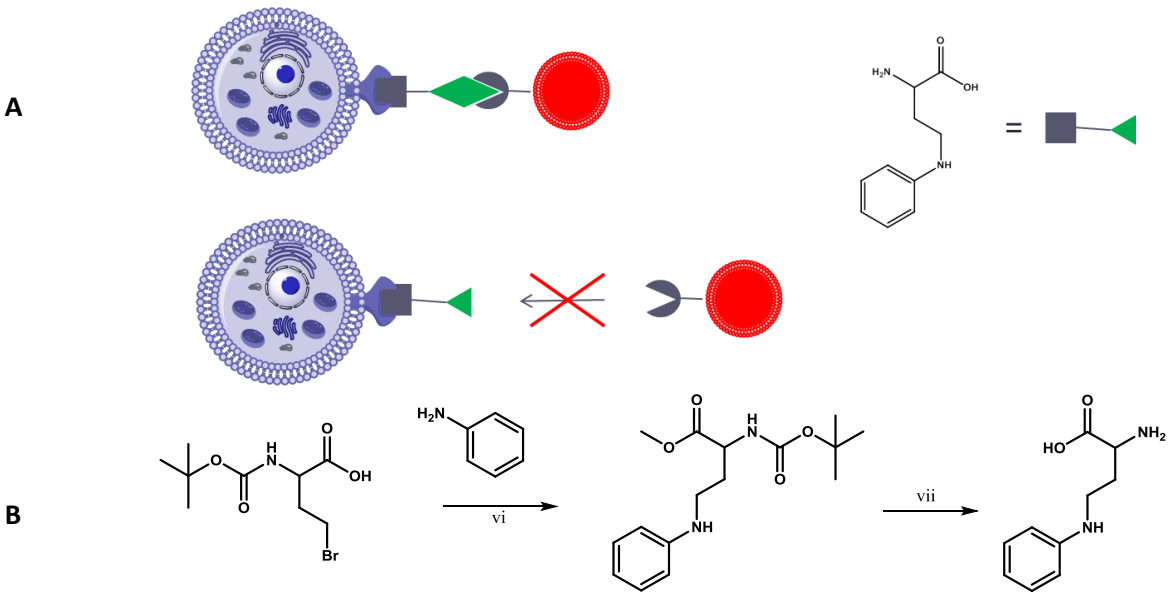


**Figure 2.10:** Proposed negative control experiment using aniline-Hse. **(A)** General scheme showing the proposed control ligand binding to the target receptor. Subsequent addition of cyclen-liposomes would be unable to bind to the ligand, leading to a lack of associated fluorescence with the cells. **(B)** Synthesis of the control compound. (vi) $NaHCO_3$ and SDS in water. (vii) The conjugate was deprotected using the same conditions as (v) in Scheme 2.2. Overall yield: 30%.

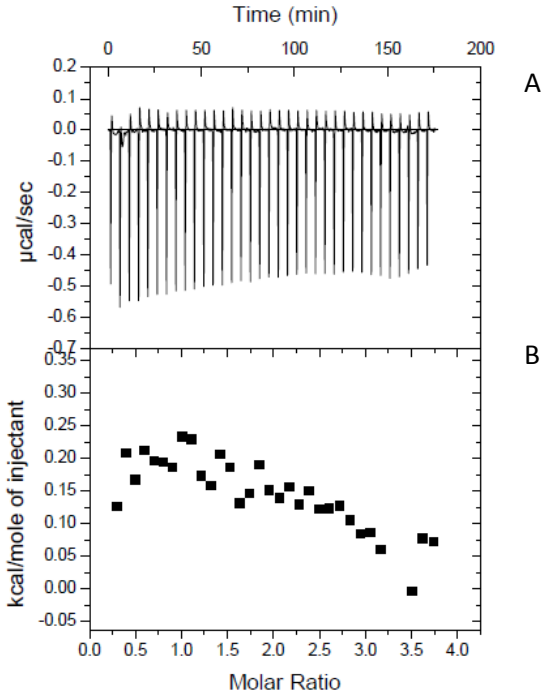


**Figure 2.11:** Isothermal titration calorimetry of aniline-Hse and cyclen **1**. (**A**) Raw data for the titration of a 0.25 mM solution of aniline-Hse with a 5 mM solution of cyclen-Ome in methanol. (**B**) Integrated data from (**A**), corrected by the heat of cyclen-Ome dilution, normalized to moles of injectant and plotted as a function of cyclen 1/aniline-Hse ratios.

## 2.6 Synthesis of Liposomes

The synthetic scheme for the modified cyclen receptor was previously developed by Kaushik et al, and is shown in **Scheme 2.2**.[67] The cyclen receptor used in the following experiments consisted of the urea-based arms with the p-OMe-phenyl group terminating each arm ($K_a$ = 9 x $10^6$ $M^{-1}$). The cyclen core included the p-$NO_2$-benzoyl group, which was reduced to the amine. This was used to make the liposomes containing the reporter dye, Rhodamine B.

Liposomes were made with the cyclen-Ome **2** receptor in the following manner. The mixture of lipids which consisted of 98.5 mol% egg yolk L-α-phophatidylcholine (EYPC) and 1.5 mol% cyclen receptor lipid were dissolved in 190 proof ethanol and dried under vacuum to form a thin film. The lipid film was hydrated using 2 mL of 50 nM Rhodamine B in phosphate

buffer solution (PBS) (10 mM sodium phosphate, 100 mM NaCl, pH 7.4). The solution was subjected to 5 freeze/thaw cycles (acetone/dry ice bath and water at room temperature). In order to achieve unilamellar vesicles of a consistent size, the solution was extruded through a 400 nm membrane 21 times. The liposomes were then purified using size-exclusion chromatography (Sephadex G-10 and the same PBS solution) to give a final volume of 1.7 mL of 400 nm cyclen functionalized liposomes encapsulating 50 nM Rhodamine B.

### 2.7 Confocal Microscopy Study

Cells studies were carried out using HEK-293 cells expressing the α1GlyR receptor.[102] Confocal microscopy was used to show HPTS-Hse binding to the receptors on the cell membranes and after addition of the liposomes to the medium, binding of cyclen to the HPTS conjugate quenched the green fluorescence and the red fluorescence of the liposomes replaced it. The results are shown in **Figure 2.12**. The following procedure was used. A culture of cells in ECS was grown on a poly-lysine cover slip. The cells were viewed in Brightfield mode first. 20 uL of 5 mM HPTS-Hse was then added to the cells. Images were taken using Brightfield mode **(A)** followed by fluorescent mode (emission at 427 nm) **(B)**. The two images were overlaid **(C)** to show that the green fluorescence was associated with the membranes of the cells. Next, 100 uL of Rhodamine B-filled liposomes was added and brightfield **(D)** and fluorescent (**E**; emission at 627 nm) were taken. Both images are overlaid in (**F**). The liposomes are clearly visible in both images, however the fluorescent image makes it clear that liposomes have associated with the membranes of the cells, leading to a clear amplification of the fluorescence associated with these cells. This labeling is clear even without washing away the unbound liposomes from the surrounding solution.

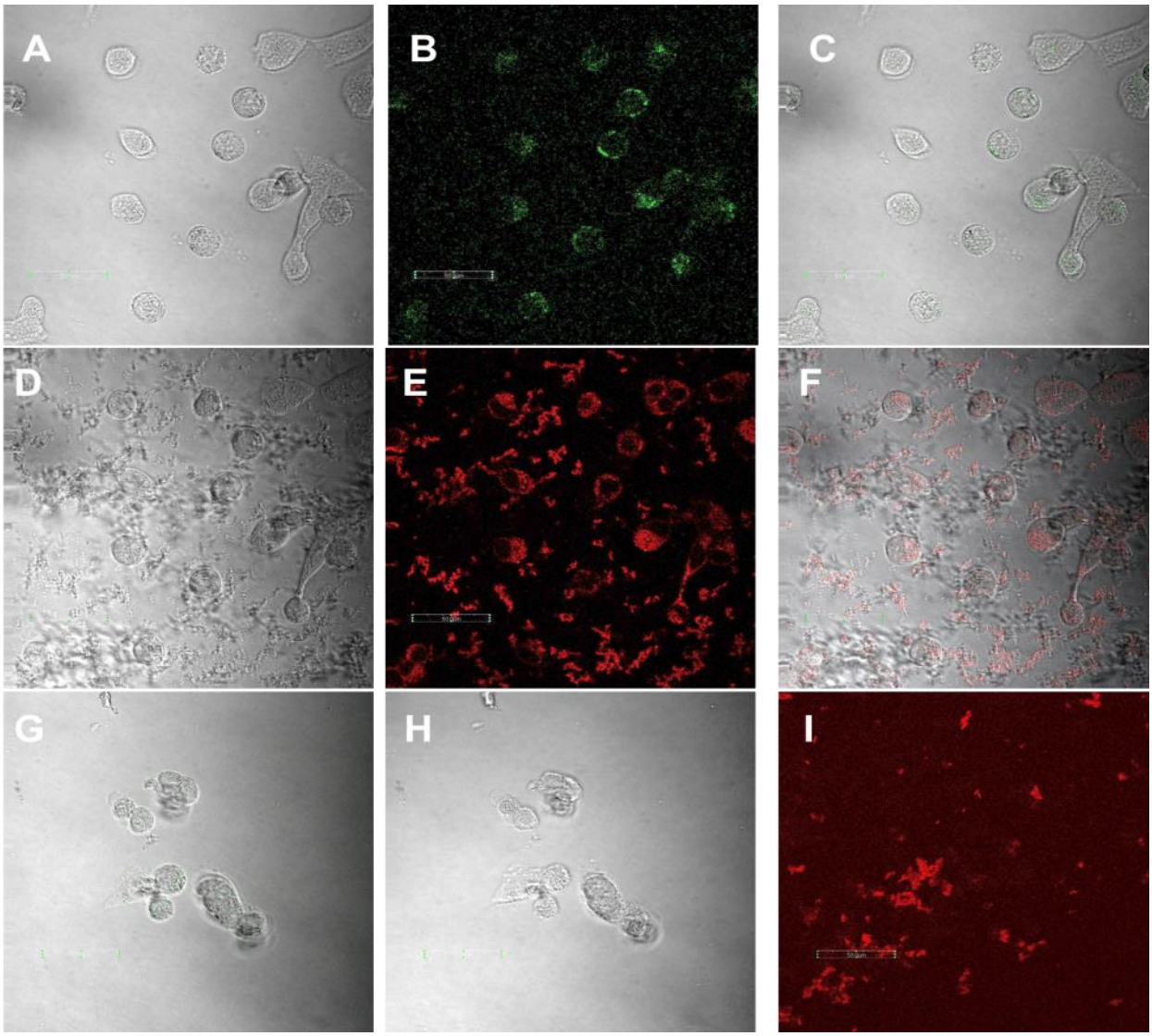


**Figure 2.12:** Confocal Microscopy Experiments Showing Amplification of Targeted Fluorescence. (**A**) Brightfield image of cells after the addition of 20 uL of 5 mM HPTS-Hse. (**B**) Fluorescent mode image of the same cells. (**C**) Combined BF and FM images. (**D**) Brightfield image of cells and HPTS-Hse with the addition of 100 uL of liposomes containing Rhodamine B. (**E**) Fluorescent mode image of these same cells. (**F**) Combined BF and FM images. (**G**) Control experiment showing Aniline-Hse bound to α1GlyR. Combined BF and FM image. (**H**) Same cells after the addition of liposomes. (**I**) FM image of the lipsomes, which are seen to have no affinity to the cells. (ECS buffer: 137 mM NaCl, 5.4 mM KCl, 10 mM HEPES, 10 mM glucose, 1 mM $CaCl_2$, 1 mM $MgCl_2$, pH 7.4)

A new plate of cells was used for the control experiment. Panel **G** shows a group of cells after the addition of 20 uL of 5 mM Hse-aniline (emission at 433 nm). After the addition of 100

uL of liposomes, there is no visible interaction between the liposomes and the cells. It is important to note that for this set of experiments, the cells were not grown on a poly-lysine coverslip. Because of this, the liposomes were found to be floating in the solution (**I**) further indicating that without the presence of pyranine for the receptor to bind, the liposomes form no non-specific interactions with the cells. This suggests that the pyranine-cyclen receptor system is a successful tool for cell labeling assays.

The presence of the liposomes results in an amplification of up to 1 million times the intensity of the fluorescence associated with the glycine receptors that are labeled by single molecule probes. The addition of the aniline-Hse compound showed no specific interactions with the liposomes.

## 2.8 Conclusions

This work demonstrates the usefulness of the specific complex formed between the cyclen 1 receptor and pyrene dye derivatives as a tool to modify techniques that require some kind of specificity. In this case, the interaction was used to provide an amplification of the fluorescence used as a labeling and visualization method for cells expressing target receptors. Although glycine was used here only as a model ligand-receptor system, other useful therapeutic targets, such as cancerous cells could be visualized using this method, as long as a specific membrane receptor could be efficiently targeted.

# Chapter 3

## Controlled Formation of Iminothiozolidinones and a Novel Nucleophile-Assisted Decyclization

### 3.1 Heterocyclic-Forming Reactions of Thioureas

In addition to the numerous applications of substituted thioureas, they also play an important role as precursors to the formation of heterocycles. The thioureas containing the ethanolamine arm, which we have used extensively, have been shown to form heterocycles in the presence of TsCl and NaOH (**Scheme 3.1**).[103-105] This reaction tolerates the changes to the arm to include amines and thiol groups. This reaction is a pathway to the synthesis of 2-amino-aza-heterocycles. These heterocycles are important in biology; chlonidine, a drug used to treat hypertension, is one example. Chlonidine analogs were synthesized using this scheme.[105]

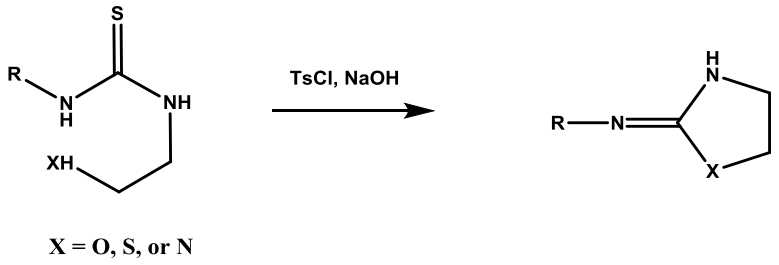


**Scheme 3.1**: Formation of 2-amino-aza-heterocycles from substituted thioureas.[105]

### 3.2 A Novel Synthesis of Iminothiozolidinones

Following the successful completion of the cell labeling assay involving the HPTS-cyclen **1** system, we planned to move forward with adapting this system to develop a methodology to selectively fuse liposomes. During this transition, we chose to revisit the synthesis of the cyclen receptor. The original reported synthesis involved building the arm onto the cyclen core in a stepwise fashion. While there were no inherent issues with this synthesis, it did involve the loss of some cyclen or cyclen-containing intermediate during each step. Cyclen, and especially p-$NO_2$-bn-cyclen, is rather expensive, so we wanted to minimize any loss. Previous work by Kaushik et al had made adjustments to the synthesis to conserve cyclen for that reason. Shown in **Scheme 3.2**, the new synthesis involved the reactions to form the complete arm first. 4-Methoxyphenyl isocyanate was reacted with ethanolamine to form 4-methoxyphenyl urea ethanolamine. This was then reacted with bromoacetyl bromide in the presence of triethylamine. These steps afforded the full arm which was then ready to react with p-$NO_2$-bn-cyclen. Following the reaction to conjugate the arm to the cyclen, the nitro group was reduced to the amine using Sn and HCl. Because of the ester bonds on the arms, the compound was dissolved in THF. HCl was generated by dripping sulfuric acid into a flask of NaCl. By controlling the conditions, this product was formed with fewer intermediates needing to be purified. The crude was dissolved in ethyl acetate and washed with ammonia water to give the final product.

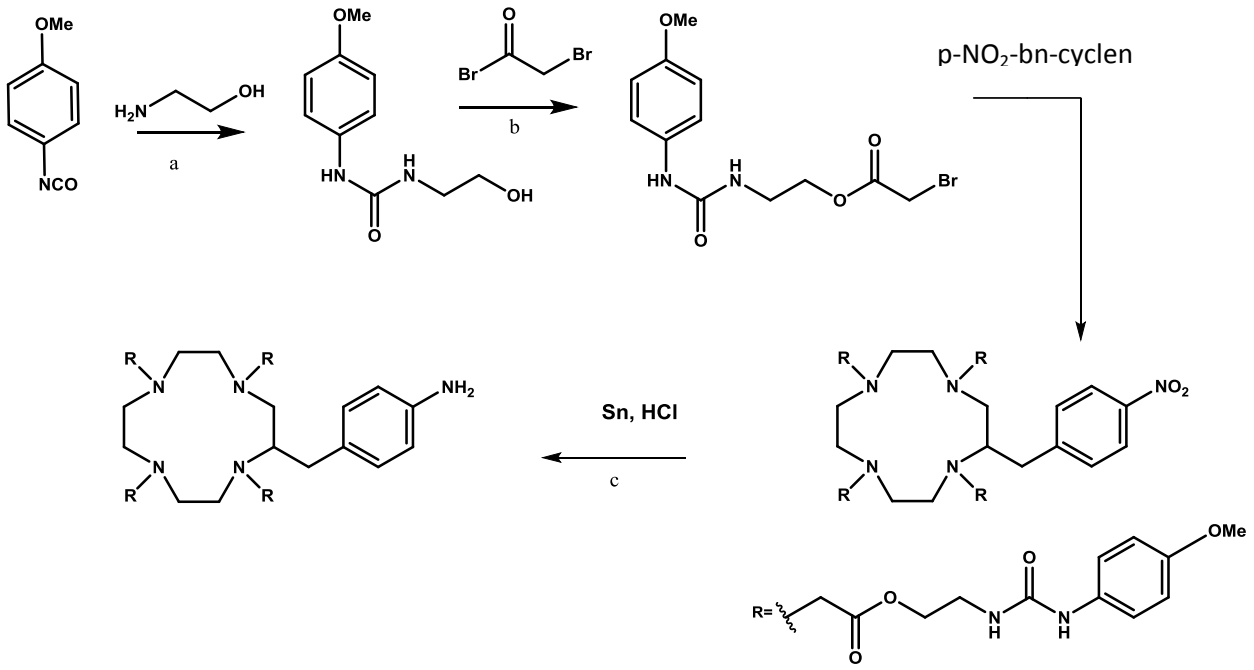


**Scheme 3.2** Modified synthesis of the cyclen **2** receptor. Note the use of the isocyanate rather than the isothiocyanate. a) ethyl acetate, rt, 1hr, 97%; b) bromoacetyl bromide, $Et_3N$, DCM, rt, 5 hrs, 90%; c) anhydrous DMF, $Na_2CO_3$, rt, 6 hrs, 62%; d) anhydrous THF, Sn/HCl(g), rt, 4hrs, 63%.

This synthesis was developed for the cyclen receptor variant that contained a urea group and terminated in 4-methoxyphenyl. We decided for this next project that we wanted to use the original cyclen **1** compound which consisted of the thiourea and naphthyl group. The first reaction between 1-naphthyl isothiocyanate and ethanolamine proceeded as expected. The second step, which was the reaction of the thiourea with bromoacetyl bromide, produced an unexpected product. After the first unexpected result, we speculated that the nitrogen of the thiourea group was possibly reacting with the acyl bromide instead of the alcohol as we had intended, so we reduced the amount of base from 2 mol eq to 1 and switched from DCM to THF. This second reaction also produced a product other than the desired ester (**Scheme 3.3)**. The products from both of these reactions were isolated and MS (ESI) revealed that the two products

were isomeric heterocycles. We decided to explore this discovery further, which will be the subject of this chapter.

The first thing that we considered was the difference between urea and thiourea. In the disubstituted urea, the electronegative oxygen would withdraw electron density from the nitrogens, making them less nucleophilic. The alcohol of the side chain would then be the strongest nucleophile of the compound, and when added to bromoacetyl bromide, the ester forms as expected. Thiourea, on the other hand, contains a sulfur rather and oxygen. In this case, the nitrogens are now able to act as nucleophiles, and this matched our observations. There are then two nucleophilic nitrogen centers and bromoacetyl bromide has two electrophilic centers. Mass spectrometry confirmed that the products we obtained were the result of an initial attack by (we suspected) the nitrogen, followed by a second intramolecular attack to close the ring. **Figure 3.1** shows that the NMR spectra of the two products are significantly different, while mass spectrometry showed the products had the same masses.

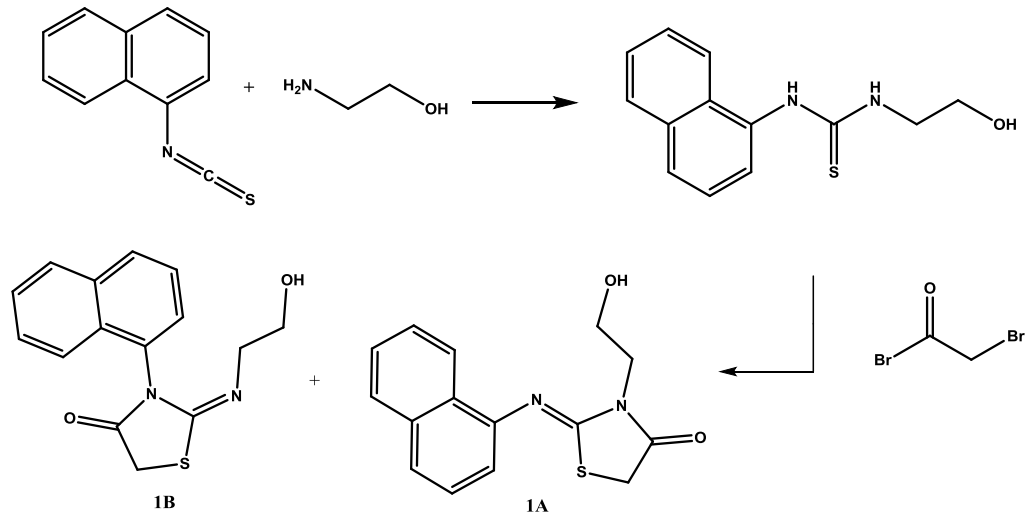


**Scheme 3.3:** Reaction of thiourea **1** forms two products.

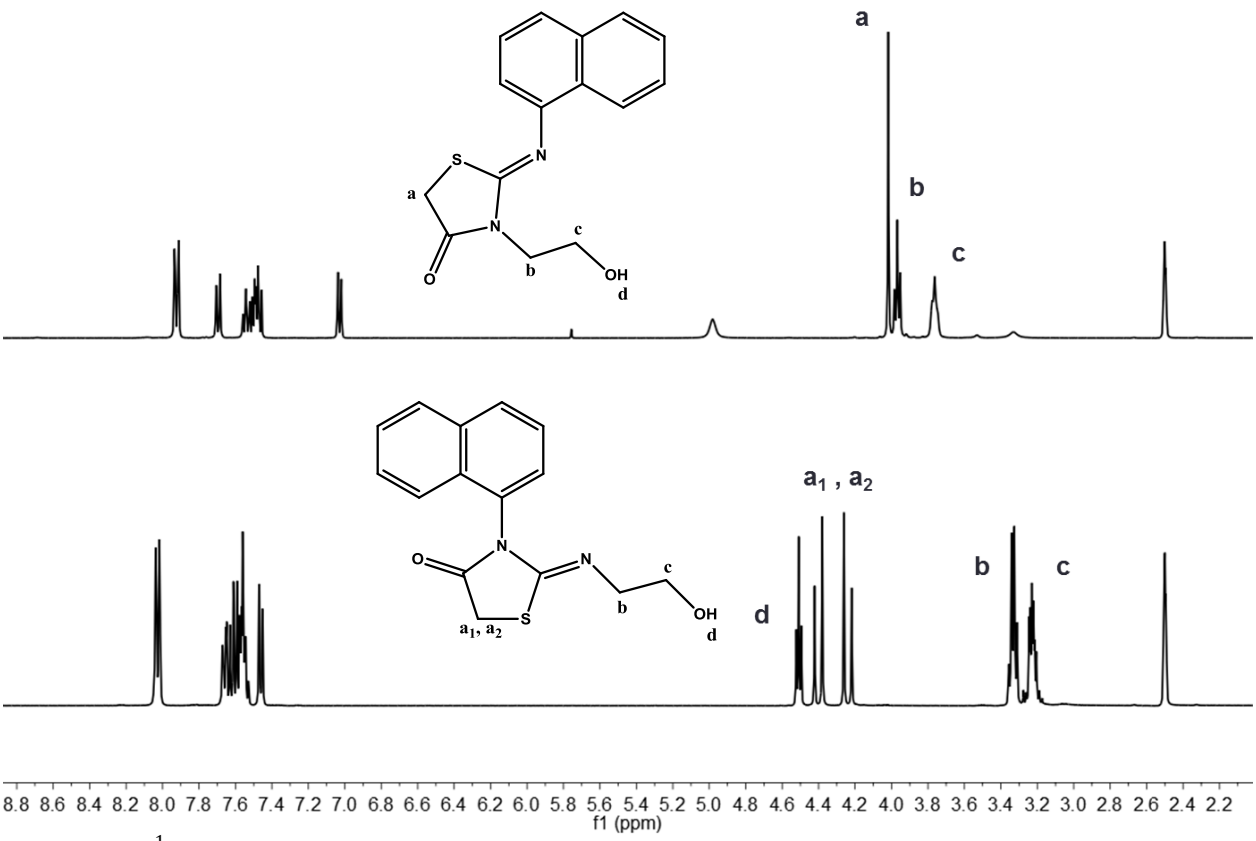


**Figure 3.1** $^{1}$H NMR of isomeric heterocycles. product **1a** is formed through the reaction at the alkyl-substituted nitrogen. **1b** forms in a similar manner through reaction at the aryl-substituted nitrogen. Peaks labeled **a** are assigned to the methylene group on the ring, **b** and **c** are the ethanol arm methylene groups, and **d** is the hydroxyl H.

The most significant aspect of this discovery was that we were able to switch which of the two isomers was the major product of the reaction by simply changing the amount of base and the solvent used. Furthermore, these reactions result in two products at most. Typically, when a compound with multiple nucleophilic centers is reacted with a compound with two electrophilic centers, a polymer mixture would be the expected result. These conditions are usually not synthetically useful. The crude NMR spectra of our reactions, however, indicate a simple mixture of two isomers with no other significant side products. We thought then that this reaction would be a useful route to the creation of a library of thiourea based heterocycles.

### 3.3 Structure Elucidation of Heterocyclic Isomers

Our first goal was to determine the structure of the isomers we had synthesized from naphthyl thiourea ethanolamine. **Figure 3.1** depicts the $^{1}$H NMR of the isomers, designated **1a** (top) and **1b** (bottom). Despite the similar structures, these two compounds have distinctly different spectra. The spectrum of **1a** is characterized by a singlet which can be attributed to the methylene that has been added to the thiourea from the haloacetyl halide. The equivalent group in **1b**, however, appears as a pair of doublets that are downfield shifted in comparison. In **1a**, the two methylene groups of the ethanol arm are found as two triplets in the vicinity of the singlet whereas in **1b** these methylene groups are the most upfield shifted and appear to have higher order splitting patterns.

The source of this dramatic difference in the two NMR spectra is a chiral center that is present in **1b**. In this structure, the naphthalene ring is unable to rotate due to the carbonyl on the neighboring five-membered ring. The rigid conformation and position on the naphthalene group causes the methylene of the five-membered ring to behave like a diastereomeric group, each hydrogen being split by the other. The naphthalene ring of **1a**, on the other hand, is an additional bond away from the equivalent methylene group, so it is unable to influence those hydrogens to the same extent. While the NMR spectra provide a clear way to tell the two products apart, they did not provide any conclusive structural information when viewed alone.

In order to better understand the structures, a series of 2D NMR experiments were run. First, the HSQC (Heteronuclear Single Quantum Correlation) experiment was run for each isomer, **1a** and **1b**. The heterocyclic products have three regional spin systems. The naphthalene group is isolated by the thiourea bond. There is a lone methylene group found on the heterocycle

that came from the bromoacetyl bromide and is further isolated by a carbonyl. Finally, the ethanol arm is on the far nitrogen of the thiourea. Additional structural information came from the subsequent HMBC (Heteronuclear Multiple Bond Correlation) experiment.

HMBC shows the association of one group to a group one or two bonds away. This leads to important connectivity information within a compound. At this point, we believed **1a** to be a five-membered ring closed through the two nitrogens of the thiourea due to the disappearance of the NH peaks. The pair of doublets in **1b** suggested a rigid structure, such as a six-membered ring, which could form if the ring closed through the alkyl nitrogen of the thiourea and the OH of the arm (**Figure 3.2**). HMBC spectra were taken in an effort to prove these hypothesized products (**Figure 3.3 and 3.4**). The HMBC of **1a** showed correlation between the methylene groups of the ethanol arm, **b** and **c**, with each other but not with the methylene of the heterocycle, **a**. That methylene, **a**, however, showed cross peaks with C=N and C=O. This pattern would fit with a five-membered heterocycle. The HMBC of **1b** shared a similar pattern of cross peaks, with a correlation between the heterocycle's methylene and the arm group notably absent, suggesting that **1b** was likely not a six-membered ring. The NMR experiments were not conclusive, however, which led us to attempt crystallization of the different compounds for single crystal x-ray crystallography.

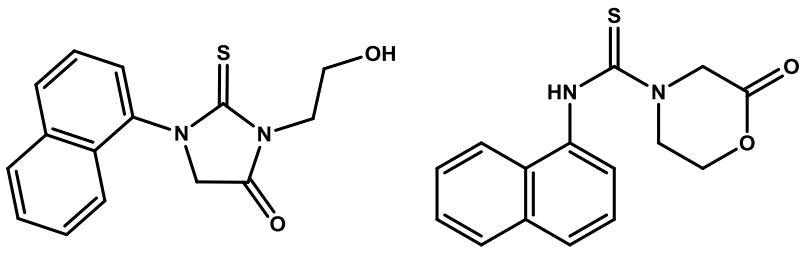


**Figure 3.2:** Possible heterocycles formed from the reaction of thiourea **1** and bromoacetyl bromide.

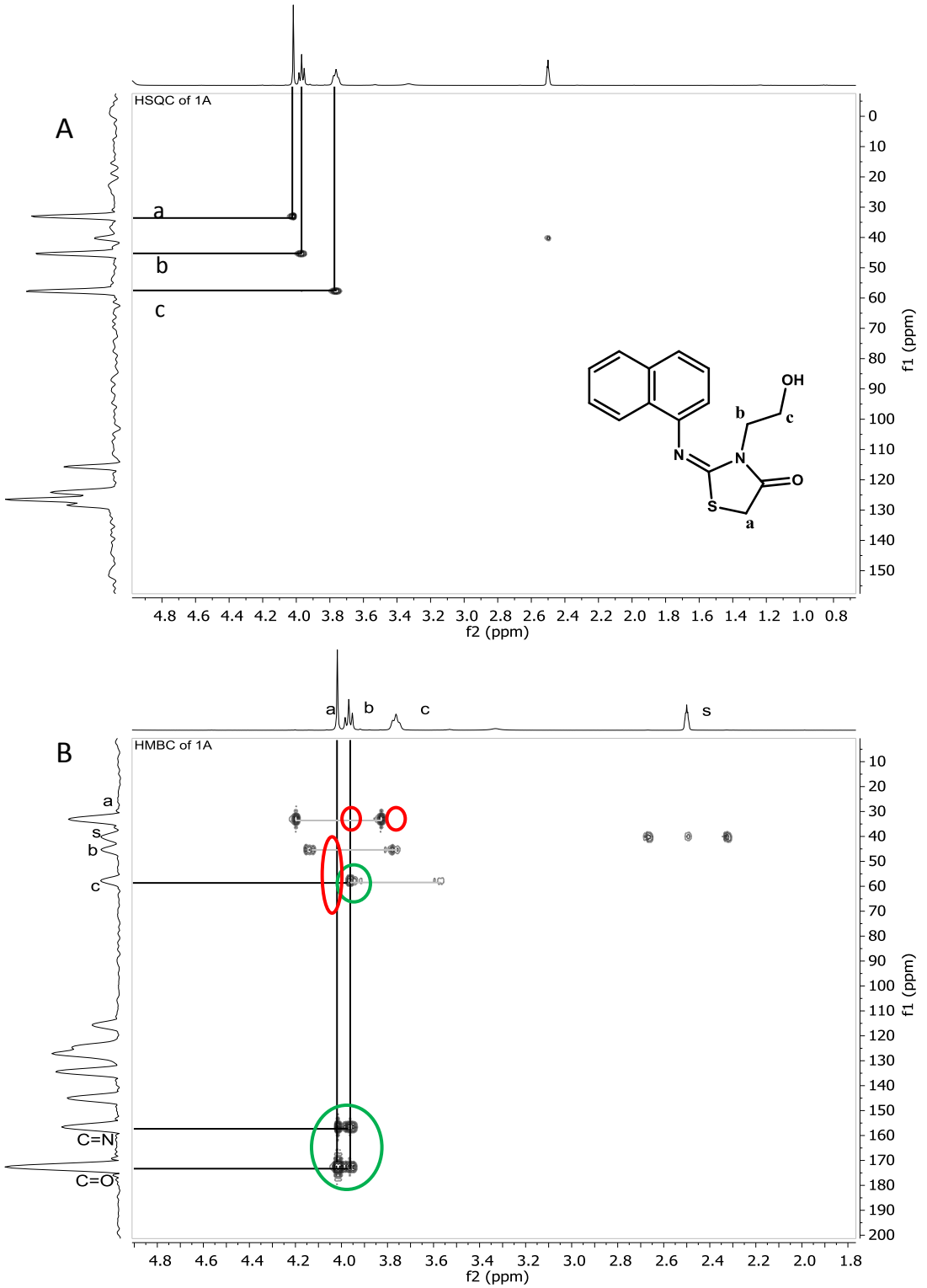


**Figure 3.3:** 2D NMR study of **1a**. (A) HSQC of **1a**. (B) HMBC of **1a**. The black lines indicate correlations between hydrogen types and other carbons. The gray lines indicate the peaks that correlate the hydrogens to the same carbon. Note that these peaks appear spaced evenly on either side of the hydrogen peak. Green circles indicate correlations we expect to see and red circles indicate correlations that are expected to be absent.

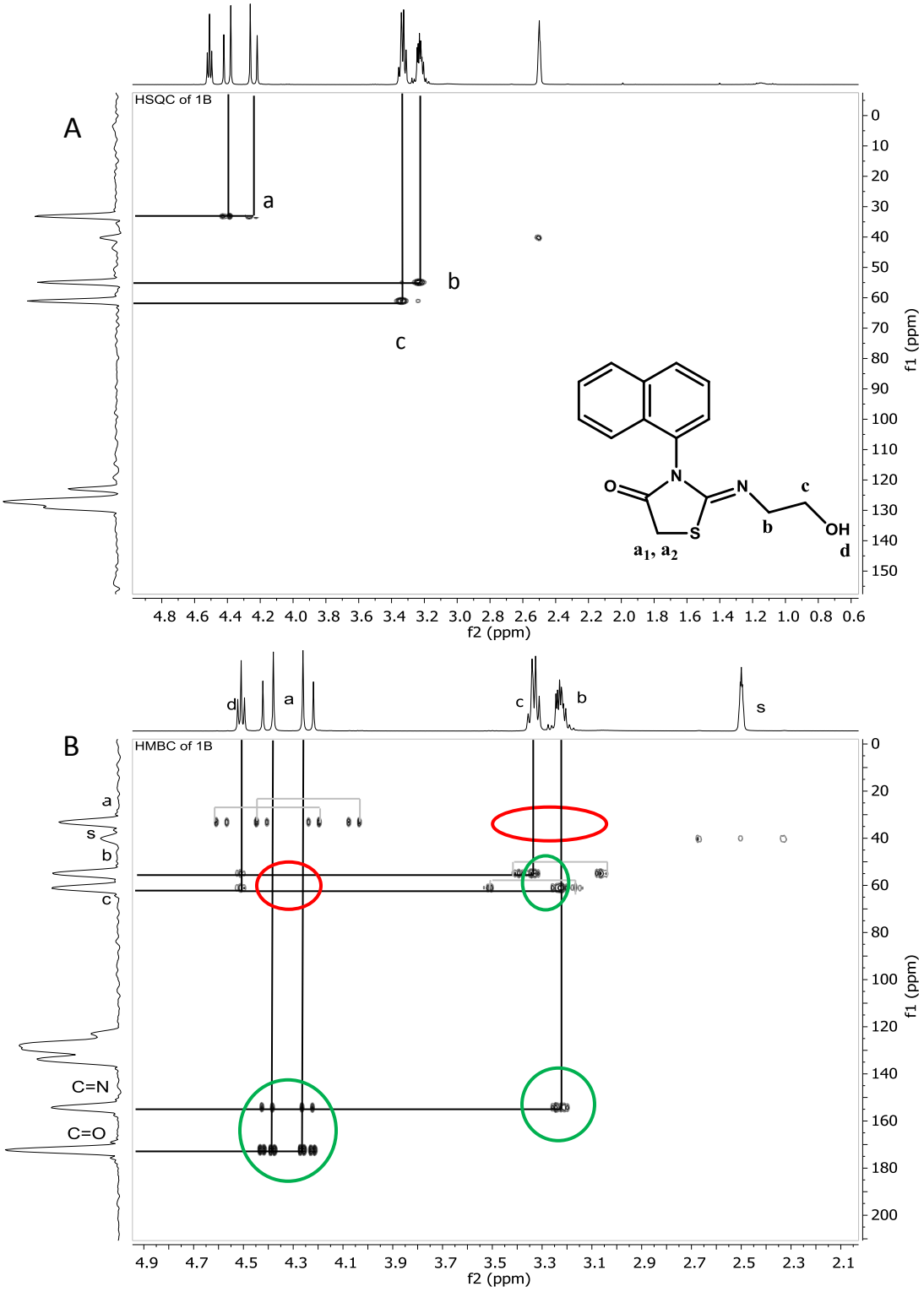


**Figure 3.4:** 2D NMR study of **1b**. (A) HSQC of **1b**. (B) HMBC of **1b**. The black lines indicate correlations between hydrogen types and other carbons. The gray lines indicate the peaks that correlate the hydrogens to the same carbon. Note that these peaks appear spaced evenly on either side of the hydrogen peak.

Three variants yielded successful crystal structures, which are shown in **Figure 3.5**.These crystal structures, obtained by Dr. Peter Zavalij of the University of Maryland, prove that the five-membered ring forms at the alkyl nitrogen and closes through the sulfur of the thiourea, resulting in an iminothiozolidinone. All products that followed this pattern, indicated by a singlet on NMR with upfield shifted aromatic peaks, were designated as **"a**" isomers." We then hypothesized that the second isomer was the product of ring formation from the aromatic nitrogen with closure through the sulfur to also form an iminothiozolidinone. These isomers were designated as "**b**" isomers and could be identified by the pair of doublets or the downfield shifted aromatic peaks.

It is important to note that the pair of doublets was seen in variants containing the naphthalene group but not the phenyl derivatives. The methylene group on the ring appears as two doublets in the naphthyl **b** rings because of the fixed orientation of the aryl group due to steric hindrance from the carbonyl, leading to a chiral C-N bond. This hindrance is absent in the **a** ring series. The p-phenyl thiourea cyclized products showed singlets for both the **a** and **b** isomers. This is because of the symmetrical nature of the ring. The phenyl derivatives were instead characterized by their aromatic peaks, which always appeared as two sets of doublets for each product.

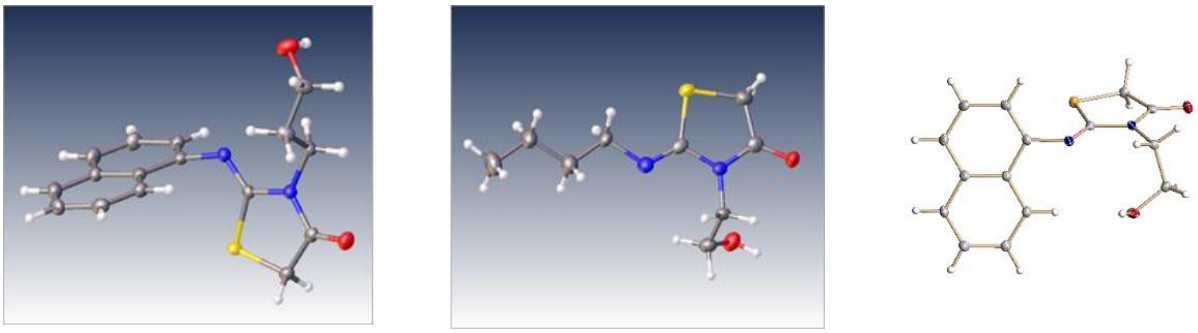

**Figure 3.5** Crystal structures of various products. **8a** (left), **5a** (middle), and **1a** (right). Nitrogens are shown in blue, oxygen in red and sulfur in yellow. Structures were solved by Dr. Peter Zavalij from the University of Maryland.

### 3.4 Library Formation

After the initial discovery of the formation of two different heterocycles, we wanted to explore the versatility of this reaction and the possible products that could be formed. We began by building a library of thioureas to be used as precursors. **Scheme 3.3** shows the general reaction between different isothiocyanates with various amines to form a thiourea. We used the naphthyl thiourea ethanolamine precursor as the base for variations.

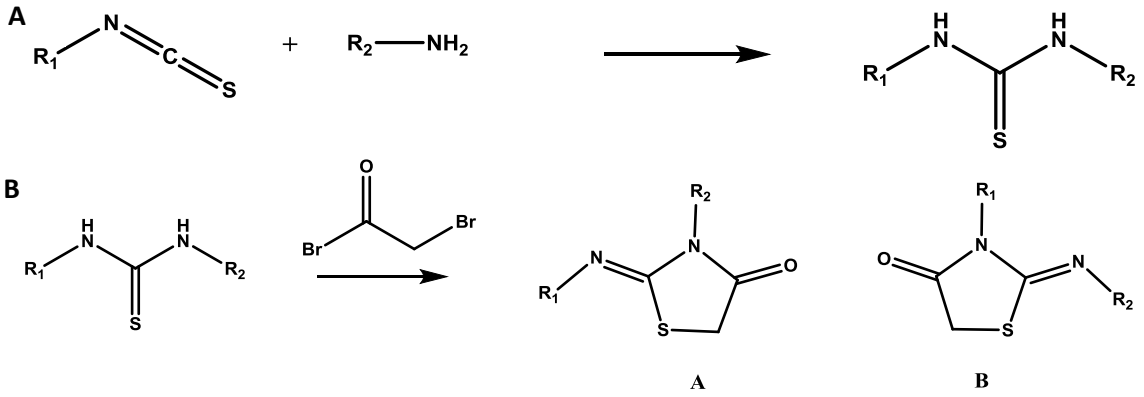


**Scheme 3.4:** Generalized scheme for the formation of thioureas and iminothiozolidinones. **A** shows the reaction to form thiourea. **B** shows the reaction to form the two isomers.

We first varied the aromatic group present while keeping the ethanolamine arm. We also made a variant with a butyl chain instead of an aromatic group. Next, we kept the use of naphthyl isothiocyanate constant and we varied the arm groups by introducing branching or lengthening the alkyl chain while keeping the alcohol function, or by removing the alcohol function by using a straight alkyl chain. A summary of these thioureas is shown in **Figure 3.6**.

All of these products could be purified by recrystallization or aqueous work up with 0.1 M HCl.. We later determined that the reaction went to completion after four hours at room

temperature and could be used without further purification (reactions monitored by NMR, not shown).

One of the reasons we chose to explore this set of reactions was the fact that we could control the reaction with base or solvent to favor one of the products over the other. For the isomer library synthesis, we decided to use the conditions that favored the **b** isomer formation. We did not want to limit the product formation to one isomer, and we felt that the **b** isomer would be the more biologically and synthetically interesting product of the two. All reactions were initially run in THF with 1 mol eq of $Et_3N$ at room temperature. Every thiourea formed the **a** isomer in yields ranging from 28% to 78%. All thioureas also formed the **b** isomer except for **4** (p-methoxyphenyl derivative). Of the ethanol arm derivatives, p-nitrophenyl thiourea formed **a** as the minor product (28%) and **b** as the major product (69%) at room temperature. The rest formed **b** as the minor product or in a similar yield to **a**. Interestingly, for the derivatives that used the propyl arm, **b** was the major product with only small amounts (~10%) of **a** produced. These structures are shown in **Figure 3.7**.

After the initial reaction, two reactions were chosen for further optimization—those that used precursors **1** and **2.** First, naphthyl thiourea ethanolamine was reacted with bromoacetyl bromide in DCM (with 2 eq of $Et_3N$). These two changes results in a yield of 67% for the **a** isomer. When the same thiourea was reacted in THF, the **b** isomer was formed in 63% yield. These two reactions demonstrate that through a minor change to reaction conditions (solvent and relative amount of base), the major product can be switched to favor either isomer.

We also compared the product distributions of the p-bromophenyl thiourea ethanolamine (**2**) reactions at two different temperatures. The first reaction was at room temperature and the second was at -78°C. Both were in THF with 1 mol eq of $Et_3N$. **Figure 3.8** shows the results of

this temperature study. The difference in product ratios is clear, with the room temperature reaction giving 1:2 (**b:a**) and the -78°C reaction giving a 10:1 (**b:a**) distribution. In this case, the only change was in temperature, rather than solvent or base. These experiments prove the ability to tune the product formation through simple adjustments to reaction conditions which we believe lend a greater synthetic usefulness for this reaction pathway.

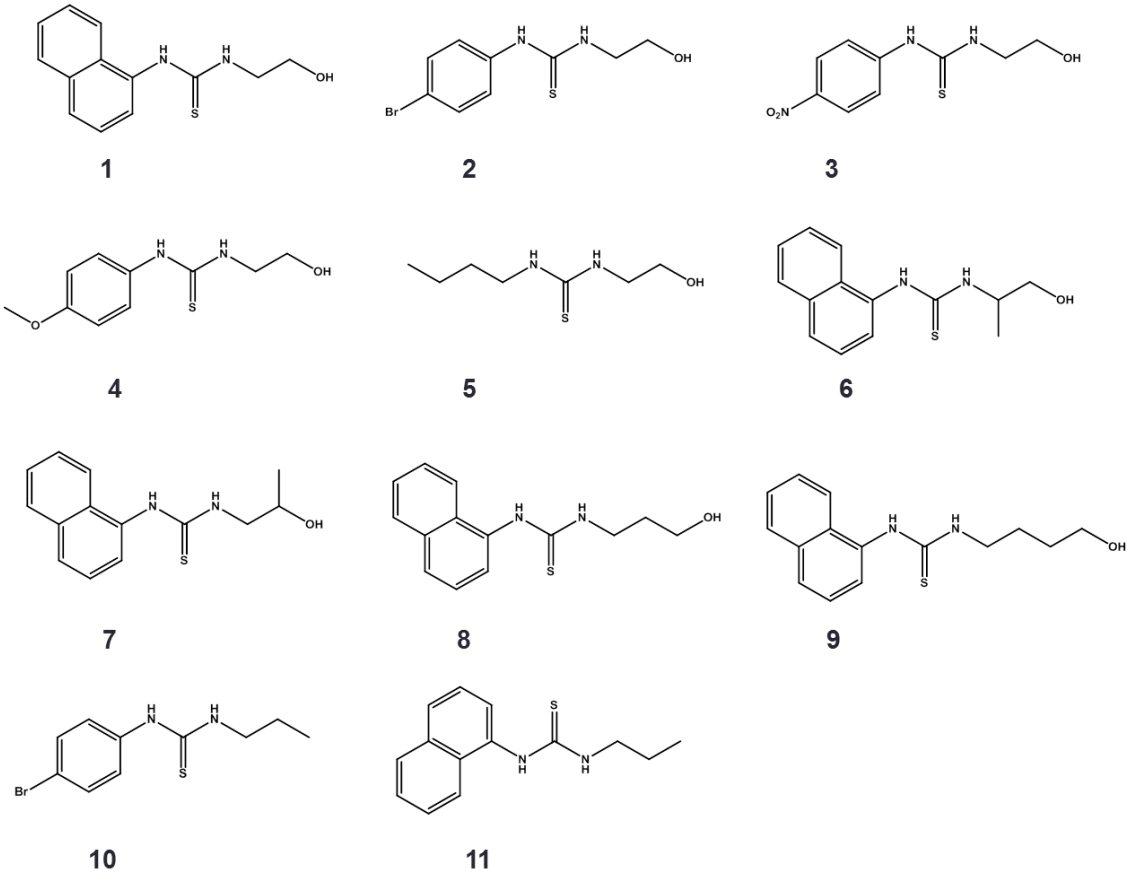


**Figure 3.6**: Library of synthesized thioureas.

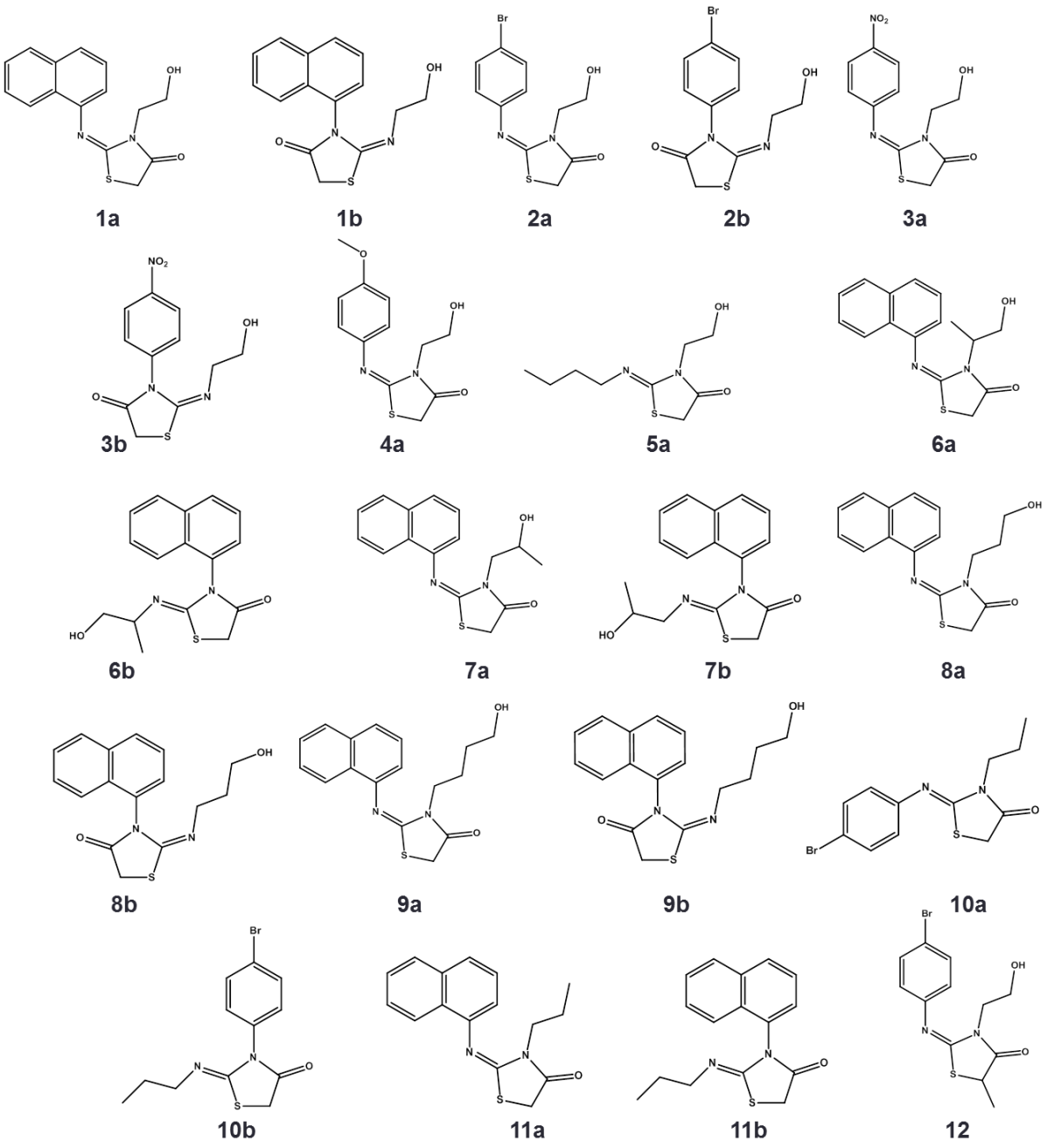


**Figure 3.7**. Library of iminothiozolidinone products formed from thiourea precursors.

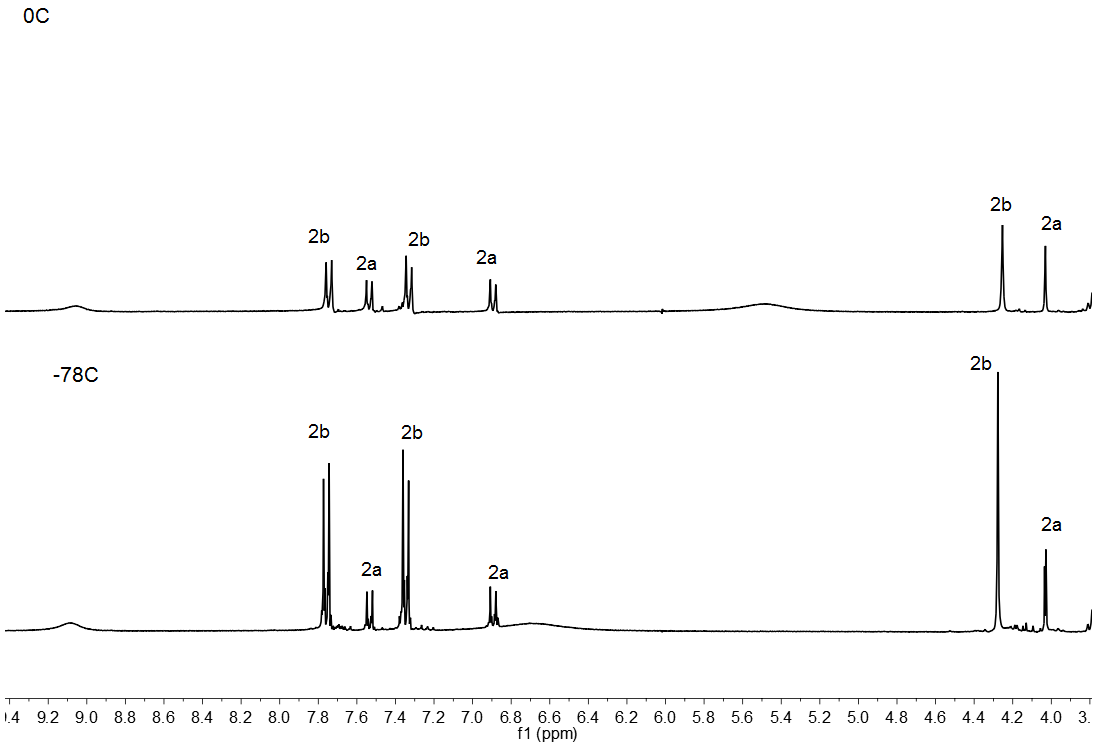


**Figure 3.8:** $^{1}$H NMR study comparing the effects of temperature on ring formation. **Top** panel shows the 0°C crude reaction, where a nearly 1:1 (**a:b**) is observed. The additional peaks in the aromatic region can be attributed to left over starting thiourea as well as a small amount of the decyclization product. The **bottom** panel is the -78°C crude mixture.

### 3.5 The Effects of Solvent and Temperature on Product Distribution

The discovery of **1a** came about from an attempt to synthesize the full thiourea arm for the cyclen receptor. The reaction was run in DCM with $Et_3N$ (2 eq) with the belief that an ester would form. When this product was not seen, the reaction conditions were adjusted, leading to the formation of **1b**. Following this realization, we wanted to explore the effects of solvent on the reaction. A series of reactions was conducted using the following conditions: **1** was dissolved in the chosen solvent and $Et_3N$ (1 eq) was added. Bromoacetyl bromide (1 eq) was added, and the reaction was stirred at room temperature for six hrs. The solvent was removed and the crude was dissolved in DCM and washed with sodium bicarbonate. The crude NMR of each reaction was

taken. The solvents chosen were acetone, acetonitrile, THF, ethyl acetate, DCM, and benzene. All solvents were aprotic and of varying polarities. All but DCM and benzene were capable of acting as hydrogen bond acceptors. **Figure 3.9** shows that there is a distinct difference in the product distribution of isomers formed in the different solvents. Both isomers are present in all of the reactions, but acetonitrile and THF favor **1b** considerably, acetone, ethyl acetate and DCM show some preference for **1b**, and benzene shows a near equal formation of the two products. The integrations of relevant peaks and calculated product ratios are shown in **Table 3.1**.

We hypothesized the hydrogen bonding capability with the alcohol arm was a driving force in the differences we observed. To test this, we ran the same series of reactions using the naphthyl propyl thiourea (**11**). The results of these experiments are shown in **Figure 3.10** and **Table 3.2**. **11b** is the major product in each reaction with close to a 90% **b** to 10% **a** yield seen in each reaction. This clearly demonstrates the importance of the auxiliary arm group in the formation of these iminothiozolidinones.

We next decided to explore the effect of the arm in controlling the reaction at different temperatures. As we noted before, the reaction of p-bromophenyl thiourea (**2)** at room temperature favored the formation of **2a** while the reaction at -78°C favored **2b**. We propose that intramolecular hydrogen bonding between the terminal alcohol and the alkyl nitrogen of the thiourea is able to form to a greater extent at the cold temperature. This hydrogen bond leads to the formation of a stable five-membered ring. The alkyl site is effectively blocked through this interaction, resulting in reaction at the aryl position. As the temperature is increased to 20°C, the solvent (THF) overcomes this complex to form an intermolecular bond. This frees the alkyl position, which we have observed to be the favored nucleophilic center in this thiourea.

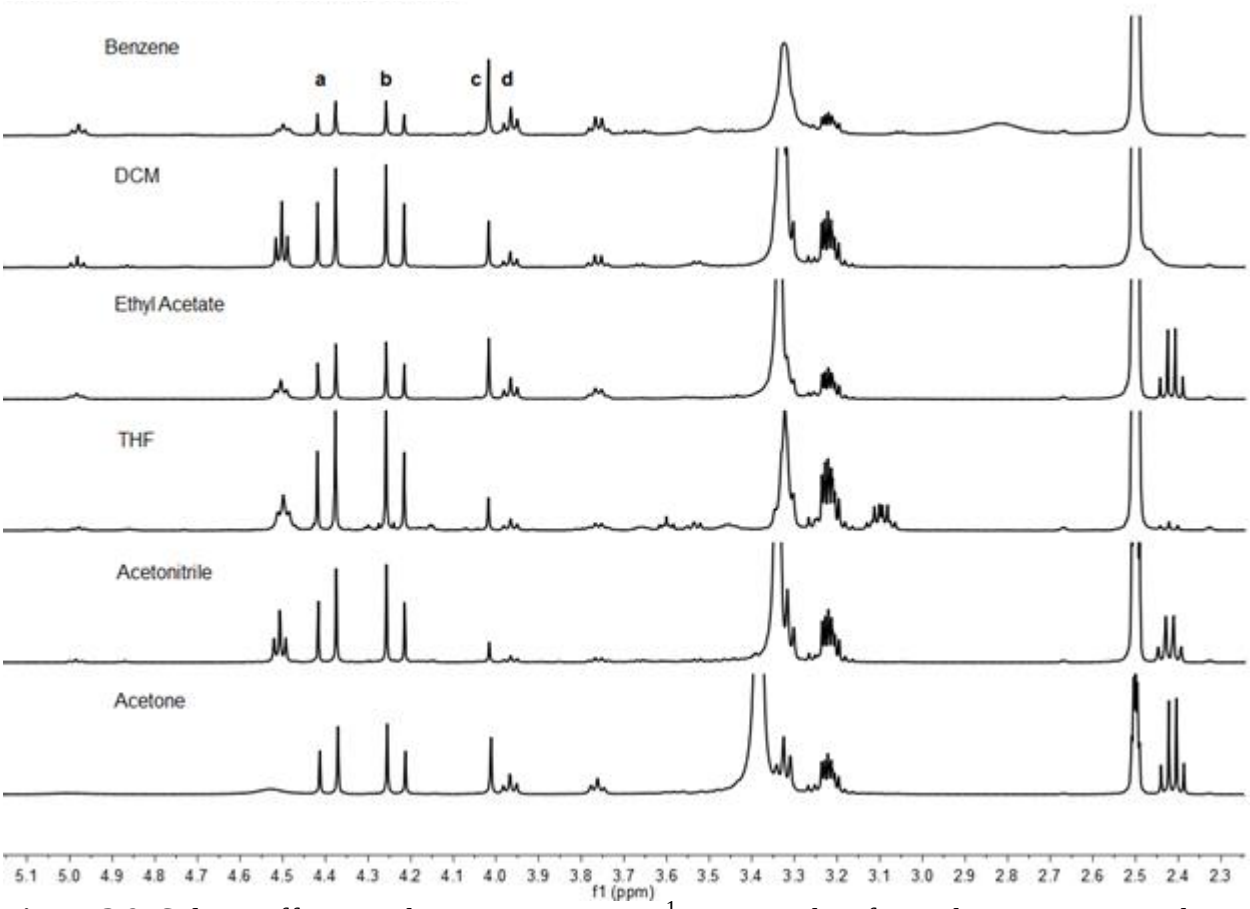


**Figure 3.9**: Solvent effects on thiourea **1** reactions. $^{1}$H NMR taken for each reaction run in the solvent indicated. All other reaction conditions were kept the same. Peaks **a** and **b** are from the $CH_2$ of the ring of isomer **1b**, peak **c** is the $CH_2$ on the ring of isomer **1a** and peak **d** is the $CH_2$ closest to the nitrogen on the arm of **1a**.

**Table 3.1:** Comparison of isomers formed from the reaction of thiourea **1**.

| **Solvent** | **Integration** | | | | |
|---|---|---|---|---|---|
| | a (CH) | b (CH) | c ($CH_2$) | d ($CH_2$) | Ratio (**1b:1a**) |
| Acetone | 1.00 | 0.97 | 0.55 | 0.56 | 4:1 |
| Acetonitrile | 1.00 | 0.98 | 0.18 | 0.17 | 12:1 |
| THF | 1.00 | 1.04 | 0.19 | 0.22 | 9:1 |
| Ethyl Acetate | 1.00 | 0.97 | 0.71 | 0.76 | 3:1 |
| DCM | 1.00 | 1.00 | 0.34 | 0.36 | 5.5:1 |
| Benzene | 1.00 | 0.92 | 1.20 | 1.33 | 1.5:1 |

The peak assignments are shown in the NMR (**Fig. 3.7**). Note that **a** and **b** both represent CH's whereas **c** and **d** both represent $CH_2$'s. The ratio of isomers was calculated using peaks **a** and **d**.

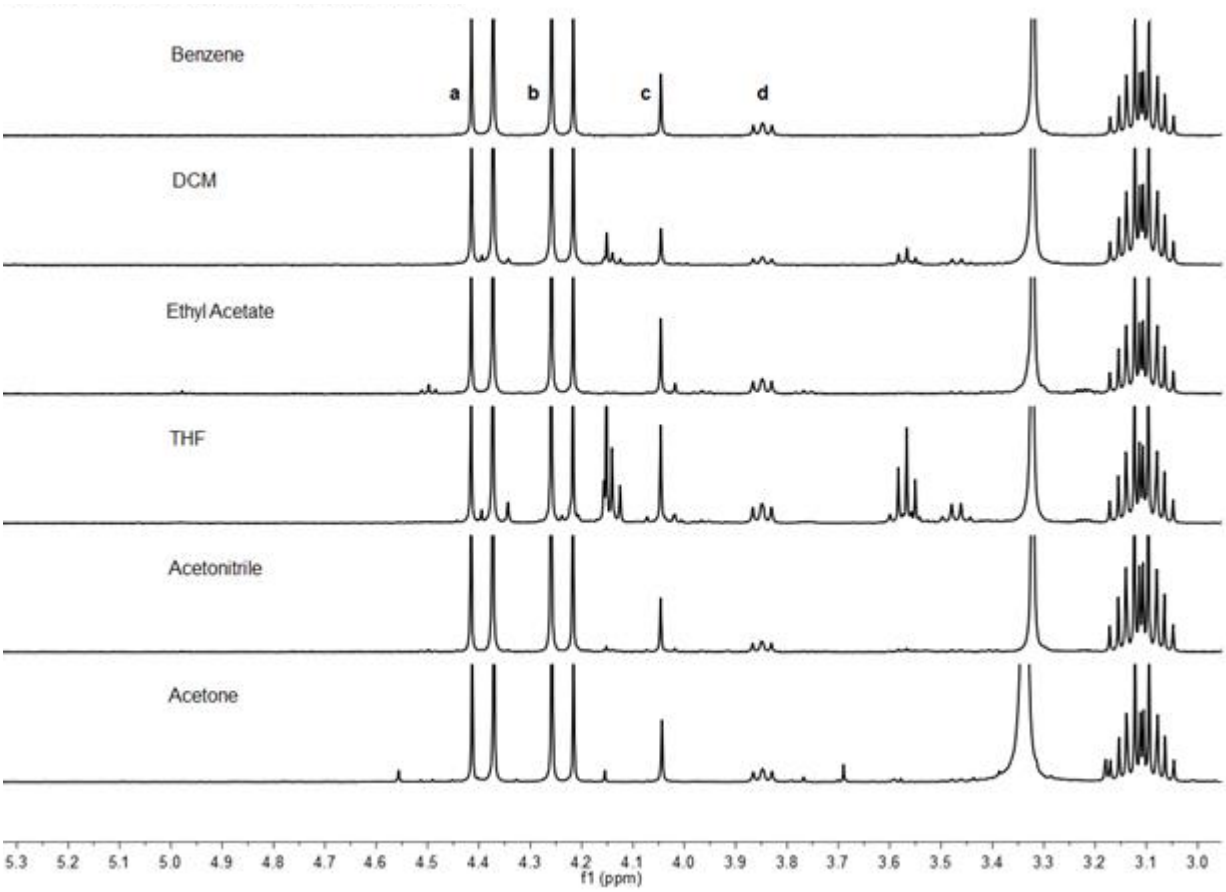


**Figure 3.10**: Solvent effects on thiourea **11** reactions. $^{1}$H NMR taken for each reaction run in the solvent indicated. All other reaction conditions were kept the same. Peaks **a** and **b** are from the $CH_2$ of the ring of **11b**, peak **c** is the $CH_2$ on the ring of **11a** and peak **d** is the $CH_2$ closest to the nitrogen on the arm of **11a**.

**Table 3.2:** Comparison of isomers formed from the reaction of thiourea **2**.

| **Solvent** | **Integration** | | | | |
|---|---|---|---|---|---|
| | a (CH) | b (CH) | c ($CH_2$) | d ($CH_2$) | Ratio (**11b:11a**) |
| Acetone | 1.00 | 0.98 | 0.19 | 0.20 | 10:1 |
| Acetonitrile | 1.00 | 1.00 | 0.15 | 0.17 | 12:1 |
| THF | 1.00 | 1.07 | 0.28 | 0.29 | 7:1 |
| Ethyl Acetate | 1.00 | 0.97 | 0.22 | 0.24 | 8:1 |
| DCM | 1.00 | 0.99 | 0.12 | 0.14 | 14:1 |
| Benzene | 1.00 | 0.96 | 0.24 | 0.26 | 8:1 |

The peak assignments are shown in the NMR (**Fig. 3.8**). Note that **a** and **b** both represent CH's whereas **c** and **d** both represent $CH_2$'s. The ratio of isomers was calculated using peaks **a** and **d**. Based on the integrations and assuming the reaction went to completion, the average product distribution is 91% **11b** and 9% **11a**.

Bromophenyl propyl thiourea is not capable of forming this hydrogen bonded complex in either case, therefore we expected that the reaction of **10** at 20°C and -78°C would result in the same product ratio. This is indeed the result that we observed, shown in **Figure 3.11**. It is interesting to point out that **12b** is the major product at either temperature with very little of **12a** present.

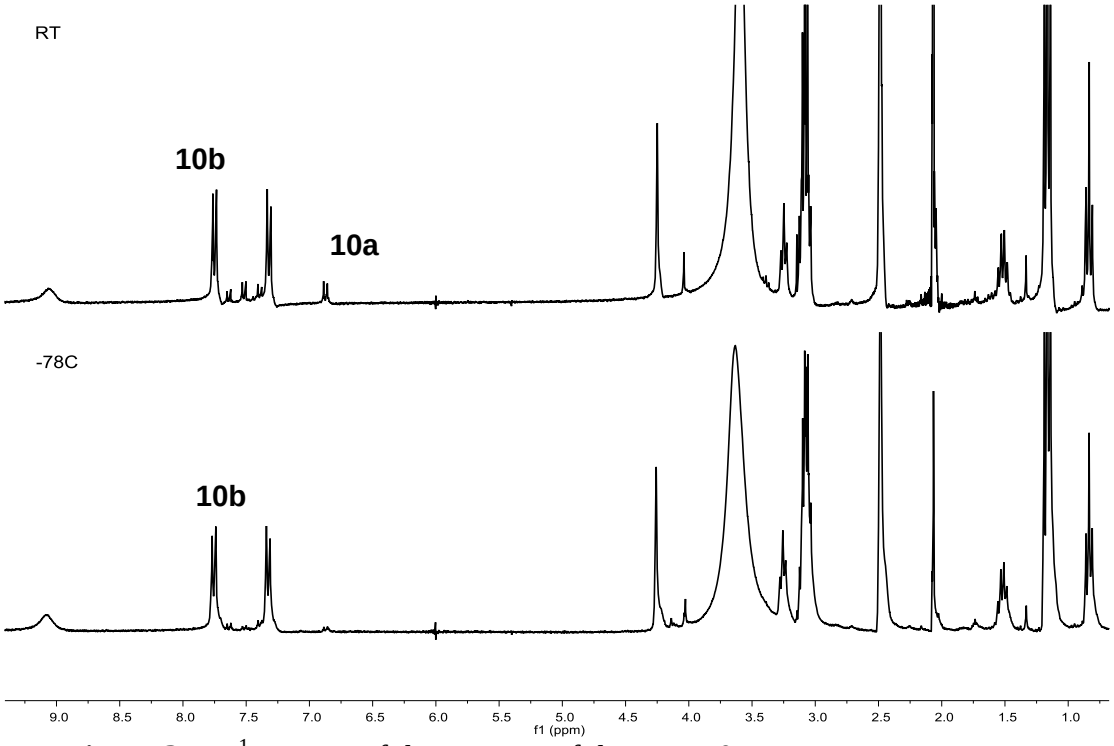


**Figure 3.11:** $^{1}$H NMR of the reaction of thiourea **10** at various temperatures.

Following the exploration of the mechanism of the iminothiozolidinone reaction, we moved forward to demonstrate that these products were stable by subjecting them to reflux conditions. **1a** was heated to 65°C in THF in the presence of HCl. The NMR (**Figure 3.12**) shows no change in the product, showing that this ring is stable and does not interconvert to **1b**. When **1b** was treated in the same manner, a change was observed. The product isolated from this reaction was not conversion to **1a** but a new product entirely **(Figure 3.13**).

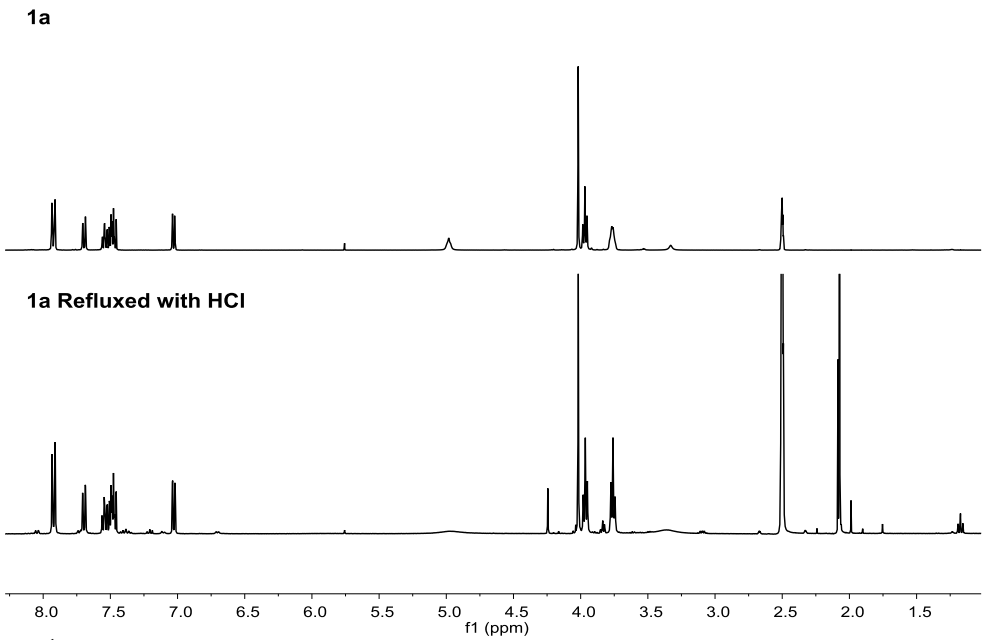


**Figure 3.12**: $^{1}$H NMR of the treatment of **1a** with HCl. The ring was dissolved in acetonitrile and HCl was added to reach a pH of 3. The reaction was heated to 65°C for 24 hours. The NMR taken was of the crude reaction. ESI MS confirms lack of any product present.

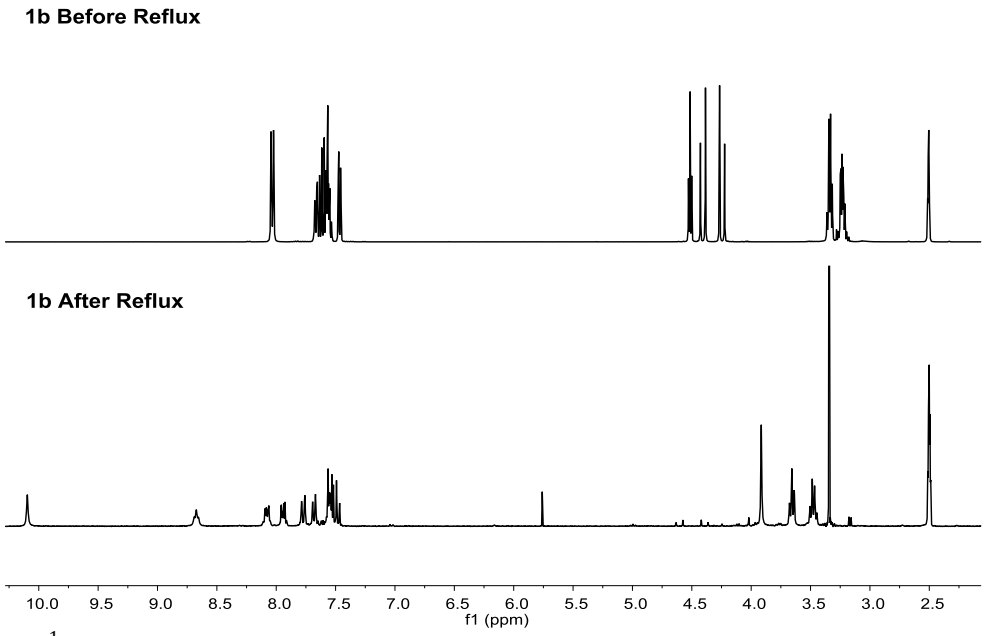


**Figure 3.13**: $^{1}$H NMR comparing **1b** before and after refluxing with HCl. Both NMRs were taken after purification of the products. The characteristic doublets, present before heating with HCl, disappear and a new singlet forms. There are also noticeable changes in the aromatic region.

### 3.6 Enthalpy vs Entropy Control of Product Formation

In 1944, Woodward and Baer studied the difference in products formed in the Diels-Alder reaction of maleic anhydride and 6,6-pentamethylenefulvene.[106] They found that both the endo and exo products formed to different extents depending on the reaction conditions. Around the same time, Catchpole, Hughes and Ingold explored in depth the similar phenomenon in the nucleophilic substitution of allylic halides.[107] While observations of differences in product distributions had been made by Meisenheimer et al as early as 1930[108], it took a number of years for the concept of thermodynamic versus kinetic control of reactions to be established in main stream chemistry.[109] Since then, the ability to control product formation by selecting conditions that favor the kinetic or thermodynamic product has been widely used in synthesis.[110] In general, the kinetic product is the product that forms due to the pathway having a lower energy barrier, compared to the thermodynamic product, which may have a higher energy barrier but leads to a more stable product. Temperature and reaction time can be used to favor isolation of one product over the other. One of the requirements in this system is the ability of these two products to interconvert from a reversible step.

The lack of conversion between the two isomers means that there is no thermodynamic product in our system. Instead, the kinetic product is always formed. At -78°C, the reaction is under entropy control. This is due to the fact that an intramolecular H-bond is able to effectively block the alkyl nitrogen through the formation of an exceptionally stable five-membered ring (**Figure 3.14A**) This results in a loss of entropy, but the formation of the ring at the aryl-N position, which is favored under these conditions, makes up for this loss. At higher temperatures, the reaction is under enthalpy control. At 20°C, the H-bonding between the OH of the arm and the solvent dominates, leaving both nitrogen positions exposed. The reaction takes place at the

alkyl-N, forming the **a** isomer and resulting in a greater release of energy than if the **b** isomer formed, due to the extension of the conjugated system (**Figure 3.14B**). When the thiourea with a propyl arm (**10**) is used instead, there is no formation of the H-bond at either temperature (**Figure 3.14C**), therefore we see the similar composition of products at both 20°C and -78°C (**Figure 3.11**).

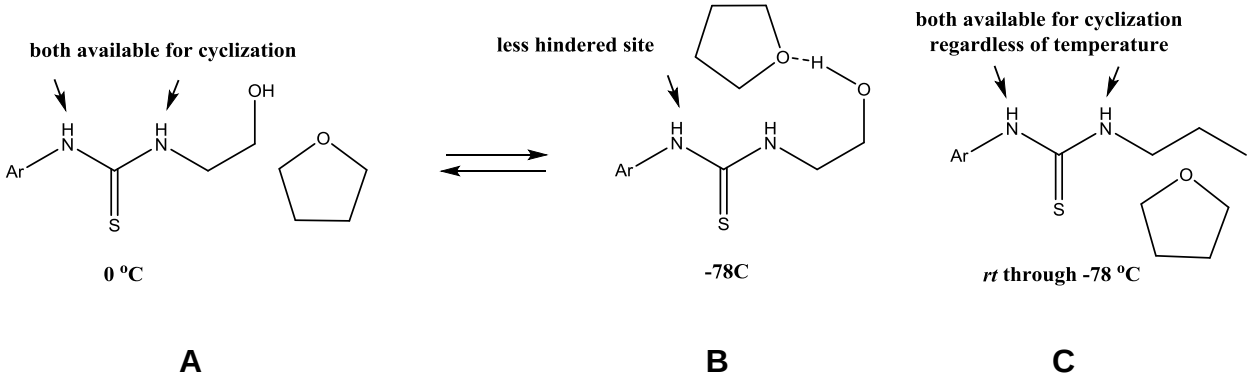


**Figure 3.14:** Depiction of temperature effects on the cyclization of functionalized *p*-bromophenyl thioureas. **(A)** Thiourea **1** at 0°C, **(B)** the same thiourea at -78°C and **(C)** thiourea **11** at either temperature. The arrow indicates the favored nucleophilic position.

While it is common perception that nitrogens of aliphatic amines are more nucleophilic than those of anilines, it might not be necessarily true in the case of thiourea nitrogens. Whereas the aromatic amines exhibit lower nucleophilicity due to the delocalization of lone pair of nitrogen into the aromatic ring, both nitrogens in thiourea are already $sp^2$ hybridized due to the resonance with thiocarbonyl moiety (**Figure 3.15**). We have found that cyclic voltammetry is a promising way to establish relative affinity of thioureas to an electron, which might serve as an estimate of relative nucleophilicity for the compounds with similar sterics (**Figure 3.16**).

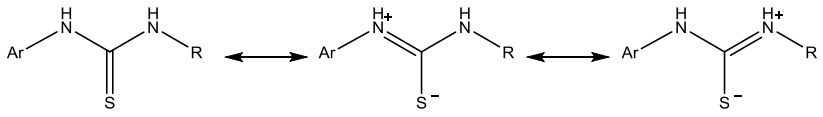

**Figure 3.15:** $sp^2$ hybridization of aliphatic and aromatic nitrogens in thioureas due to the resonance delocalization of lone pairs.

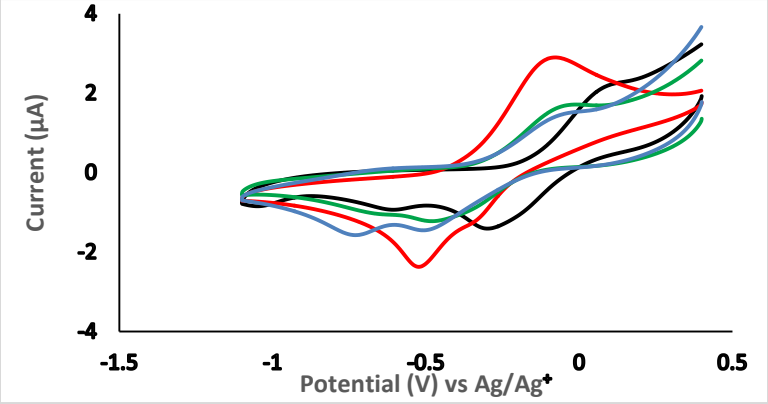


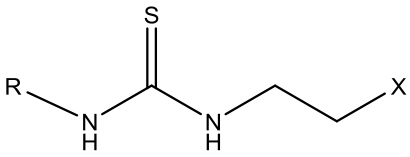


**1** R = 1-naphthyl, X = OH
**2** R = *p*-bromophenyl, X = OH
**5** R = butyl, X = OH
**11** R = 1-naphthyl, X = $CH_3$

**Figure 3.16:** Cyclic Voltammetric Study of Nucleophilicity of Various Thioureas. **A.** Cyclic voltammetric response on gold electrode of 1 mM THF solution of butyl ethanolamine thiourea **5** (red line), naphthyl ethanolamine thiourea **1** (green line), naphthyl propylamine thiourea **11** (blue line), bromophenyl ethanolamine thiourea **2** (black line) and 0.1 M $TBAPF_6$. Scan rate: 0.1V/s. **B.** Structures of compounds used in cyclic voltammetry.

Four compounds used to validate the applicability of cyclic voltammetry to study of relative affinity of thiureas to electrons differ in the following way: an aliphatic thiourea **5** was supposed to have two nitrogens of similar nucleophilicity and was used as a reference compound. Two naphthyl thioureas **1** and **11** were different in the terminal group X: whereas thiourea **1** was triply nucleophilic due to the presence of an OH group, the thiourea **11** was terminated with an inert methyl group. Finally, bromophenyl thiourea **2** was different from **1** by the electron withdrawing nature of its aromatic moiety. The reduction and oxidation potentials for compounds **1**, **5** and **11** were very similar (the reduction was observed at -0.5 V, and oxidation was observed at – 0.07 V), however the corresponding potential for compound **2** were quite different (-0.34 V for reduction and 0.11 V for oxidation). These observations suggest the following: 1) relative affinity of compounds **1**, **5** and **11** to an electron was very similar; implying similar effects of alkyl and 1-naphthyl groups, as well as negligible influence of an OH auxiliary; 2) significantly higher affinity of compound **2** to an electron was observed, which is in line with its relative electron deficiency.

### 3.7 A Novel Nucleophile-Assisted Decyclization of Iminothiozolidinones

During the study of the effect of temperature as a means of control, we discovered an additional reaction taking place. **1b**, when treated with a nucleophile under acidic conditions at reflux, underwent a decyclization that resulted in the conversion of iminothiozolidinone into aminooxoethylcarbamothionate. **2b** also reacted in a similar fashion and the crystal structures of these two are shown in **Figure 3.17.**

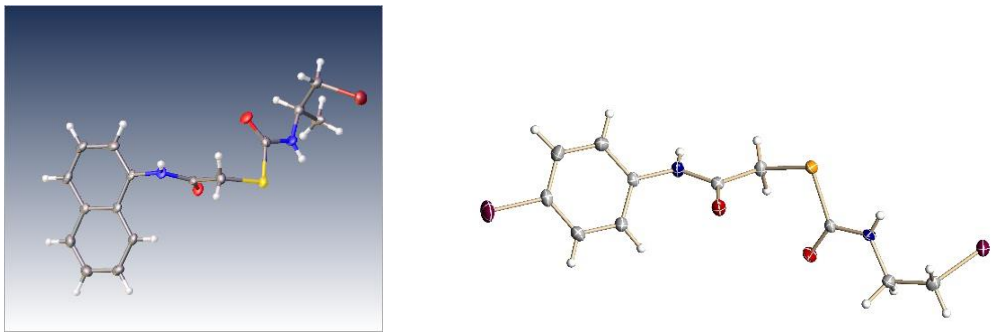

**Figure. 3.17**: Crystal structures of various decyclization products. **15** (left) and **16** (right) Nitrogens are shown in blue, oxygen in red, and sulfur in yellow. These structures were solved by Dr. Peter Zavalij of the University of Maryland.

The decyclization was first observed when the crude reaction mixture of bromophenyl ethanolamine thiourea **2** formed at -78°C was heated to 65°C. The NMR shows a loss of the pair of doublets and the emergence of a singlet in their place. Additional changes to the aromatic peaks can be seen. This NMR was also different from that of **2a**. MS (ESI) and crystal structures confirm that the following reaction took place: Substitution of the auxiliary alcohol by the nucleophile, bromine, triggered the decylization of the iminothiozolidinone. The intermolecular nucleophile, OH, attacks the electrophilic carbonyl center, leading to an opening of the ring and subsequent loss of the parent thiourea scaffold. This reaction requires an external nucleophile, in this case from the triethylammonium bromide formed during the previous step, as well as $H^+$ from an acidic medium. For reasons stated previously, there was only one equivalent of base

used, leading to an excess of acid in the final crude mixture. The proposed mechanism is shown in **Scheme 3.5. Scheme 3.6** shows all of the decyclized products that have been synthesized in a similar manner.

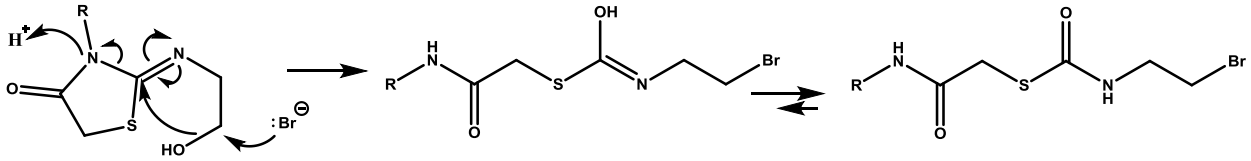

**Scheme 3.5**: Proposed termolecular mechanism for decyclization of iminothiozolidinones. Note that this mechanism involves a cascade of steps, with no intermediate being observed.

**13** R = Naphthyl, X = Br, Z = H
**14** R = Naphthyl, X = Cl, Z = H
**15** R = Naphthyl, X = Br, Z = $CH_3$
**16** R = p-Br-ph, X = Br, Z = H

**Scheme 3.6:** Formation of different decyclization products. The general reaction involved dissolving the ring in acetonitrile or THF and adding enough HBr or HCl to achieve a pH of 3. The reaction was heated to 65°C for 4-6 hrs. Products may also be formed by heating up the crude ring formation reaction in certain conditions.

This reaction is an example of a termolecular mechanism. It is dependent on the external nucleophile as well as the internal nucleophile found on the arm. We attempted to prove this through a control experiment using bromophenyl thiourea propylamine **11b**. The crude reaction to form this compound was treated to the same reflux conditions with the addition of water and the reaction was monitored by NMR before and after reflux. **Figure 3.14** shows that there was no significant change in the compound after reflux, illustrating the role of the pendant OH in the decyclization. This group must be present in the compound to undergo decyclization. The presence of an internal nucleophile is required so that the reaction relies one the attack of only the external nucleophile to begin. It is interesting that the series of **b** isomers will undergo this

cyclization, but ethanolamine-based **a** isomers tested, no decyclization was observed by NMR (**Figure 3.18**) or MS.

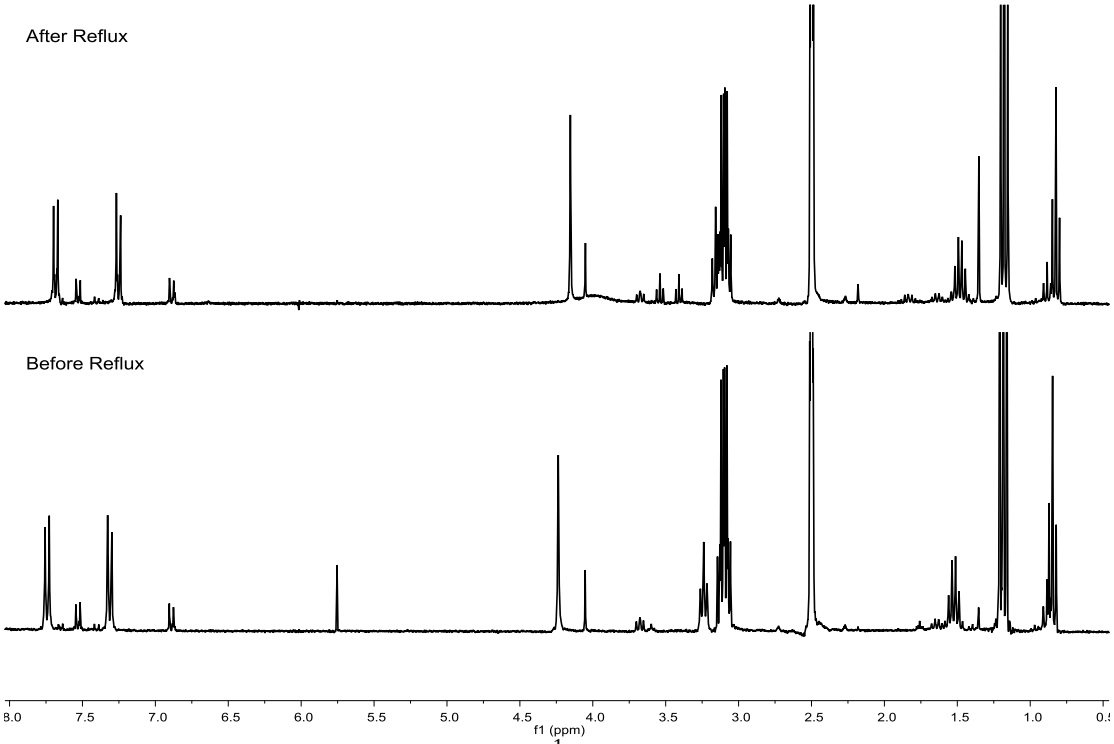


**Figure 3.18**: Reflux of **10b** ring crude reaction. $^{1}$H NMR comparing the mixture before and after reflux in the presence of HBr. A small amount of water was added to show that the OH source must be intramolecular. The NMR indicates that no significant change took place, suggesting the ternary molecular mechanism takes place. This also shows lack of interconversion between the two isomers.

The proposed mechanism is believed to be correct based on several observations. First, the –OH group must be present on the molecule, it cannot come from external conditions, as shown in Figure 3.18. Next, the reaction requires an acidic environment, which was proven when the same reaction was run using 3 equivalents of triethylamine instead of 1, resulting in no formation of the decyclized product. Finally, additional mechanisms were considered following some helpful discussions with Dr. Hartman. (**Scheme 3.7**), but ultimately it was the lack of a discernible intermediate that led to the final proposed mechanism.

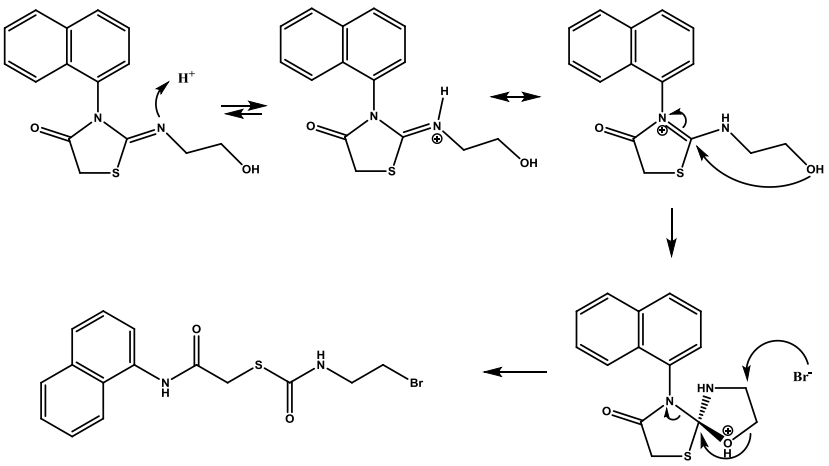

**Scheme 3.7.** Alternative possible mechanism for the decyclization reaction.

The mechanism we have proposed could be drawn in a step-wise fashion, as shown in **Scheme 3.8**, however this too was not selected due to the formation of an intermediate. If this was the reaction pathway, the intermediate is the same for both **a** and **b,** which would mean both rings form the same product, or lead to the degradation of **a**. However, several experiments contradict this finding. The treatment of **1a** with HCl and heat leads to no change in the ring, and if **Scheme 3.8** was accurate, this reaction of **1a** should have led to the formation of **14**. An experiment in which a mixture of **2a** and **2b** were heated in the presence of HBr resulted in the loss of all of **2b** to form the decyclized product, but none of **2a** reacted. These observations, when taken together, led us to proposed the mechanism in **Scheme 3.5**.

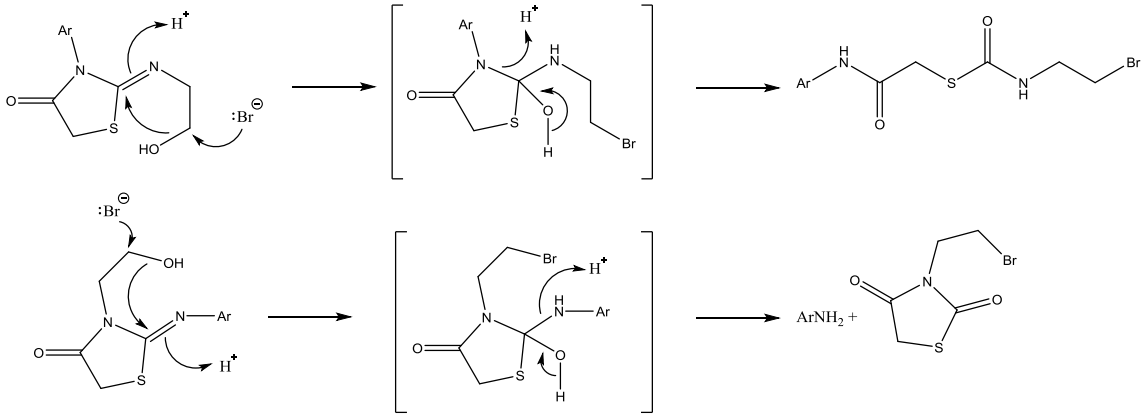

**Scheme 3.8.** Possible step-wise mechanism for the decyclization reaction. The reaction of **b** is shown in the top while the reaction of **a** is shown in the bottom.

### 3.8 Conclusions

The initial reaction of thiourea **1** to form the two different isomers was expanded to create a library of 20 different products using 11 thioureas. The products and yields from these reactions are summarized in **Scheme 3.9**.

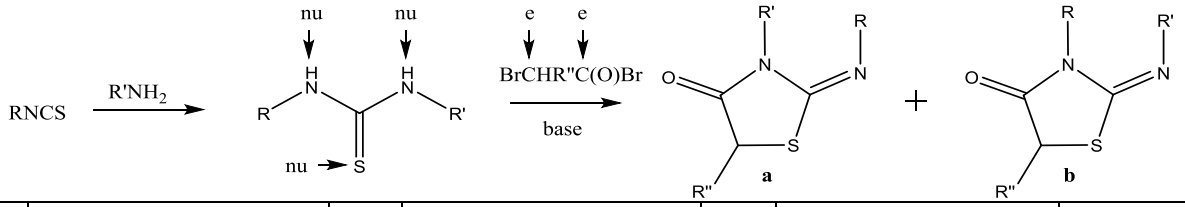


| | | | | | | |
|---|---|---|---|---|---|---|
| **1** | R = 1-Naphthyl<br>R' = $CH_2CH_2OH$ | **1a** | R = 1-Naphthyl<br>R' = $CH_2CH_2OH$ | **1b** | R = 1-Naphthyl<br>R' = $CH_2CH_2OH$ | 67% / 20%<br>26% / 63% |
| **2** | R = 4-Bromophenyl<br>R' = $CH_2CH_2OH$ | **2a** | R = 4-Bromophenyl<br>R' = $CH_2CH_2OH$ | **2b** | R = 4-Bromophenyl<br>R' = $CH_2CH_2OH$ | 14% / 65% |
| **3** | R = 4-Nitrophenyl<br>R' = $CH_2CH_2OH$ | **3a** | R = 4-Nitrophenyl<br>R' = $CH_2CH_2OH$ | **3b** | R = 4-Nitrophenyl<br>R' = $CH_2CH_2OH$ | 28% / 69% |
| **4** | R = 4-Methoxyphenyl<br>R' = $CH_2CH_2OH$ | **4a** | R = 4-Methoxyphenyl<br>R' = $CH_2CH_2OH$ | **4b** | Not observed | 60% |
| **5** | R = *n*-Butyl<br>R' = $CH_2CH_2OH$ | **5a** | R = *n*-Butyl<br>R' = $CH_2CH_2OH$ | **5b** | Not observed | 20% |
| **6** | R = 1-Naphthyl<br>R' = $CH(CH_3)CH_2OH$ | **6a** | R = 1-Naphthyl<br>R' = $CH_(CH_3)CH_2OH$ | **6b** | R = 1-Naphthyl<br>R' = $CH_(CH_3)CH_2OH$ | 27% / 17% |
| **7** | R = 1-Naphthyl<br>R' = $CH_2CH(CH_3)OH$ | **7a** | R = 1-Naphthyl<br>R' = $CH_2CH(CH_3)OH$ | **7b** | R = 1-Naphthyl<br>R' = $CH_2CH(CH_3)OH$ | 29% / 11% |
| **8** | R = 1-Naphthyl<br>R' = $CH_2CH_2CH_2OH$ | **8a** | R = 1-Naphthyl<br>R' = $CH_2CH_2CH_2OH$ | **8b** | R = 1-Naphthyl<br>R' = $CH_2CH_2CH_2OH$ | 37% / 36% |
| **9** | R = 1-Naphthyl<br>R' = $CH_2CH_2CH_2CH_2OH$ | **9a** | R = 1-Naphthyl<br>R' = $CH_2CH_2CH_2CH_2OH$ | **9b** | R = 1-Naphthyl<br>R' = $CH_2CH_2CH_2CH_2OH$ | 28% / 19% |
| **10** | R = 4-Bromophenyl<br>R' = $CH_2CH_2CH_3$ | **10a** | R = 4-Bromophenyl<br>R' = $CH_2CH_2CH_3$ | **10b** | R = 4-Bromophenyl<br>R' = $CH_2CH_2CH_3$ | 9% / 79% |
| **11** | R = 1-Naphthyl<br>R' = $CH_2CH_2CH_3$ | **11a** | R = 1-Naphthyl<br>R' = $CH_2CH_2CH_3$ | **11b** | R = 1-Naphthyl<br>R' = $CH_2CH_2CH_3$ | 17% / 60% |
| **12** | R = 4-Bromophenyl<br>R' = $CH_2CH_2OH$ | **12a** | R = 4-Bromophenyl<br>R' = $CH_2CH_2OH$ | **12b** | Not isolated | 27% |

**Scheme 3.9**. Summary of functionalized thioureas and iminothiozolidinone derivatives. R'' equals to H for all compounds, except **12a**. For **12a** R''= $CH_3$. Labels "nu" denote nucleophilic centers in thioureas, and labels "e" denote electrophilic centers in bromoacyl bromides. Note, that thioureas **1**-**9** and **12** have an additional nuclephilic OH group. The yields are reported as a% / b% as isolated from a given reaction. These values were measured after column purification. Note that only the reaction of **1** was optimized for yield, and the two sets of yields provided come from two different reactions.

This work has expanded on the potential reactions of thioureas to form biologically relevant products. These reactions have no other side products, making purification straightforward after simple optimization of column conditions. In addition, a novel decyclization was discovered. The products of this decyclization were proven using x-ray crystallography and a potential mechanism was proposed based on experimental observations.

# Chapter 4

# Future Work

## 4.1. Experimental Support of a Termolecular Mechanism

Reactions involving termolecular mechanisms are a rare class as they involve the collision between three different species. We were able to obtain crystal structures of two of the decyclization products, **15** and **16**, providing irrefutable proof of the formation of these aminooxoethylcarbamothionates from the iminothiozolidinone **b** isomers. We were also able to demonstrate that the pendant OH is necessary for the decyclization, as well as an external nucleophile. **Figure 4.1** further proves that the decyclization requires acidic protons to be present. These experiments have led us to suggest a plausible termolecular mechanism.

We would like to conduct a kinetic study of this reaction to further support this proposed mechanism. Specifically, we would monitor the decyclization reaction by variable temperature NMR. A kinetic profile could be established by varying the concentrations of iminothiozolidinone, acid, and nucleophile in $CD_3CN$. This this could be used to either support or disprove our proposed termolecular mechanism.

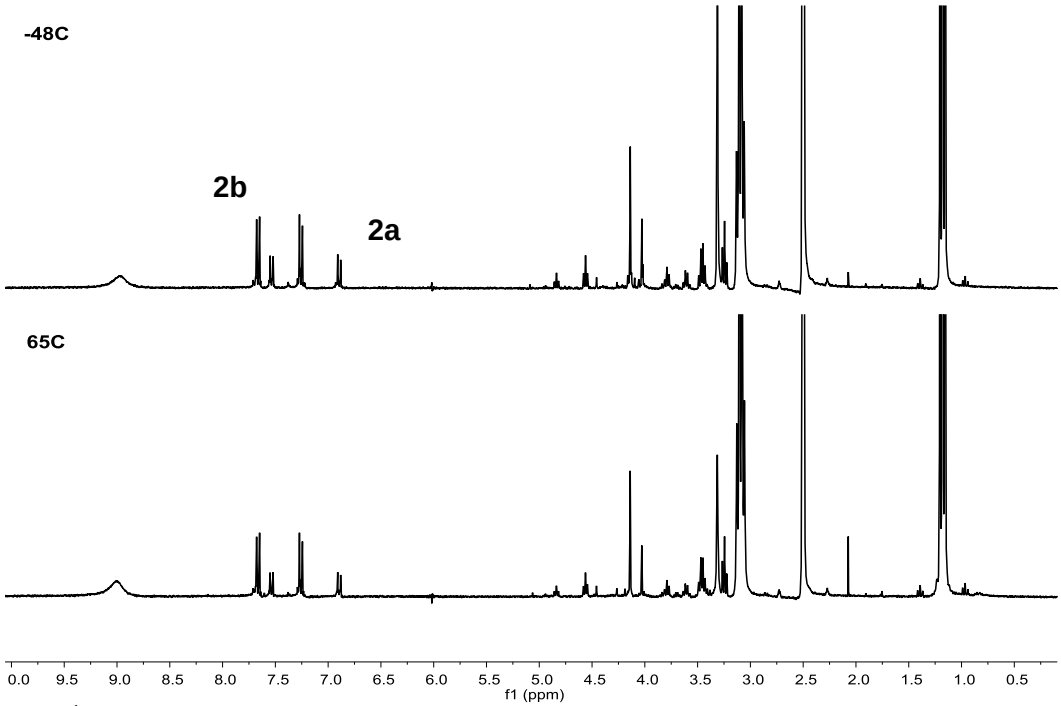


**Figure 4.1:** $^{1}$H NMR of the ring formation step followed by heating in the presence of excess base. The precursor was thiourea **2**.

### 4.2 One Pot Synthesis of Aminooxoethylcarbamothionates

We were able to show that this series of experiments are well-suited to a one-pot synthesis protocol. The reaction of isothiocyanate and the amine that have been added 1:1 will go to completion within four hrs at room temperature (monitored by NMR). This step can also be done in any of the solvents that are suitable for the next step. Next, triethylamine and bromoacetyl bromide can be added to the same pot, leading to the ring formation. This step can be done at room temperature or cold temperatures (-45°C when in acetonitrile) to control the product distribution and finishes within 6 hrs. Finally, this mixture need only be heated to 65°C for 4 hrs to promote the decylization of any **b** isomer formed in the previous step. Any **a** isomer formed would remain unchanged. Therefore, the formation of aminooxoethylcarbamotionates can be achieved in 14 hrs by simply controlling the temperature. There is no need to change the

solvent at any step, which is important for the conversion of traditional syntheses to continuous flow protocols which are common in large-scale industrial syntheses. Additionally, the crude NMRs taken show that the reaction results in a clean mixture of products with no additional side products to be removed. Aqueous work up will remove the triethylamine and salts while the aminooxoethylcarbamothionate has a sufficiently different polarity that separation from the iminothiozolidinone via chromatography is easily done. **Figure 4.2** shows the results of this series.

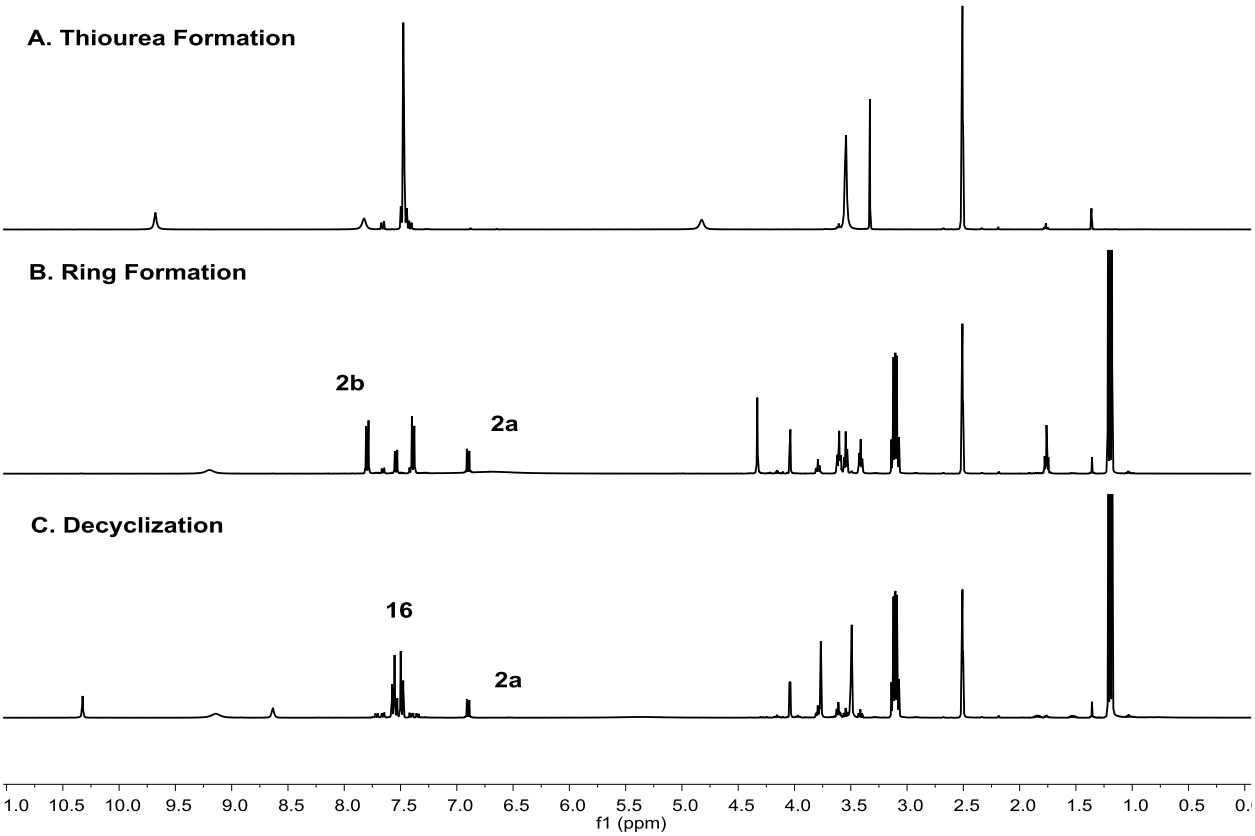


**Figure 4.2:** One-pot reaction series forming aminooxoethylcarbamothionate from isothiocyanate.

### 4.3 Potential HIV-1 Reverse Transcriptase Inhibitors

This reaction that we have discovered is, to the best of our knowledge, completely unprecedented. We observe a complete rearrangement of the inherited RNC(S)NR scaffold to the $RNC(O)CH_2SC(O)NR$. This is a remarkable reaction that deserves to be explored in its entirety. In addition, the aminooxoethylcarbamothionates that are formed are known to be a privileged motif.[111] in HIV-1 reverse transcriptase inhibitors.[112-116] Thus the products of this decyclization are of biological interest as well. The major advantage to formation of these products using our method is the quick, inexpensive synthesis that allows for multiple points of variation. We have already established a protocol to synthesize these products from fairly cheap, commercially available starting materials that could be easily adapted to an automated system for large scale production.

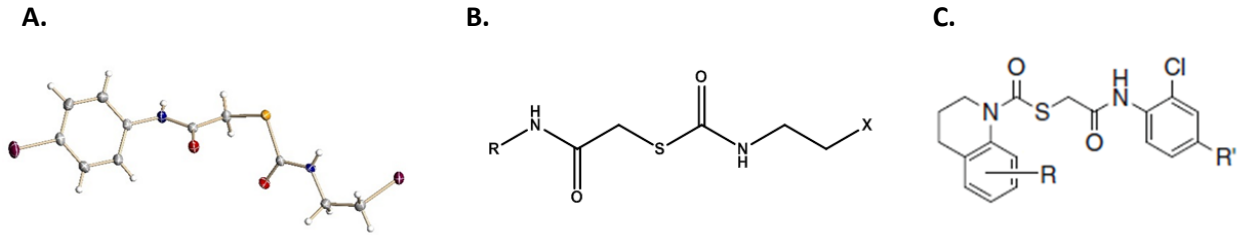


**Figure 4.3**: Comparison of **16** to a known class of HIV reverse transcriptase inhibitors. (A) The crystal structure of **16** has been redrawn for comparison. (B) The general structure of the aminooxoethylcarbamothionates formed in the newly reported decyclization of iminothiozolidinones. (C) General structure of compounds known to be HIV-1 RTIs.

Our next goal would be to continue to expand the class of products that can be synthesized in this manner. To date, we have only considered bromoacetyl bromide or 1-bromopropionyl bromide. We would like to explore the use of other capping agents as a means to synthesize other heterocycles**. Figure 4.4** shows some possible cyclization products that could be formed using the same thioureas with different capping agents. We expect that we can achieve

a similar control over the reaction through solvent and temperature due to the presence of the same auxiliary OH. We have somewhat explored the auxiliary chain length but we would like to find the limit at which we can exert control over the reaction in this manner. We can synthesize thioureas that terminate in amines instead of alcohols, but we have not explored their effect on the ring formation reaction. We would also like to expand the external nucleophiles that can participate in the decyclization step. The hydrohalogen acids are the most successful, however we have also seen promising results with 2-mercaptoethanol and amines. This would provide another avenue for diversity in the potential HIV transcriptase inhibitors.

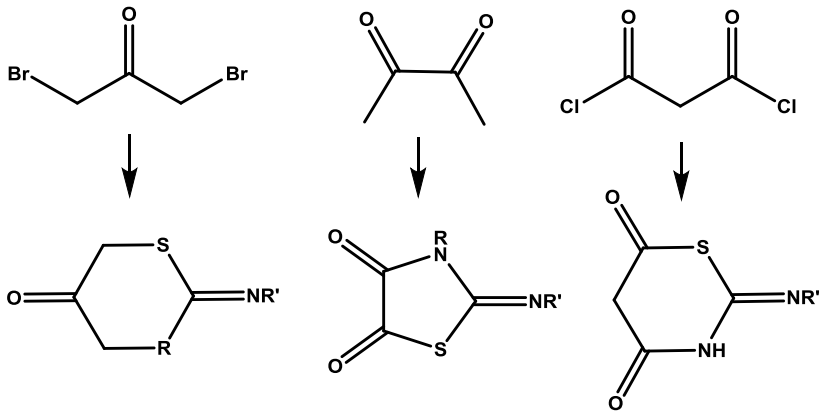


**Figure 4.4:** Potential reactions of N,N'-disubstituted thioureas with other capping agents. Each capping agent is doubly electrophilic. These reactions could make synthesis of other heterocycles more accessible.

Although we have identified the importance of base in the ring formation, we have not yet explored this in depth. We would like to explore the effect of base in combination with different solvents in the future in an attempt to push the reaction towards 100% formation of the **a** isomers. We are currently working on the synthesis of a third isomer using the naphthyl thiourea ethanolamine precursor. In an effort to synthesize this compound, we have proposed a different synthetic route. We will form naphthyl thiourea morpholinone through the reaction of naphthyl isothiocyanate and morpholin-3-one with NaH in THF. Crude NMRs suggest the

formation of this product, however purification and characterization are still necessary. The structure of this isomer would be characterized by HSQC and HMBC.

### 4.4 Cyclic Voltammetry as a Means to Assess Relative Nucleophilicity

A protocol for assessment of relative nucleophilicity of two nitrogens in asymmetric thioureas will be developed. Chapter 3 included a cyclic voltammogram used to compare the redox potentials of selected thioureas in an effort to explain the differences in product distributions formed from various reactions with these precursors. Similar studies will be carried out on the number of thioureas that are subject to cyclization under conditions mimicking the reaction conditions, including a variety of solvents and temperature variations that allowed us to control the outcome of syntheses. Through a series of cyclic voltammetry experiment, we expect to find a relationship between relative reactivity of individual thioureas and the conditions of reactions.

References


1. Rizzo, M. A.; Davidson, M. W.; Piston, D. W. Fluorescent Protein Tracking and Detection: Applications Using Fluorescent Proteins in Living Cells. *Cold Spring Harb. Protoc.* **2009**, *12*.

2. Bao, G.; Rhee, W. J.; Tsourkas, A. Fluorescent Probes for Live-Cell RNA Detection. *Annu. Rev. Biomed. Eng.* **2009**, *11*, 25-47.

3. Paik, S.; Bryant, J.; Tan-Chiu, E., et al. Real-World Performance of HER2 Testing-National Surgical Adjuvant Breast and Bowel Project Experience. *J. Natl. Cancer Inst.* **2002**, *94*, 852-854.

4. Zwirglmaier, K. Detection of prokaryotic cells with fluorescence in situ hybridization. *Methods Mol. Biol.* **2010**, *659*, 349-362.

5. Engvall, E. Quantitative enzyme immunoassay (ELISA) in microbiology. *Med. Biol.* **1977**, *55*, 193-200.

6. Bao, S.; Wu, Q.; Sathornsumetee, S., et al. Stem Cell-like Glioma Cells Promote Tumor Angiogenesis through Vascular Endothelial Growth Factor. *Cancer Res.* **2006**, *66*, 7843-7848.

7. Li, J.; Sun, K.; Chen, Z.; Shi, J.; Zhou, D.; Xie, G. A fluorescence biosensor for VEGF detection based on DNA assembly structure switching and isothermal amplification. *Biosens. Bioelectron.* **2017**, *89*, 964-969.

8. Goncalves, V.; Gautier, B.; Garbay, C.; Vidal, M.; Inguimbert, N. Development of a chemiluminescent screening assay for detection of vascular endothelial growth factor receptor 1 ligands. *Anal. Biochem.* **2007**, *366*, 108-110.

9. Takahashi, H.; Nomura; Nishida, J.; Fujino, Y.; Yanagi, Y.; Kawashima, H. Vascular Endothelial Growth Factor (VEGF) Concentration Is Underestimated by Enzyme-Linked Immunosorbent Assay in the Presence of Anti-VEGF Drugs. *Biochem. and Mol. Bio.* **2016**, *57*, 462-466.

10. Matsuura-Tokita, K.; Takeuchi, M.; Ichihara, A.; Mikuriya, K.; Nakano, A. Live imaging of yeast Golgi cisternal maturation. *Nature* **2006**, *441*, 1007-1010.

11. Mochizuki, N.; Yamashita, S.; Kurokawa, K.; Ohba, Y.; Nagai, T.; Miyawaki, A.; Matsuda, M. Spatio-temporal images of growth-factor-induced activation of Ras and Rap1. *Nature* **2001**, *441*, 1065-1068.

12. Miyawaki, A. Visualization of the spatial and temporal dynamics of intracellular signaling. *Dev. Cell* **2003**, *4*, 295-305.

13. Suzuki, T.; Matsuzaki, T.; Hagiwara, H.; Aoki, T.; Takata, K. Recent Advances in Fluorescent Labeling Techniques for Fluorescence Microscopy *Acta. Histochem Cytochem* **2007**, *40*, 131-137.

14. Giepmans BN; Adams SR; FAU - Ellisman, M. H.; Ellisman MH; FAU - Tsien, R. Y.; Tsien RY The fluorescent toolbox for assessing protein location and function. *Science*.**2006** *312*, 217-24.

15. Keppler, A.; Gendreizig, S.; Gronemeyer, T.; Pick, H.; Vogel, H.; Johnsson, K. A general method for the covalent labeling of fusion proteins with small molecules in vivo. *Nature Biotech.* **2003**, *21*, 89.

16. Chen, X.; Wu, Y. Selective chemical labeling of proteins. *Org. Biomol. Chem.* **2016**, *14*, 5417-5439.

17. Marks, K. M.; Nolan, G. P. Chemical labeling strategies for cell biology. *Nature Methods* **2006**, *3*, 596.

18. Betzig, E.; Patterson, G.; Sougrat, R.; Lindwasser, O.; Olenych, S.; Bonifacino, J.; Davidson, M.; Lippincott-Schwartz, J.; Hess, H. Imaging intracellular fluorescent proteins at nanometer resolution. *Science* **2006**, *313*, 1642-1645.

19. Betzig, E. Proposed method for molecular optical imaging. *Opt. Lett.* **1995**, *20*, 237-239.

20. Dickson, R. M.; Cubitt, A. B.; Tsien, R. Y.; Moerner, W. E. On/off blinking and switching behavior of single molecules of green fluorescent protein. *Nature* **1997**, *388*, 355-358.

21. Moerner, W. E.; Kador, L. Optical detection and spectroscopy of single molecules in a solid. *Phys. Rev. Lett.* **1989**, *62*, 2535-2538.

22. Klar, T. A.; Jakobs, S.; Dyba, M.; Egner, A.; Hell, S. W. Fluorescence microscopy with diffraction resolution barrier broken by simulated emission. *Proc. Natl. Acad. Sci. USA* **2000**, *97*, 8206-8210.

23. Mondal, S. B.; Gao, S.; Zhu, N.; Liang, R.; Gruev, V.; Achilefu, S. *Adv. Cancer Res.* **2014**, *124*, 211.

24. Nguyen, Q. T.; Tsien, R. Y. *Nat. Rev. Cancer* **2013**, *13*, 662.

25. Andersson H; Baechi T; FAU - Hoechl, M.; Hoechl M; FAU - Richter, C.; Richter C Autofluorescence of living cells. - *J Microsc.***1998** ,*191*,1-7.

26. Ramanujam N; Mitchell MF; Mahadevan, A.; Mahadevan A; Warren, S.; Warren S; Thomsen, S.; Thomsen S; Silva, E.; Silva E; Richards-Kortum, R.; Richards-Kortum R In vivo diagnosis of cervical intraepithelial neoplasia using 337-nm-excited laser-induced fluorescence. - *Proc Natl Acad Sci U S A.***1994**, *91*, 10193-7.

27. Resch-Genger, U.; Grabolle, M.; Cavaliere-Jaricot, S.; Nitschke, R.; Nann, T. Quantum dots versus organic dyes as fluorescent labels. *Nature Methods* **2008**, *5*, 763-775.

28. Frasco, M. F.; Chaniotakis, N. Semiconductor Quantum Dots in Chemical Sensors and Biosensors. *Sensors* **2009**, *9*, 7266-7286.

29. Sapsford, K. E.; Pons, T.; Medintz, I. L.; Mattoussi, H. Biosensing with Luminescent Semiconductor Quantum Dots. *Sensors* **2006**, *6*, 925-953.

30. Norris, D. J.; Bawendi, M. G. Measurement and assignment of the size-dependent optical spectrum in CdSe quantum dots. *Phys. Rev. B.* **1996**, *53*, 16338.

31. Huang, C. -.; Li, Y. -.; Chen, T. -. A highly sensitive system for urea detection by using CdSe/ZnS core-shell quantum dots. *Biosensors & Bioelectronics* **2007**, *22*, 1835-1838.

32. Medintz, I. L.; Clapp, A. R.; Mattoussi, H.; Goldman, E. R.; Fisher, B.; Mauro, J. M. Self-assembled nanoscale biosensors based on quantum dot FRET donors. *Nat. Mater.* **2003**, *2*, 630-638.

33. Ji, X.; Zheng, J.; Xu, J.; Rastogi, V. K.; Cheng, T.; DeFrank, J. J.; Leblanc, R. M. (CdSe)ZnS Quantum Dots and Organophosphorus Hydrolase Bioconjugate as Biosensors for Detection of Paraoxon. *J. Phys. Chem. B* **2005**, *109*, 3793-3799.

34. Dabbousi, B. O.; et al (CdSe)ZnS core-shell qds: synthesis and characterization of a size series of highly luminescent nanocrystallites. *J. Phys. Chem. B.* **1997**, *101*, 9463-9475.

35. Xing, Y. et. al. Bioconjugated quantum dots for multiplexed and quantitative immunohistochemistry. *Nat. Protoc.* **2007**, *2*, 1152-1165.

36. Medintz, I. L.; Uyeda, H.; Goldman, E.; Mattoussi, H. QD bioconjugates for imaging, labelling, and sensing. *Nat. Mater.* **2005**, *4*, 435-446.

37. Mason, J. N. et al. Novel fluorescence-based approaches for the study of biogenic amine transporter localization, activity, and regulation. *J. Neurosci. Methods* **2005**, *143*, 3-25.

38. Wang, M.; Thanou, M. Targeting nanoparticles to cancer. *Pharmacological Research* **2010**, *62*, 90-99.

39. Boisselier, E.; Astruc, D. Gold nanoparticles in nanomedicine: preparations, imaging, diagnostics, therapies and toxicity. *Chem. Soc. Rev.* **2009**, *38*, 1759-1782.

40. Janib, S. M.; Moses, A. S.; MacKay, J. A. Imaging and drug delivery using theranostic nanoparticles. *Adv. Drug Deliv. Rev.* **2010**, *62*, 1052-1063.

41. Al-Jamal, W. T.; Kostarelos, K. Liposomes: From a Clinically Established Drug Delivery System to a Nanoparticle Platform for Theranostic Nanomedicine. *Acc. Chem. Res.* **2011**, *44*, 1094-1104.

42. Lasic, D. D.; Papahadjopoulos, D. Medical applications of liposomes. *Elsevier Science* **1998**.

43. Wehunt, M. P.; Winschel, C. A.; Khan, A. K.; Guo, T.; Abdrakhmanova, G.; Sidorov, V. Controlled drug-release system based on pH-sensitive chloride-triggerable liposomes. *J. of Liposome Res.* **2013**, *23*, 37-46.

44. Al-Jamal, W. T.; Kostarelos, K. Liposome-nanoparticle hybrids for multimodal diagnostic and therapeutic applications. *Nanomedicine* **2007**, *2*, 85-98.

45. Rasch, M. R.; Rossinyol, E.; Hueso, J. L.; Goodfellow, B. W.; Arbiol, J.; Korgel, B. A. Hydrophobic gold nanoparticle self-assembly with phosphatidylcholine lipid: membrane-loaded and janus vesicles. *Nano. Lett.* **2010**, *10*, 3733-3739.

46. Passonen, L.; Laaksonen, T.; Johans, C.; Yliperttula, M.; Urtti, A. Gold nanoparticles enable selective light-induced contents release from liposomes. *J. Controlled Release* **2007**, *122*, 86-93.

47. Park, S. H.; Oh, S. G.; Mun, J. Y.; Han, S. S. Loading of gold nanoparticles inside the DPPC bilayers of liposome and their effects on membrane fluidities. *2006* **48**, *112*, 118.

48. Mertschenk, B.; Knott, A.; Bauer, W. Thiourea and Thiourea Derivatives. In *Ullmann's Encyclopedia of Industrial Chemistry*Wiley-VCH Verlag GmbH & Co. KGaA: 2000; .

49. Waris, G.; Siddiqi, H. M.; Twyman, L. J.; Hussain, R.; Akhter, Z.; Butt, M. S. Novel flame retardant poly(thiourea-sulfone-imide)s for high temperature applications: synthesis and characterization. *Turkish Journal of Chemistry* **2013**, *37*, 946-958.

50. SCHROEDER, D. Thioureas. *Chem. Rev.* **1955**, *55*, 181-228.

51. Shakeel, A.; Altaf, A. A.; Qureshi, A. M.; Badshah, A. Thioureas derivatives in drug design and medicinal chemistry: A short review. *J. of Drug Design and Med. Chem.* **2016**, *2*, 10-20.

52. Rodriguez-Fernandez, E.; Garcia, E.; Hermosa, M.; Jimenez-Sanchez, A.; Sanchez, M.; Monte, E.; Criado, J. Chloride and ethyl ester morpholine thiourea derivatives and their Ni(II) complexes. Crystal and molecular structures of the thiourea derivative L-leucine methyl ester and its complexes with Cu(II) and Pt(II). Growth of the pathogenic fungus Botrytis cinerea. *J. Inorg. Biochem.* **1999**, *75*, 181-188.

53. del Campo, R.; Criado, J.; Gheorghe, R.; Gonzalez, F.; Hermosa, M.; Sanz, F.; Manzano, J.; Monte, E.; Rodriguez-Fernandez, E. N-benzoyl-N'-alkylthioureas and their complexes with Ni(II), Co(III) and Pt(II) - crystal structure of 3-benzoyl-l-butyl-l-methyl-thiourea: activity against fungi and yeast. *J. Inorg. Biochem.* **2004**, *98*, 1307-1314.

54. Rodriguez-Fernandez, E.; Del-Campo, R.; Criado, J.; Manzano, J.; Sanz, F. The antifungal agent methyl 2-benzyl-6-diethylamino-4-phenyl-2H-1,3,5-thiadiazine-2-carboxylate. *Acta Crystallographica Section E-Structure Reports Online* **2004**, *60*, O713-O715.

55. Rodriguez-Fernandez, E.; Manzano, J.; Benito, J.; Hermosa, R.; Monte, E.; Criado, J. Thiourea, triazole and thiadiazine compounds and their metal complexes as antifungal agents. *J. Inorg. Biochem.* **2005**, *99*, 1558-1572.

56. Wu, J.; Shi, Q.; Chen, Z.; He, M.; Jin, L.; Hu, D. Synthesis and Bioactivity of Pyrazole Acyl Thiourea Derivatives. *Molecules* **2012**, *17*, 5139-5150.

57. CUNNINGHAM, A.; HURLEY, J. Alpha-Naphthyl-Thiourea-Induced Pulmonary Edema in Rat - Topographical and Electron-Microscope Study. *J. Pathol.* **1972**, *106*, 25-+.

58. Cantrell, A.; Engelhardt, P.; Hogberg, M.; Jaskunas, S.; Johansson, N.; Jordan, C.; Kangasmetsa, J.; Kinnick, M.; Lind, P.; Morin, J.; Muesing, M.; Noreen, R.; Oberg, B.; Pranc, P.; Sahlberg, C.; Ternansky, R.; Vasileff, R.; Vrang, L.; West, S.; Zhang, H. Phenethylthiazolylthiourea (PETT) compounds as a new class of HIV-1 reverse transcriptase inhibitors .2. Synthesis and further structure-activity relationship studies of PETT analogs. *J. Med. Chem.* **1996**, *39*, 4261-4274.

59. Gavriliu, D.; Fossey, C.; Ciurea, A.; Delbederi, Z.; Sugeac, E.; Laduree, D.; Schmidt, S.; Laumond, G.; Aubertin, A. Synthesis and anti-HIV activity of [D4U]-[Trovirdine analogue] and [D4T]-[Trovirdine analogue] heterodimers as inhibitors of HIV-1 reverse transcriptase. *Nucleosides Nucleotides & Nucleic Acids* **2002**, *21*, 505-533.

60. Mehanna, A. S.; Belani, J. D.; Kelley, C. J.; Pallansch, L. A. Design, synthesis and biological evaluation of a series of thioamides as non-nucleoside reverse transcriptase inhibitors. *Medicinal Chemistry* **2007**, *3*, 513-519.

61. Sugeac, E.; Fossey, C.; Laduree, D.; Schmidt, S.; Laumond, G.; Aubertin, A. Synthesis and anti-HIV activity of some heterodimers [NRTI]-glycyl-succinyl-[Trovirdine Analogue] of known HIV-1 reverse transcriptase inhibitors. *Journal of Enzyme Inhibition and Medicinal Chemistry* **2003**, *18*, 175-186.

62. Venkatachalam, T.; Sudbeck, E.; Mao, C.; Uckun, F. Stereochemistry of halopyridyl and thiazolyl thiourea compounds is a major determinant of their potency as nonnucleoside inhibitors of HIV-1 reverse transcriptase. *Bioorg. Med. Chem. Lett.* **2000**, *10*, 2071-2074.

63. Schreiner, P. Metal-free organocatalysis through explicit hydrogen bonding interactions. *Chem. Soc. Rev.* **2003**, *32*, 289-296.

64. Winschel, C. A.; Kalidinid, A.; Zgani, I.; Magruder, J. L.; Sidorov, V. Receptor for Anionic Pyrene Derivatives Provides the Basis for New Biomembrane Assays. *J. Am. Chem. Soc.* **2005**, *127*, 14704-14713.

65. Winschel, C. A.; Kaushik, V.; Abdrakhmanova, G.; Aris, S. M.; Sidorov, V. New Noninvasive Methodology for Real-Time Monitoring of Lipid Flip. *Bioconjug. Chem.* **2007**, *18*, 1507-1515.

66. Kaushik V, Cook N, Liang AY, Desai UR, Sidorov V. Chemoselective precipitation of lactose from a lactose/sucrose mixture: Proof of concept for a new separation methodology. *Supramol. Chem.* **2010**, *22*, 751-757.

67. Kaushik, V. Synthesis of cyclen based receptors and their use in separations biotechnology, Virginia Commonwealth University, Richmond, VA, 2011.

68. Nishimura, T.; Shinoda, S.; Tsukube, H. Chirality induction in supramolecular aggregate: Chiral recognition between armed cyclen-Na+ complexes having quadruplicated helical geometry. *Chirality* **2002**, *14*, 555-557.

69. Shinoda, S.; Nishimura, T.; Tadokoro, M.; Tsukube, H. Ester-armed cyclens having quadruplicated helical geometry: Remarkably stable and selective encapsulation of Na+ ion. *J. Org. Chem.* **2001**, *66*, 6104-6108.

70. Daleke, D. L. Regulation of transbilayer plasma membrane phospholipid asymmetry. *J. Lipid Res.* **2003**, *44*, 233-242.

71. Castegna, A.; Lauderback, C. M.; Mohmmad-Abdul, H.; Butterfield, D. A. Modulation of phospholipid asymmetry in synaptosomal membranes by the lipid peroxidation products, 4-hydroxynonenal and acrolein: implications for Alzheimer's disease. *Brain Res.* **2004**, *1004*, 193-197.

72. Fadok, V. A.; Voelker, D. R.; Campbell, P. A.; Cohen, J. J.; Bratton, D. L.; Henson, P. M. Exposure of phosphatidylserine on the surface of apoptotic lymphocytes triggers specific recognition and removal by macrophages. *J. Immunol.* **1992**, *148*, 2207-2216.

73. Williamson, P.; Schlegel, R. A. Transbilayer phospholipid movement and the clearance of apoptotic cells. *Biochim. Biophys. Acta* **2002**, *1585*, 53-63.

74. Borisenko, G. G.; Matsura, T.; Liu, S. X.; Tyurin, V. A.; Jianfei, J.; Serinkan, F. B.; Kagan, V. E. Macrophage recognition of externalized phosphatidylserine and phagocytosis of apoptotic Jurkat cells—existence of a threshold. *Arch. Biochem. Biophys.* **2003**, *413*, 41-52.

75. Hamon, Y.; Chambenoit, O.; Chimini, G. ABCA1 and the engulfment of apoptotic cells. *Biochim. Biophys. Acta* **2002**, *1585*, 64-71.

76. Chung, S. M.; Bae, O. N.; Lim, K. M.; Noh, J. Y.; Lee, M. Y.; Jung, Y. S.; Chung, J. H. Lysophosphatidic acid induces thrombogenic activity through phosphatidylserine exposure and procoagulant microvesicle generation in human erythrocytes. *Arterioscler. Thromb. Vasc. Biol* **2007***, 27*, 414-421.

77. Zwaal, R. F. A.; Schroit, A. J. Pathophysiologic implications of membrane phospholipid asymmetry in blood cells. *Blood* **1997**, *89*, 1121-1132.

78. Pomorski, T.; Muller, P.; Zimmermann, B.; Burger, K.; Devaux, P. F.; Herrmann, A. Transbilayer movement of fluorescent and spin-labeled phospholipids in the plasma membrane of human fibroblasts: A quantitative approach. *J. Cell Sci.* **1996**, 687-698.

79. McIntyre, J. C.; Sleight, R. G. Fluorescence assay for phospholipid membrane asymmetry. *Biochem.* **1991**, *30*, 11819-11827.

80. Armstrong, V. T.; Brzustowicz, M. R.; Wassall, S. R.; Jenski, L. J.; Stillwell, W. Rapid flip-flop in polyunsaturated (docosahexaenoate) phospholipid membranes. *Arch. Biochem. Biophys.* **2003**, *414*, 74-82.

81. Bhushan R, K. S. TLC separation of some common sugars on silica gel plates impregnated with transition metal ions. *Biomed. Chromatogr*, **1997***, 11*, 59-60.

82. Chavez-Servin JL, Castellote AI, Lopez-Sabater MC Analysis of mono- and disaccharides in milk-based formulae by high-performance liquid chromatography with refractive index detection. *J. Chromatogr. A* **2004**, *1043*, 211-215.

83. Ahmadi S., Lippross S., Neuhuber W. L. and Zeilhofer H. U. PGE2 selectively blocks inhibitory glycinergic neurotransmission onto rat superficial dorsal horn neurons. *Nat. Neurosci.* **2002**, *5*, 34-40.

84. Sobetzko D., Sander T. and Becker C. M. Genetic variation of the human glycine receptor subunit genes GLRA3 and GLRB and susceptibility to idiopathic generalized epilepsies. *Am. J. Med. Genet.* **2001**, *105*, 534-538.

85. Ramanathan S., Woodroffe A. and Flodman P. L. A case of autism with an interstitial deletion on 4q leading to hemizygosity pentameric ligand-gated ion channels. *Proc. Natl. Acad. Sci USA* **2004**, *102*, 18207-18212.

86. Thathiah, A.; De Strooper, B. The role of G protein-coupled receptors in the pathology of Alzheimer's disease. *Nat. Rev. Neurosci.* **2011**, *12*, 73-87.

87. Zhao, Y.; Inayat, S.; Dikin, D. A.; Singer, J. H., et al Patch clamp technique: review of the current state of the art and potential contributions from nanoengineering. *Proc. IMechE, 222 Part N: J. Nanoengineering and Nanosystems* **2009**, *149*, 1-11.

88. Hopkin, J. M.; , N., M.J. The release of 14C-glycine from electrically stimulated rat spinal cord slices. *Br. J. Pharmacol* **1970**, *40*, 136-138.

89. Shank, R. P.; Aprison, M. H. The metabolism in vivo of glycine and serine in eight areas of the rat central nervous system. *J. Neurochem.* **1970**, *17*, 1461-1475.

90. Garrett, R.; Grisham, C. *Biochemistry, 4th ed.* 2009; .

91. Hatva, E.; Kaipainen, A.; Mentula, P.; Jaaskelainen, J.; Paetau, A.; Haltia, M.; Alitalo, K. Expression of Endothelial Cell-Specific Receptor Tyrosine Kinases and Growth Factors in Human Brain Tumors. *Am. J. of Pathol.* **1995**, *146*, 368-378.

92. Rich, J., N.; Sathornsumetee, S.; Keir, S. T., et al. ZD6474, a Novel Tyrosine Kinase Inhibitor of Vascular Endoethelial Growth Factor Receptor and Epidermal Growth Factor Receptor, Inhibits Tumor Growth of Multiple Nervous System Tumors. *Clin. Cancer Res.* **2005**, *11*, 8145-8157.

93. Gao, J. Cancer stem Cells: the lessons from pre-cancerous stem cells. *J. Cell. Mol. Med.* **2008**, *12*, 67-96.

94. Duffy, M. J. Role of tumor markers in patients with solid cancers: A critical review. *Euro. J. of Internal. Med.* **2007**, *18*, 175-184.

95. Thivierge, C.; Kurbegovic, A.; Couillard, M., et al Overexpression of PKD1 Causes Polycystic Kidney Disease. *Mol. Cell. Biol.* **2006**, *26*, 1538-1548.

96. . Lemoine, D.; Jiang, R.; Taly, A., et al. Ligand-Gated Ion Channels: New Insights into Neurological Disorders and Ligand Recognition. *Chem. Rev.* **2012**, *112*, 6285-6318.

97. . Hernandes, M. S.; Troncone, L. R. P. Glycine as a neurotransmitter in the forebrain: a short review. *J. Neural Transm.* **2009**, *116*, 1551-1560.

98. . Langosch, D.; Laube, B.; Rundstrom, N., et al. Decreased agonist affinity and chloride conductance of mutant glycine receptors associated with human hereditary hyperekplexia. *The EMBO Journal* **1994**, *13*, 4223-4228.

99. . Betz, H.; Laube, B. Glycine receptors: recent insights into their structural organization and functional diversity. *J. of Neurochem.* **2006**, *97*, 1600-1610.

100. Lynch, J. W. Molecular Structure and Function of the Glycine Receptor Chloride Channel. *Physiol. Rev.* **2004**, *84*, 1051-1095.

101. Rajendra, S.; Lynch, J. W.; Schofield, P. R. The glycine receptor. *Pharmacol Ther* **1997**, *73*, 121-146.

102. . Jensen, A. A.; Kristiansen, U. Functional characterization of the human α1 glycine receptor in a fluorescence-based membrane potential assay. *Biochemical Pharmacology* **2004**, *67*, 1789-1799.

103. Kim, T. H.; Lee, N.; Lee, G.; Kim, J. N. A mild cyclodesulfurization of N-(2-hydroxyethyl)-N'-phenyl thioureas to 2-phenylamino-2-oxazolines using TsCl/NaOH. *Tetrahedron* **2001**, *57*, 7137-7141.

104. Lee, G.; Kim, J. N.; Kim, T. H. Investigation of the cyclization of N-(2-hydroxyethyl)-N'-phenyl thioureas: Mitsunobu conditions vs TsCl/NaOH system. *Bull. Korean Chem. Soc.* **2002**, *23*, 19-20.

105. Heinelt, U.; Schultheis, D.; Jager, S.; Lindenmaier, M.; Pollex, A.; Beckmann, H. S. G. A convenient method for the synthesis of 2-amino substituted aza-heterocycles from N,N'-disubstituted thioureas using TsCl/NaOH. *Tetrahedron* **2004**, *60*, 9883-9888.

106. Woodward, R. B.; Baer, H. Studies on Diene-addition Reactions. II.1 The Reaction of 6,6-Pentamethylenefulvene with Maleic Anhydride. *J. Am. Chem. Soc.* **1944**, *66*, 645-649.

107. Catchpole, A. G.; Hughes, E. D.; Ingold, C. K. Rearrangement and substitution in anionotropic systems. Part III. Mechanism of, and equilibrium in, anionotropic change. *J. Chem. Soc.* **1948**, 8-17.

108. Meisenheimer, J.; Link, J. Über die Verschiebung in der Allyl-Gruppe. 3. Mitteilung über Substitution und Addition. *Justus Liebigs Ann. Chem.* **1930**, *479*, 211-277.

109. Berson, J. A. Kinetics, Thermodynamics, and the Problem of Selectivity: The Maturation of an Idea. *Angewandte Chemie International Edition* **2006**, *45*, 4724-4729.

110. Wang, Y.; He, J.; Liu, C.; Chong, W. H.; Chen, H. Thermodynamics versus Kinetics in Nanosynthesis. *Angewandte Chemie International Edition* **2015**, *54*, 2022-2051.

111. Barreiro, E. J. Privileged Scaffolds in Medicinal Chemistry: An Introduction. In *Privileged Scaffolds in Medicinal Chemistry: Design, Synthesis, Evaluation*; Brase, S., Ed.; Royal Society of Chemistry: 2016; .

112. Su, D. -.; Lim, J. J.; Tinney, E.; et al. Substituted tetrahydroquinolines as potent allosteric inhibitors of reverse transcriptase and its key mutants. *Bioorg. Med. Chem. Lett.* **2009**, *19*, 5119-5123.

113. Muraglia, E.; Kinzel, O.; Laufer, R.; et al. Tetrazole thioacetanilides: Potent non-nucleoside inhibitors of WT HIV reverse transcriptase and its K103N mutant. *Bioorg. Med. Chem. Lett.* **2006**, *16*, 2748-2752.

114. De La Rosa, M.; Kim, H. W.; Gunic, E.; et al. Tri-substituted triazoles as potent non-nucleoside inhibitors of the HIV-1 reverse transcriptase. *Bioorg. Med. Chem. Lett.* **2006**, *16*, 4444-4449.

115. O'Meara, J. A.; Jakalian, A.; LaPlante, S., et al. Scaffold hopping in the rational design of novel HIV-1 non-nucleoside reverse transcriptase inhibitors. *Bioorg. Med. Chem. Lett.* **2007**, *17*, 3362-3366.

116. Gagnon, A.; Amad, M. H.; Bonneau, P. R.; et al. Thiotetrazole alkynylacetanilides as potent and bioavailable non-nucleoside inhibitors of the HIV-1 wild type and K103N/Y181C double mutant reverse transcriptases. *Bioorg. Med. Chem. Lett.* **2007**, *17*, 4437-4441.

# Appendix A.

## Experimental Information for Chapter 2

### General

L-Homoserine was purchased from TCI Chemicals and EYPC was purchased from Avanti Polar Lipids. All other chemicals were purchased from Sigma, Fisher, or Acros. Reactions were monitored by thin layer chromatography using silica gel plates with F254 indicator. Plates were visualized using UV and $I_2$. Products were purified by silica gel column chromatography (silica gel 60, particle size 0.04mm-0.063mm) or size exclusion chromatography (Sephadex G-10 purchased from Sigma). NMR spectra were taken on a Varian Mercury instrument operating at 299.865 MHz or an Agilent 400 MHz NMR operating at 400.130 MHz. Chemical shifts were reported in ppm relative to the residual solvent peak. The $^{13}C$ NMR spectra were taken on the same instruments at 75.408 MHz and 100.613 respectively. All NMRs were taken in DMSO-$d_6$. Mass spectra were recorded on a Micromass Q-TOF 2 instrument (Manchester, UK) or a LCMS-IT-TOF (Shimadzu Corporation, Columbia, MD) using the electrospray technique (positive mode). All spectrophotometric experiments were carried out on a Fluoromax 3 (Jobin-Yvon/Horriba) spectrophotometer. Microcalorimic titrations were performed using a VP-ITC microcalorimeter (MicroCal, LLC, Northampton, MA) and analyzed using Origin-7 software.

**Methyl homoserinate hydrochloride (i)**

L-Homoserine (0.536 g, 4.50 mmol) was suspended in methanol (21.5 mL) under inert atmosphere. The suspension was cooled to $0^0$C. Trimethylsilyl chloride (0.125 mL, 9.90 mmol) was added dropwise via syringe. The reaction was stirred for 22 hours at $20^0$C. The solvent was removed using a high vacuum rotary evaporator to give the product in quantitative yield. This compound has been previously synthesized. $^1$H NMR (300 MHz, DMSO-$d_6$) δ 8.45 (br s, 2H), 4.45 (t, *J* = 9.5 Hz, 1H), 4.41 – 4.18 (m, 2H), 4.07 (br s, 1H), 3.74 (s, 3H), 2.58 (m, 1H), 2.43 – 2.16 (m, 1H).

**Methyl (tert-butoxycarbonyl)homoserinate (ii)**

Methyl homoserinate hydrochloride **(i)** (0.743 g, 4.38 mmol) was suspended in anhydrous acetonitrile (15 mL) at $20^0$C. Boc anhydride (1.05 g, 4.95 mmol) was added to the suspension. Triethylamine (1.22 mL, 9.0 mmol) was added slowly via syringe and the reaction was stirred for 16 hours. Methylene chloride (60 mL) was added to the reaction. The organic layer was washed with distilled water, followed by 1 N HCl, saturated sodium bicarbonate and brine. The organic layer was dried over anhydrous sodium sulfate and then evaporated to give a white solid containing the desired product as well as the lactone by product. This was used in the next step without further purification. This compound had been previously synthesized. $^1$H NMR (300 MHz, $CDCl_3$) δ ppm 1.45 (s, 9H), 2.23-2.30 (m, 1H), 2.63-2.72 (m, 1H), 3.75 (s, 3H), 4.21-4.30 (m. 2H), 4.40 (br s, 1H), 4.43 (t, *J*=3 Hz, 1H), 5.59 (br s, 1H).

**Methyl 4-bromo-2-((tert-butoxycarbonyl)amino)butanoate (iii)**

The N-boc-Hse-OMe and lactone by product from **(ii)** was dissolved in anhydrous methylene chloride (20 mL) and cooled to $0^0$C. Carbon tetrabromide (1.052 g, 4.95 mmol) and triphenylphosphine (0.832 g, 4.95 mmol) were added to the solution in that order. The reaction was allowed to come to room temperature and stir for a total of 90 minutes. The solvent was removed by rotary evaporation to give an orange solid. This was dissolved in ethyl acetate and then filtered. The filtrate was collected and evaporated. The solid was then dissolved in a minimal amount of ethyl acetate and hexanes (3:7). The filtrate was added to a silica gel column. The final product was eluted with the same ethyl acetate and hexanes mixture. The overall yield for these three steps was 15%. $^1$H NMR (300 MHz, $CDCl_3$) δ ppm 1.44 (s, 9H), 2.15-2.27 (m, 1H), 2.34-2.47 (m, 1H), 3.43 (t, *J*=2 Hz, 2H), 3.76 (s, 3H), 4.41 (t, *J*=3 Hz, 1 H), 5.13 (br s, 1H); $^{13}$C NMR (75 MHz, $CDCl_3$) δ 192.67, 149.09, 107.87, 77.70, 77.27, 76.84, 71.16, 67.86, 67.64, 52.83, 36.06, 29.71, 28.49, 24.03, 0.21. ESI MS *m/z* 296.07 and 298.07 $(M+H)^+$ found, calculated for $C_{10}H_{19}BrNO_4$, 296.04.

**Sodium 8-(3-((tert-butoxycarbonyl)amino)-4-methoxy-4-oxobutoxy)-3a1,9-dihydropyrene-1,3,6-trisulfonate (iv)**

HPTS (0.048 g, 0.101 mmol) and cesium carbonate (0.132 g, 0.404 mmol) were suspended in anhydrous acetone (6 mL; pH 8). Tetrabutylammonium fluoride (150 uL) was added until all HPTS was in solution. N-boc-Br-Homoserine methyl ester (0.030 g, 0.101 mmol) was added to the solution. The reaction was stirred for 20 hours at $45^0$C. During the course of the reaction, the solution turned orange and some of the unreacted HPTS dropped out of solution. The unreacted

HPTS was removed via filtration and the filtrate was collected and the solvent removed on a rotary evaporator. The product was purified on a silica gel column, using methanol/chloroform (1:5) to elute. Once the product started coming off the column, the solvent was gradually increased to 35% methanol/65% chloroform. After collecting and drying the product, the HPTS-boc-Hse-TBAF conjugate was dissolved in 5 mL acetone and 20 equivalents of NaI (0.250 g) was added. The solution was stirred overnight to remove the TBAF. The HPTS-boc-HSE conjugate precipitated out of the acetone and was collected via centrifugation. Yield: 0.052 g, 70% $^{1}$H NMR (300 MHz, DMSO-$D_6$) δ ppm 1.38 (s, 9H), 2.24-2.35 (m, 1H), 2.39-2.50 (m, 1H), 3.64 (s, 3H), 4.40-4.49 (m, 3H), 7.56 (br s, 1H), 8.18 (s, 1H), 8.34 (d, *J*=3 Hz, 1 H), 8.92 (d, *J*=1 Hz, 1H), 9.01 (d, *J*= 4 Hz, 1H), 9.10 (d, *J*=2 Hz, 1H), 9.16 (s, 1H). $^{13}$C NMR (75 MHz, DMSO) δ 220.04, 207.31, 156.26, 143.82, 141.25, 140.35, 140.13, 128.70, 128.32, 126.98, 126.57, 126.08, 125.77, 125.10, 121.18, 79.07, 52.61, 49.27, 40.97, 40.69, 40.41, 40.13, 39.86, 39.58, 39.30, 31.40, 28.83. ESI MS *m/z* 185.15 $(M+H)^{4+}$ found, calculated for $C_{26}H_{26}NNa_3O_{14}S_3$ 741.02.

**Sodium 8-(3-amino-3-carboxypropoxy)-3a1,9-dihydropyrene-1,3,6-trisulfonate (v)**

To remove the boc protecting group, HPTS-boc-Hse was stirred in TFA and DCM (1:1) for 3 hours. The TFA was then removed via rotary evaporator. The HPTS-Hse TFA salt was then dissolved in deionized water and sodium bicarbonate was used to adjust the pH from 1 to 7. The salts were removed by running the crude on a Sephadex column, eluting with di$H_2O$. $^{1}$H NMR (300 MHz, DMSO-$D_6$) δ ppm 2.09-2.19 (m, 1H), 2.29-2.39 (m, 1H), 3.64 (s, 3H), 3.72 (t, *J*=2 Hz, 1H), 4.42-4.47 (m, 2H), 8.16 (s, 1H), 8.32 (d, *J*=3 Hz, 1H), 8.92 (d, *J*=3 Hz, 1H), 9.00 (d, *J*=2 Hz, 1H), 9.05 (d, *J*=3 Hz, 1H), 9.14 (s, 1H). $^{13}$C NMR (300 MHz, DMSO-$D_6$) δ ppm 38.95,

49.16, 50.53, 60.38, 121.35, 121.60, 121.72, 124.19, 125.77, 127.14, 128.42, 128.86, 137.85, 139.90, 143.60, 151.75, 171.76. . ESI MS *m/z* 161.05 $(M+H)^{4+}$. Calculated for $C_{20}H_{16}NNa_3O_{12}S_3$ 626.95

**Methyl 2-((tert-butoxycarbonyl)amino)-4-(phenylamino)butanoate (vi)**

Aniline (2.50 mmol), sodium bicarbonate (3 mmol), and sodium dodecyl sulfate (10 mg) were dissolved in deionized water (10mL) and heated to $45^0$C for ten minutes. Then N-boc-Br-Homoserine methyl ester (3 mmol) was added to the reaction. The reaction was run at $45^0$C for 48 hours and then the solvent was removed by rotary evaporation. The product was purified on a silica gel column using 1:9 Ethyl acetate/hexanes. $^1$H NMR (300 MHz, $CDCl_3$) δ ppm 1.46 (s, 9H), 1.81-1.93 (m, 1H), 2.11-2.22 (m, 1H), 3.17-3.32 (m, 2H), 3.70 (s, 3H), 4.42 (t, *J*=5 Hz, 1H), 5.20 (br s, 1H), 6.59 (d, *J*=3 Hz, 2H), 6.70 (t, *J*=3 Hz, 1H), 7.17 (t, *J*=2 Hz, 2 H), 7.26 (br s, 1H). $^{13}$C NMR (75 MHz, DMSO) δ 171.76, 170.57, 159.91, 159.41, 158.91, 158.41, 151.75, 143.60, 140.13, 139.95, 139.90, 137.85, 128.86, 128.42, 127.14, 125.77, 124.19, 121.72, 117.88, 114.05, 110.21, 86.51, 79.79, 60.38, 53.58, 50.53, 49.16, 40.76, 40.48, 40.38, 40.21, 39.93, 39.65, 39.37, 39.09, 38.95, 31.19, 30.42. ESI MS *m/z* 309.20 $(M+H)^+$ found, calculated for $C_{16}H_{25}N_2O_4$ 309.17.

**2-amino-4-(phenylamino)butanoic acid (vii)**

The protecting group was removed using the same procure as in **(v)**. Instead of a column, the product was extracted into ethyl acetate and the solvent removed. Overall Yield: 30% $^1$H NMR (600 MHz, $CDCl_3$) δ ppm 1.89-1.94 (m, 1H) 2.07-2.12 (m, 1H), 3.18 (br s, 3H), 3.28-3.37 (m, 2H), 3.60-3.70 (m, 1H), 3.71 (s, 3H), 6.62 (d, j=2 Hz, 2H), 6.72 (d, j=1 Hz, 1H), 7.19 (t, j=2 Hz,

2H). $^{13}C$ NMR (75 MHz, $CDCl_3$) δ 173.38, 147.93, 129.48, 117.66, 113.08, 80.37, 77.64, 77.42, 77.22, 76.80, 52.59, 51.71, 41.24, 40.04, 36.14, 32.57, 29.90, 28.52, 28.50, 28.42, 27.97, 1.22, 0.20. ESI MS (DI, MeOH) *m/z* 209.22 $(M+H)^+$ found, calculated for $C_{11}H_{16}N_2O_2$ 208.12.

**Synthesis of cyclen 2 lipid**

Prepared as directed.[67]

**Preparation of Liposomes**

Egg yolk L-α-phosphatidylcholine and cyclen **2** lipid were combined in ethanol to make a 98.5% EYPC/1.5% cyclen **2** lipid mixture. The solvent was removed on a high vacuum to make a thin lipid film. This lipid film was hydrated in 2 mL PBS (10 mM sodium phosphate, 100 mM NaCl, pH 7.4) containing 50 nM Rhodamine B. During hydration the mixture was subjected to 5 freeze- thaw cycles (dry ice/acetone bath, room temperature water bath). The resulting suspension was subjected to 21 high pressure extrusions through a 0.4 uM polycarbonate membrane to afford liposomes. These were purified via size exclusion chromatography using Sephadex G-10 and PBS minus Rhodamine B as the eluant. The liposomes eluted over 1.7 mL.

**Patchclamp Recordings**

α1GlyR-HEK293 cells (generously provided by Jensen[102]) were bathed in the extracellular recording solution (ECS). The cells were constantly perfused with the ECS using a gravity fed perfusion system. Micropipettes of approx. 2-3 MΩ resistance were used to patch each individual cell. The micropippettes contained a silver wire electrode and inctracellular solution (ICS). Voltage clamp readings were taken in the whole cell configuration using the range of

concentrations tested. Glycine and homoserine solutions were prepared in distilled water at 100x the concentrations needed and diluted with ECS. The concentration-response relationship was modeled using the Hill equation $I = I_{max}/ (1 + (EC_{50}/[drug])^{n})$ where I is the current induced by the drug at that concentration, $I_{max}$ is the maximum current the drug can induce, $EC_{50}$ is the concentration that gives half of the maximal current and n is the Hill coefficient[102].

**Isothermal Titration Calorimetry**

0.25 mM aniline-Hse and 5 mM cyclen-OMe receptor was prepared in MeOH. The solution of cyclen-OMe was in the syringe and injected into the cell containing the aniline-Hse solution. The reference cell contained pure methanol. Injections were 7 uL. There were a total of 35 with 300 s between each injection. The temperature was set to 25C. Data was corrected using a dilution experiment in which the same cyclen-OMe solution was titrated into a cell of pure MeOH.

## Appendix B.

## Experimental Information for Chapter 3

### General Information:

All chemicals were purchased from Sigma, Aldrich, Fisher, or Acros. Reactions were monitored by thin layer chromatography using silica gel plates with F254 indicator (200 uM from Dynamic Adsorbents). The formation of imidithiozolidinones using N-alkoxy-thioureas was monitored by eluting plates in 5:95 MeOH:DCM. The N-alkyl-thiourea reactions were monitored by eluting plates in 1:99 EtOAc:DCM. Plates were visualized using UV and $I_2$. Products were purified by silica gel column chromatography (silica gel 60, particle size 0.04mm-0.063mm). NMR spectra were taken on a Varian Mercury instrument operating at 299.865 MHz or an Agilent 400 MHz NMR operating at 400.130 MHz. Chemical shifts were reported in ppm relative to the residual solvent peak. The $^{13}C$ NMR spectra were taken on the same instruments at 75.408 MHz and 100.613 respectively. All NMRs were taken in DMSO-$d_6$. Mass spectra were recorded on a ThermoFisher Scientific LTQ Orbitrap Velos using the electrospray technique (positive mode).

### 1-(2-hydroxyethyl)-3-(naphthalen-1-yl)thiourea (1)

1-naphthyl isothiocyanate (0.250 g, 1.35 mmol) was dissolved in ethyl acetate (10 mL). Ethanolamine (0.0815 mL, 1.35 mmol) was added and the reaction was stirred at room temperature for 1 hr. The solvent was removed *in vacuo*. The crude solid was recrystallized in

toluene to give **1** as a white powder (0.293 g, 88 %). This compound was previously characterized.[64]

**3-(2-hydroxyethyl)-2-(naphthalen-1-ylimino)thiazolidin-4-one (1a)**

**1** (0.106 g, 0.43 mmol) was dissolved in dichloromethane (10 mL) and triethylamine (0.120 mL, 0.86 mmol) was added. The mixture was stirred for 10 minutes and then bromoacetyl bromide (0.0477 mL, 0.516 mmol) in dichloromethane (1 mL) was added dropwise within five minutes. This reaction was stirred at room temperature for 8 hr. The crude was washed once with water (15 mL) and once with brine (15 mL) and then was concentrated under reduced pressure. The crude oil was purified using column chromatography (silica gel, MeOH/DCM 1:99) to give **1a** as an orange oil (.0818 g, 67 %) $^{1}$H NMR (300 MHz, DMSO-$d_6$) δ 7.92 (d, $J$ = 9.1 Hz, 2H), 7.78 – 7.64 (m, 1H), 7.64 – 7.32 (m, 3H), 7.16 – 6.91 (m, 1H), 4.99 (t, $J$ = 6.0 Hz, 1H), 4.02 (s, 2H), 3.97 (t, $J$ = 6.2 Hz, 2H), 3.76 (q, $J$ = 6.1 Hz, 2H); $^{13}$C NMR (75 MHz, dmso) δ 172.15, 156.14, 144.56, 133.93, 127.89, 126.87, 126.45, 125.96, 125.70, 124.14, 123.22, 115.16, 57.23, 44.90, 32.60. MS (ESI) ([M+H]$^{+}$): found 287.08, calculated for $C_{15}H_{15}N_2O_2S$ 287.08.

**2-((2-hydroxyethyl)imino)-3-(naphthalen-1-yl)thiazolidin-4-one (1b)**

**1** (0.142 g, 0.576 mmol) was dissolved in anhydrous THF (6 mL) and triethylamine (0.0583 mL, 0.576 mmol) was added. The mixture was stirred for 10 minutes and then bromoacetyl bromide (0.0533 mL, 0.576 mmol) in THF (1 mL) was added dropwise within 5 minutes. The reaction was stirred at room temperature for 11 hr. The precipitate that formed was collected by vacuum filtration. The solid was rinsed with THF followed by DCM. This solid, crude **1b**, was suspended in DCM (10 mL) and triethylamine (0.0583 mL, 0.576 mmol) was added to neutralize the HBr

that had formed. This was then washed 2x with water (15 mL) and once with brine (15 mL). The organic layer was then dried over $MgSO_4$ and the solvent removed *in vacuo* to give **1b** as a pale yellow oil (0.103 g, 63 %). The filtrate from the reaction was concentrated under reduced pressure to yield crude **1a**, which was purified using the same column conditions as above to give 0.0429g (26 %). **1b** was characterized as follows: $^1$H NMR (400 MHz, DMSO-$d_6$) δ 8.04 (d, $J$ = 8.4 Hz, 2H), 7.77 – 7.39 (m, 6H), 4.53 (s, 1H), 4.48 – 4.19 (m, 2H), 3.33 (d, $J$ = 5.8 Hz, 2H), 3.30 – 3.14 (m, 2H); $^{13}$C NMR (101 MHz, DMSO) δ 170.67, 152.61, 132.70, 131.35, 128.38, 127.92, 127.12, 126.16, 125.77, 125.21, 124.59, 121.36, 59.43, 53.29, 31.52. MS (ESI) ($[M+H]^+$): found 287.08, calculated for $C_{15}H_{15}N_2O_2S$ 287.08.

**1-(4-bromophenyl)-3-(2-hydroxyethyl)thiourea (2)**

4-Bromophenyl isothiocyanate (0.250 g, 1.17 mmol) was dissolved in ethyl acetate (10 mL). Ethanolamine (0.0705 mL, 1.17 mmol) was added and the reaction was stirred at room temperature for 11 hr. The solvent was removed *in vacuo*. The crude solid was recrystallized in toluene to give **4a** as a white powder (0.284 g, 88 %). $^1$H NMR (300 MHz, DMSO-$d_6$) δ 9.67 (s, 1H), 7.82 (s, 1H), 7.46 (m, 4H), 4.82 (s, 1H), 3.54 (m, 4H); $^{13}$C NMR (75 MHz, dmso) δ 180.43, 138.94, 131.24, 124.61, 115.69, 59.16, 46.43. MS (ESI) ($[M+H]^+$): found 274.98 and 276.98, calculated for $C_9H_{12}BrN_2OS$ 274.98.

**2-((4-bromophenyl)imino)-3-(2-hydroxyethyl)thiazolidin-4-one (2a)**

**2** (0.100 g, 0.363 mmol) was dissolved in anhydrous THF (5 mL) and triethylamine (0.0506 mL, 0.363 mmol) was added. The mixture was stirred for 10 minutes and then bromoacetyl bromide (0.0336 mL, 0.363 mmol) in THF (1 mL) was added dropwise within 5 minutes. The reaction

was stirred at room temperature for 8 hr. The reaction mixture was vacuum filtered to remove the precipitate. The filtrate was concentrated *in vacuo* and then redissolved in DCM (10 mL). The crude was washed once with water (15 mL) and once with brine (15 mL) and then dried over $MgSO_4$. The solvent was removed to give **2a** as an orange oil (0.0404 g, 78 %). $^1$H NMR (300 MHz, DMSO-$d_6$) δ 7.54 (d, $J$ = 8.7 Hz, 2H), 6.90 (d, $J$ = 8.7 Hz, 2H), 4.85 (s, 1H), 4.03 (s, 2H), 3.79 (t, $J$ = 6.3 Hz, 2H), 3.61 (t, $J$ = 5.9 Hz, 2H); $^{13}$C NMR (75 MHz, dmso) δ 168.99, 153.19, 144.50, 129.17, 120.25, 113.42, 53.91, 41.68, 29.68. MS (ESI) ($[M+H]^+$): found 314.98 and 316.98, calculated for $C_{11}H_{12}BrN_2O_2S$ 314.98.

**3-(4-bromophenyl)-2-((2-hydroxyethyl)imino)thiazolidin-4-one (2b)**

**2** (0.100 g, 0.363 mmol) was dissolved in anhydrous THF (5 mL) and triethylamine (0.0506 mL, 0.363 mmol) was added. The mixture was cooled to -78°C using an acetone/dry ice bath. It was stirred for 10 minutes and then bromoacetyl bromide (0.0336 mL, 0.363 mmol) in THF (1 mL) was added dropwise within 5 minutes. After the reaction was stirred at -78°C for 6.5 hr, it was allowed to come up to room temperature. The precipitate that formed was collected by vacuum filtration. The solid was rinsed with THF followed by DCM. This solid, crude **2b**, was suspended in DCM (10 mL) and triethylamine (0.0506 mL, 0.363 mmol) was added to neutralize the HBr that had formed. This was then washed 2x with water (15 mL) and once with brine (15 mL). The organic layer was then dried over $MgSO_4$ and the solvent removed in vacuo to give **2b** as a pale orange oil (0.0741 g, 65 %). $^1$H NMR (400 MHz, DMSO-$d_6$) δ 7.66 (d, $J$ = 8.8 Hz, 2H), 7.26 (d, $J$ = 8.7 Hz, 2H), 4.59 (s, 1H), 3.45 (q, $J$ = 6.0 Hz, 2H), 3.24 (t, $J$ = 6.2 Hz, 2H); $^{13}$C NMR (101 MHz, DMSO) δ 171.78, 153.87, 135.29, 132.28, 131.16, 121.69, 61.18, 54.92, 33.00. MS (ESI) ($[M+H]^+$): found 314.98 and 316.98, calculated for $C_{11}H_{12}BrN_2O_2S$ 314.98.

**1-(2-hydroxyethyl)-3-(4-nitrophenyl)thiourea (3)**

4-nitrophenyl isothiocyanate (0.250 g, 1.39 mmol) was dissolved in ethyl acetate (10 mL). Ethanolamine (0.0837 mL, 1.39 mmol) was added and the reaction was stirred at room temperature for 11 hr. The solvent was removed *in vacuo*. The crude solid was recrystallized in toluene to give **3** as a pale yellow powder (0.280 g, 83 %). $^{1}$H NMR (400 MHz, DMSO-$d_6$) δ 10.23 (s, 1H), 8.24 (s, 1H), 8.17 (d, $J$ = 9.3 Hz, 2H), 7.88 (d, $J$ = 9.2 Hz, 2H), 4.89 (s, 1H), 3.57 (s, 4H); $^{13}$C NMR (101 MHz, DMSO) δ 180.51, 146.89, 142.22, 124.96, 120.67, 59.29, 46.97. MS (ESI) ($[M+H]^+$): found 242.06, calculated for $C_9H_{12}N_3O_3S$ 242.05.

**3-(2-hydroxyethyl)-2-((4-nitrophenyl)imino)thiazolidin-4-one (3a)**

**3** (0.20 g, 0.83 mmol) was dissolved in anhydrous THF (8 mL) and triethylamine (0.116 mL, 0.83 mmol) was added. The mixture was stirred for 10 minutes and then bromoacetyl bromide (0.0766 mL, 0.83 mmol) in THF (1 mL) was added dropwise within 5 minutes. The reaction was stirred at room temperature for 8 hr. The reaction mixture was vacuum filtered and the precipitate was reserved for further purification (see **3b** below). The filtrate was concentrated *in vacuo*. This crude was purified using column chromatography (silica gel, MeOH/DCM 1:99) to give **3a** as a hard yellow oil (0.067 g, 28%). For **3a**:$^{1}$H NMR (400 MHz, DMSO-$d_6$) δ 8.24 (d, $J$ = 9.0 Hz, 2H), 7.16 (d, $J$ = 9.1 Hz, 2H), 4.08 (s, 2H), 3.81 (t, $J$ = 6.2 Hz, 2H), 3.62 (t, $J$ = 6.2 Hz, 3H), 3.40 (t, $J$ = 7.5 Hz, 1H). $^{13}$C NMR (101 MHz, DMSO) δ 171.91, 157.26, 154.50, 143.71, 125.23, 122.01, 56.89, 44.77, 32.93. MS (ESI) ($[M+H]^+$): found 282.05, calculated for $C_{11}H_{12}N_3O_4S$ 282.05.

**2-((2-hydroxyethyl)imino)-3-(4-nitrophenyl)thiazolidin-4-one (3b)**

The precipitate separated from the crude of **3a** was rinsed with THF followed by DCM. The solid was then suspended in DCM (10 mL) and triethylamine (0.116 mL, 0.83 mmol) was added to neutralize the HBr. The solid dissolved completely after 30 s of sonication. This was washed once with water (15 mL) and once with brine (15 mL) and the organic layer was dried over $MgSO_4$. The solvent was removed *in vacuo* to give **3b** as a light yellow solid (0.162 g, 69%). For **3b**: $^1$H NMR (300 MHz, DMSO-$d_6$) δ 8.33 (d, $J$ = 9.1 Hz, 2H), 7.64 (d, $J$ = 9.1 Hz, 2H), 4.20 (s, 2H), 3.47 (t, $J$ = 6.1 Hz, 2H), 3.28 (t, $J$ = 6.1 Hz, 2H); $^{13}$C NMR (75 MHz, dmso) δ 170.89, 147.75, 139.06, 130.26, 124.74, 109.54, 59.40, 52.24, 34.06. MS (ESI) ($[M+H]^+$): found 282.05, calculated for $C_{11}H_{12}N_3O_4S$ 282.05.

**1-(2-hydroxyethyl)-3-(4-methoxyphenyl)thiourea (4)**

4-methoxyphenyl isothiocyanate (0.211 mL, 1.51 mmol) was dissolved in ethyl acetate (10 mL). Ethanolamine (0.0913 mL, 1.51 mmol) was added and the reaction was stirred at room temperature for 1 hr. The solvent was removed *in vacuo*. The crude solid was recrystallized in toluene to give **4** as a white powder (0.315 g, 92 %). $^1$H NMR (300 MHz, DMSO-$d_6$) δ 9.41 (s, 1H), 7.46 (s, 1H), 7.24 (d, $J$ = 8.9 Hz, 2H), 6.89 (d, $J$ = 9.0 Hz, 2H), 4.78 (s, 1H), 3.73 (s, 3H), 3.51 (d, $J$ = 4.8 Hz, 4H); $^{13}$C NMR (75 MHz, dmso) δ 180.81, 156.47, 131.83, 125.73, 113.92, 59.38, 55.27, 46.5. MS (ESI) ($[M+H]^+$): found 227.08,calculated for $C_{10}H_{15}N_2O_2S$ 227.08.

**3-(2-hydroxyethyl)-2-((4-methoxyphenyl)imino)thiazolidin-4-one (4a)**

**4** (0.227 g, 1.0 mmol) was dissolved in anhydrous THF (8 mL) and triethylamine (0.140 mL, 1.0 mmol) was added. The mixture was stirred for 10 minutes and then bromoacetyl bromide

(0.0927 mL, 1.0 mmol) in THF (1 mL) was added dropwise within 5 minutes. The reaction was stirred at room temperature for 11 hr. The solvent was removed *in vacuo* and the crude was redissolved in DCM (10 mL). Triethylamine (0.140 mL, 1.0 mmol) was added to neutralize the HBr that had formed. This was then washed once with water (15 mL) and once with brine (15 mL). The organic layer was concentrated *in vacuo.* A column was used to purify the crude (silica gel, MeOH/DCM (1:99) to give **4a** as an off-white solid (0.159 g, 60 %). $^{1}$H NMR (300 MHz, DMSO-$d_6$) δ 6.90 (q, $J$ = 9.0 Hz, 4H), 3.99 (s, 2H), 3.79 (t, $J$ = 6.4 Hz, 2H), 3.74 (s, 3H), 3.60 (t, $J$ = 6.3 Hz, 2H), 3.38 (s, 3H); $^{13}$C NMR (75 MHz, dmso) δ 171.99, 156.04, 154.91, 141.09, 121.94, 114.46, 56.96, 55.18, 44.62, 32.48. MS (ESI) ($[M+H]^+$): found 267.08, calculated for $C_{12}H_{15}N_2O_3S$ 267.07.

**1-butyl-3-(2-hydroxyethyl)thiourea (5)**

Butyl isothiocyanate (0.209 mL, 1.74 mmol) was dissolved in ethyl acetate (10 mL). Ethanolamine (0.1048 mL, 1.74 mmol) was added. The reaction was stirred at room temperature for 16 hr. The reaction was concentrated *in vacuo* and the crude oil was recrystallized using a mixed solvent system of ethyl acetate and cyclohexane to give **5** as a white powder (0.251 g, 82 %). $^{1}$H NMR (400 MHz, DMSO-$d_6$) δ 7.48 (s, 1H), 7.31 (s, 1H), 4.76 (s, 1H), 3.65 – 3.39 (m, 4H), 1.44 (q, $J$ = 7.5 Hz, 2H), 1.38 – 1.18 (m, 2H), 0.89 (t, $J$ = 7.3 Hz, 3H). $^{13}$C NMR (101 MHz, DMSO) δ 158.39, 60.14, 55.38, 46.62, 31.36, 20.03, 14.19. MS (ESI) ($[M+H]^+$): found 177.10, calculated for $C_7H_{17}N_2OS$ 177.10.

**2-(2-(butylimino)thiazolidin-3-yl)ethan-1-ol (5a)**

**5** (0.197 g, 1.12 mmol) was dissolved in anhydrous THF (10 mL) and triethylamine (0.156 mL, 1.12 mmol) was added. The reaction was stirred for 10 minutes then bromoacetyl bromide (0.098

mL, 1.12 mmol) was added dropwise within 5 minutes. The reaction was stirred at room temperature for 24 hr. The solvent was removed *in vacuo* and the crude was purified using column chromatography (silica gel, MeOH/DCM 1:99) to give **5a** as an oil (0.048 g, 20 %). $^{1}$H NMR (400 MHz, DMSO-$d_6$) δ 4.76 (t, *J* = 5.9 Hz, 1H), 3.98 (d, *J* = 7.1 Hz, 2H), 3.65 (t, *J* = 6.4 Hz, 2H), 3.62 – 3.54 (m, 1H), 3.49 (q, *J* = 6.3 Hz, 2H), 3.20 (t, *J* = 6.7 Hz, 2H), 1.65 – 1.41 (m, 2H), 1.41 – 1.28 (m, 2H), 0.89 (t, *J* = 7.4 Hz, 3H). $^{13}$C NMR (101 MHz, DMSO) δ 172.10, 152.60, 57.48, 55.38, 51.42, 44.76, 32.82, 20.42, 14.23. MS (ESI) ($[M+H]^+$): found 217.10, calculated for $C_9H_{17}N_2O_2S$ 217.09.

**1-(1-hydroxypropan-2-yl)-3-(naphthalen-1-yl)thiourea (6)**

1-naphthyl isothiocyanate (0.125 g, 0.675 mmol) was dissolved in ethyl acetate (6 mL). 2-amino-1-propanol (0.0521 mL, 0.675 mmol) was added and the reaction was stirred at room temperature for 16 hr. The solvent was removed *in vacuo* to give an oil. The crude was recrystallized using a mixed solvent system of ethyl acetate and cyclohexane to give **6** as a white powder (0.095 g, 54%). $^{1}$H NMR (300 MHz, DMSO-$d_6$) δ 9.56 (s, 1H), 8.30 – 7.73 (m, 4H), 7.68 – 7.28 (m, 5H), 4.85 (s, 1H), 4.55 – 4.15 (m, 1H), 3.58 – 3.42 (m, 3H), 1.12 (d, 3H); $^{13}$C NMR (75 MHz, dmso) δ 181.34, 134.80, 133.96, 129.70, 128.19, 126.37, 126.18, 125.66, 124.93, 122.84, 63.91, 51.51, 16.98. MS (ESI) ($[M+H]^+$): found 261.10, calculated for $C_{14}H_{17}N_2OS$ 261.10.

**3-(1-hydroxypropan-2-yl)-2-(naphthalen-1-ylimino)thiazolidin-4-one (6a)**

**6** (0.095 g, 0.518 mmol) was dissolved in anhydrous THF (5 mL) and triethylamine (0.0722 mL, 0.518 mmol) was added. The mixture was stirred for 10 minutes and then bromoacetyl bromide

(0.0479 mL, 0.518 mmol) in THF (1 mL) was added dropwise within five minutes. The reaction was stirred at room temperature for 21 hr. Triethylamine (0.0722 mL, 0.518 mmol) was added and after stirring for 5 minutes, the solvent was removed *in vacuo*. The crude was dissolved in DCM (10 mL) and washed once with water (15 mL) and once with brine (15 mL) and dried over $MgSO_4$. The solvent was removed again and the crude oil was purified using column chromatography (silica gel, MeOH/DCM 1:99) to give **6a** as a hard oil (0.042 g, 27 %) and **6b** (0.026 g, 17 %). For **6a**: $^{1}$H NMR (300 MHz, DMSO-$d_6$) δ 10.07 (s, 1H), 8.53 (d, *J* = 7.1 Hz, 1H), 8.06 (d, *J* = 6.2 Hz, 1H), 7.93 (d, *J* = 3.2 Hz, 1H), 7.72 (dd, *J* = 28.6, 7.8 Hz, 2H), 7.60 – 7.32 (m, 3H), 4.21 – 3.99 (m, 1H), 3.89 (s, 2H), 3.70 – 3.51 (m, 2H), 1.18 (d, *J* = 6.7 Hz, 3H); $^{13}$C NMR (75 MHz, dmso) δ 168.13, 165.49, 134.11, 133.73, 128.59, 128.08, 126.52, 126.34, 126.01, 125.86, 122.95, 121.88, 48.52, 33.99, 31.13, 19.02. MS (ESI) ($[M+H]^+$): found 301.10, calculated for $C_{16}H_{17}N_2O_2S$ 301.09.

**2-((1-hydroxypropan-2-yl)imino)-3-(naphthalen-1-yl)thiazolidin-4-one (6b)**

Synthesized and purified as stated above (see **6a).** For **6b**: $^{1}$H NMR (400 MHz, DMSO-$d_6$) δ 8.04 (d, *J* = 8.8 Hz, 2H), 7.76 – 7.51 (m, 4H), 7.48 (d, *J* = 8.2 Hz, 1H), 4.49 (s, 1H), 4.41 (d, *J* = 16.9 Hz, 1H), 4.25 (d, *J* = 16.9 Hz, 1H), 3.51 (dd, *J* = 11.3, 5.8 Hz, 1H), 3.27 – 3.10 (m, 1H), 3.08 – 2.90 (m, 1H), 0.83 (d, *J* = 6.2 Hz, 2H). 13C NMR (101 MHz, DMSO) δ 206.94, 172.28, 134.31, 133.02, 130.01, 129.54, 128.75, 127.73, 127.31, 126.82, 126.20, 122.97, 66.41, 60.08, 33.20, 21.73. MS (ESI) ($[M+H]^+$): found 301.10, calculated for $C_{16}H_{17}N_2O_2S$ 301.09

**1-(2-hydroxypropyl)-3-(naphthalen-1-yl)thiourea (7)**

1-naphthyl isothiocyanate (0.125 g, 0.675 mmol) was dissolved in ethyl acetate (6 mL). 1-amino-2-propanol (0.0521 mL, 0.675 mmol) was added and the reaction was stirred at room temperature for 16 hr. The solvent was removed *in vacuo*. The crude was recrystallized in toluene to give **7** as a white powder (0.133 g, 76%). $^{1}$H NMR (300 MHz, DMSO-$d_6$) δ 9.69 (s, 1H), 8.11 – 7.73 (m, 3H), 7.73 – 7.33 (m, 5H), 4.76 (s, 1H), 3.83 (m, 1H), 3.56 (m, 1H), 3.31 (m, 1H), 1.05 (d, $J$ = 6.1 Hz, 3H); $^{13}$C NMR (75 MHz, dmso) δ 182.59, 134.98, 134.36, 130.17, 128.57, 126.86, 126.59, 126.06, 125.40, 123.20, 65.17, 52.04, 21.64. MS (ESI) ($[M+H]^+$): found 261.10, calculated for $C_{14}H_{17}N_2OS$ 261.10.

**3-(2-hydroxypropyl)-2-(naphthalen-1-ylimino)thiazolidin-4-one (7a)**

**7** (0.066 g, 0.357 mmol) was dissolved in anhydrous THF (5 mL) and triethylamine (0.050 mL, 0.357 mmol) was added. The mixture was stirred for 10 minutes and then bromoacetyl bromide (0.034 mL, 0.357 mmol) in THF (1 mL) was added dropwise within five minutes. The reaction was stirred at room temperature for 21 hr. Triethylamine (0.050 mL, 0.357 mmol) was added and after stirring for 5 minutes, the solvent was removed *in vacuo*. The crude was dissolved in DCM (10 mL) and washed once with water (15 mL) and once with brine (15 mL) and dried over $MgSO_4$. The solvent was removed again and the crude oil was purified using column chromatography (silica gel, MeOH/DCM 1:99) to give **7a** as a hard oil (0.030g, 29 %) and **7b** (0.012 g, 11 %). For **7a**: $^{1}$H NMR (300 MHz, DMSO-$d_6$) δ 7.91 (d, $J$ = 9.3 Hz, 2H), 7.69 (d, $J$ = 8.3 Hz, 1H), 7.57 – 7.31 (m, 3H), 7.01 (d, $J$ = 6.2 Hz, 1H), 5.01 (d, $J$ = 5.1 Hz, 1H), 4.37 – 4.10 (m, 1H), 4.00 (s, 2H), 3.90 (dd, $J$ = 12.2, 8.5 Hz, 1H), 3.72 (dd, $J$ = 13.0, 5.3 Hz, 1H), 1.16 (d, $J$ = 6.3 Hz, 3H). $^{13}$C NMR (75 MHz, dmso) δ 172.69, 156.80, 145.09, 134.38, 128.33, 127.28,

126.87, 126.40, 126.13, 124.56, 123.66, 115.64, 63.38, 50.18, 33.00, 21.53. MS (ESI) ($[M+H]^+$): found 301.10, calculated for $C_{16}H_{17}N_2O_2S$ 301.09.

**2-((2-hydroxypropyl)imino)-3-(naphthalen-1-yl)thiazolidin-4-one (7b)**

Synthesized and purified as stated above (**7a**). For **7b**: $^1$H NMR (400 MHz, DMSO-$d_6$) δ 8.03 (d, $J$ = 8.3 Hz, 2H), 7.70 – 7.51 (m, 4H), 7.48 (d, $J$ = 8.3 Hz, 1H), 4.55 (t, $J$ = 5.7 Hz, 1H), 4.40 (d, $J$ = 16.9 Hz, 1H), 4.25 (d, $J$ = 16.9 Hz, 1H), 3.40 – 3.23 (m, 1H), 3.23 – 3.03 (m, 2H), 0.86 (d, $J$ = 6.3 Hz, 3H). $^{13}$C NMR (101 MHz, DMSO) δ 172.30, 152.56, 134.34, 133.04, 129.95, 129.49, 128.76, 127.79, 127.28, 126.80, 126.24, 122.98, 66.42, 60.36, 32.95, 18.28. MS (ESI) ($[M+H]^+$): found 301.10, calculated for $C_{16}H_{17}N_2O_2S$ 301.09.

**1-(3-hydroxypropyl)-3-(naphthalen-1-yl)thiourea (8)**

1-naphthyl isothiocyanate (0.300 g, 1.62 mmol) was dissolved in ethyl acetate (8 mL). 3-amino-1-propanol (0.126 mL, 1.62 mmol) was added. The reaction was stirred at room temperature for 16 hr. The solvent was removed *in vacuo*. The crude was recrystallized in toluene to give **8** as a white powder (0.322 g, 76 %). $^1$H NMR (300 MHz, DMSO-$d_6$) δ 9.58 (s, 1H), 7.90 (dd, $J$ = 34.7, 6.3 Hz, 3H), 7.77 – 7.28 (m, 5H), 4.40 (s, 1H), 3.75 – 3.05 (m, 4H), 1.82 – 1.39 (m, 2H); $^{13}$C NMR (75 MHz, dmso) δ 181.61, 134.36, 133.96, 129.85, 128.06, 126.62, 126.12, 125.69, 125.07, 122.84, 58.61, 31.72, 30.65. MS (ESI) ($[M+H]^+$): found 261.10, calculated for $C_{14}H_{17}N_2OS$ 261.10.

**3-(3-hydroxypropyl)-2-(naphthalen-1-ylimino)thiazolidin-4-one (8a)**

**8** (0.191 g, 0.734 mmol) was dissolved in anhydrous THF (6 mL) and triethylamine (0.102 mL, 0.734 mmol) was added. The mixture was stirred for 10 minutes. Bromoacetyl bromide (0.0678 mL, 0.734 mmol) in THF (1 mL) was added dropwise within 5 minutes. The reaction was stirred at room temperature for 24 hr. The precipitate was collected by gravity filtration and rinsed with DCM. This gummy solid was reserved for purification (see **8b** below). The filtrate was concentrated *in vacuo*. The crude was dissolved in DCM (10 mL) and washed once with water (15 mL) and once with brine (15 mL). The organic layer was concentrated and purified by column chromatography (silica gel, MeOH/DCM 1:99) to give **8a** as a yellow oil (0.0817 g, 37 %). For **8a**: $^{1}$H NMR (300 MHz, DMSO-$d_6$) δ 10.07 (s, 1H), 8.46 (s, 1H), 8.19 – 7.85 (m, 2H), 7.73 (dd, $J$ = 26.0, 7.7 Hz, 2H), 7.60 – 7.40 (m, 3H), 3.89 (s, 2H), 3.48 (d, $J$ = 29.7 Hz, 4H), 2.17 – 1.76 (m, 2H). $^{13}$C NMR (75 MHz, dmso) δ 168.15, 165.84, 134.12, 133.79, 128.58, 128.06, 126.50, 126.33, 126.00, 125.81, 122.97, 121.80, 39.75, 34.03, 32.70, 32.48. MS (ESI) ($[M+H]^+$): found 301.10, calculated for $C_{16}H_{17}N_2O_2S$ 301.09.

**2-((3-hydroxypropyl)imino)-3-(naphthalen-1-yl)thiazolidin-4-one (8b)**

The precipitate from **8a** (above) was suspended in DCM (10 mL) and triethylamine (0.102 mL, 0.734 mmol) was added. After sonication, all of the solid dissolved. The organic solution was washed once with water (15 mL) and once with brine (15 mL) and dried over $MgSO_4$. The DCM was removed *in vacuo* to give **8b** as a yellow oil (0.0781 g, 36 %). $^{1}$H NMR (300 MHz, DMSO-$d_6$) δ 8.03 (d, $J$ = 8.6 Hz, 2H), 7.88 – 7.30 (m, 5H), 4.49 – 4.08 (m, 3H), 3.26 – 3.01 (m, 4H), 1.66 – 1.37 (m, 2H). $^{13}$C NMR (75 MHz, dmso) δ 172.19, 153.28, 134.30, 133.01, 130.00,

129.52, 128.73, 127.65, 127.34, 126.82, 126.17, 122.90, 48.89, 33.65, 33.16, 29.47. MS (ESI) ($[M+H]^+$): found 301.10, calculated for $C_{16}H_{17}N_2O_2S$ 301.09.

**1-(4-hydroxybutyl)-3-(naphthalen-1-yl)thiourea (9)**

1-naphthyl isothiocyanate (0.200 g, 1.08 mmol) was dissolved in ethyl acetate (10 mL). 4-amino-1-butanol (0.995 mL, 1.08 mmol) was added and the reaction was stirred at room temperature for 16 hr. The solvent was removed *in vacuo*. The crude was recrystallized in toluene to give **9** as a white solid (0.1756 g, 52 %). $^1$H NMR (300 MHz, DMSO-$d_6$) δ 9.54 (s, 1H), 8.20 – 7.75 (m, 3H), 7.75 – 7.39 (m, 5H), 4.38 (s, 1H), 3.66 – 3.36 (m, 4H), 1.73 – 1.20 (m, 4H). $^{13}$C NMR (75 MHz, dmso) δ 182.07, 134.86, 134.43, 130.34, 128.54, 127.03, 126.57, 126.17, 125.52, 123.32, 60.96, 44.50, 30.30, 25.86. MS (ESI) ($[M+H]^+$): found 275.12, calculated for $C_{15}H_{19}N_2OS$ 275.11.

**3-(4-hydroxybutyl)-2-(naphthalen-1-ylimino)thiazolidin-4-one (9a)**

**9** (0.301 g, 1.09 mmol) was dissolved in anhydrous THF (10 mL) and triethylamine (0.153 mL, 1.09 mmol) was added. Bromoacetyl bromide (0.096 mL, 1.09 mmol) in THF (1 mL) was added dropwise within 5 minutes. The reaction was stirred at room temperature for 24 hr. The solvent was removed *in vacuo*. The crude was purified using column chromatography (silica gel, MeOH/DCM 1:99) to give **9a** as a clear oil (0.095 g, 28 %) as well as **9b** as a clear oil (0.065 g, 19 %). For **9a**: $^1$H NMR (300 MHz, DMSO-$d_6$) δ 8.04 – 7.81 (m, 2H), 7.69 (d, $J$ = 8.3 Hz, 1H), 7.63 – 7.37 (m, 3H), 7.02 (d, $J$ = 8.3 Hz, 1H), 4.48 (t, $J$ = 5.1 Hz, 1H), 4.03 (s, 2H), 3.88 (t, $J$ = 7.2 Hz, 2H), 3.47 (q, $J$ = 7.8, 7.1 Hz, 2H), 1.93 – 1.63 (m, 2H), 1.63 – 1.38 (m, 2H). $^{13}$C NMR (75 MHz, dmso) δ 172.53, 156.39, 144.99, 134.39, 128.37, 127.28, 126.87, 126.39, 126.21,

124.62, 123.49, 115.67, 60.80, 42.96, 32.97, 30.30, 24.19. MS (ESI) ($[M+H]^+$): found 315.11, calculated for $C_{17}H_{19}N_2O_2S$ 315.11.

**2-((4-hydroxybutyl)imino)-3-(naphthalen-1-yl)thiazolidin-4-one (9b)**

Synthesized and purified as stated above (see **9a).** For **9b**: $^1$H NMR (300 MHz, DMSO-$d_6$) δ 8.02 (d, $J$ = 8.4 Hz, 2H), 7.79 – 7.29 (m, 5H), 4.55 – 4.08 (m, 3H), 3.24 – 2.90 (m, 4H), 1.45 – 1.11 (m, 4H). $^{13}$C NMR (75 MHz, dmso) δ 172.20, 153.02, 134.29, 133.04, 130.00, 129.51, 128.73, 127.64, 127.33, 126.82, 126.18, 122.91, 60.80, 51.87, 33.10, 30.56, 26.99. MS (ESI) ($[M+H]^+$): found 315.11, calculated for $C_{17}H_{19}N_2O_2S$ 315.11.

**1-(4-bromophenyl)-3-propylthiourea (10)**

4-Bromophenyl isothiocyanate (0.400 g, 1.87 mmol) was dissolved in ethyl acetate (10 mL). Propylamine (0.1536 mL, 1.87 mmol) was added and the reaction was stirred at room temperature for 3 hr. The solvent was removed *in vacuo*. The crude NMR showed a pure product with no starting material left, so the product was used without further purification. **10** was produced as a hard oil (0.498 g, 98 %). $^1$H NMR (400 MHz, DMSO-$d_6$) δ 9.51 (s, 1H), 7.84 (s, 1H), 7.47 (d, $J$ = 8.9 Hz, 2H), 7.41 (d, $J$ = 8.9 Hz, 2H), 3.41 (s, 2H), 1.54 (h, $J$ = 7.4 Hz, 2H), 0.88 (t, $J$ = 7.4 Hz, 3H). $^{13}$C NMR (101 MHz, DMSO) δ 180.77, 139.37, 131.71, 125.15, 116.16, 46.05, 22.17, 11.87. MS (ESI) ($[M+H]^+$): found 273.0 and 275.0, calculated for $C_{10}H_{14}BrN_2S$ 273.00.

**2-((4-bromophenyl)imino)-3-propylthiazolidin-4-one (10a)**

**10** (0.050 g, 0.183 mmol) was dissolved in acetonitrile (5 mL) and triethylamine (0.0255 mL, 0.183 mmol) was added. The mixture was stirred for 10 minutes and then bromoacetyl bromide (0.0169 mL, 0.183 mmol) in acetonitrile (1 mL) was added dropwise within 5 minutes. The reaction was stirred at room temperature for 6 hr. The solvent was concentrated *in vacuo* and then dissolved in DCM (10 mL). Triethylamine (0.0255 mL, 0.183 mmol) was added. The product was purified by column chromatography (silica gel, eluted with 100 % DCM)) to give **10a** (0.005 g, 9 %) and **10b** as a yellow oil (0.045 g, 79 %). For **10a**: $^{1}$H NMR (400 MHz, DMSO-$d_6$) δ 7.53 (d, $J$ = 8.7 Hz, 2H), 6.89 (d, $J$ = 8.7 Hz, 2H), 4.05 (s, 2H), 3.68 (t, $J$ = 7.0 Hz, 2H), 1.64 (h, $J$ = 7.4 Hz, 2H), 0.89 (t, $J$ = 7.5 Hz, 3H). $^{13}$C NMR (101 MHz, DMSO) δ 172.44, 156.55, 148.01, 132.62, 123.68, 116.87, 44.31, 33.06, 20.50, 11.64. . MS (ESI) ($[M+H]^+$): found 312.99 and 314.99, calculated for $C_{12}H_{14}BrN_2OS$ 312.99

**3-(4-bromophenyl)-2-(propylimino)thiazolidin-4-one (10b)**

Synthesized and purified as stated above (see **10a**). For **10b**: $^{1}$H NMR (400 MHz, DMSO-$d_6$) δ 7.67 (d, $J$ = 8.7 Hz, 2H), 7.24 (d, $J$ = 8.7 Hz, 2H), 4.13 (s, 2H), 3.14 (t, $J$ = 6.8 Hz, 2H), 1.47 (h, $J$ = 7.2 Hz, 2H), 0.82 (t, $J$ = 7.4 Hz, 3H). $^{13}$C NMR (101 MHz, DMSO) δ 171.71, 152.84, 135.36, 132.29, 131.11, 121.69, 53.57, 32.98, 23.77, 12.28. MS (ESI) ($[M+H]^+$): found 312.99 and 314.99, calculated for $C_{12}H_{14}BrN_2OS$ 312.99.

**1-(naphthalen-1-yl)-3-propylthiourea (11)**

1-Naphthyl isothiocyanate (0.151 g, 0.817 mmol) was dissolved in ethyl acetate. Propylamine (0.067 mL, 0.817 mmol) was added and the reaction was stirred at room temperature for 16 hrs.

The crude was washed with 1 M HCl (2x), once with brine, and dried over $MgSO_4$. The solvent was removed *in vacuo* to give the product **11** as a pale yellow solid in quantitative yield. $^1$H NMR (400 MHz, DMSO-$d_6$) δ 9.55 (s, 1H), 7.97 (d, *J* = 9.4 Hz, 1H), 7.87 (t, *J* = 9.6 Hz, 2H), 7.68 – 7.37 (m, 5H), 3.40 (q, *J* = 6.5 Hz, 2H), 1.67 – 1.44 (m, 2H), 0.83 (t, *J* = 7.0 Hz, 3H). $^{13}$C NMR (101 MHz, DMSO) δ 182.15, 134.93, 134.46, 130.36, 128.57, 127.09, 126.61, 126.21, 125.54, 123.34, 46.35, 22.38, 11.78. MS (ESI) ($[M+H]^+$): found 245.10, calculated for $C_{14}H_{17}N_2S$ 245.10.

**2-(naphthalen-1-ylimino)-3-propylthiazolidin-4-one (11a)**

**11** (0.100 g, 0.54 mmol) was dissolved in THF (5 mL). Triethylamine (0.075 mL, 0.54 mmol) was added and the reaction was stirred for 5 min. Bromoacetyl bromice (0.050 mL, 0.54 mmol) was added. The reaction was stirred at room temperature for 16 hours. The solvent was removed *in vacuo*. DCM (10 mL) was added and the crude was washed with a solution of sodium bicarbonate (pH 8) and dried over $MgSO_4$. The organic layer was concentrated *in vacuo* and purified via column chromatography (silica gel, 0.5% EtOAC and 99.5% DCM eluting solvent) to give **11a** (0.02 g, 17%) and **11b** (0.07 g, 60 %) For **11a**: $^1$H NMR (400 MHz, DMSO-$d_6$) δ 7.94 (d, *J* = 7.3 Hz, 1H), 7.88 (d, *J* = 8.6 Hz, 1H), 7.71 (d, *J* = 8.3 Hz, 1H), 7.64 – 7.39 (m, 3H), 7.04 (d, *J* = 8.3 Hz, 1H), 4.06 (s, 2H), 3.86 (t, J = 6.9 Hz, 2H), 1.80 (h, *J* = 7.4 Hz, 2H), 0.99 (t, *J* = 7.5 Hz, 3H). $^{13}$C NMR (101 MHz, DMSO) δ 172.59, 156.49, 145.02, 134.42, 128.42, 127.30, 126.89, 126.43, 126.24, 124.65, 123.44, 115.70, 44.54, 33.01, 20.78, 11.75. MS (ESI) ($[M+H]^+$): found 285.10, calculated for $C_{16}H_{17}N_2OS$ 285.10

**3-(naphthalen-1-yl)-2-(propylimino)thiazolidin-4-one (11b)**

Synthesized and purified as stated above (see **11a**). For **11b:** $^{1}$H NMR (400 MHz, DMSO-$d_6$) δ 8.04 (d, *J* = 8.4 Hz, 2H), 7.75 – 7.51 (m, 4H), 7.46 (d, *J* = 7.3 Hz, 1H), 4.40 (d, *J* = 16.9 Hz, 1H), 4.25 (d, *J* = 16.9 Hz, 1H), 3.24 – 3.01 (m, 2H), 1.47 – 1.26 (m, 2H), 0.71 (t, *J* = 7.4 Hz, 3H). $^{13}$C NMR (101 MHz, DMSO) δ 172.24, 153.09, 134.33, 133.09, 130.03, 129.54, 128.76, 127.68, 127.34, 126.84, 126.21, 122.94, 53.63, 33.15, 23.63, 12.09. MS (ESI) ($[M+H]^+$): found 285.10, calculated for $C_{16}H_{17}N_2OS$ 285.10

**3-(2-hydroxyethyl)-5-methyl-2-(naphthalen-1-ylimino)thiazolidin-4-one (12)**

4-Bromophenyl thiourea (**2**) (0.200 g, 0.753 mmol) was dissolved in anhydrous THF (8 mL) and triethylamine (0.105 mL, 0.753 mmol) was added. The mixture was stirred for 10 minutes then bromoacetyl bromide (0.0790 mL, 0.753 mmol) in THF (1 mL) was added dropwise within 5 minutes. The reaction was stirred at room temperature for 24 hr. The solvent was removed *in vacuo* and the crude was dissolved in DCM (15 mL). The organic layer was washed once with water (15 mL), once with 1 M HCl (15 mL), and once with brine (15 mL). The organic layer was concentrated *in vacuo* and purified by column chromatography (silica gel, MeOH/DCM 1:99) to yield the product **12** as a white powder (0.067 g, 27%). $^{1}$H NMR (400 MHz, DMSO-$d_6$) δ 7.53 (d, *J* = 8.7 Hz, 2H), 6.90 (d, *J* = 8.7 Hz, 2H), 4.81 (s, 1H), 4.34 (q, *J* = 7.2 Hz, 1H), 3.80 (t, *J* = 7.0 Hz, 2H), 3.61 (t, *J* = 6.3 Hz, 2H), 1.50 (d, *J* = 7.2 Hz, 3H). $^{13}$C NMR (101 MHz, DMSO) δ 175.52, 155.34, 148.00, 132.56, 123.71, 116.87, 57.39, 45.21, 42.67, 19.21. MS (ESI) ($[M+H]^+$): found 328.99 and 330.99, calculated for $C_{12}H_{14}BrN_2O_2S$ 328.99.

**2-(naphthalen-1-ylamino)-2-oxoethyl) (2-bromoethyl)carbamothioate (13)**

The solid precipitate formed in the reaction of **1** with BrAcBr (crude **1b** HBr salt) (0.023 g, 0.06 mmol) was dissolved in acetonitrile (3 mL) and heated to 65°C. The reaction was run for 5 hr then concentrated *in vacuo*. The crude was purified by column chromatography (silica gel, MeOH/DCM 0.5:99.5) to give the product as a pale yellow oil (0.006 g, 26 %). $^{1}$H NMR (400 MHz, DMSO-$d_6$) δ 10.08 (s, 1H), 8.69 (s, 1H), 8.16 – 8.00 (m, 1H), 8.00 – 7.88 (m, 1H), 7.77 (d, $J$ = 8.2 Hz, 1H), 7.69 (d, $J$ = 7.3 Hz, 1H), 7.63 – 7.40 (m, 3H), 3.92 (s, 2H), 3.62 – 3.48 (m, 4H). $^{13}$C NMR (101 MHz, DMSO) δ 168.01, 166.26, 134.14, 133.80, 128.60, 128.07, 126.52, 126.33, 126.03, 125.83, 123.03, 121.84, 55.39, 34.09, 32.42. MS (ESI) ($[M+H]^+$): found 367.01 and 369.00, calculated for $C_{15}H_{16}BrN_2O_2S$ 367.00.

**2-(naphthalen-1-ylamino)-2-oxoethyl) (2-chloroethyl)carbamothioate (14)**

**1b** (0.015 g, 0.0524 mmol) was dissolved in acetonitrile (3 mL) and heated to 60°C. Enough HCl was added to give the reaction a pH of 4, checked using litmus paper. The reaction was run for 16 hr then concentrated *in vacuo*. The crude was purified by column chromatography (silica gel, MeOH/DCM 1:9) to give the product as a pale yellow oil (0.0145 g, 86%). $^{1}$H NMR (300 MHz, DMSO-$d_6$) δ 10.10 (s, 1H), 8.67 (s, 1H), 8.15 – 8.01 (m, 1H), 8.01 – 7.85 (m, 1H), 7.77 (d, $J$ = 8.2 Hz, 1H), 7.68 (d, $J$ = 7.3 Hz, 1H), 7.62 – 7.39 (m, 3H), 3.91 (s, 2H), 3.66 (t, $J$ = 6.0 Hz, 2H), 3.48 (q, $J$ = 5.8 Hz, 2H); $^{13}$C NMR (75 MHz, dmso) δ 168.00, 166.28, 134.11, 133.77, 128.58, 128.04, 126.51, 126.31, 126.01, 125.80, 123.01, 121.83, 43.67, 43.09, 34.04. MS (ESI) ($[M+H]^+$): found 323.06, calculated for $C_{15}H_{16}ClN_2O_2S$ 323.05.

**2-(naphthalen-1-ylamino)-2-oxoethyl) (1-bromopropan-2-yl)carbamothioate (15)**

1-naphthyl isothiocyanate (0.100 g, 0.54 mmol) was dissolved in THF (5 mL) and 2-amino-1-propanol (0.043 mL, 0.54 mmol) was added. The reaction was stirred at room temperature for 2 hrs. After this time, triethylamine (0.0752 mL, 0.54 mmol) was added, followed by bromoacetyl bromide (0.050 mL, 0.54 mmol) after waiting a period of 5 min. The reaction was stirred at room temperature for 14 hrs then heated to 65C for an additional 8 hrs. The solvent was removed *in vacuo*. The crude was purified using column chromatography (silica gel, 1:99 MeOH/DCM) to give the product as a slightly yellow hard oil (0.052 g, 25 % yield). $^{1}$H NMR (400 MHz, DMSO-$d_6$) δ 10.10 (s, 1H), 8.56 (d, $J$ = 7.0 Hz, 1H), 8.10 (d, $J$ = 9.5 Hz, 1H), 7.94 (t, $J$ = 8.5 Hz, 1H), 7.78 (d, $J$ = 8.2 Hz, 1H), 7.71 (d, $J$ = 7.3 Hz, 1H), 7.61 – 7.47 (m, 4H), 4.17 – 4.02 (m, 1H), 3.92 (s, 2H), 3.64 – 3.47 (m, 2H), 1.20 (d, $J$ = 6.7 Hz, 3H). $^{13}$C NMR (101 MHz, DMSO) δ 168.11, 165.49, 134.15, 133.81, 128.61, 128.07, 126.52, 126.33, 126.03, 125.82, 123.01, 121.83, 48.54, 38.42, 34.07, 19.05. MS (ESI) ($[M+H]^+$): found 381.0 and 383.0 (10% intensity) and ($[M+Na]^+$) 403.00 and 405.00 (100% intensity), calculated for $C_{16}H_{18}BrN_2O_2S$ 381.02.

**2-((4-bromophenyl)amino)-2-oxoethyl) (2-bromoethyl)carbamothioate (16)**

**2b** (0.015 g, 0.0478 mmol) was dissolved in acetonitrile (2 mL) and heated to 65°C. Enough HBr was added to give the reaction a pH of 4, checked using litmus paper. The reaction was run for 24 hr then concentrated *in vacuo*. The crude was purified by column chromatography (silica gel, DCM 100%) to give the product as a pale yellow oil (0.0124 g, 66 %). $^{1}$H NMR (400 MHz, DMSO-$d_6$) δ 10.30 (s, 1H), 8.64 (s, 1H), 7.56 (d, $J$ = 9.0 Hz, 2H), 7.49 (d, $J$ = 8.9 Hz, 2H), 3.76 (s, 2H), 3.50 (s, 4H); $^{13}$C NMR (101 MHz, DMSO) δ 167.29, 165.93, 138.80, 132.04, 121.44,

115.37, 43.05, 34.49, 32.37. MS (ESI) ($[M+H]^+$): found 394.90 (50%), 396.90 (100%), and 398.90 (50%), calculated for $C_{11}H_{13}B_{r2}N_2O_2S$ 394.90.

**Treatment of 1b to decyclization conditions**

**1b** (0.022 g, 0.08 mmol) was dissolved in acetonitrile (3 mL). Concentrated HCl (10 uL) was added and the reaction was stirred at 65C for 24 hours. There was little significant change in the NMR taken of the crude reaction and ESI MS showed the ring (($[M+H]^+$): 287) but no peak for what would be the product (($[M+H]^+$): 322).

**Treatment of 10b to decyclization conditions**

A small amount of the crude reaction mixture of **10b** (0.0317 g,) was dissolved in THF (3 mL) with a drop of water added. The mixture was heated at 60°C for 24 hr. The solvent was removed *in vacuo* and an NMR was taken of this crude. The NMR indicated that there was no change in the composition of the products when refluxed in the presence of 1 mol. eq. of HBr that forms during the course of the reaction.

**Crude brph -78 to reflux with and without base**

**2** (0.075 g, 0.273 mmol) was dissolved in THF (4 mL) and triethylamine (0.038 mL, 0.273 mmol) was added. The mixture was cooled to -78°C using an acetone/dry ice bath. Bromoacetyl bromide (0.0252 mL, 0.273 mmol) was added. The reaction was stirred at -78°C for 6 hr. At this time, a portion of the reaction (200 uL) was removed for an NMR. The rest of the reaction was allowed to stir at room temperature for 0.5 hr then heated to 60°C. The reaction was run at this

temperature for 16 hr. The solvent was removed *in vacuo* and some of the crude was taken for another NMR. Comparison of the NMRs shows that **2b** formed and then reacted to form **16**.

**2** (0.013 g, 0.0472 mmol) was dissolved in acetonitrile (3 mL). Triethylamine (0.01975 mL, 0.1416 mmol) was added. The reaction was cooled to -10°C using a salt/ice bath. Bromoacetyl bromide (0.00437 mL, 0.0472 mmol) was added. The reaction was stirred for 6 hr. At this time, some of the mixture was removed for an NMR while the rest was heated up to 60°C. The reaction was stirred at this temperature for 16 hr. The solvent was removed *in vacuo* and an NMR of the crude was taken.

**Temperature study of product distribution of 10a and 10b formed at -45°C**

**10** (0.050 g, 0.183 mmol) was dissolved in acetonitrile (5 mL) and triethylamine (0.0255 mL, 0.183 mmol) was added. The mixture was stirred for 10 minutes and then bromoacetyl bromide (0.0169 mL, 0.183 mmol) in acetonitrile (1 mL) was added dropwise within 5 minutes. The reaction was stirred in an acetonitrile/dry ice bath (-45C) for 6 hr. The crude reaction was treated in the same manner as above to yield **10b** (0.042 g, 73 %) and **10a** (0.003 g, 5 %).

**Study of the effects of different solvents on product distribution**

**1** (0.025 g, 0.102 mmol) was dissolved in 2 mL of the chosen solvent. The solvents used were acetone, acetonitrile, THF, ethyl acetate, DCM, or benzene. Triethylamine (0.0141 mL, 0.102 mmol) was added with stirring followed by bromoacetyl bromide (0.0094 mL, 0.102 mmol). The reactions were stirred at room temperature for 19 hrs. The solvent was removed *in vacuo*. Each

crude reaction was dissolved in DCM (1 mL) and washed with sat. $NaHCO_3$. 250 uL of the organic layer was removed, dried, and dissolved in 500 uL of DMSO-$d_6$ for NMR.

The same procedure was followed using **11** (0.025 g, 0.102 mmol) and the same set of solvents.

**One-pot multi-step synthesis series**

Bromophenyl isothiocyanate (0.100 g, 0.509 mmol) was dissolved in THF (5 mL). Ethanolamine (0.0307 mL, 0.509 mmol) was added and the reaction was stirred at room temperature for 19 hrs. 200 uL of the reaction mixture was removed for NMR. Triethylamine (0.071 mL, 0.509 mmol) was added and the reaction was cooled to -78C using an acetone/dry ice bath. Bromoacetyl bromide (0.0444 mL, 0.509 mmol) was added and the reaction was stirred for 6 hrs at -78C. 200 uL of the reaction mixture was removed for NMR. The reaction was allowed to stir for 30 min at room temperature then heated to 65C on an oil bath. The reaction stirred at this temperature for 4 hrs. After this time, 200 uL of the reaction mixture was removed for NMR and the reaction was stopped by removing the solvent *in vacuo*.

The same procedure was followed for the second series with one difference. After the addition of triethylamine, the reaction was kept at room temperature for the addition of bromoacetyl bromide and for the six hrs of reaction time, followed by 4 hrs of heating at 65C.

**HSQC and HMBC analysis**

**1a** (16 mg) and **1b** (22 mg) were each dissolved in 0.6 mL of DMSO-$d_6$. A H NMR (16 scans), C NMR (1024 scans), HSQC (8 scans, expt HSQCGP), and HMBC (32 scans, expt HMBCGPND)

were taken for each of the samples. NMRS were run on a Bruker NanoBay AVANCE III 400 MHz running TopSpin 3.2 using the default experimental settings.

**Crystallization of samples for single crystal x-ray analysis**

The same general procedure was followed for growing crystals of **1a**, **8a**, **15**, and **16**: 17-20 mg of the sample was dissolved in 0.5 mL of DCM in a 4 mL vial. This was placed into a 10 mL vial containing 2 mL of cyclohexane and the cap of the outer vial was secured and covered with parafilm. The samples were allowed to sit undisturbed for 2 weeks. **16** was crystallized using THF instead of DCM. **5a** was crystallized by dissolving 20 mg in 0.5 mL DCM and heating. Cyclohexane was added until the solution turned cloudy (1.5 mL) The sample was heated again until clear and then the cap was secured and covered with parafilm. The sample was left undisturbed for 2 weeks.

# Appendix C.

## $^{1}$H and $^{13}$C NMR Spectra

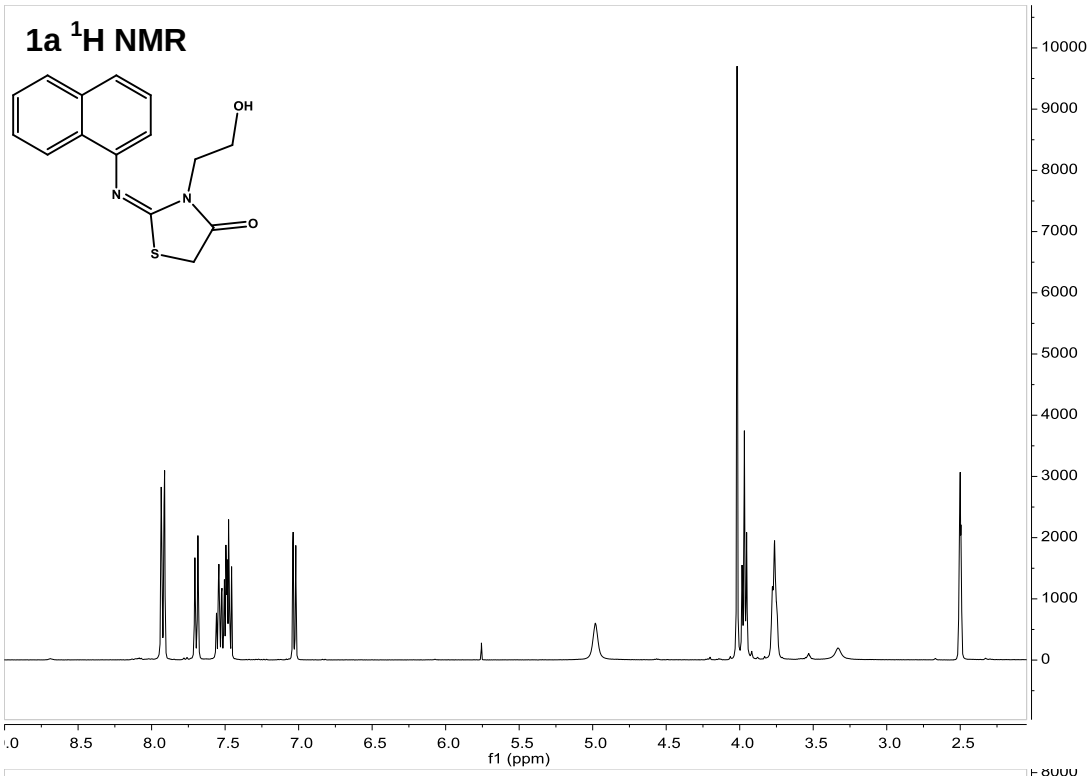
1a $^{1}$H NMR
OH
N
N
O
S
10000
9000
8000
7000
6000
5000
4000
3000
2000
1000
0
8.5
8.0
7.5
7.0
6.5
6.0
5.5
5.0
4.5
4.0
3.5
3.0
2.5
f1 (ppm)

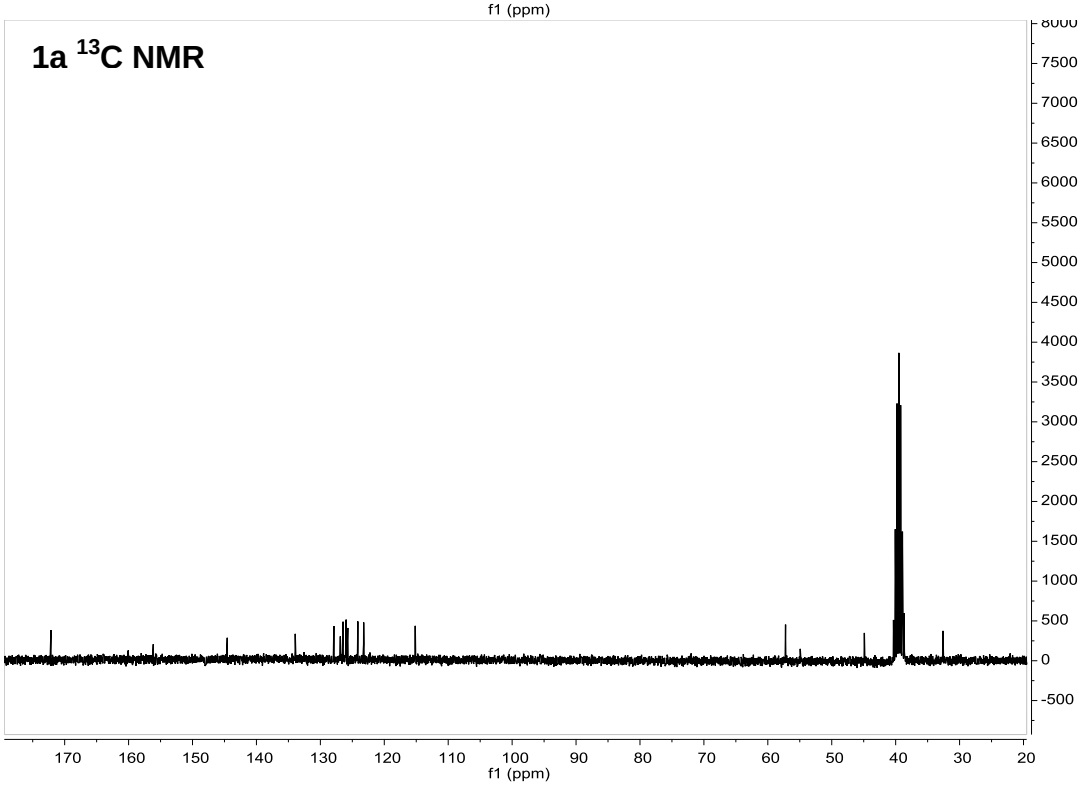
1a $^{13}$C NMR
7500
7000
6500
6000
5500
5000
4500
4000
3500
3000
2500
2000
1500
1000
500
0
-500
170
160
150
140
130
120
110
100
90
80
70
60
50
40
30
20
f1 (ppm)

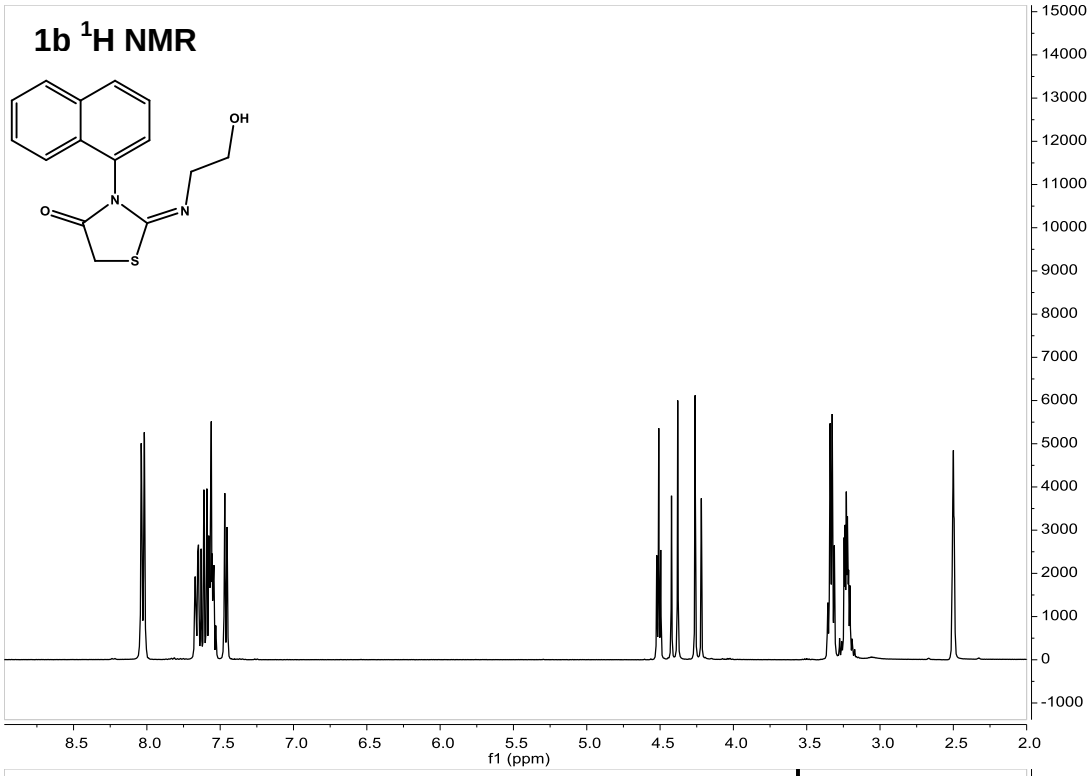
1b 1H NMR
OH
N
O
N
S
15000
14000
13000
12000
11000
10000
9000
8000
7000
6000
5000
4000
3000
2000
1000
0
-1000
8.5
8.0
7.5
7.0
6.5
6.0
5.5
5.0
4.5
4.0
3.5
3.0
2.5
2.0
f1 (ppm)

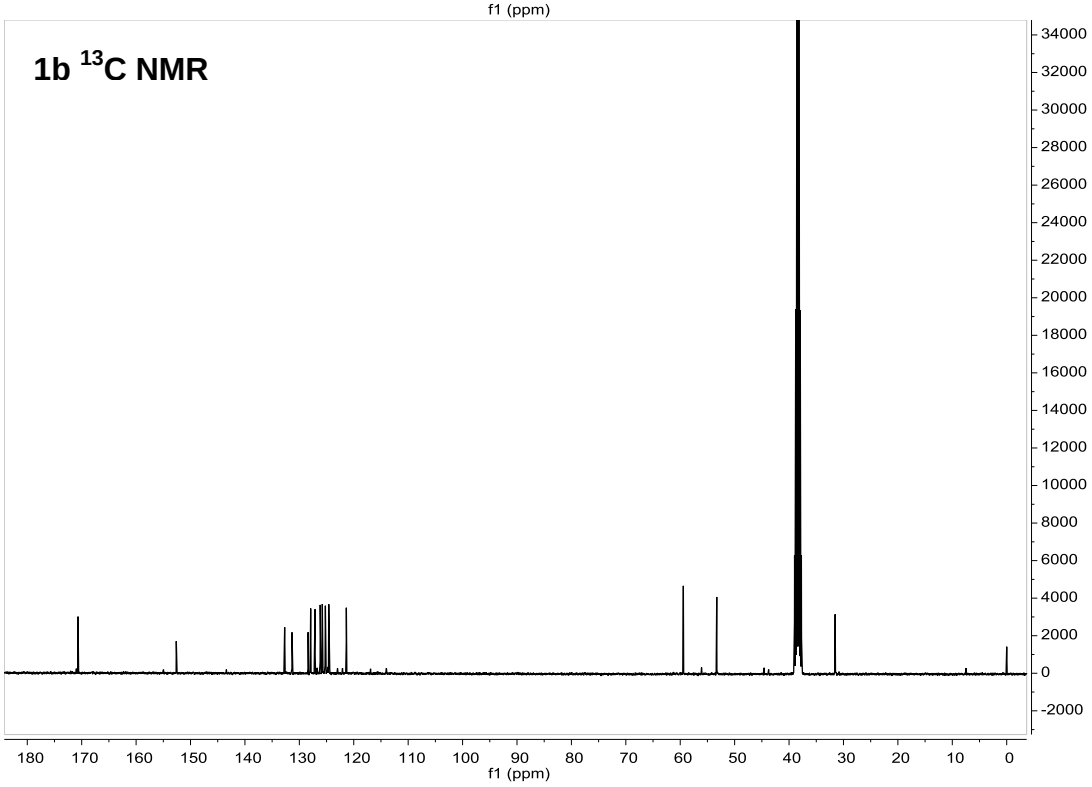
1b 13C NMR
34000
32000
30000
28000
26000
24000
22000
20000
18000
16000
14000
12000
10000
8000
6000
4000
2000
0
-2000
180
170
160
150
140
130
120
110
100
90
80
70
60
50
40
30
20
10
0
f1 (ppm)

**2 $^{1}$H NMR**

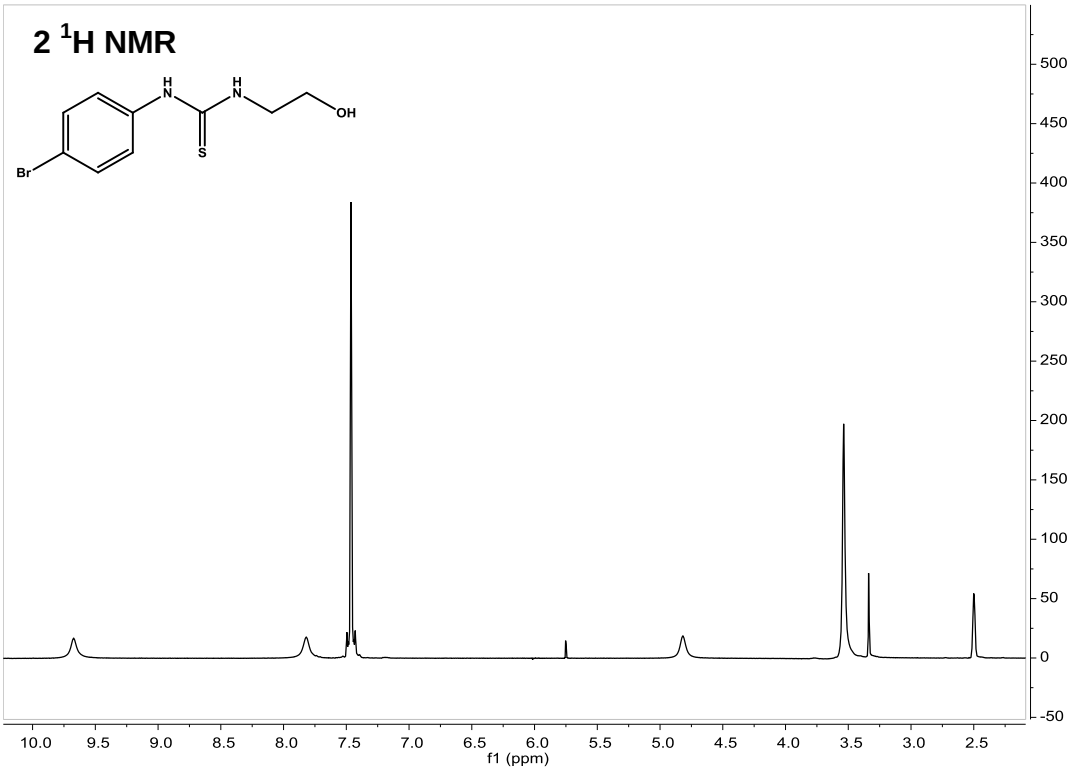


**2 $^{13}$C NMR**

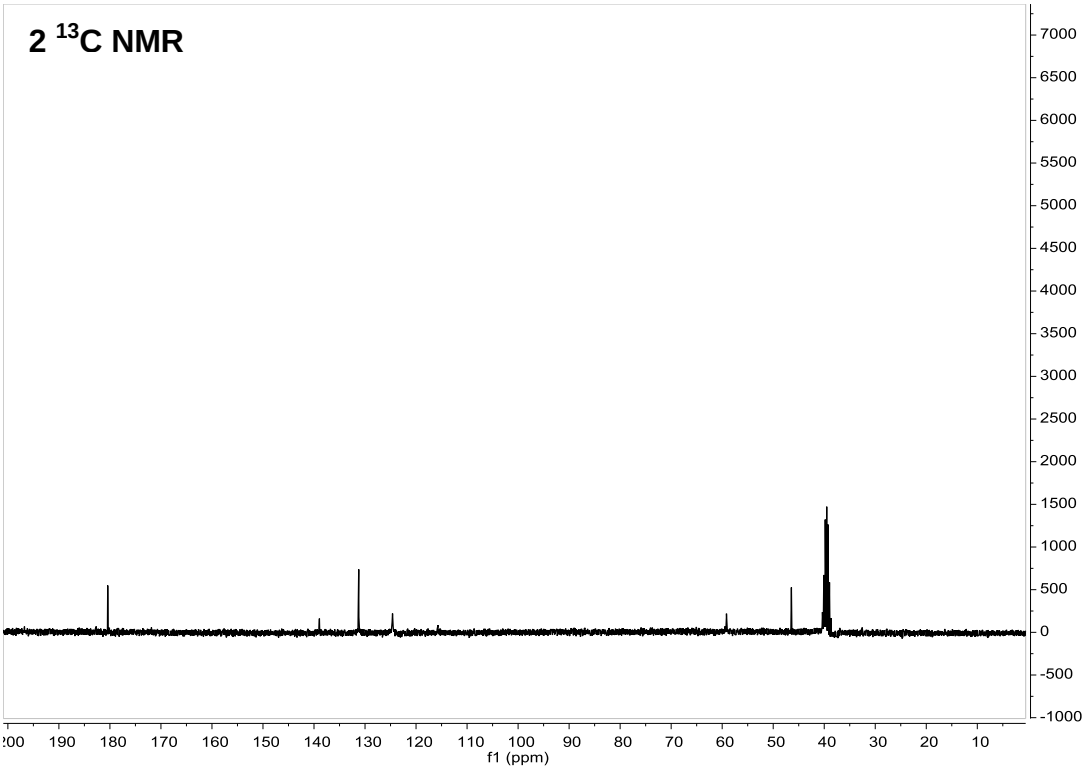

**2a $^{1}$H NMR**

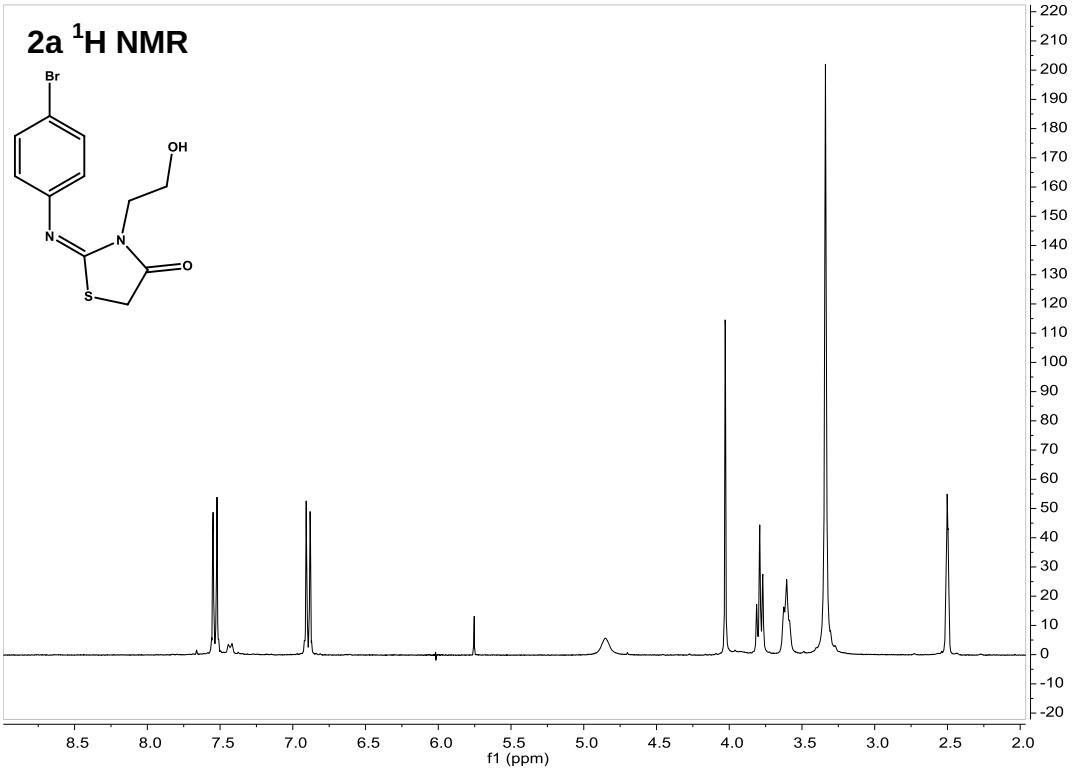


**2a $^{13}$C NMR**

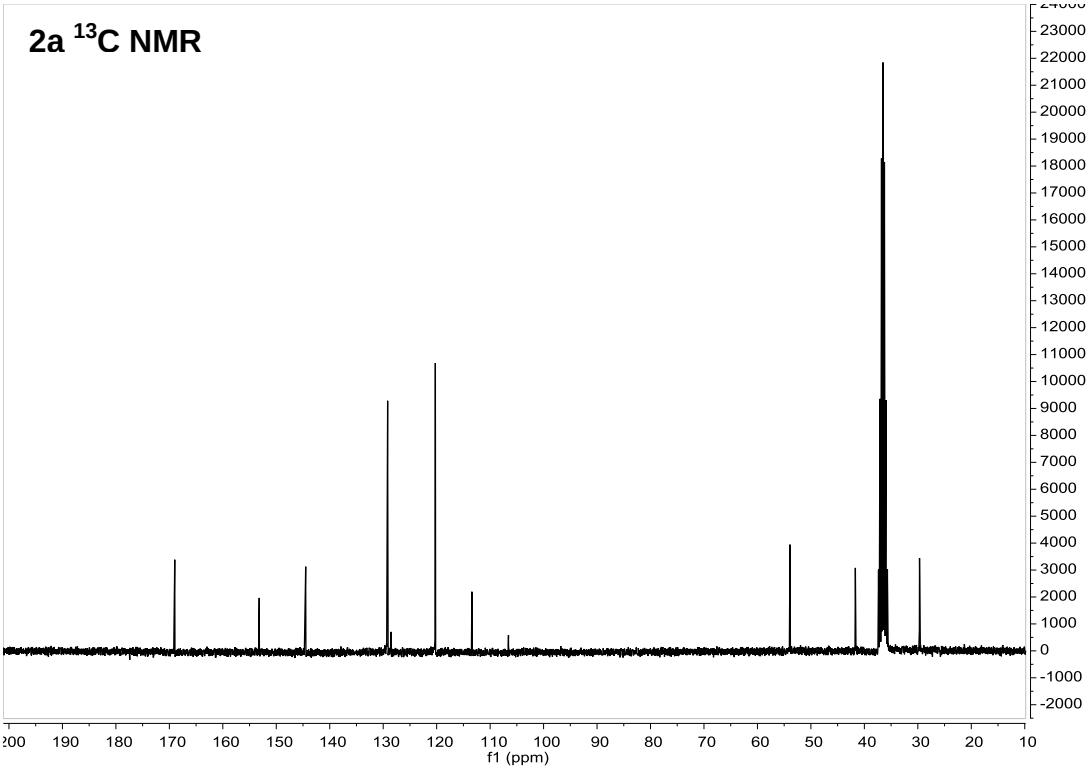

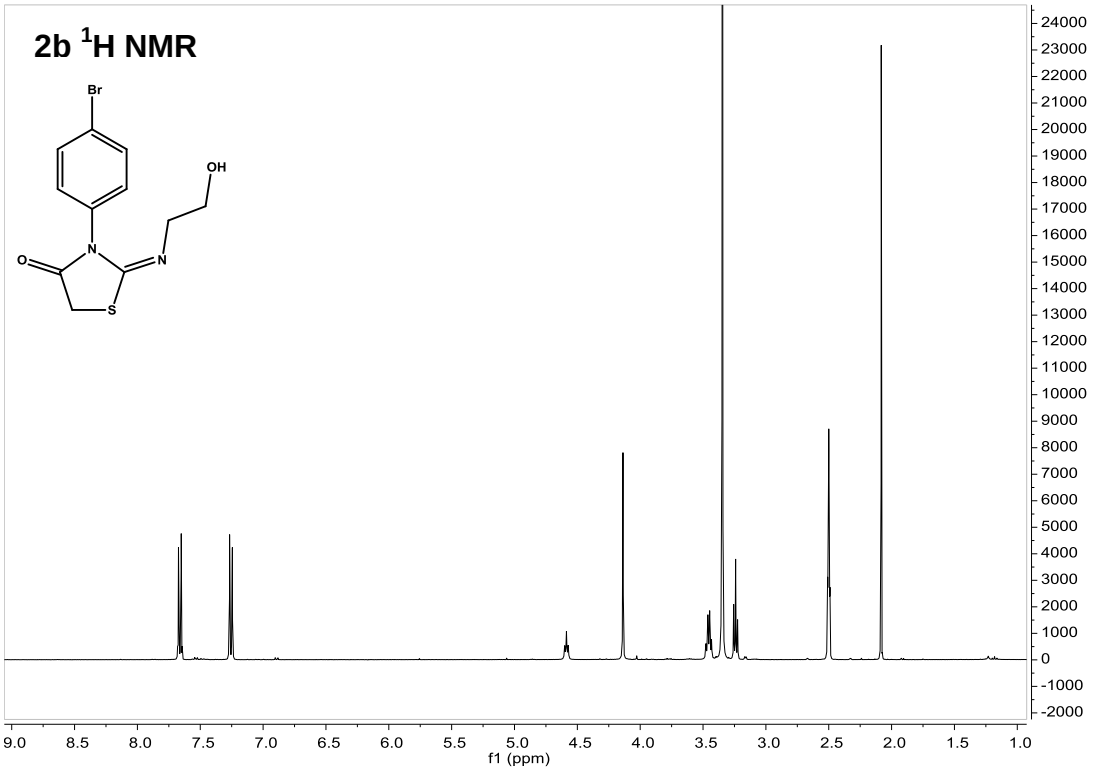
2b $^{1}$H NMR
Br
OH
N
O
N
S
24000
23000
22000
21000
20000
19000
18000
17000
16000
15000
14000
13000
12000
11000
10000
9000
8000
7000
6000
5000
4000
3000
2000
1000
0
-1000
-2000
9.0
8.5
8.0
7.5
7.0
6.5
6.0
5.5
5.0
4.5
4.0
3.5
3.0
2.5
2.0
1.5
1.0
f1 (ppm)

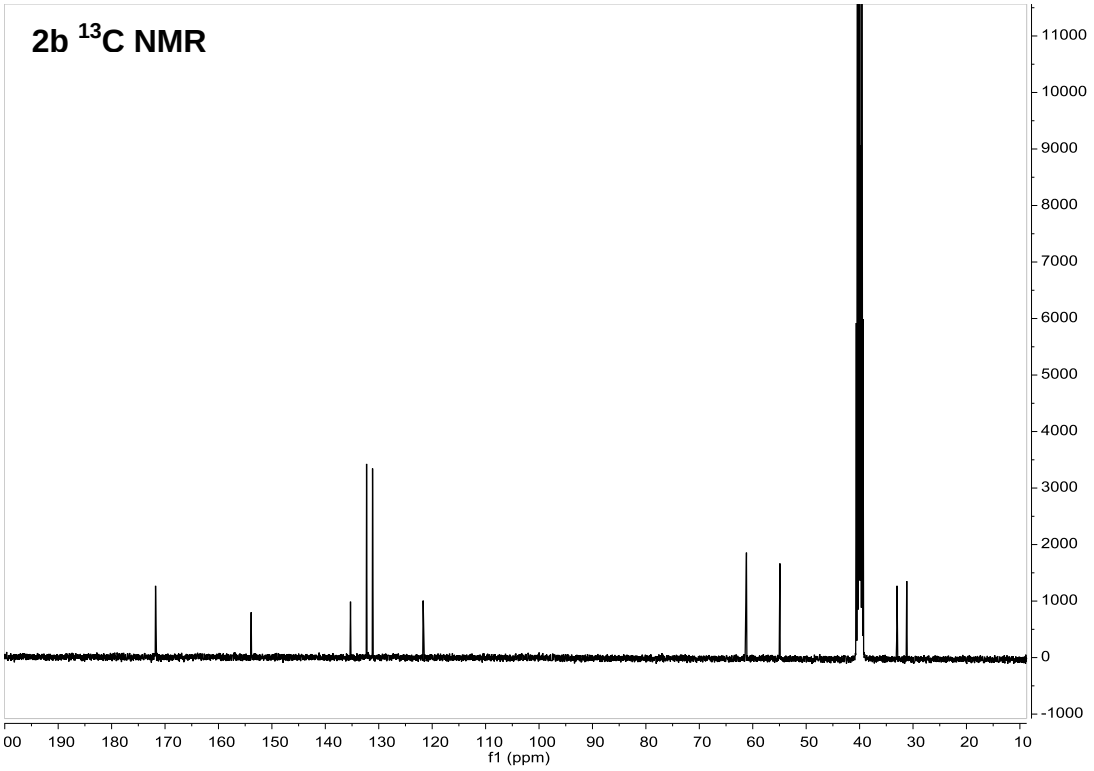
2b $^{13}$C NMR
11000
10000
9000
8000
7000
6000
5000
4000
3000
2000
1000
0
-1000
00
190
180
170
160
150
140
130
120
110
100
90
80
70
60
50
40
30
20
10
f1 (ppm)

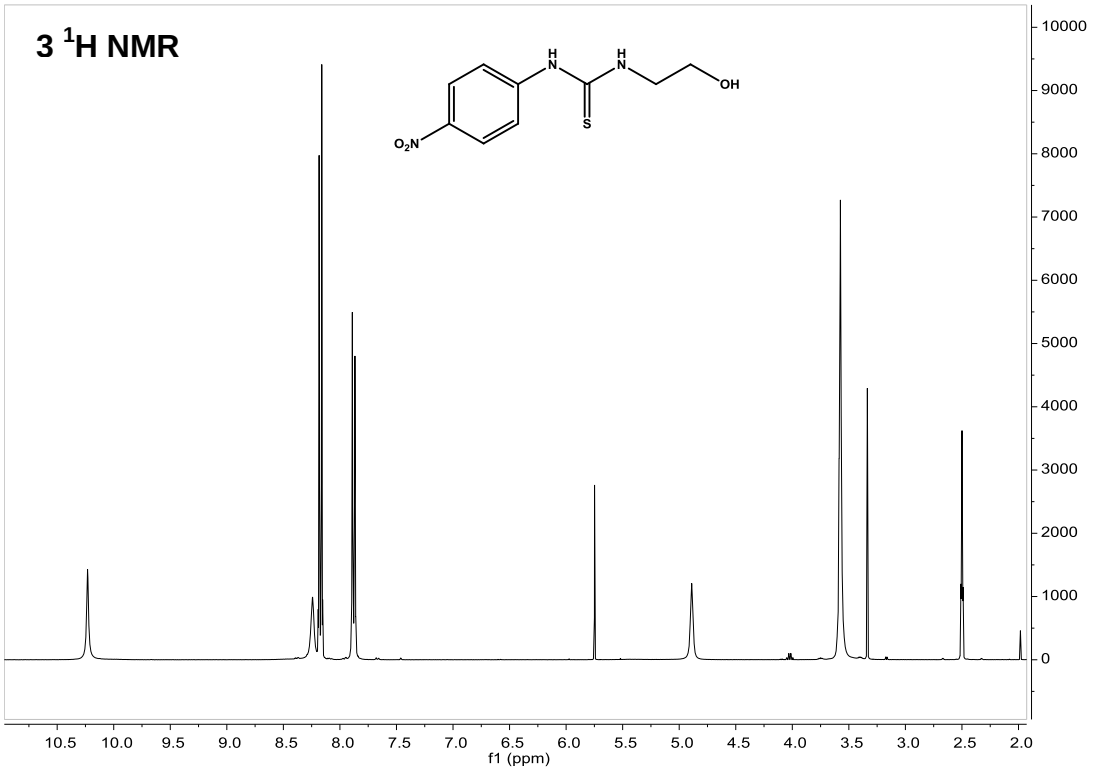
3 1H NMR
H
N
H
N
OH
S
O2N
10000
9000
8000
7000
6000
5000
4000
3000
2000
1000
0
10.5 10.0 9.5 9.0 8.5 8.0 7.5 7.0 6.5 6.0 5.5 5.0 4.5 4.0 3.5 3.0 2.5 2.0
f1 (ppm)

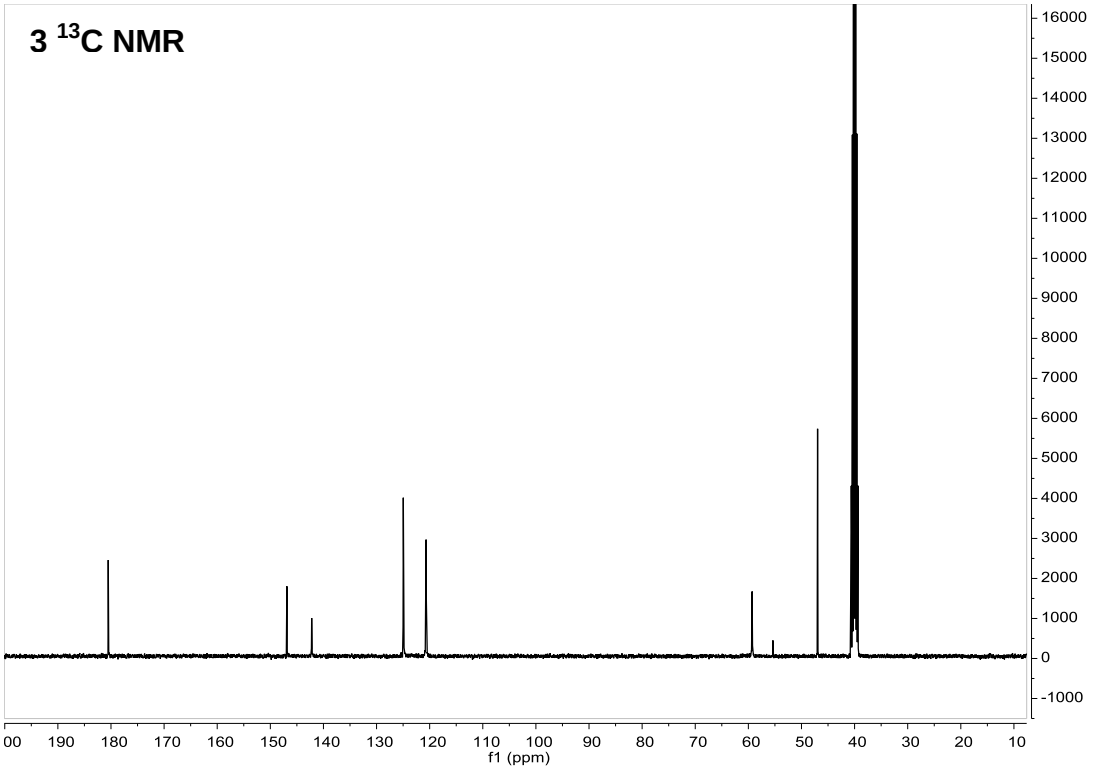
3 13C NMR
16000
15000
14000
13000
12000
11000
10000
9000
8000
7000
6000
5000
4000
3000
2000
1000
0
-1000
00 190 180 170 160 150 140 130 120 110 100 90 80 70 60 50 40 30 20 10
f1 (ppm)

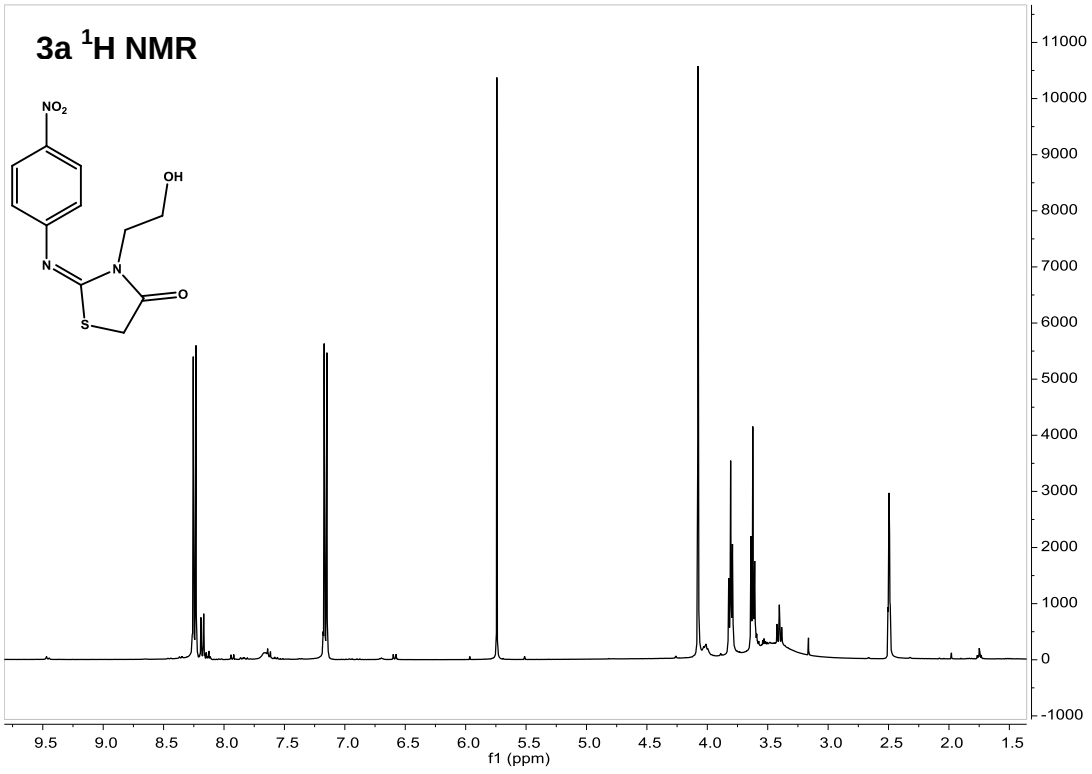
3a 1H NMR
NO2
OH
N
N
O
S
11000
10000
9000
8000
7000
6000
5000
4000
3000
2000
1000
0
-1000
9.5 9.0 8.5 8.0 7.5 7.0 6.5 6.0 5.5 5.0 4.5 4.0 3.5 3.0 2.5 2.0 1.5
f1 (ppm)

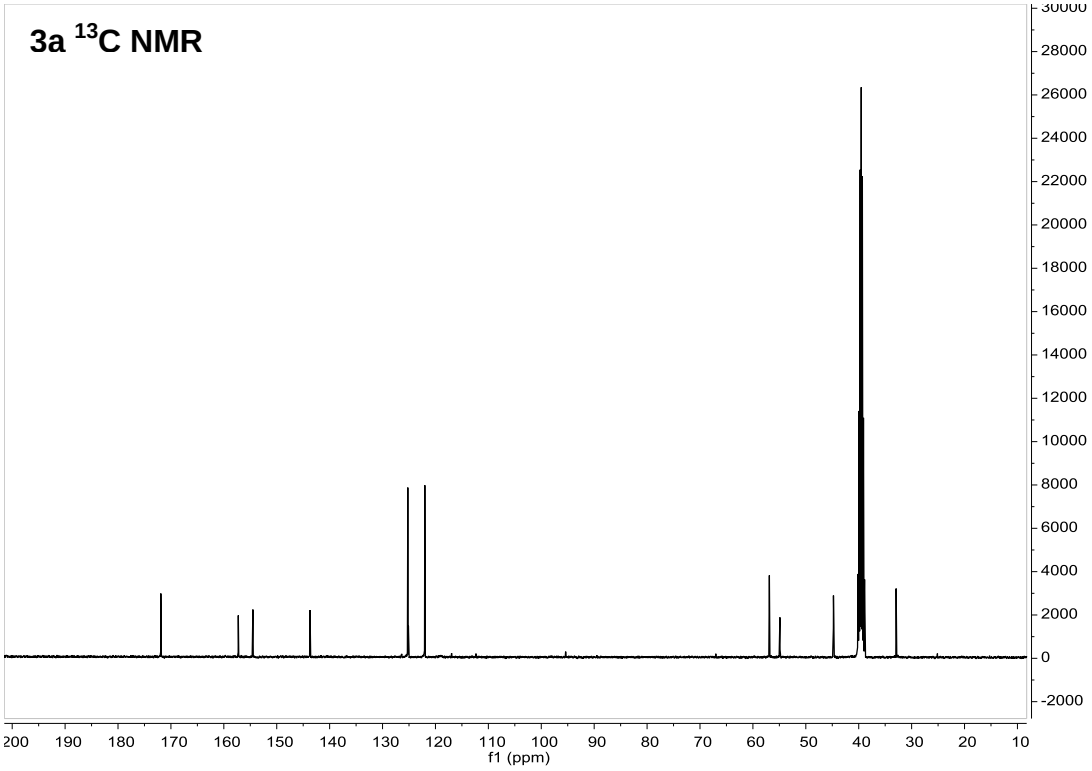
3a 13C NMR
30000
28000
26000
24000
22000
20000
18000
16000
14000
12000
10000
8000
6000
4000
2000
0
-2000
200 190 180 170 160 150 140 130 120 110 100 90 80 70 60 50 40 30 20 10
f1 (ppm)

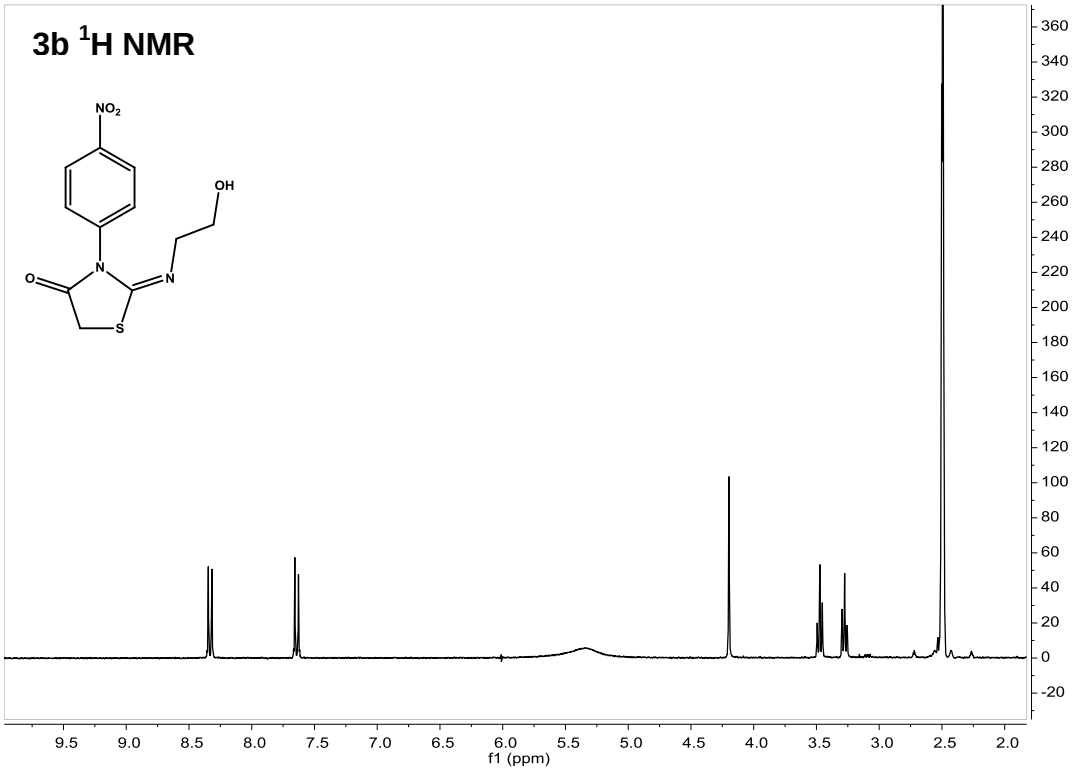
3b $^{1}$H NMR
NO2
OH
O
N
N
S
f1 (ppm)

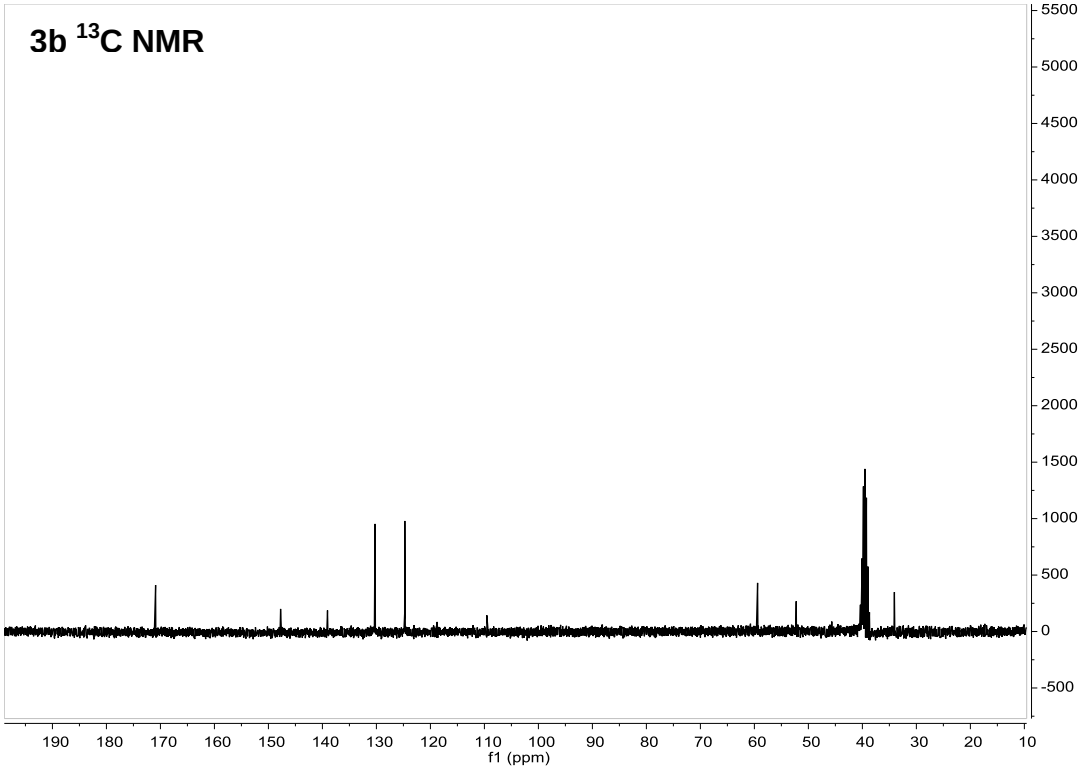
3b $^{13}$C NMR
f1 (ppm)

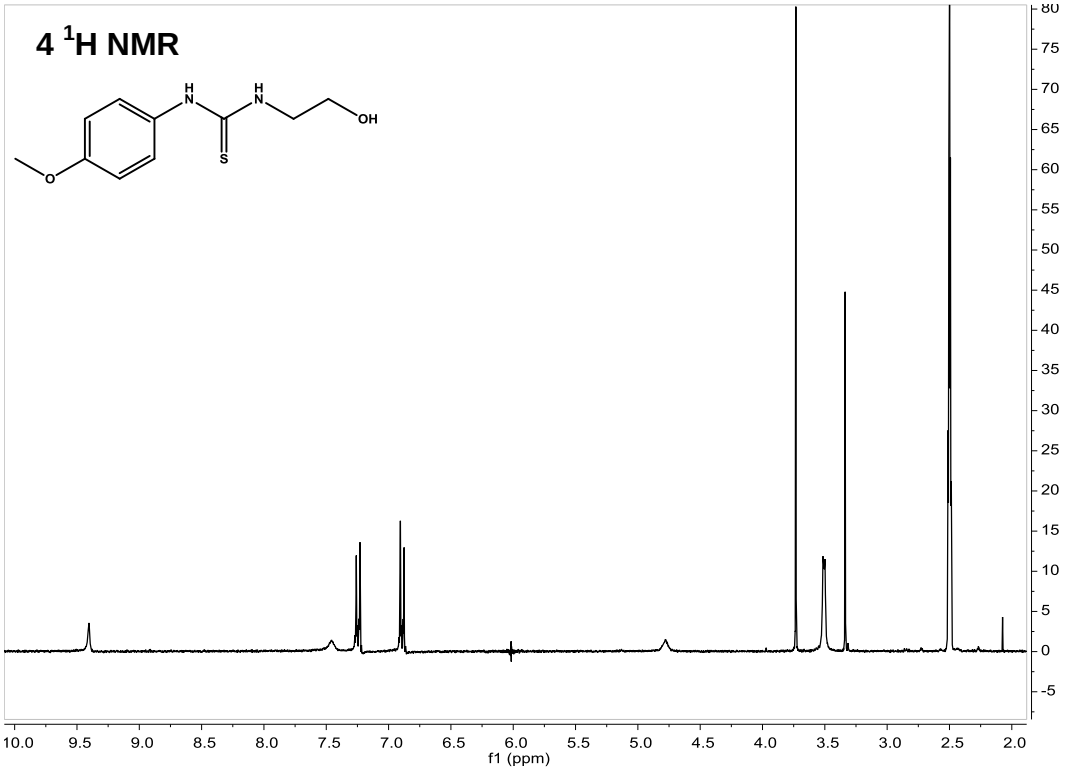
4 1H NMR
H
N
H
N
OH
S
O
80
75
70
65
60
55
50
45
40
35
30
25
20
15
10
5
0
-5
10.0
9.5
9.0
8.5
8.0
7.5
7.0
6.5
6.0
5.5
5.0
4.5
4.0
3.5
3.0
2.5
2.0
f1 (ppm)

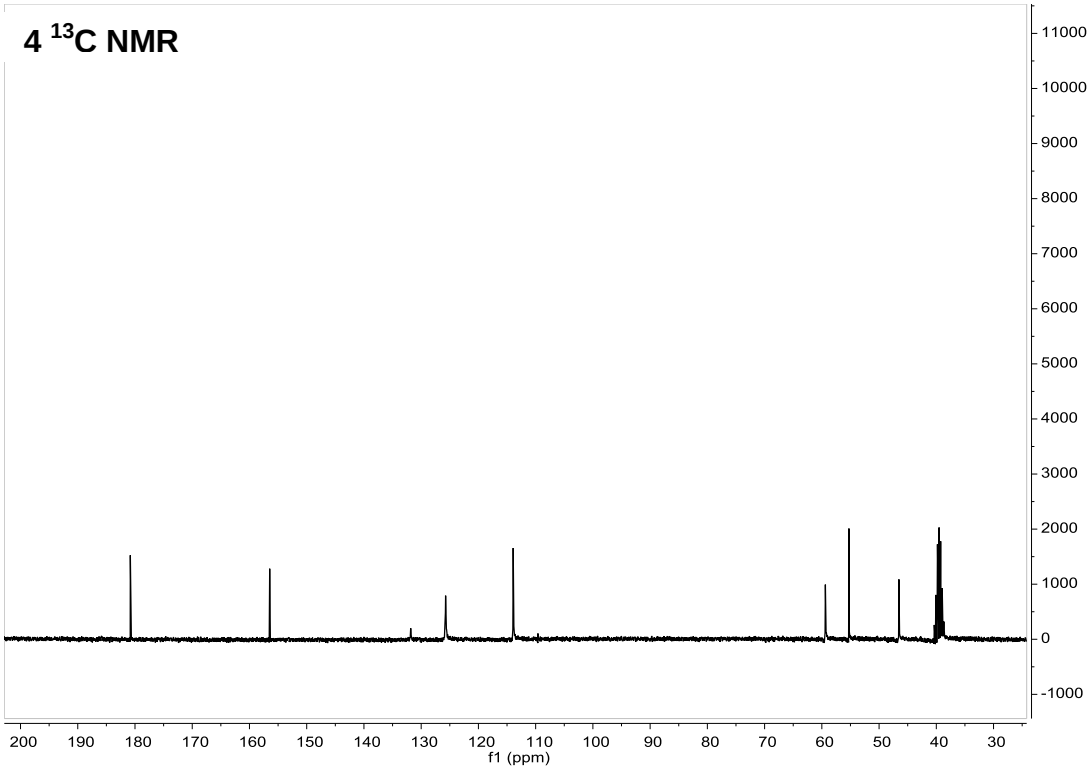
4 13C NMR
11000
10000
9000
8000
7000
6000
5000
4000
3000
2000
1000
0
-1000
200
190
180
170
160
150
140
130
120
110
100
90
80
70
60
50
40
30
f1 (ppm)

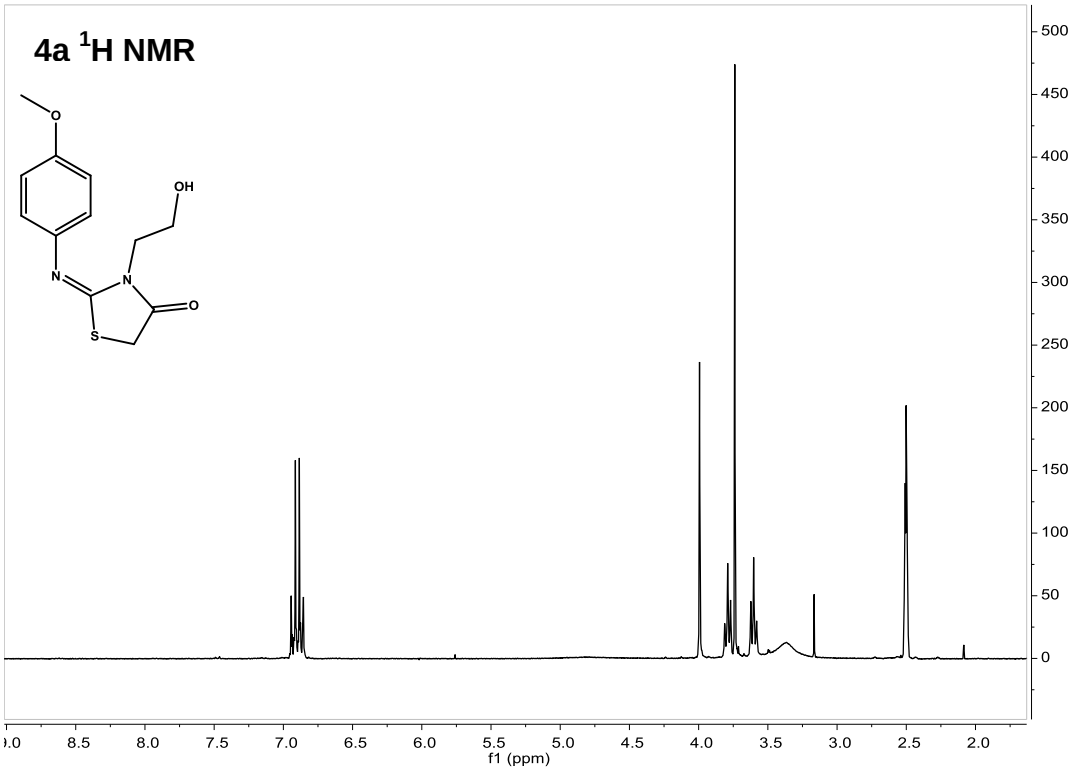
4a 1H NMR
O
OH
N
N
O
S
500
450
400
350
300
250
200
150
100
50
0
8.5
8.0
7.5
7.0
6.5
6.0
5.5
5.0
4.5
4.0
3.5
3.0
2.5
2.0
f1 (ppm)

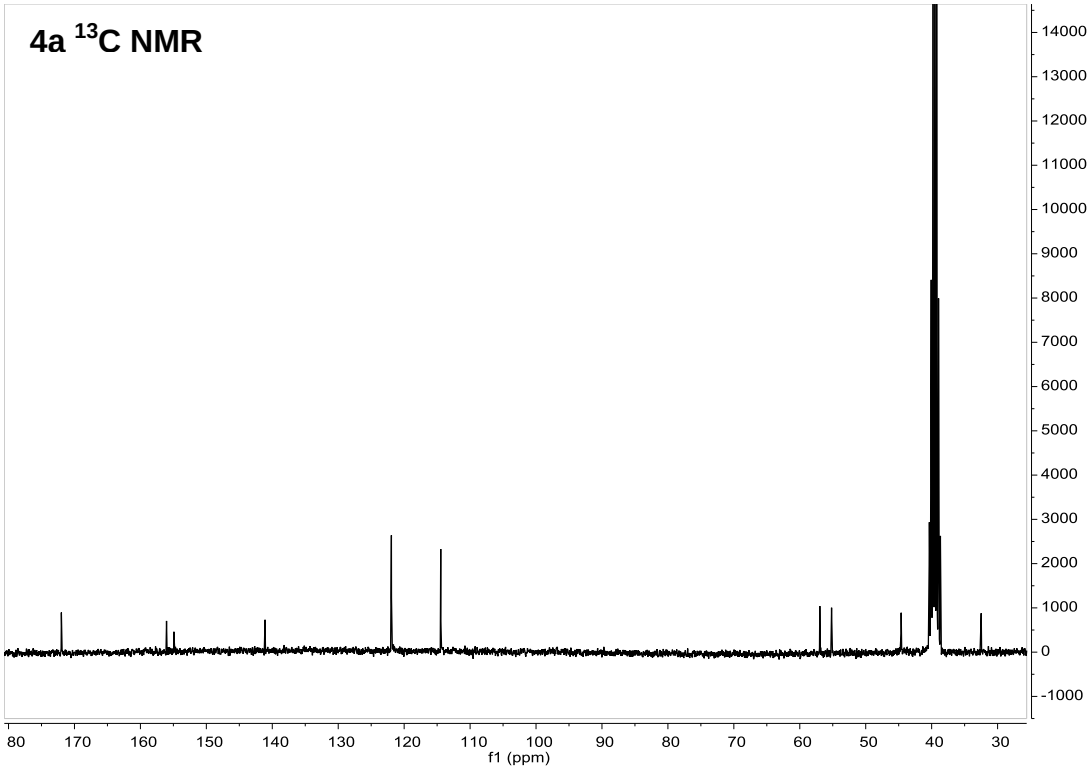
4a 13C NMR
14000
13000
12000
11000
10000
9000
8000
7000
6000
5000
4000
3000
2000
1000
0
-1000
170
160
150
140
130
120
110
100
90
80
70
60
50
40
30
f1 (ppm)

**5 $^{1}$H NMR**

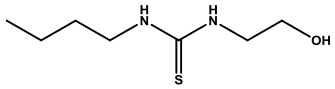





**5 $^{13}$C NMR**

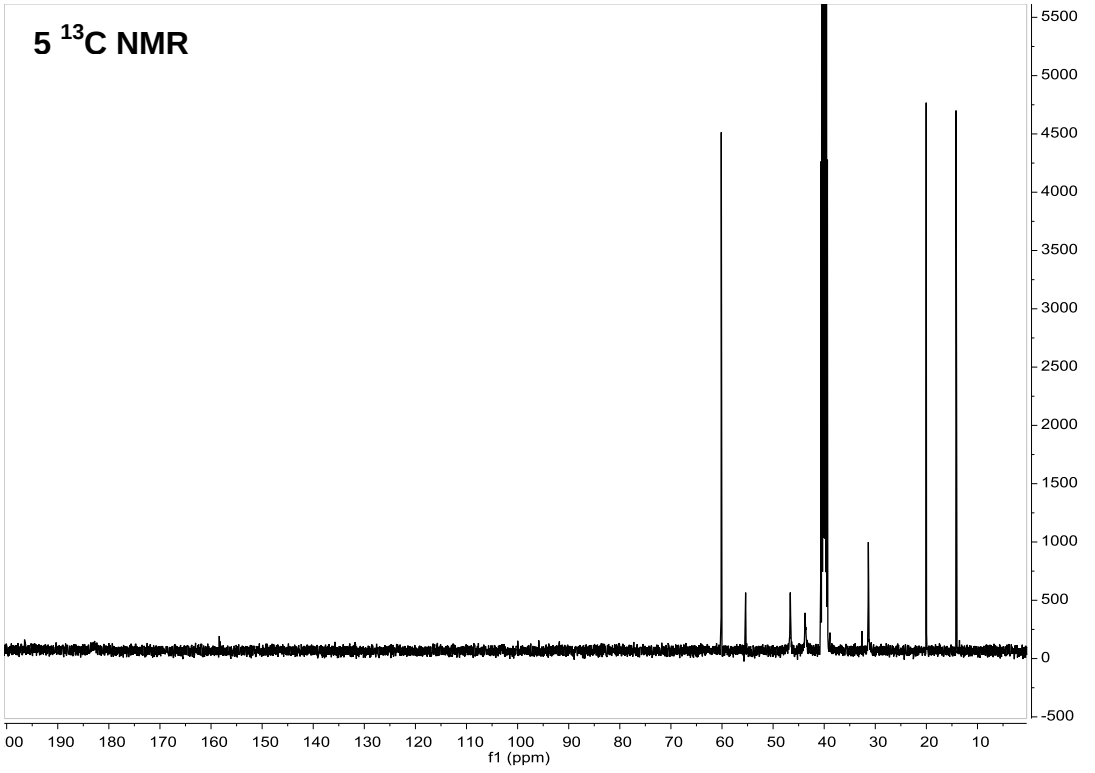

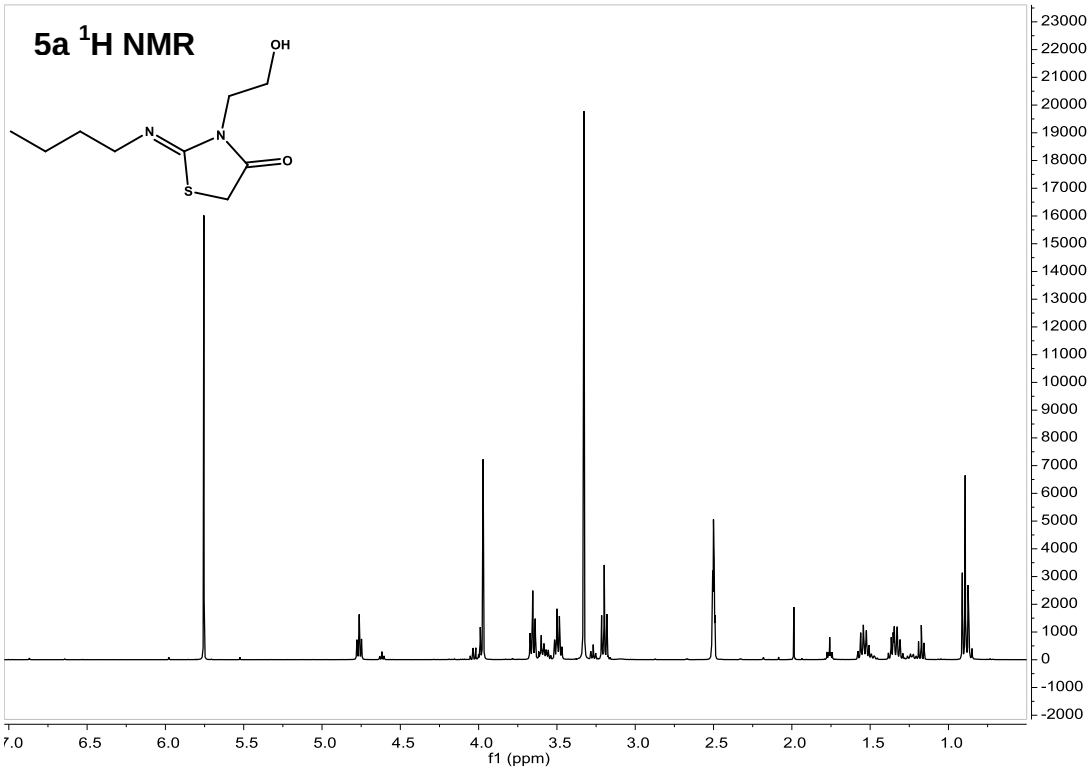
5a $^{1}$H NMR
OH
N
N
O
S
f1 (ppm)

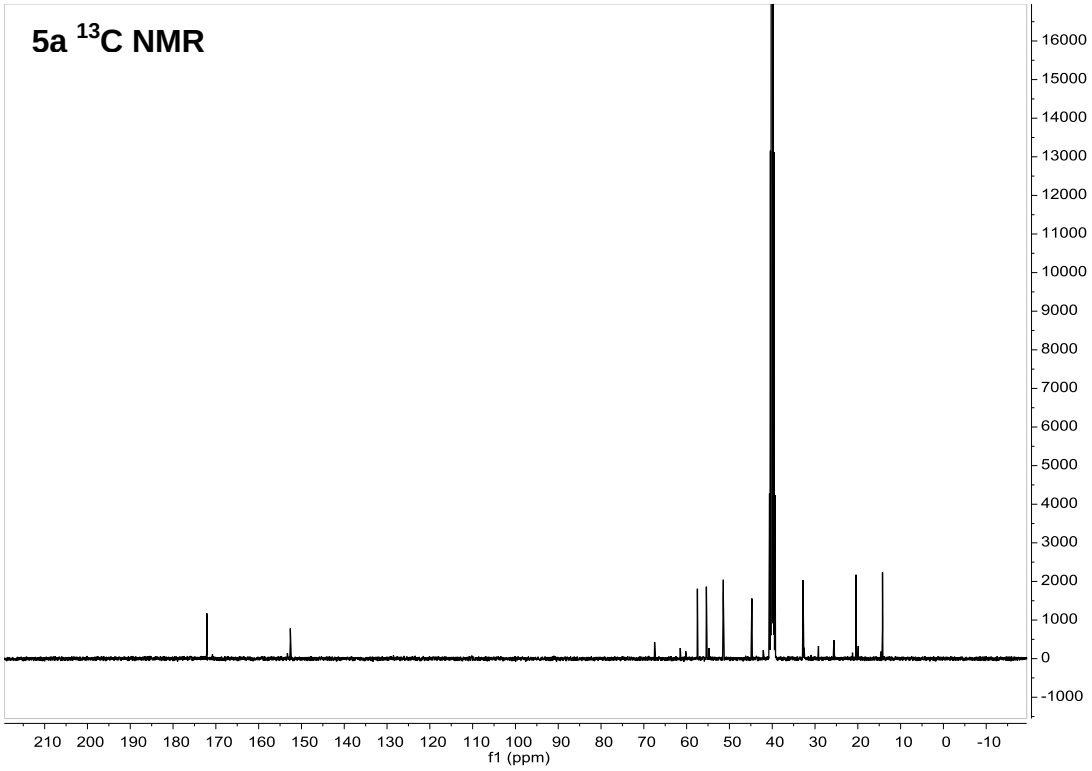
5a $^{13}$C NMR
f1 (ppm)

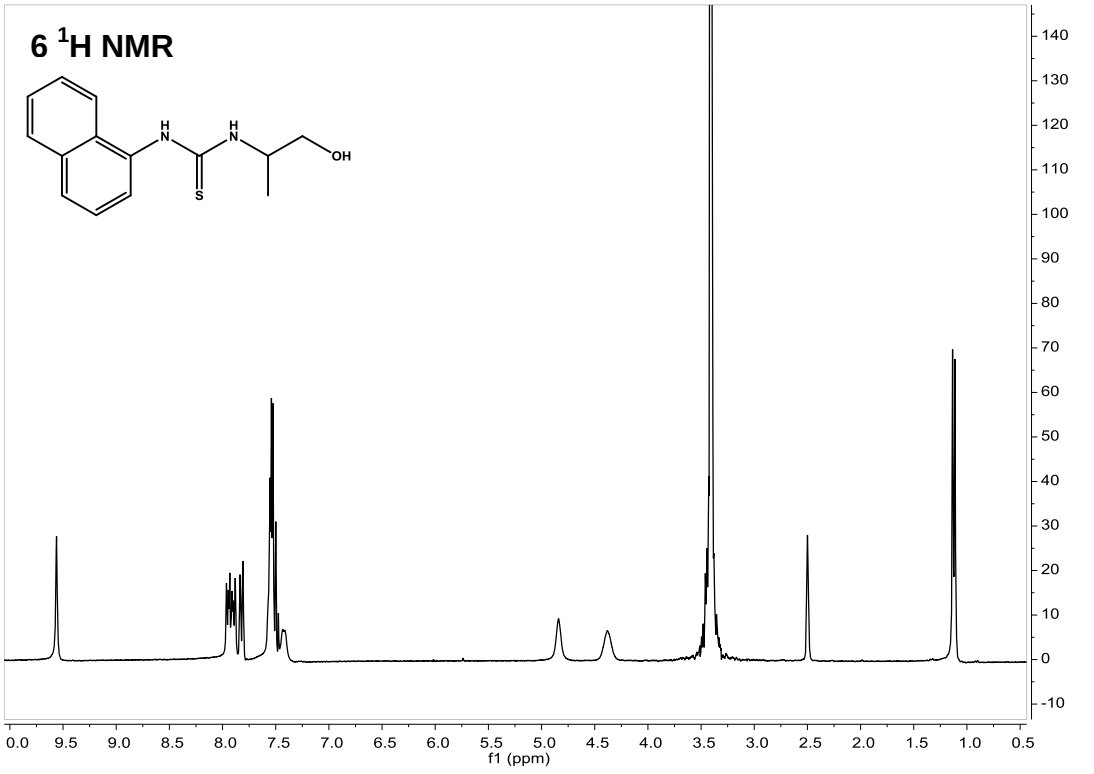
6 1H NMR
H
N
H
N
OH
S
140
130
120
110
100
90
80
70
60
50
40
30
20
10
0
-10
0.0 9.5 9.0 8.5 8.0 7.5 7.0 6.5 6.0 5.5 5.0 4.5 4.0 3.5 3.0 2.5 2.0 1.5 1.0 0.5
f1 (ppm)

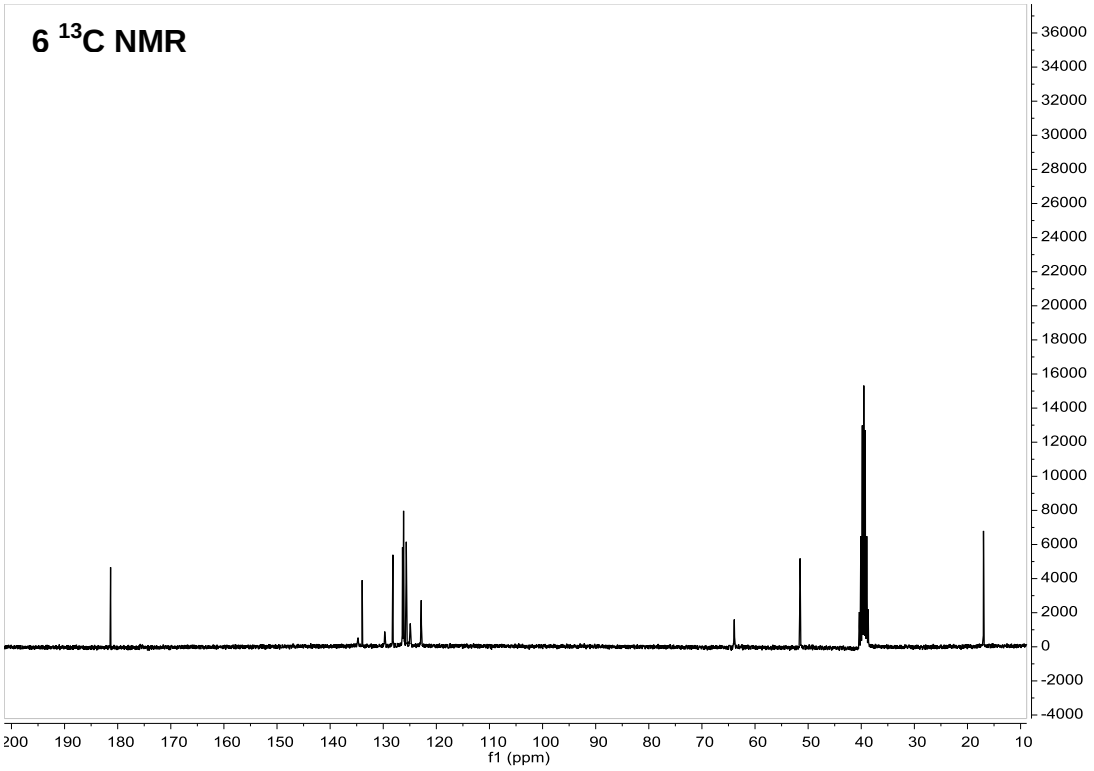
6 13C NMR
36000
34000
32000
30000
28000
26000
24000
22000
20000
18000
16000
14000
12000
10000
8000
6000
4000
2000
0
-2000
-4000
200 190 180 170 160 150 140 130 120 110 100 90 80 70 60 50 40 30 20 10
f1 (ppm)

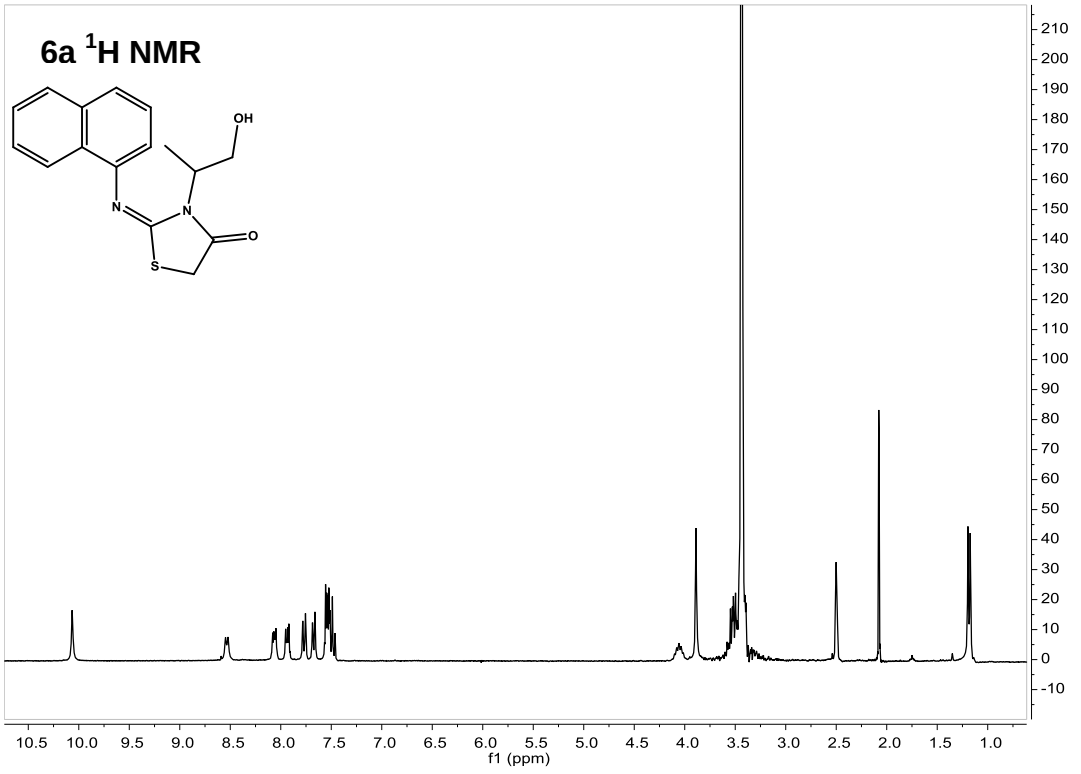
6a 1H NMR
OH
N
N
O
S
f1 (ppm)

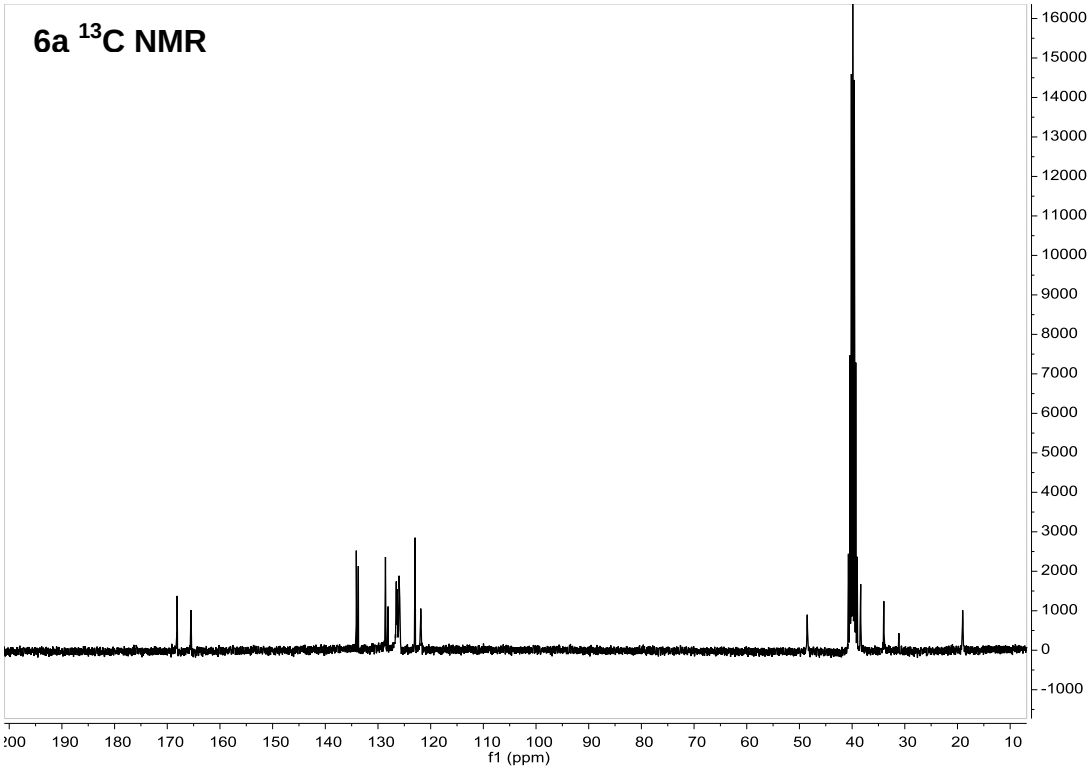
6a 13C NMR
f1 (ppm)

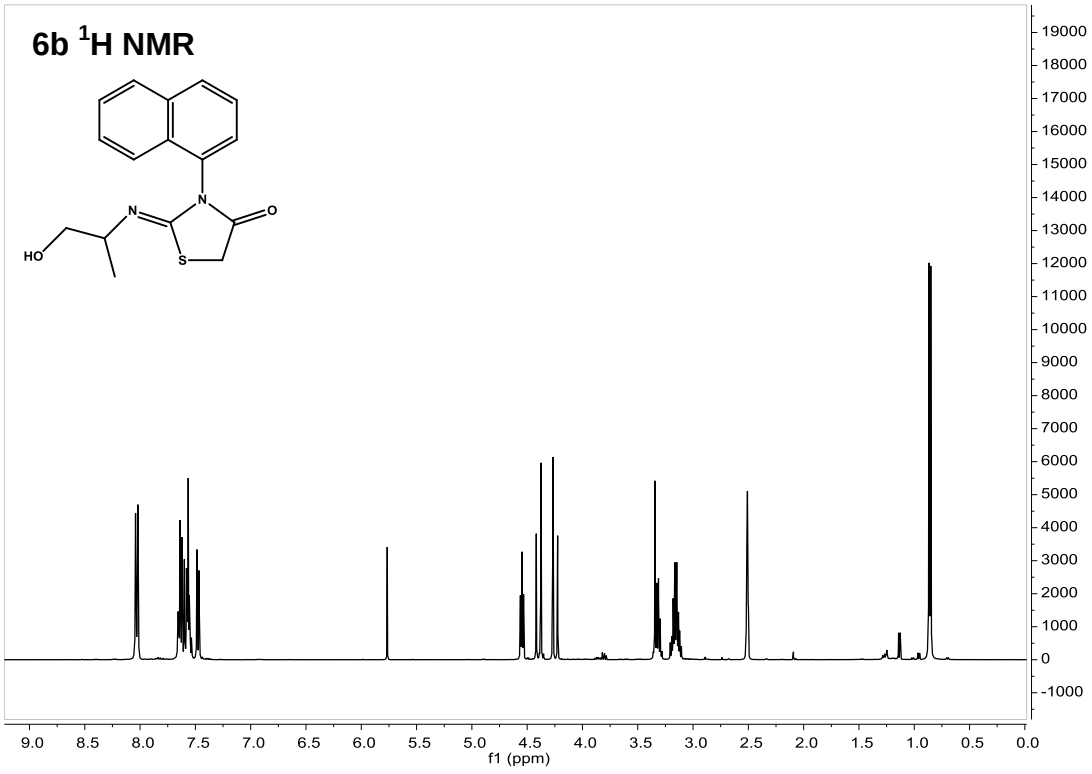
6b 1H NMR
HO
N
N
O
S
19000
18000
17000
16000
15000
14000
13000
12000
11000
10000
9000
8000
7000
6000
5000
4000
3000
2000
1000
0
-1000
9.0 8.5 8.0 7.5 7.0 6.5 6.0 5.5 5.0 4.5 4.0 3.5 3.0 2.5 2.0 1.5 1.0 0.5 0.0
f1 (ppm)

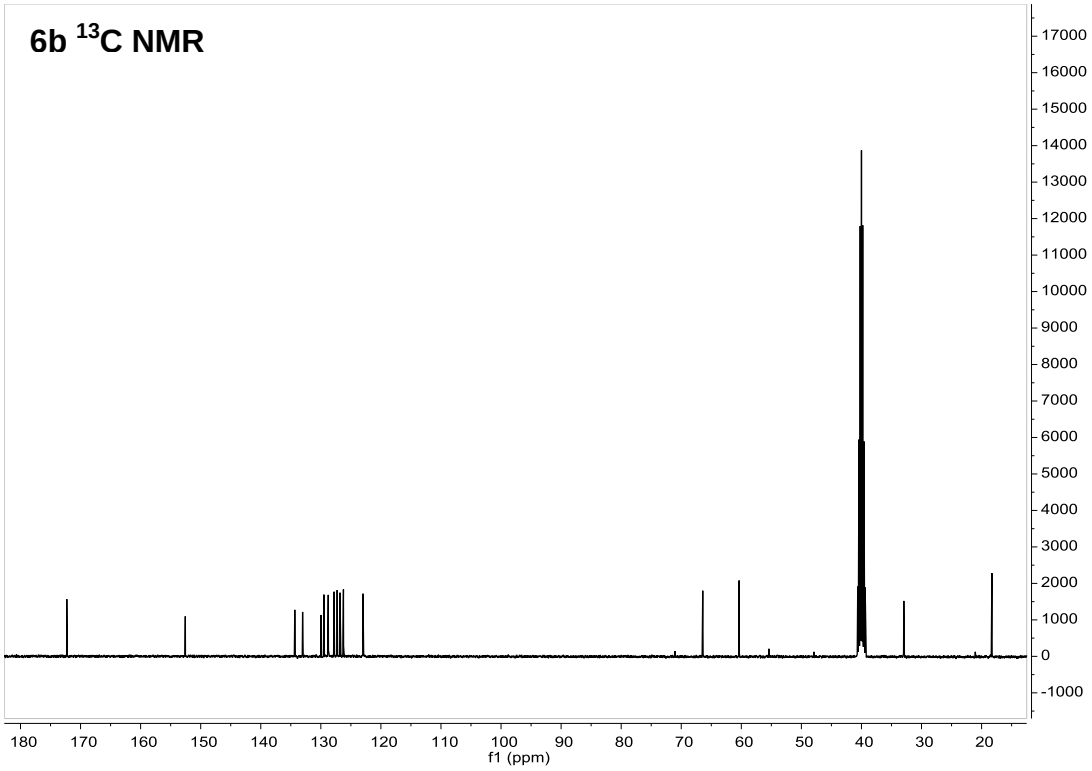
6b 13C NMR
17000
16000
15000
14000
13000
12000
11000
10000
9000
8000
7000
6000
5000
4000
3000
2000
1000
0
-1000
180 170 160 150 140 130 120 110 100 90 80 70 60 50 40 30 20
f1 (ppm)

**7 $^{1}$H NMR**

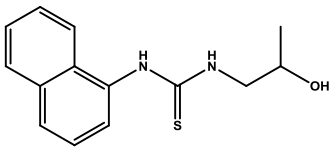





**7 $^{13}$C NMR**

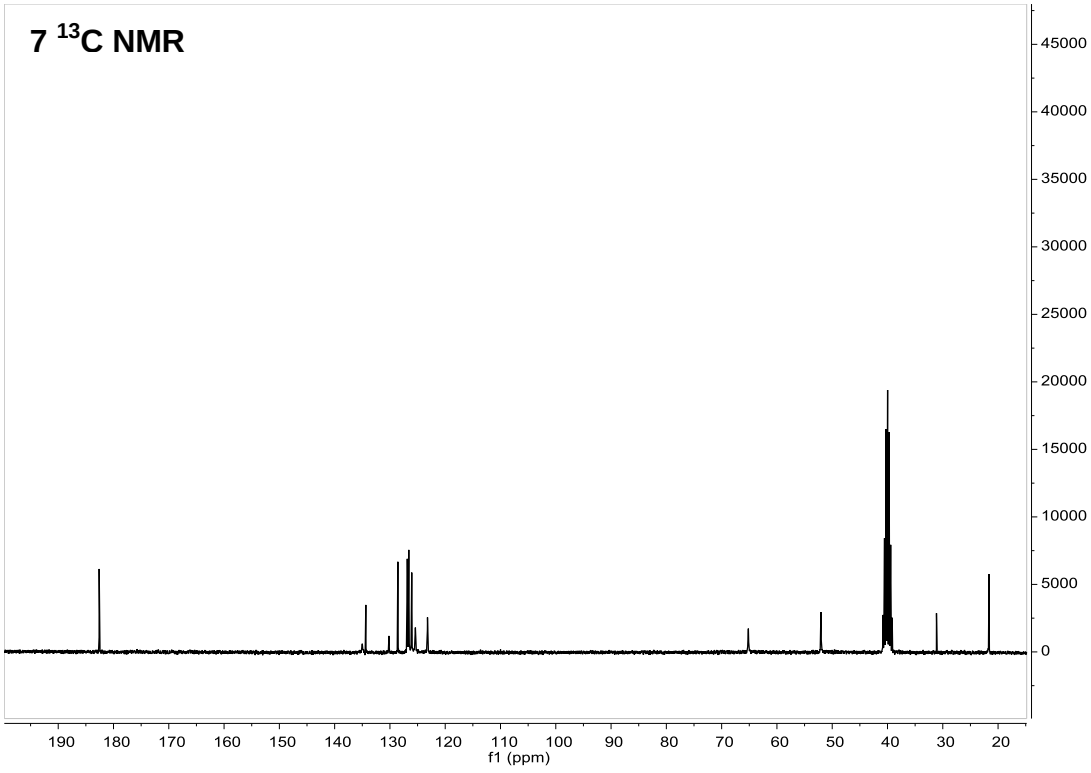

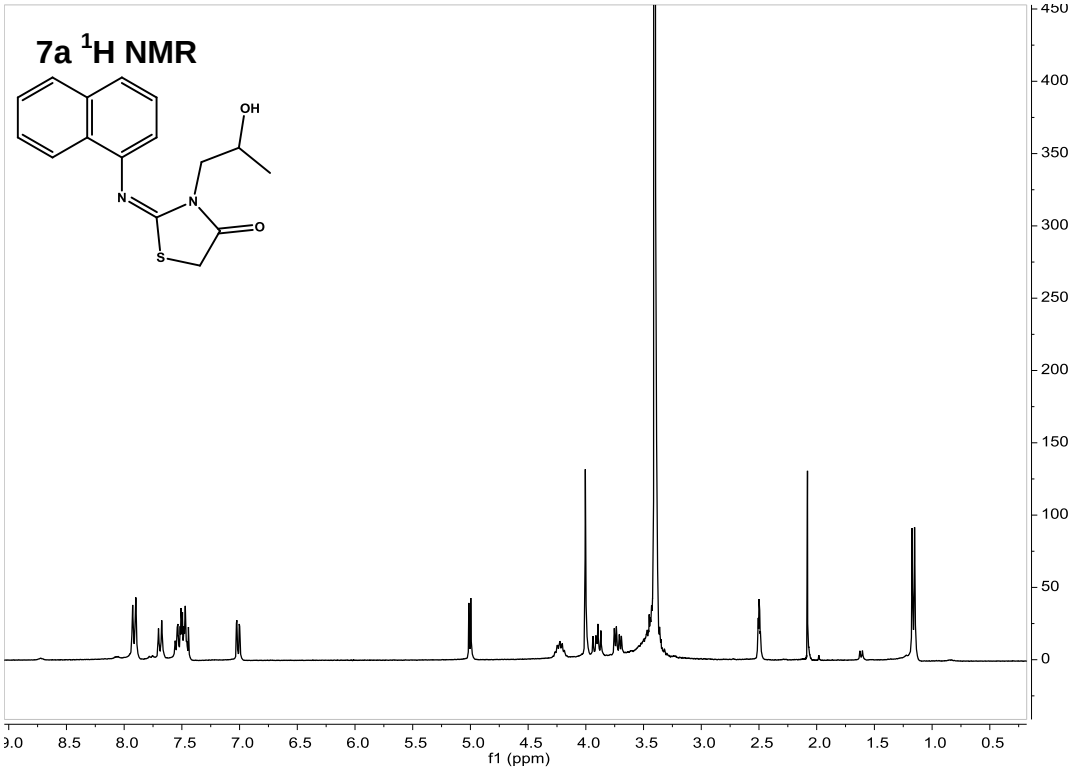
7a $^{1}$H NMR
OH
N
N
O
S
450
400
350
300
250
200
150
100
50
0
8.5
8.0
7.5
7.0
6.5
6.0
5.5
5.0
4.5
4.0
3.5
3.0
2.5
2.0
1.5
1.0
0.5
f1 (ppm)

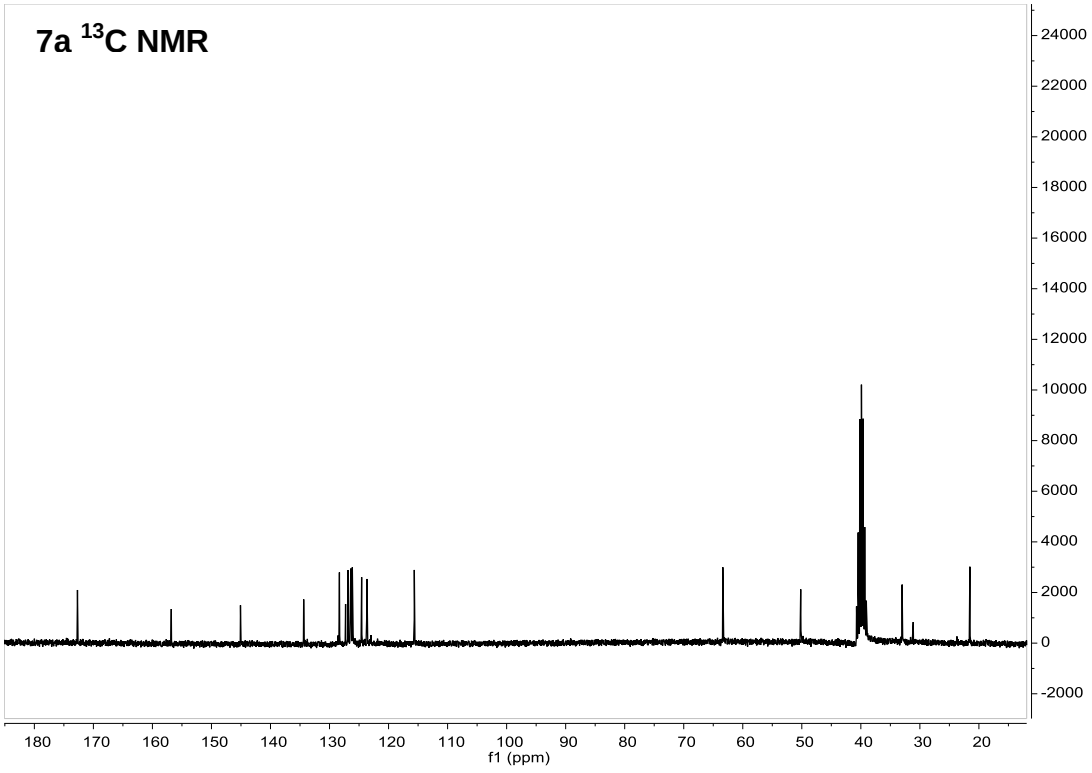
7a $^{13}$C NMR
24000
22000
20000
18000
16000
14000
12000
10000
8000
6000
4000
2000
0
-2000
180
170
160
150
140
130
120
110
100
90
80
70
60
50
40
30
20
f1 (ppm)

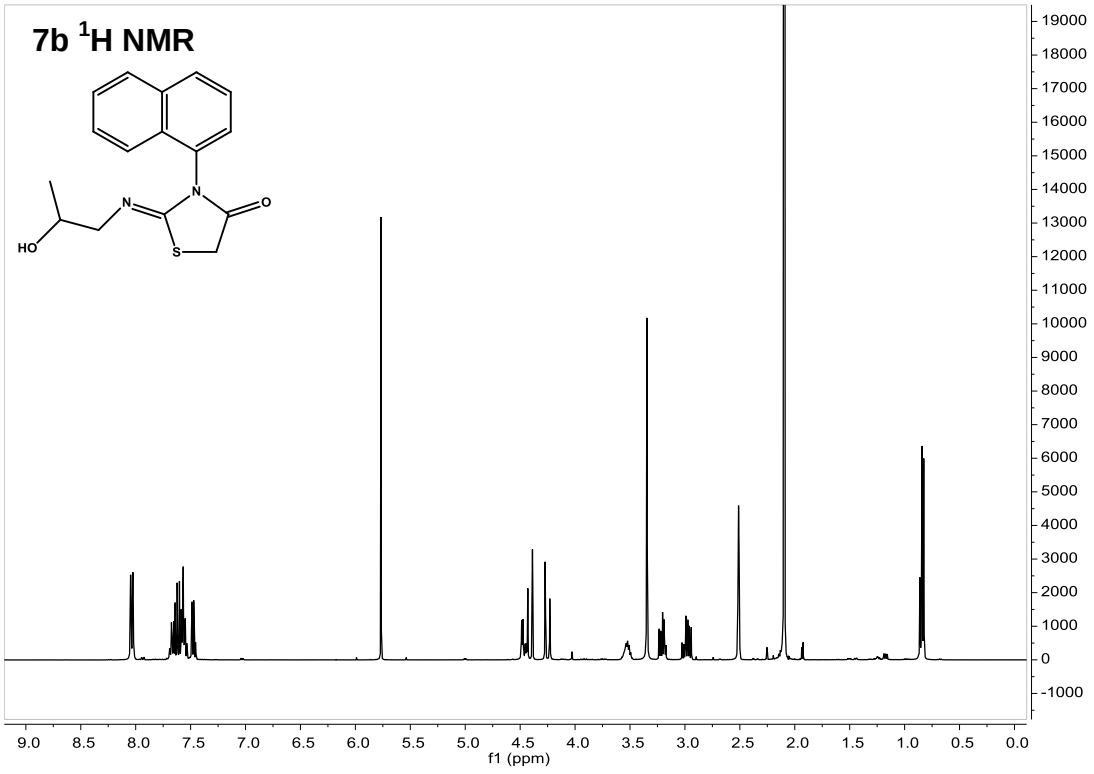
7b $^{1}$H NMR
HO
N
N
O
S
19000
18000
17000
16000
15000
14000
13000
12000
11000
10000
9000
8000
7000
6000
5000
4000
3000
2000
1000
0
-1000
9.0 8.5 8.0 7.5 7.0 6.5 6.0 5.5 5.0 4.5 4.0 3.5 3.0 2.5 2.0 1.5 1.0 0.5 0.0
f1 (ppm)

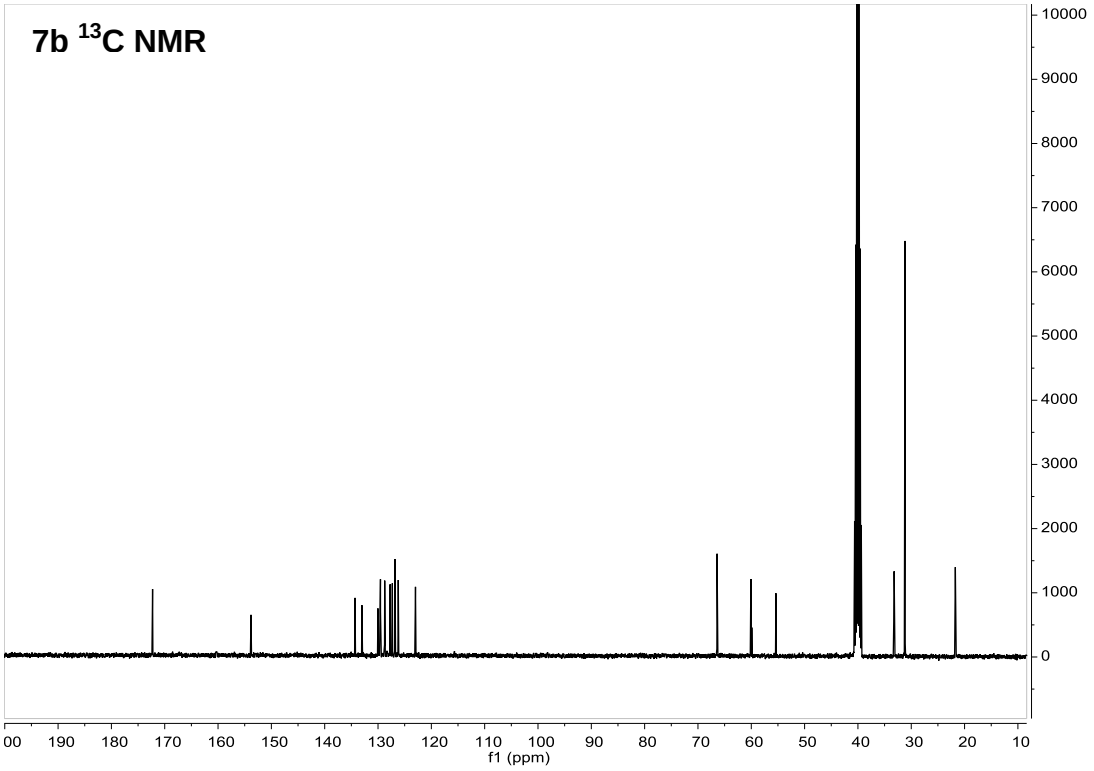
7b $^{13}$C NMR
10000
9000
8000
7000
6000
5000
4000
3000
2000
1000
0
00 190 180 170 160 150 140 130 120 110 100 90 80 70 60 50 40 30 20 10
f1 (ppm)

**8 $^{1}$H NMR**

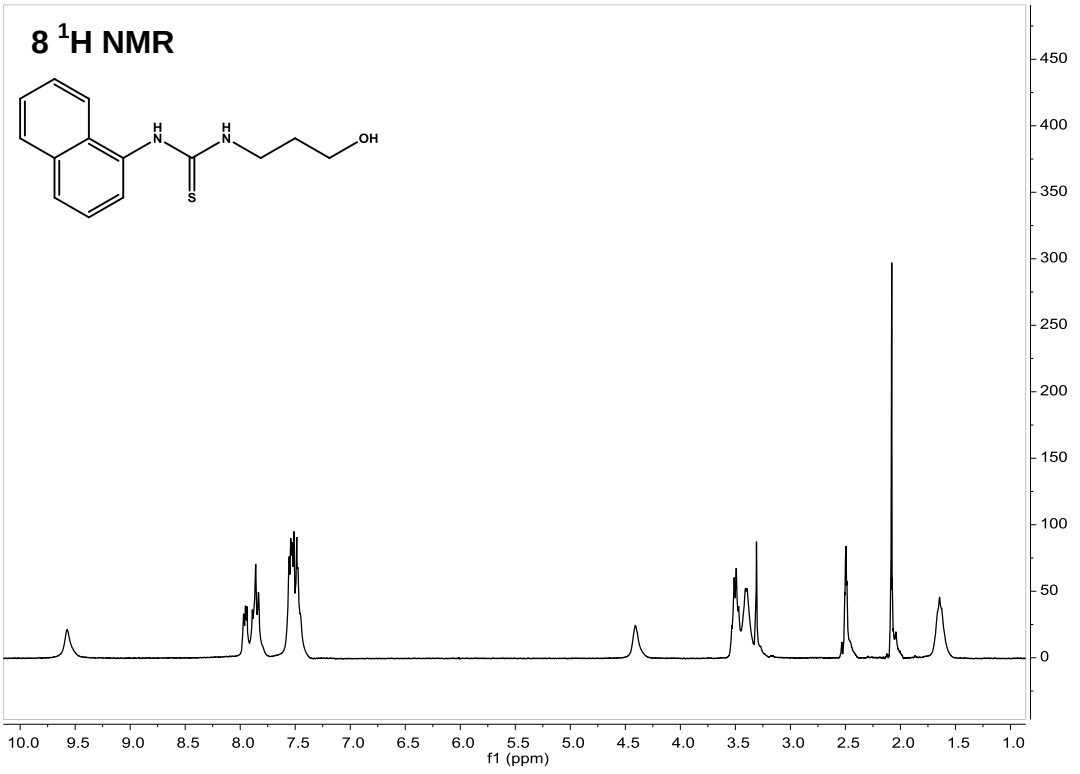


**8 $^{13}$C NMR**

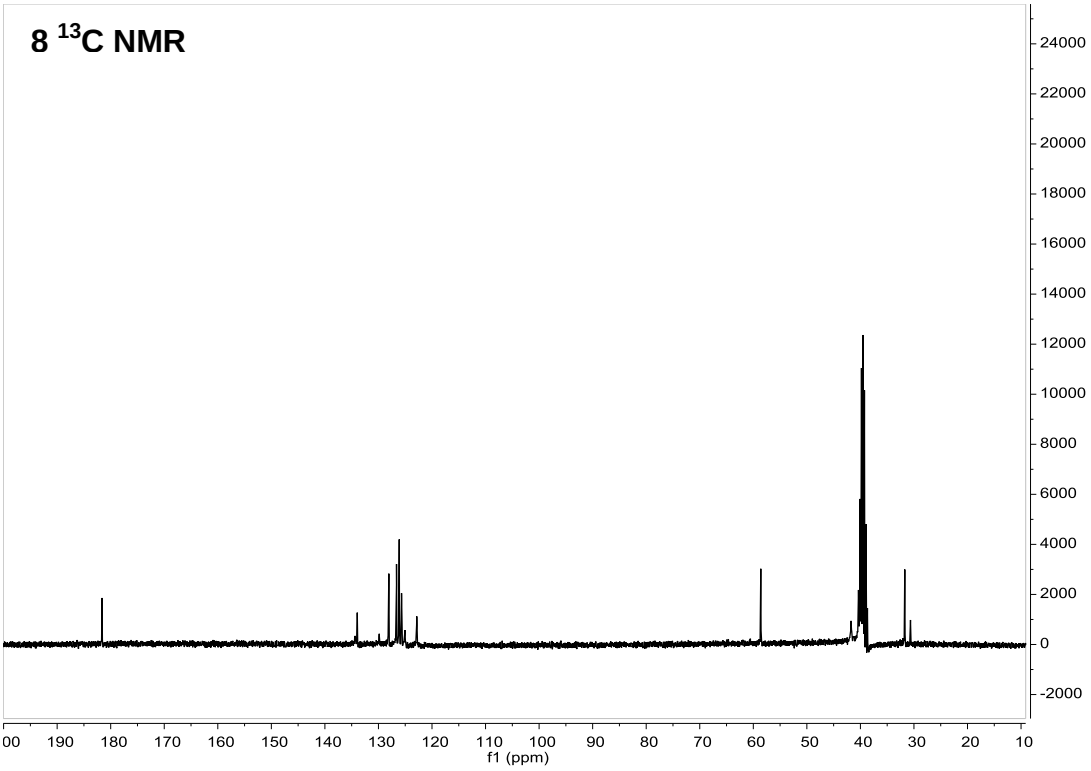

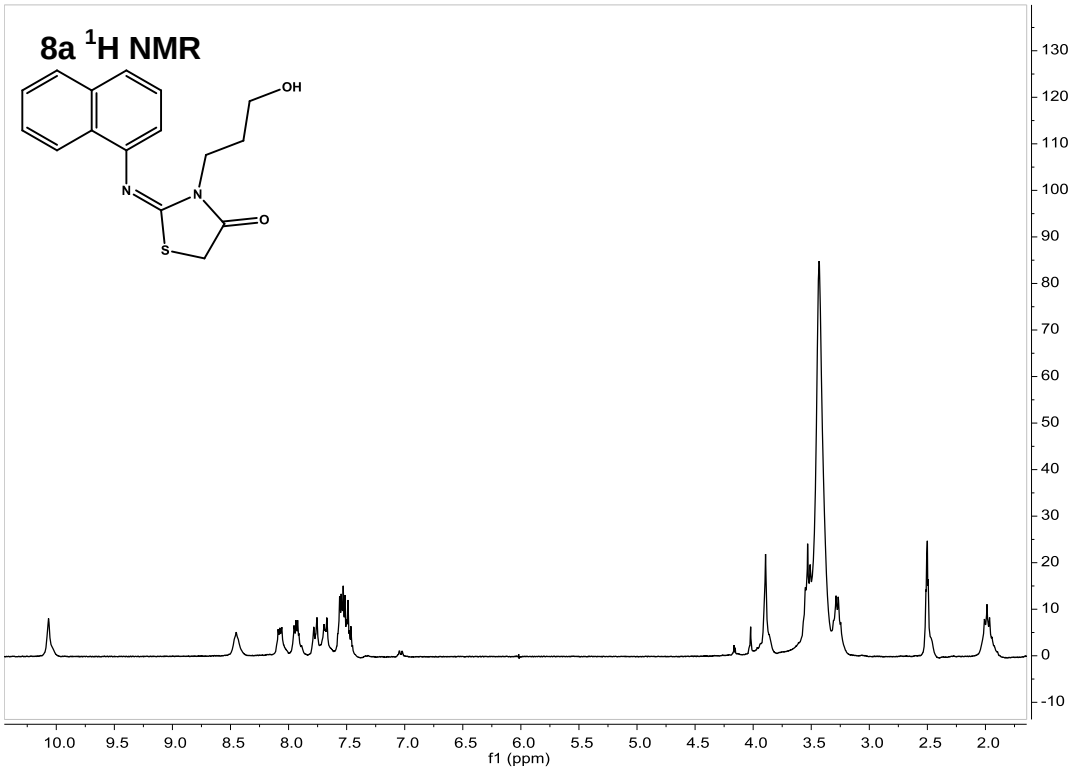
8a $^{1}$H NMR
OH
N
N
O
S
130
120
110
100
90
80
70
60
50
40
30
20
10
0
-10
10.0 9.5 9.0 8.5 8.0 7.5 7.0 6.5 6.0 5.5 5.0 4.5 4.0 3.5 3.0 2.5 2.0
f1 (ppm)

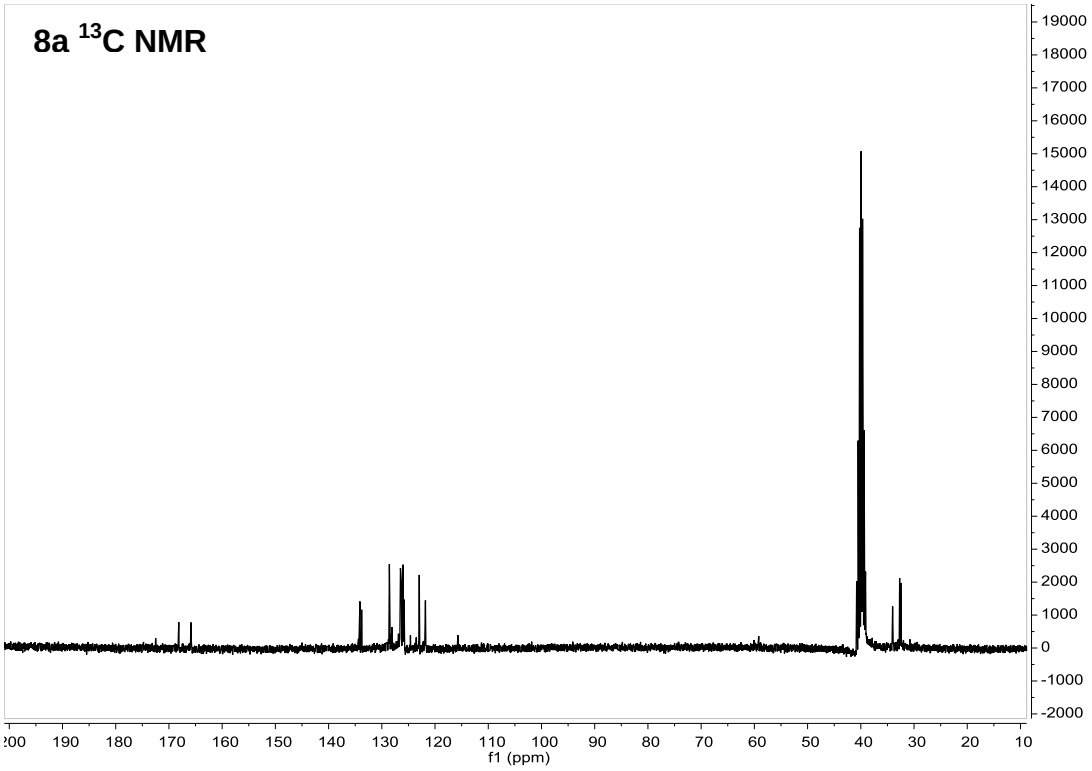
8a $^{13}$C NMR
19000
18000
17000
16000
15000
14000
13000
12000
11000
10000
9000
8000
7000
6000
5000
4000
3000
2000
1000
0
-1000
-2000
200 190 180 170 160 150 140 130 120 110 100 90 80 70 60 50 40 30 20 10
f1 (ppm)

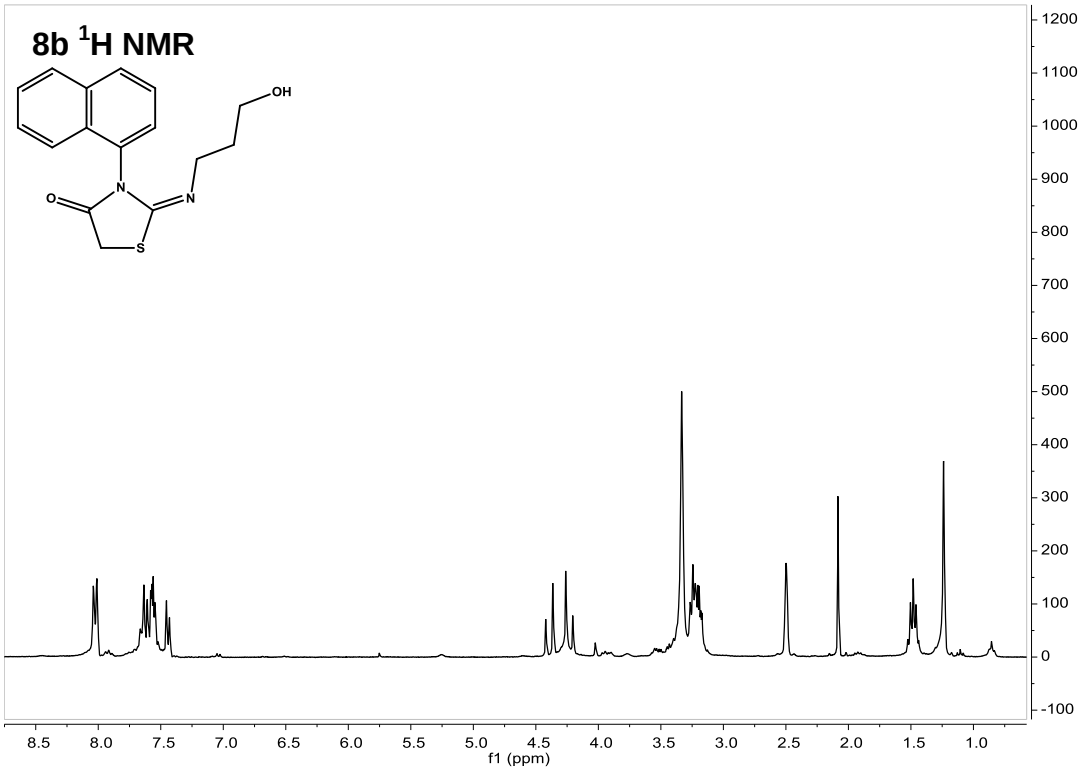
8b $^{1}$H NMR
OH
N
O
N
S
1200
1100
1000
900
800
700
600
500
400
300
200
100
0
-100
8.5 8.0 7.5 7.0 6.5 6.0 5.5 5.0 4.5 4.0 3.5 3.0 2.5 2.0 1.5 1.0
f1 (ppm)

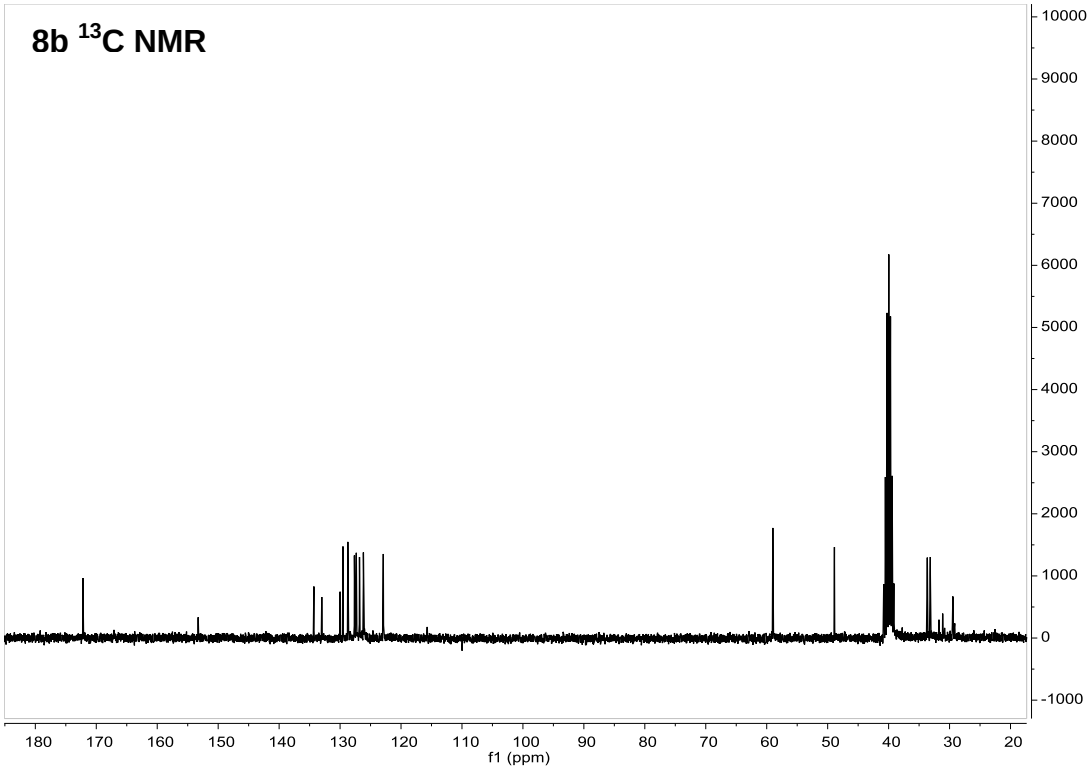
8b $^{13}$C NMR
10000
9000
8000
7000
6000
5000
4000
3000
2000
1000
0
-1000
180 170 160 150 140 130 120 110 100 90 80 70 60 50 40 30 20
f1 (ppm)

**9 $^{1}$H NMR**

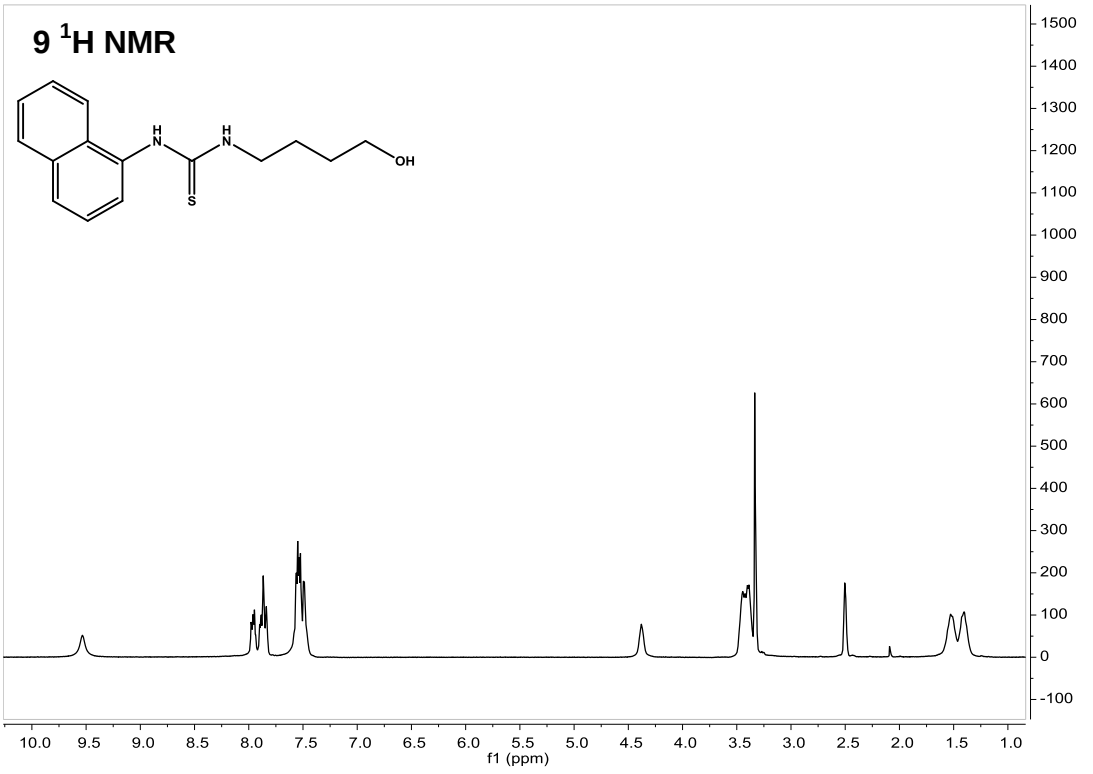


**9 $^{13}$C NMR**

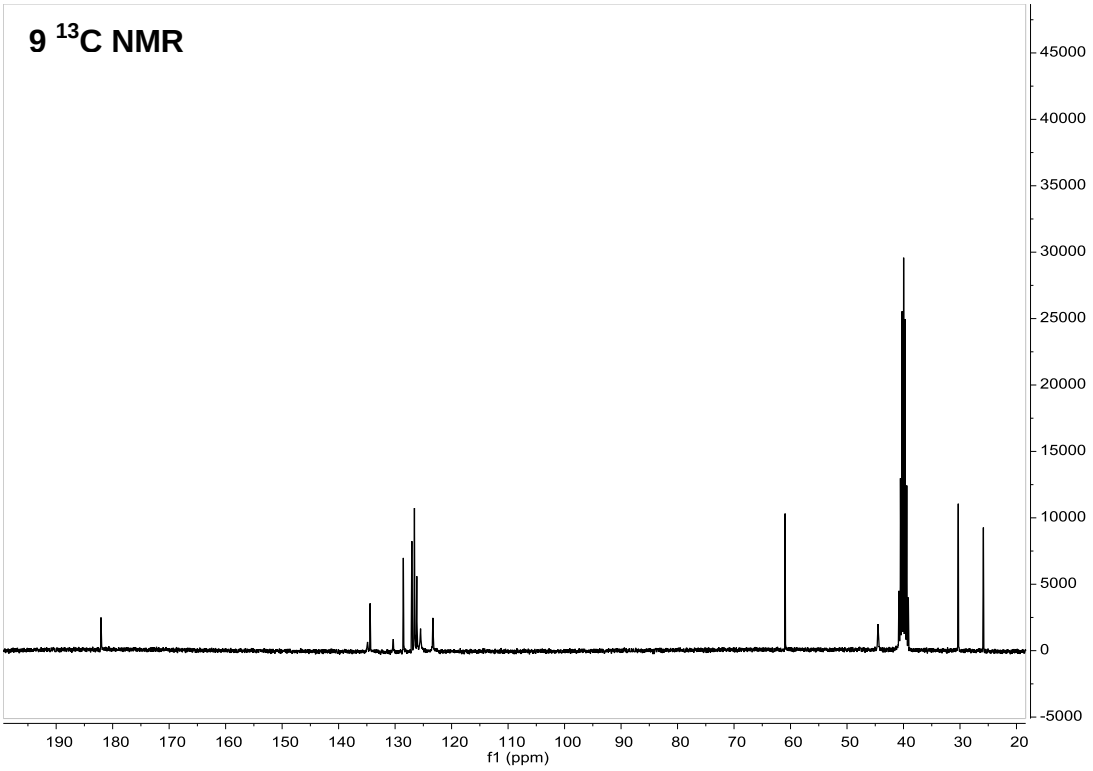

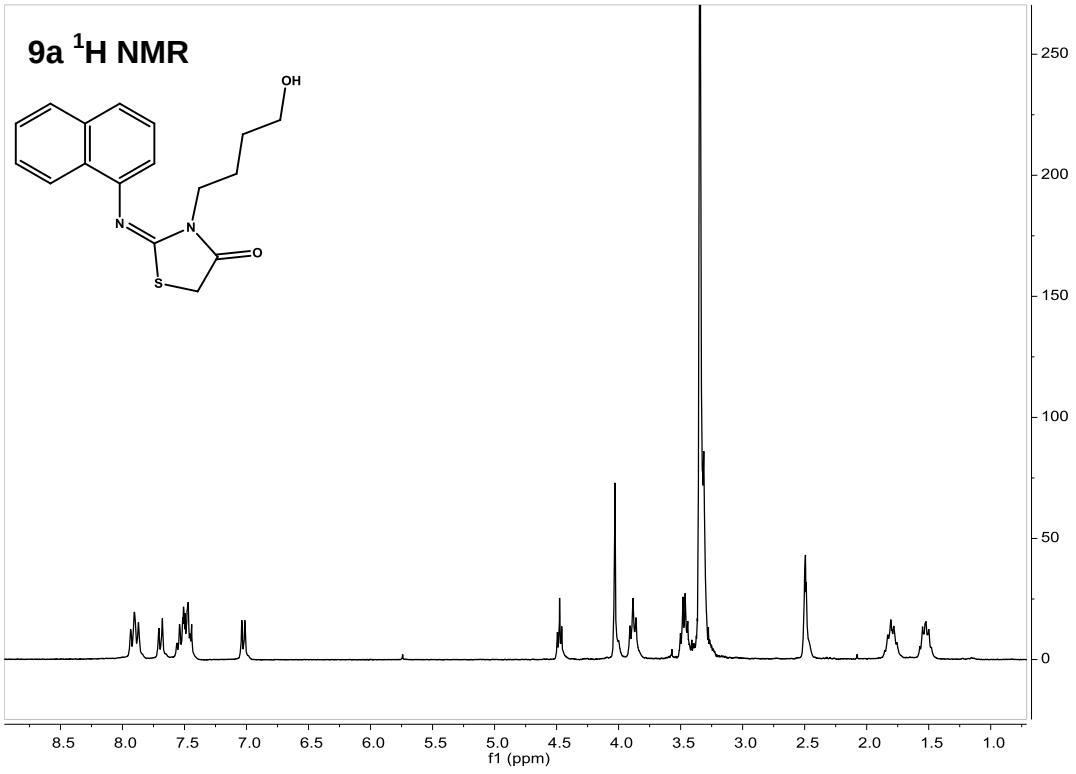
9a 1H NMR
OH
N
N
O
S
250
200
150
100
50
0
8.5
8.0
7.5
7.0
6.5
6.0
5.5
5.0
4.5
4.0
3.5
3.0
2.5
2.0
1.5
1.0
f1 (ppm)

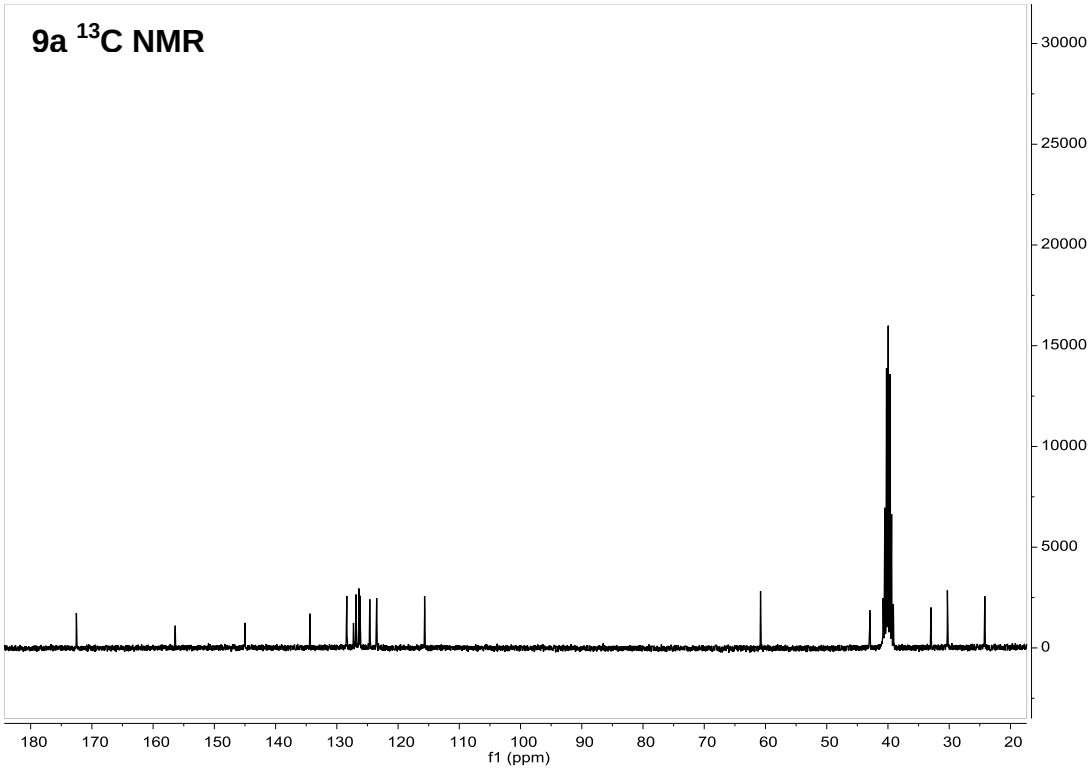
9a 13C NMR
30000
25000
20000
15000
10000
5000
0
180
170
160
150
140
130
120
110
100
90
80
70
60
50
40
30
20
f1 (ppm)

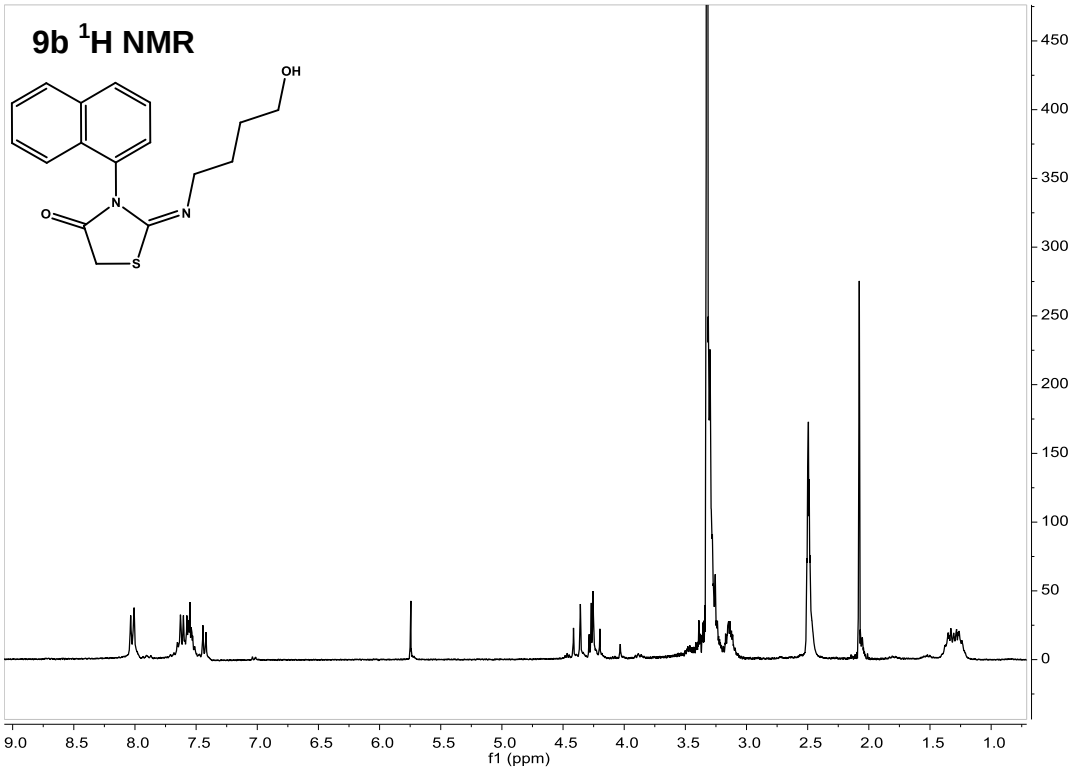
9b 1H NMR
OH
O
N
N
S
450
400
350
300
250
200
150
100
50
0
9.0
8.5
8.0
7.5
7.0
6.5
6.0
5.5
5.0
4.5
4.0
3.5
3.0
2.5
2.0
1.5
1.0
f1 (ppm)

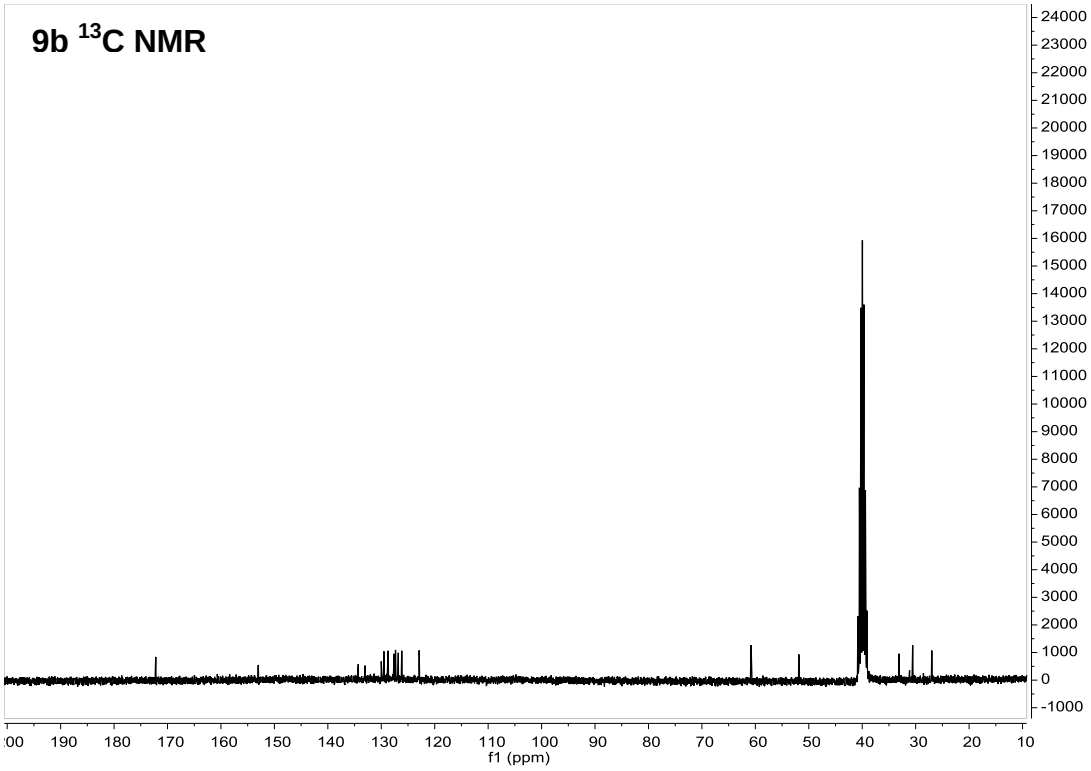
9b 13C NMR
24000
23000
22000
21000
20000
19000
18000
17000
16000
15000
14000
13000
12000
11000
10000
9000
8000
7000
6000
5000
4000
3000
2000
1000
0
-1000
190
180
170
160
150
140
130
120
110
100
90
80
70
60
50
40
30
20
10
f1 (ppm)

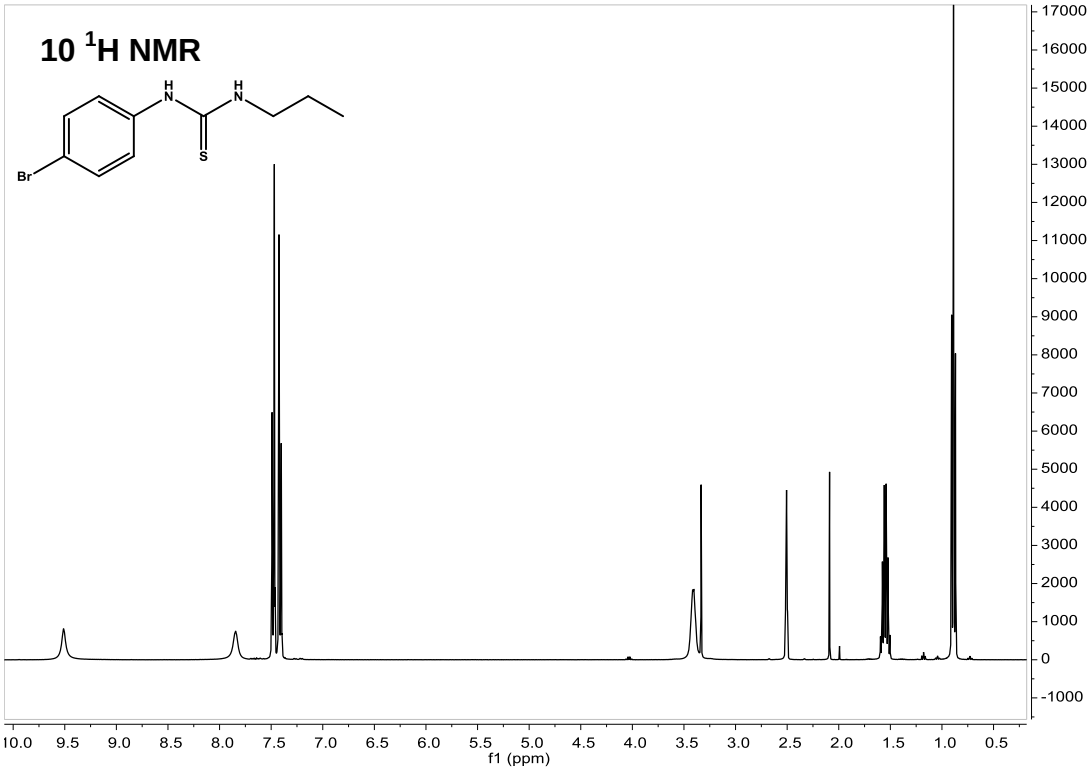
10 1H NMR
Br
H
N
H
N
S
17000
16000
15000
14000
13000
12000
11000
10000
9000
8000
7000
6000
5000
4000
3000
2000
1000
0
-1000
10.0 9.5 9.0 8.5 8.0 7.5 7.0 6.5 6.0 5.5 5.0 4.5 4.0 3.5 3.0 2.5 2.0 1.5 1.0 0.5
f1 (ppm)

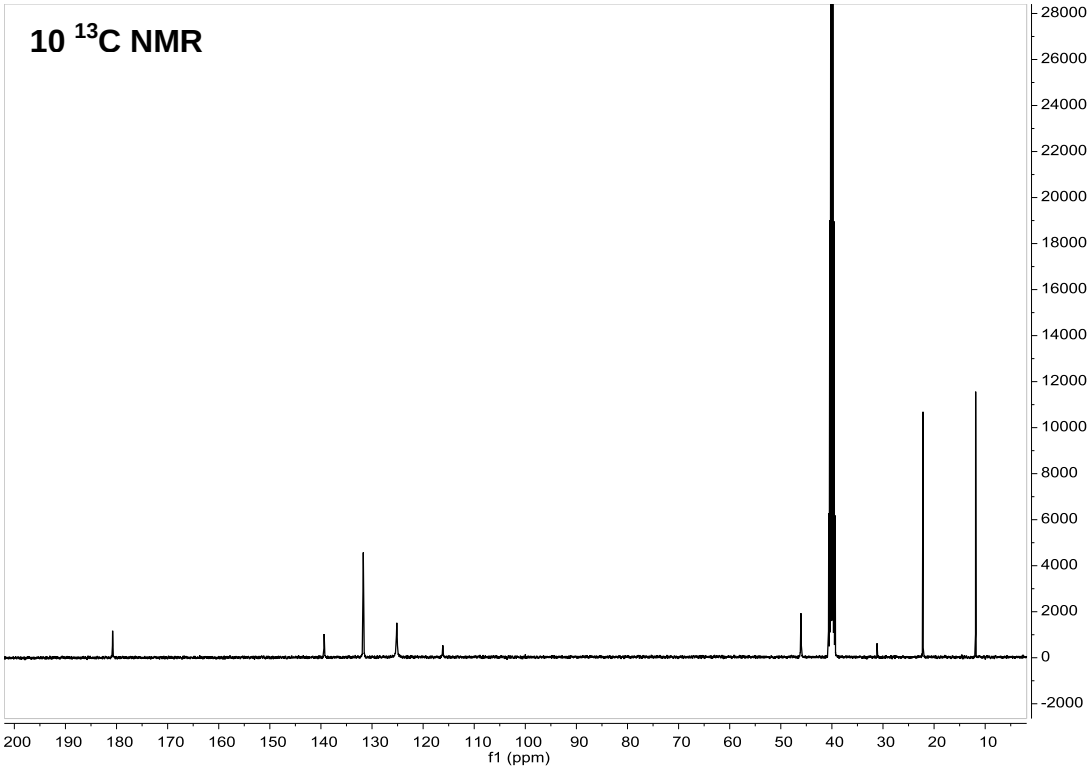
10 13C NMR
28000
26000
24000
22000
20000
18000
16000
14000
12000
10000
8000
6000
4000
2000
0
-2000
200 190 180 170 160 150 140 130 120 110 100 90 80 70 60 50 40 30 20 10
f1 (ppm)

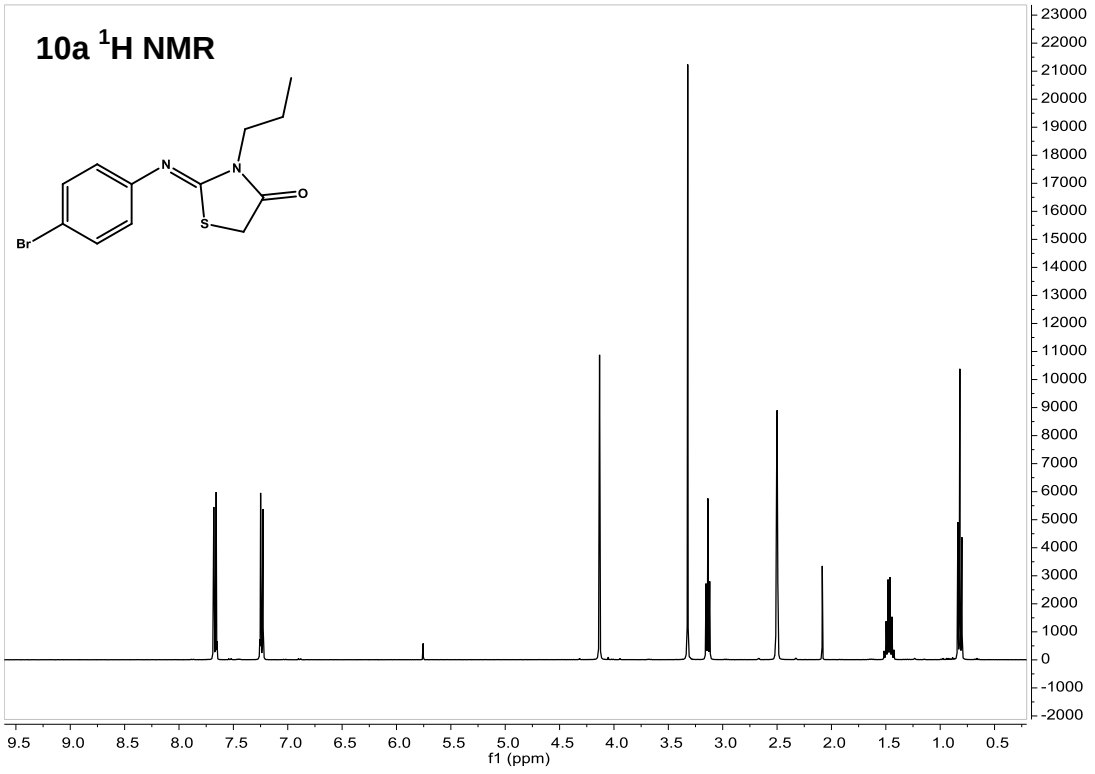
10a 1H NMR
Br
N
N
S
O
23000
22000
21000
20000
19000
18000
17000
16000
15000
14000
13000
12000
11000
10000
9000
8000
7000
6000
5000
4000
3000
2000
1000
0
-1000
-2000
9.5 9.0 8.5 8.0 7.5 7.0 6.5 6.0 5.5 5.0 4.5 4.0 3.5 3.0 2.5 2.0 1.5 1.0 0.5
f1 (ppm)

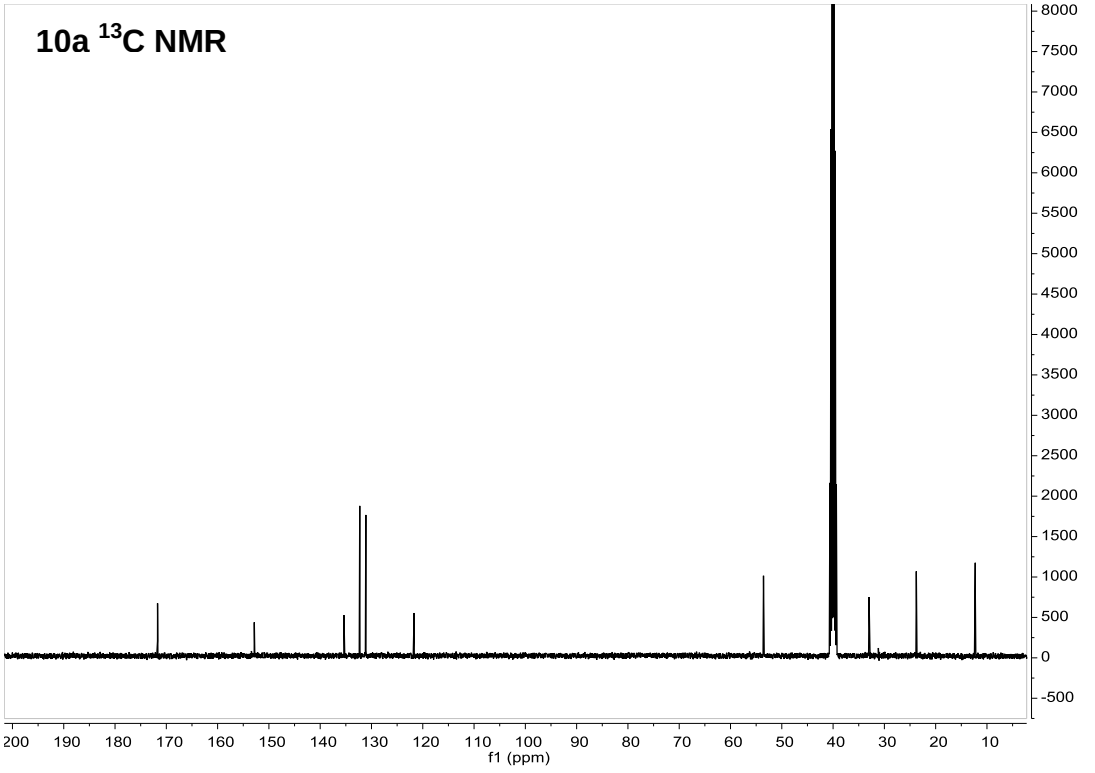
10a 13C NMR
8000
7500
7000
6500
6000
5500
5000
4500
4000
3500
3000
2500
2000
1500
1000
500
0
-500
200 190 180 170 160 150 140 130 120 110 100 90 80 70 60 50 40 30 20 10
f1 (ppm)

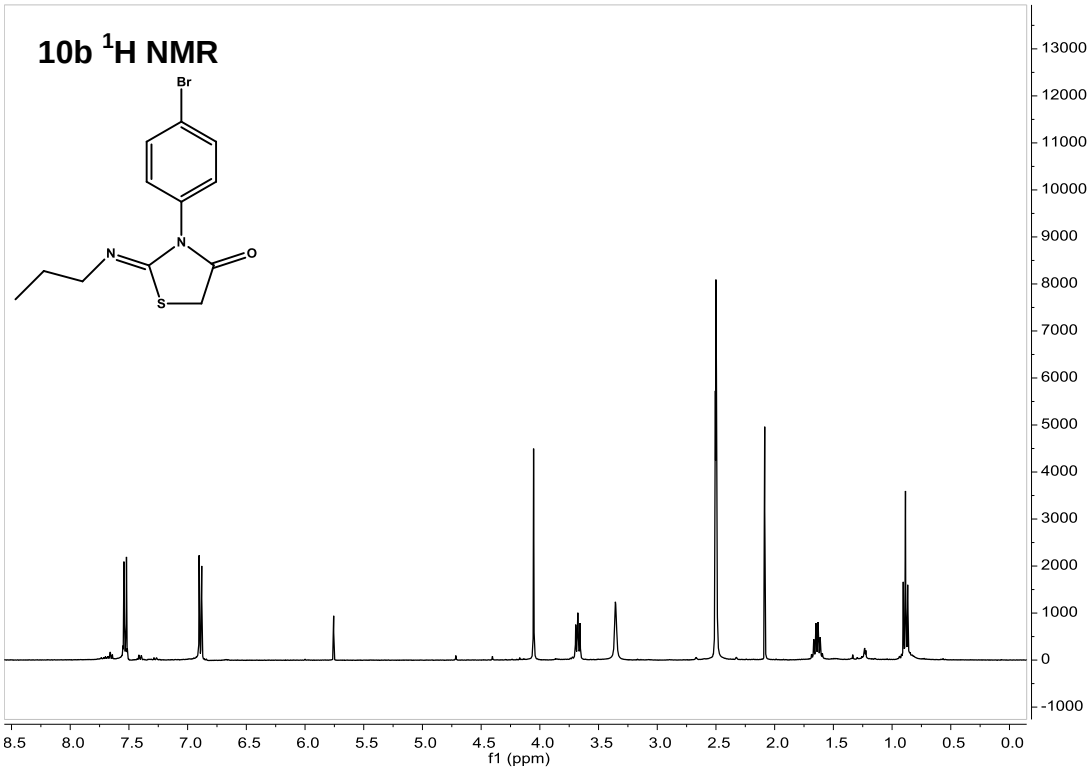
10b 1H NMR
Br
N
N
O
S
13000
12000
11000
10000
9000
8000
7000
6000
5000
4000
3000
2000
1000
0
-1000
8.5 8.0 7.5 7.0 6.5 6.0 5.5 5.0 4.5 4.0 3.5 3.0 2.5 2.0 1.5 1.0 0.5 0.0
f1 (ppm)

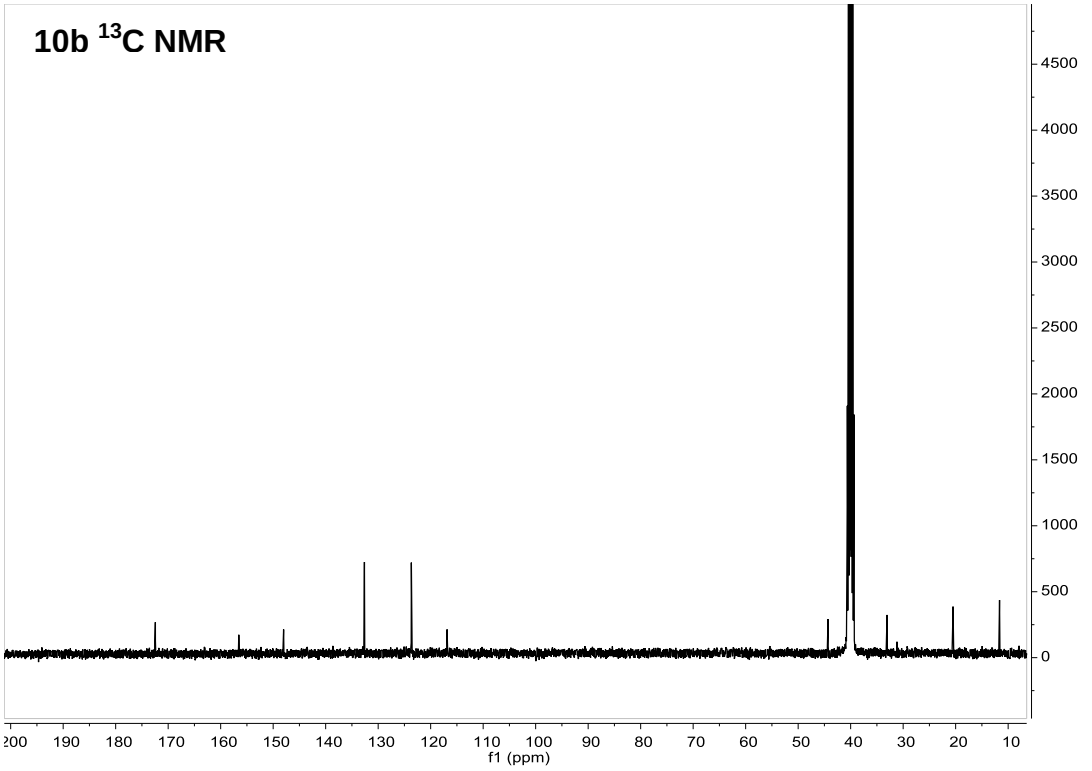
10b 13C NMR
4500
4000
3500
3000
2500
2000
1500
1000
500
0
200 190 180 170 160 150 140 130 120 110 100 90 80 70 60 50 40 30 20 10
f1 (ppm)

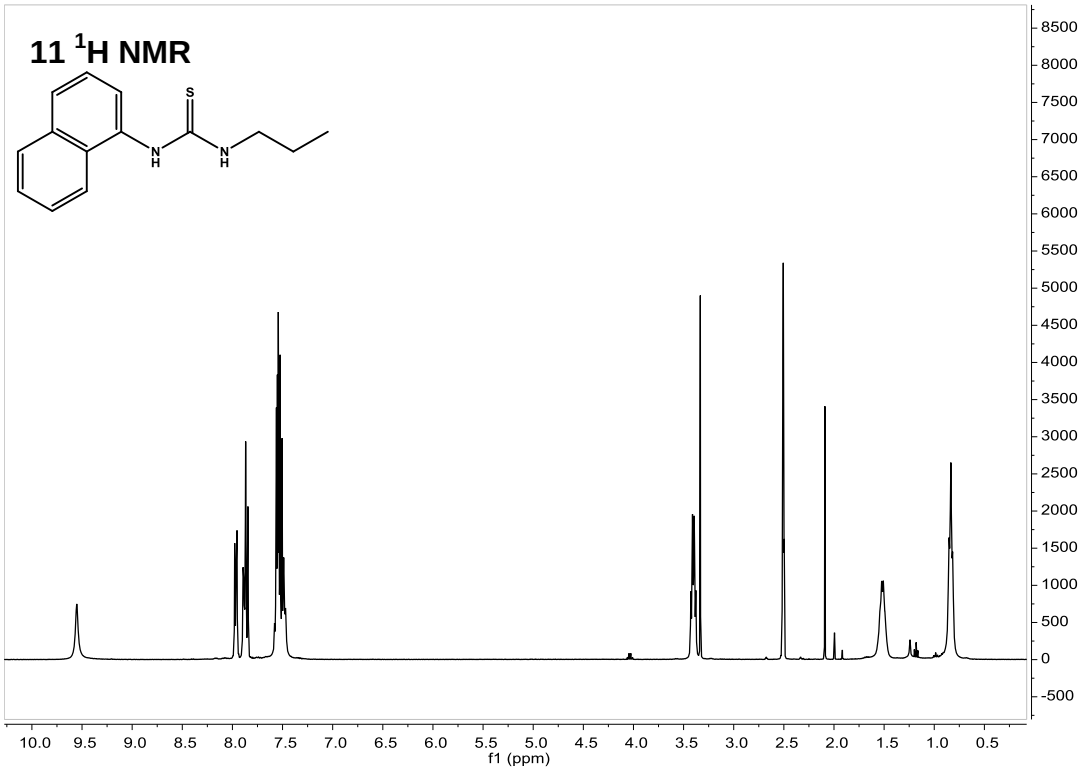
11 1H NMR
S
N
H
N
H
8500
8000
7500
7000
6500
6000
5500
5000
4500
4000
3500
3000
2500
2000
1500
1000
500
0
-500
10.0 9.5 9.0 8.5 8.0 7.5 7.0 6.5 6.0 5.5 5.0 4.5 4.0 3.5 3.0 2.5 2.0 1.5 1.0 0.5
f1 (ppm)

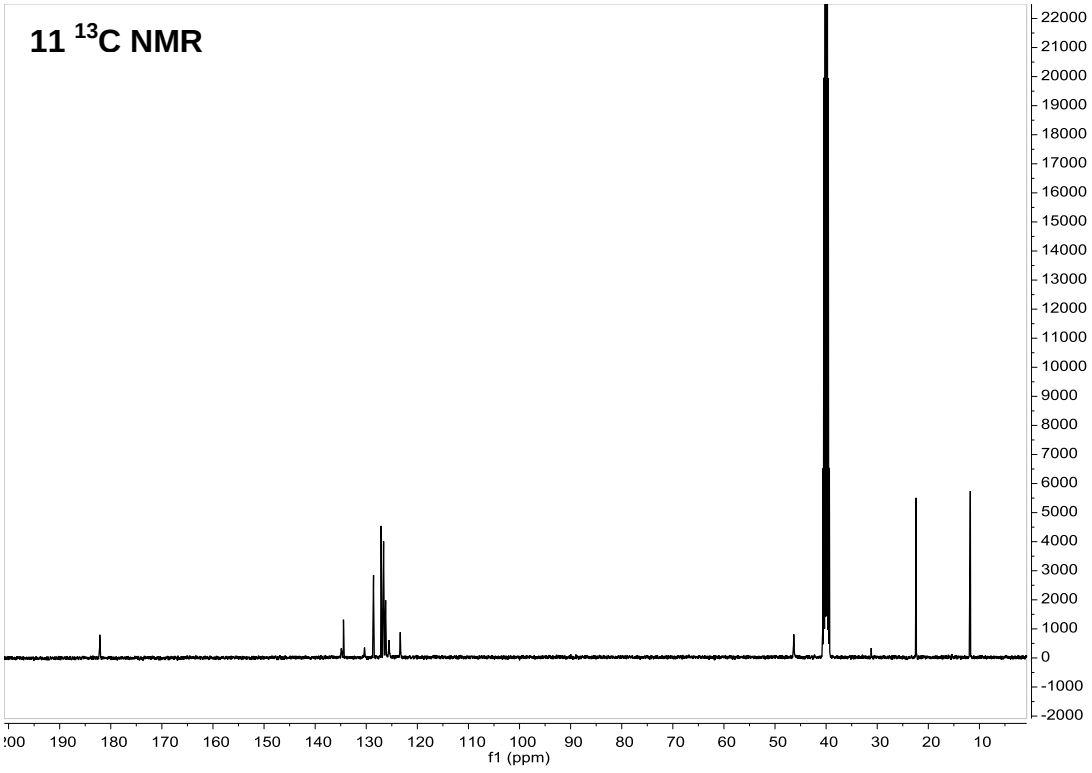
11 13C NMR
22000
21000
20000
19000
18000
17000
16000
15000
14000
13000
12000
11000
10000
9000
8000
7000
6000
5000
4000
3000
2000
1000
0
-1000
-2000
190 180 170 160 150 140 130 120 110 100 90 80 70 60 50 40 30 20 10
f1 (ppm)

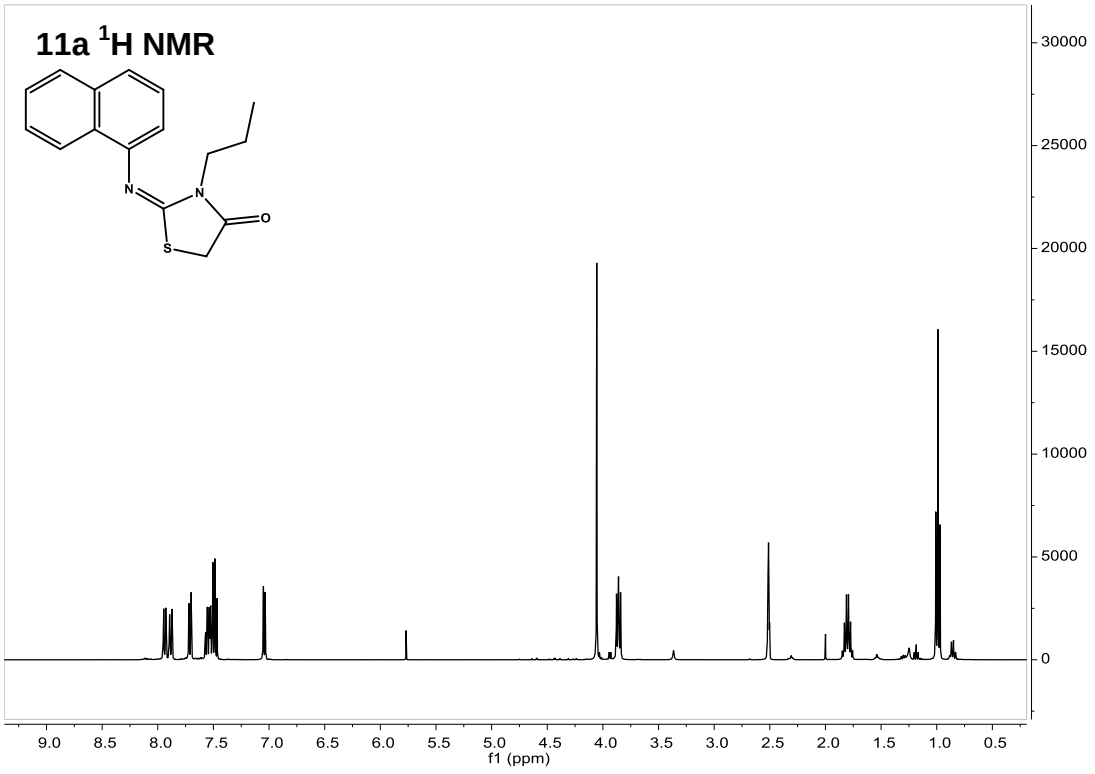
11a 1H NMR
N
N
O
S
30000
25000
20000
15000
10000
5000
0
9.0 8.5 8.0 7.5 7.0 6.5 6.0 5.5 5.0 4.5 4.0 3.5 3.0 2.5 2.0 1.5 1.0 0.5
f1 (ppm)

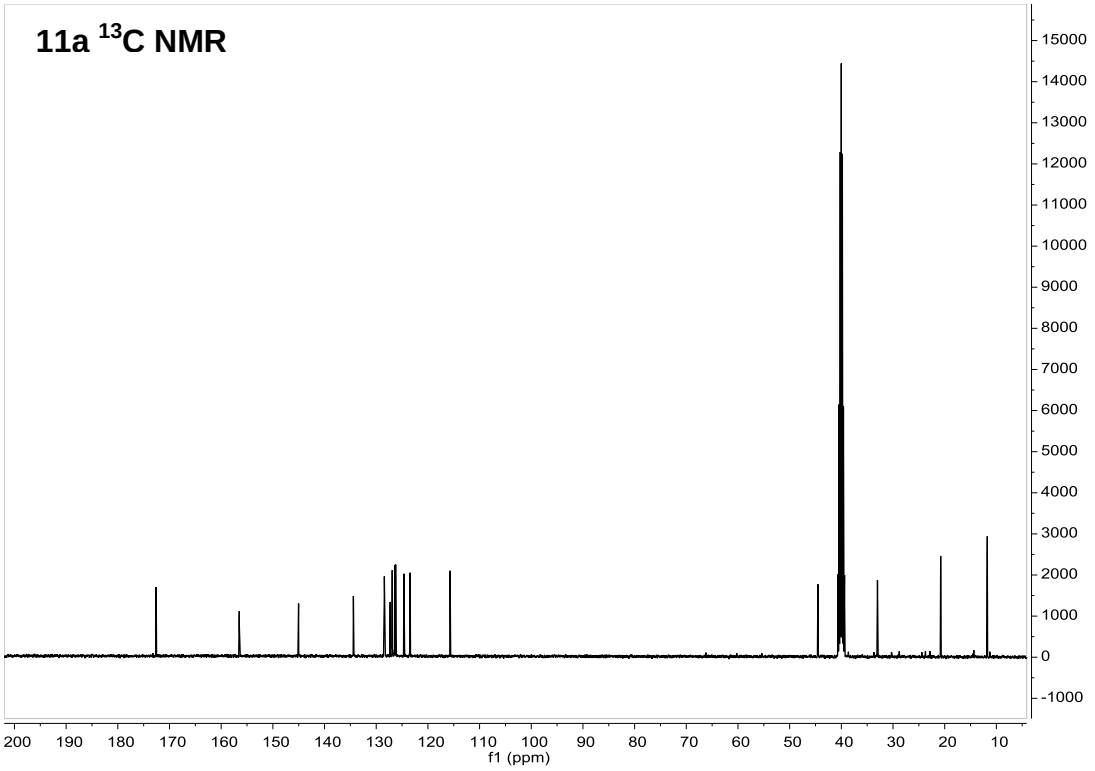
11a 13C NMR
15000
14000
13000
12000
11000
10000
9000
8000
7000
6000
5000
4000
3000
2000
1000
0
-1000
200 190 180 170 160 150 140 130 120 110 100 90 80 70 60 50 40 30 20 10
f1 (ppm)

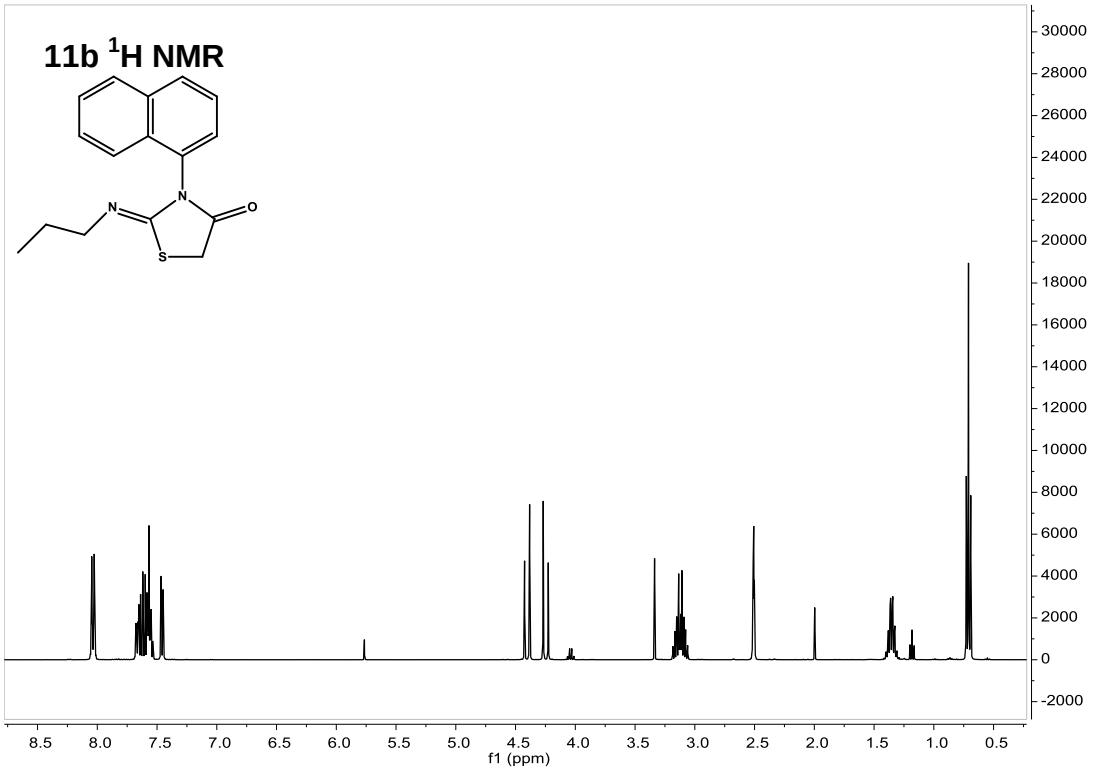
11b $^{1}$H NMR
N
N
O
S
30000
28000
26000
24000
22000
20000
18000
16000
14000
12000
10000
8000
6000
4000
2000
0
-2000
8.5 8.0 7.5 7.0 6.5 6.0 5.5 5.0 4.5 4.0 3.5 3.0 2.5 2.0 1.5 1.0 0.5
f1 (ppm)

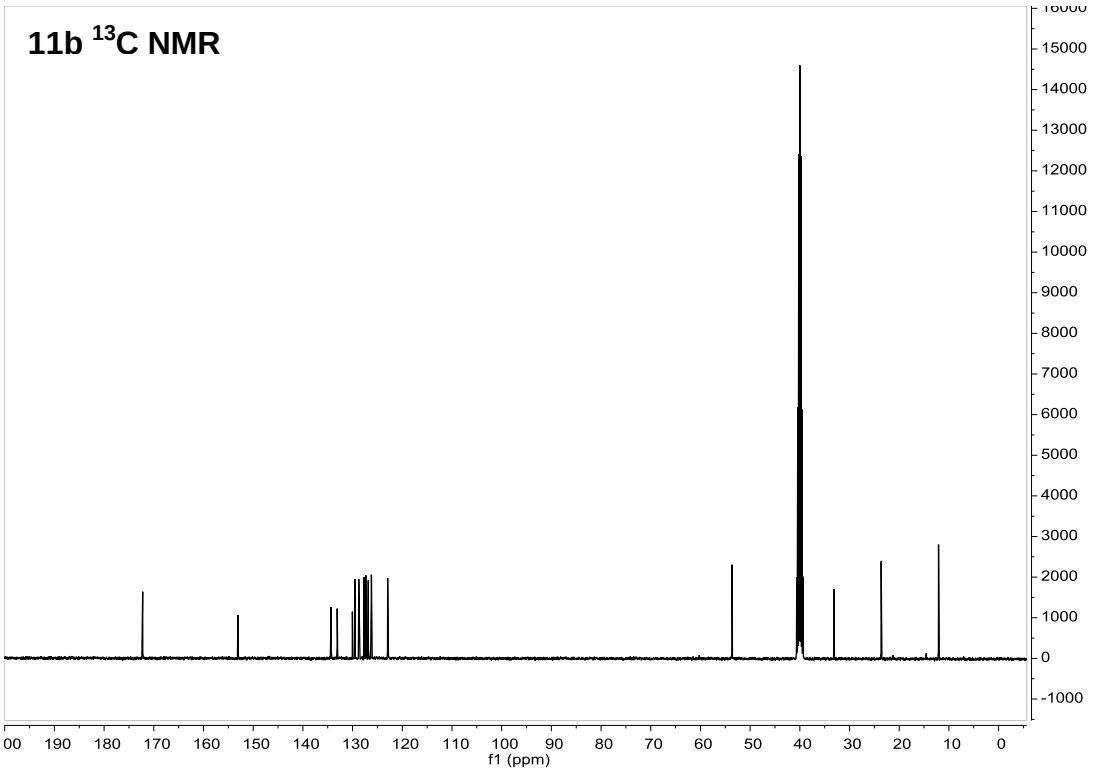
11b $^{13}$C NMR
15000
14000
13000
12000
11000
10000
9000
8000
7000
6000
5000
4000
3000
2000
1000
0
-1000
00 190 180 170 160 150 140 130 120 110 100 90 80 70 60 50 40 30 20 10 0
f1 (ppm)

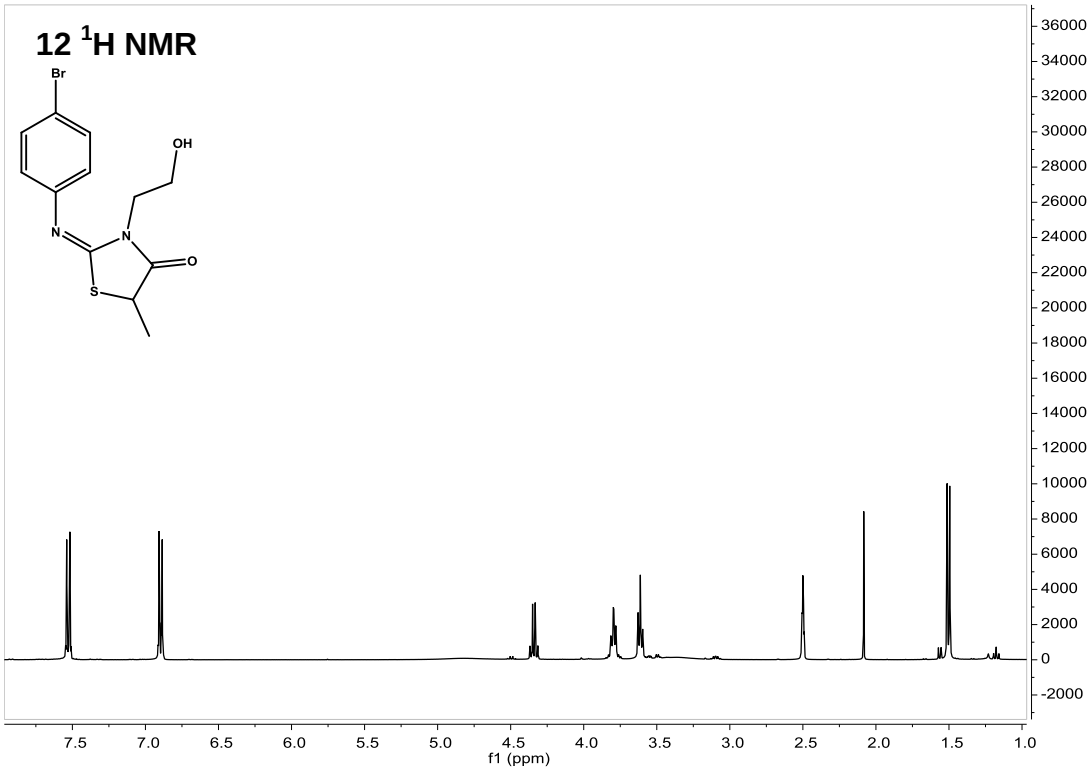
12 1H NMR
Br
OH
N
N
O
S
36000
34000
32000
30000
28000
26000
24000
22000
20000
18000
16000
14000
12000
10000
8000
6000
4000
2000
0
-2000
7.5 7.0 6.5 6.0 5.5 5.0 4.5 4.0 3.5 3.0 2.5 2.0 1.5 1.0
f1 (ppm)

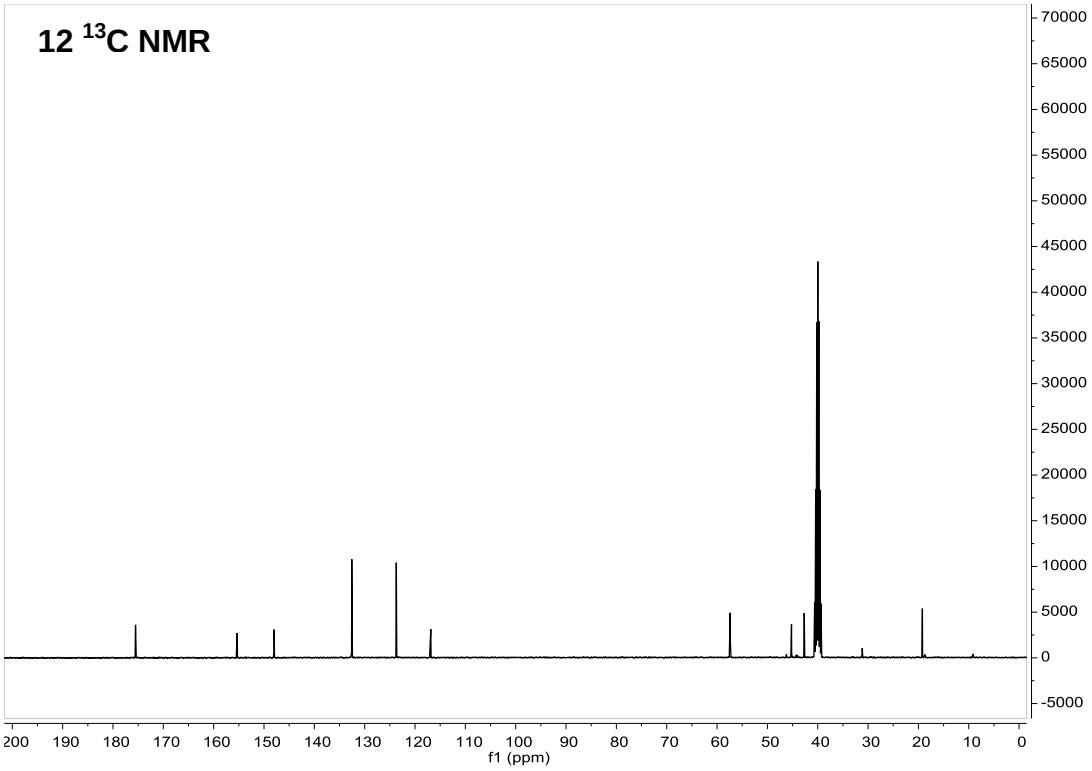
12 13C NMR
70000
65000
60000
55000
50000
45000
40000
35000
30000
25000
20000
15000
10000
5000
0
-5000
200 190 180 170 160 150 140 130 120 110 100 90 80 70 60 50 40 30 20 10 0
f1 (ppm)

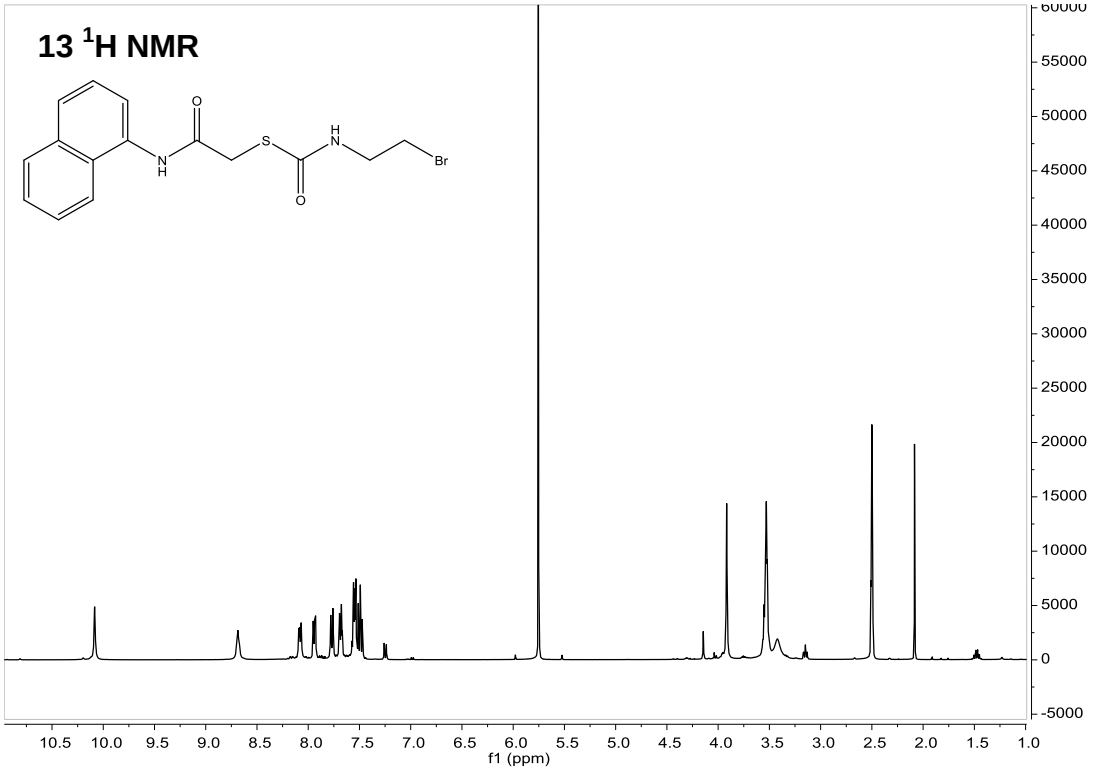
13 1H NMR
O
S
H
N
N
H
Br
O
60000
55000
50000
45000
40000
35000
30000
25000
20000
15000
10000
5000
0
-5000
10.5 10.0 9.5 9.0 8.5 8.0 7.5 7.0 6.5 6.0 5.5 5.0 4.5 4.0 3.5 3.0 2.5 2.0 1.5 1.0
f1 (ppm)

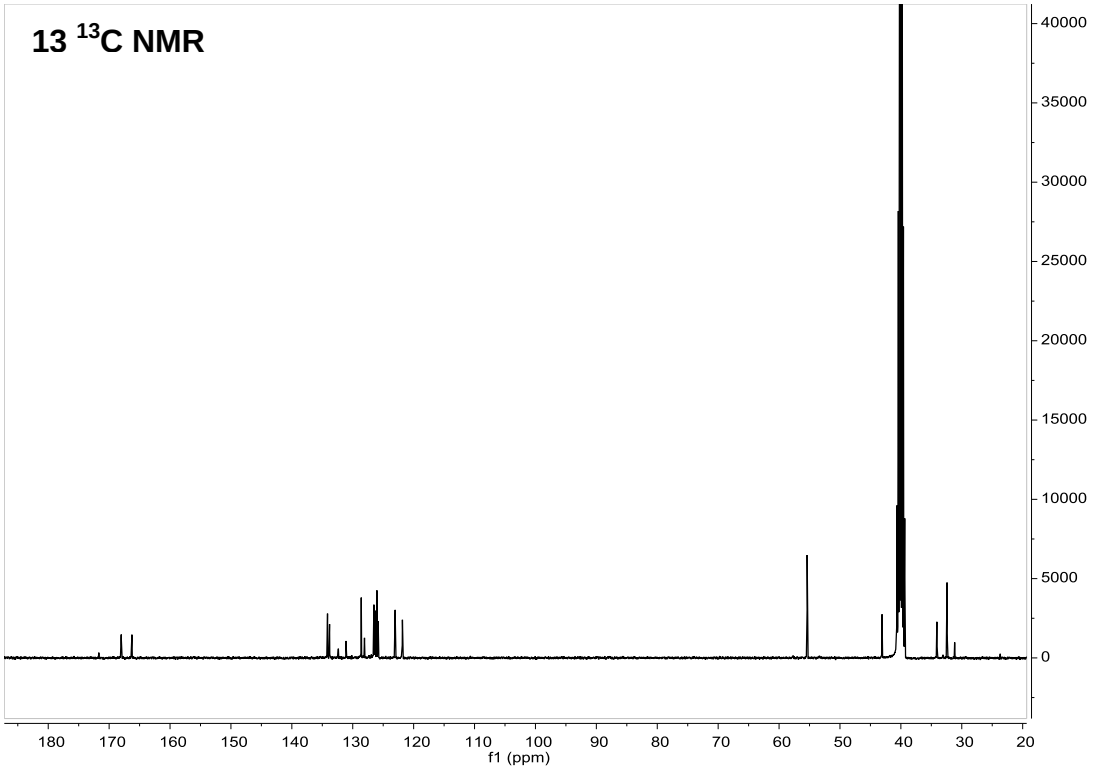
13 13C NMR
40000
35000
30000
25000
20000
15000
10000
5000
0
180 170 160 150 140 130 120 110 100 90 80 70 60 50 40 30 20
f1 (ppm)

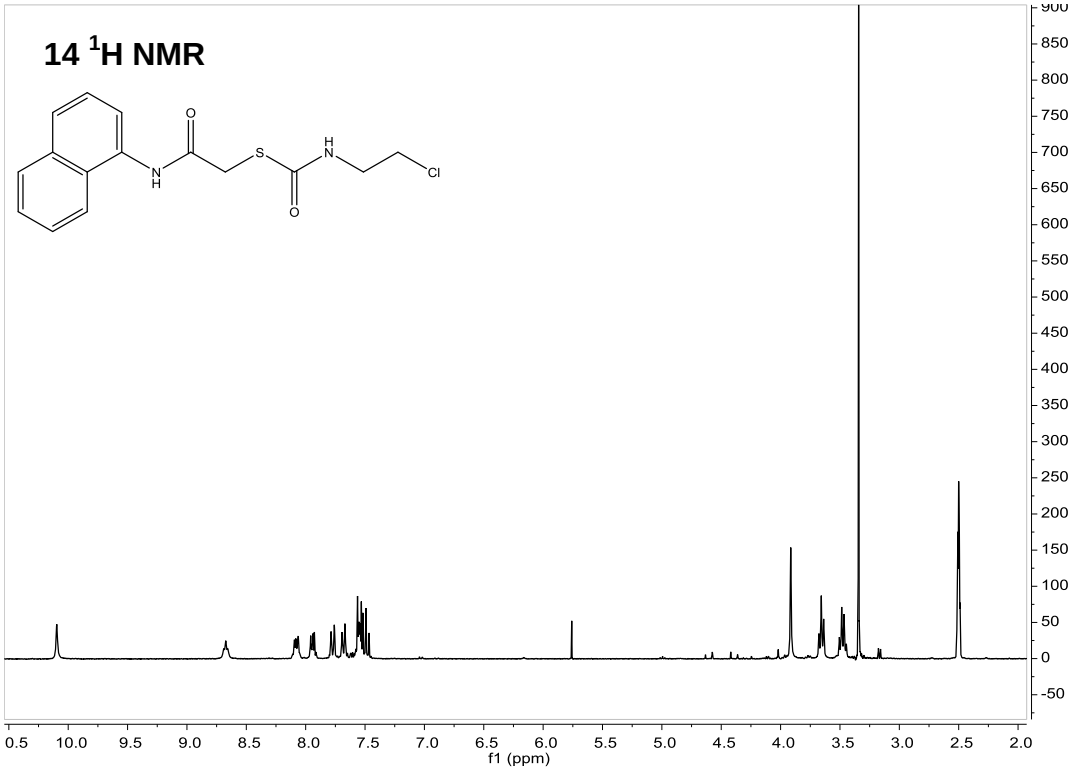
14 1H NMR
O
S
H
N
N
H
Cl
O
900
850
800
750
700
650
600
550
500
450
400
350
300
250
200
150
100
50
0
-50
0.5 10.0 9.5 9.0 8.5 8.0 7.5 7.0 6.5 6.0 5.5 5.0 4.5 4.0 3.5 3.0 2.5 2.0
f1 (ppm)

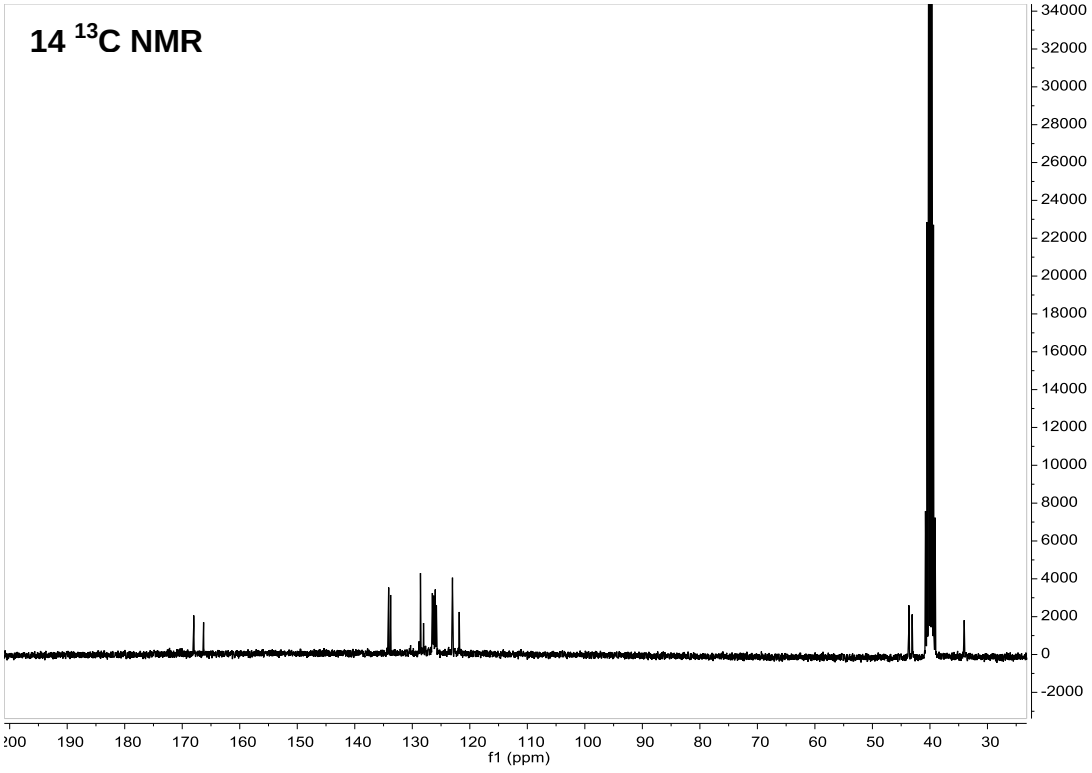
14 13C NMR
34000
32000
30000
28000
26000
24000
22000
20000
18000
16000
14000
12000
10000
8000
6000
4000
2000
0
-2000
200 190 180 170 160 150 140 130 120 110 100 90 80 70 60 50 40 30
f1 (ppm)

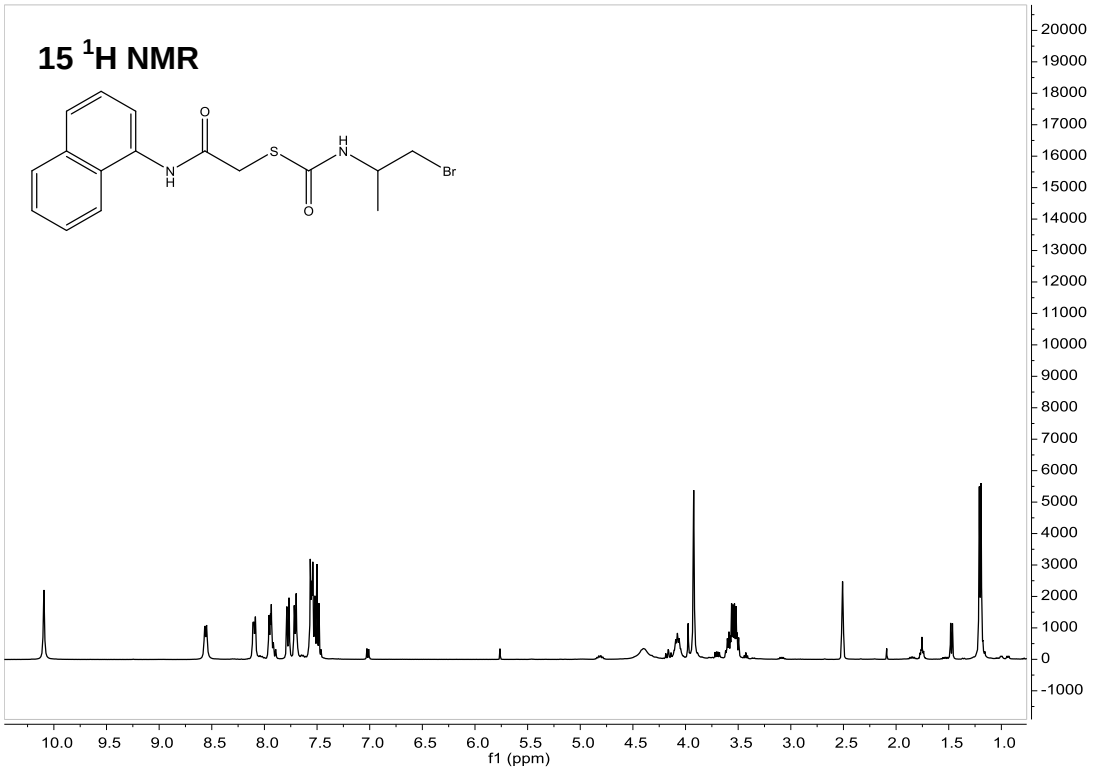
15 1H NMR
O
N
H
S
H
N
Br
O
20000
19000
18000
17000
16000
15000
14000
13000
12000
11000
10000
9000
8000
7000
6000
5000
4000
3000
2000
1000
0
-1000
10.0 9.5 9.0 8.5 8.0 7.5 7.0 6.5 6.0 5.5 5.0 4.5 4.0 3.5 3.0 2.5 2.0 1.5 1.0
f1 (ppm)

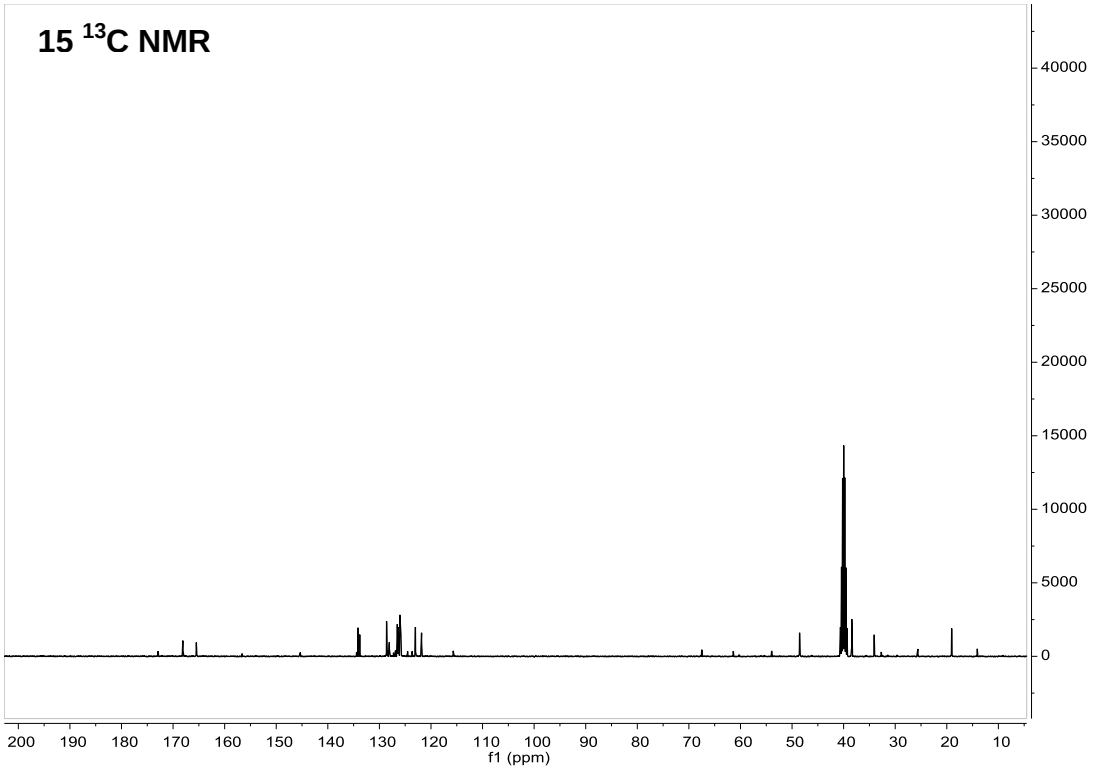
15 13C NMR
40000
35000
30000
25000
20000
15000
10000
5000
0
200 190 180 170 160 150 140 130 120 110 100 90 80 70 60 50 40 30 20 10
f1 (ppm)

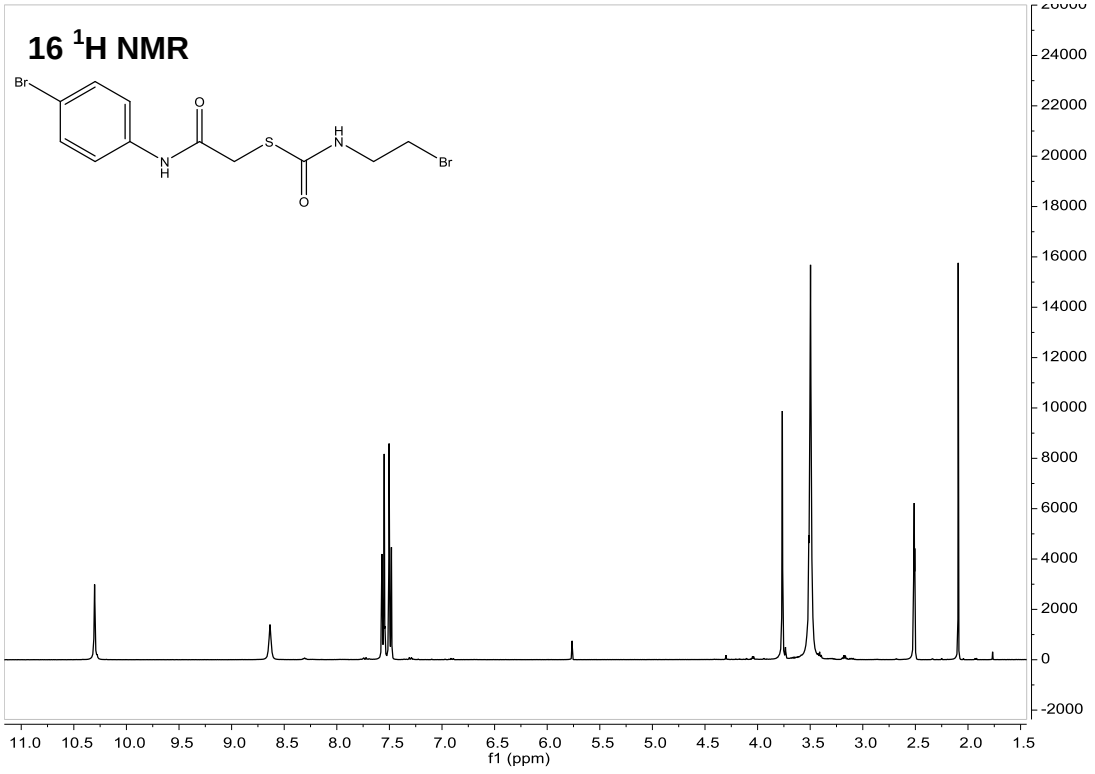
16 1H NMR
Br
O
S
H
N
N
H
Br
O
24000
22000
20000
18000
16000
14000
12000
10000
8000
6000
4000
2000
0
-2000
11.0 10.5 10.0 9.5 9.0 8.5 8.0 7.5 7.0 6.5 6.0 5.5 5.0 4.5 4.0 3.5 3.0 2.5 2.0 1.5
f1 (ppm)

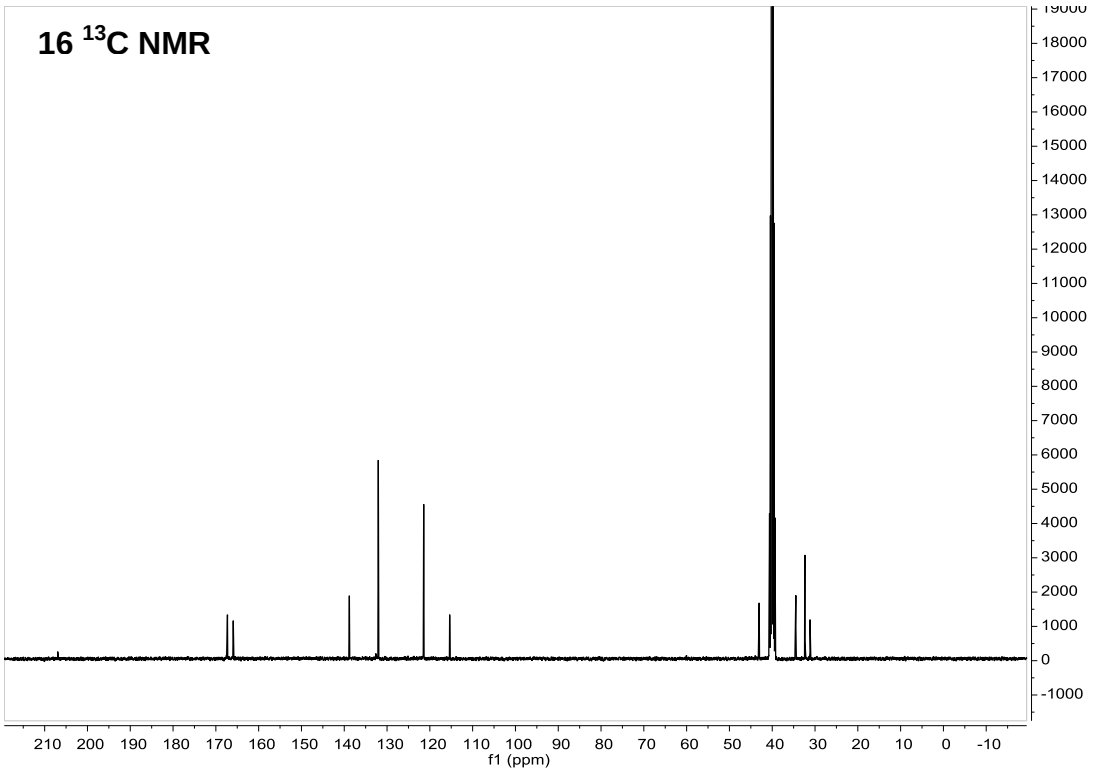
16 13C NMR
18000
17000
16000
15000
14000
13000
12000
11000
10000
9000
8000
7000
6000
5000
4000
3000
2000
1000
0
-1000
210 200 190 180 170 160 150 140 130 120 110 100 90 80 70 60 50 40 30 20 10 0 -10
f1 (ppm)

## Vita

Constance Devan Franklin was born on January 30, 1989 in Lewisville, Texas. Shortly after, she moved to Bedford, Virginia. She graduated from Jefferson Forest High School in 2007. From 2010-2011, while an undergraduate student at the University of Virginia, she worked in the lab of Dr. Derewenda under the mentorship of Dr. David Cooper. Work done included the purification and crystallization of an ABC transporter found in C*oxiella burnetti*. She received a Bachelor of Science with a Specialization in Biochemistry with ACS Certification from the University of Virginia, Charlottesville, VA in 2011. In the same year, she began graduate school at Virginia Commonwealth University where she joined the lab of Dr. Vladimir Sidorov.